



**The University of
Nottingham**

UNITED KINGDOM · CHINA · MALAYSIA

**MOLECULAR PHARMACOLOGICAL STUDIES
OF CHF1-FXII INTERACTION AND FXII
FUNCTION**

BADRALDIN KAREEM HAMAD

B.Pharm, MSc.

**Thesis submitted to the University of Nottingham for the
degree of Doctor of Philosophy**

October 2015

Abstract

Corn Hageman factor inhibitor (CHFI) is a bifunctional serine protease / α -amylase inhibitor protein having 127 residues and a molecular weight of 13.6-kDa. CHFI is selective toward FXIIa without affecting the function of the other coagulation factors. Coagulation FXII is a serine protease recognized to cause kinin generation and blood coagulation, cleaving plasma kallikrein and FXI. Results from FXII-deficient animal models proposed that this protein contributes to stable thrombosis that can cause obstruction of the blood vessels and its subsequent complications such as ischemic stroke. In contrast to other blood coagulation factors, deficiency in FXII is not related with haemorrhage in patients or in animals. These findings propose that specific inhibition of FXII could be an attractive medicine and a new method of anticoagulation to treat or prevent pathological thrombosis that could have a lower risk for bleeding and a safer anticoagulation profile than the currently available anticoagulants.

Therefore, the current PhD project aimed at pharmacological investigation into CHFI-FXII interaction and FXII function at molecular level through the following objectives: first, developing an efficient expression and purification system for generating soluble and functional recombinant native type CHFI and establishing an inhibitory activity assay against FXIIa to verify the proper function of the recombinant protein. The second objective was testing the different recombinant variants of CHFI with the desired point mutations guided by a proper prediction study of CHFI-FXII interaction. The third was to investigate into the hypothesis of the tight-binding property of CHFI via

different approaches of enzyme inhibition mechanisms and kinetic data analysis. The last objective was to investigate into the function of FXII by examining the effect of Cys466 and glycosylated peptide remnant from the proline-rich region on the function of the catalytic domain via characterizing the different recombinant variants of the catalytic domain of FXIIa, FXIIc, FXIIac, HISTF- β FXII, and MBP- β -FXIIa.

In the current study, an efficient system for soluble expression, single step purification and proper storage of functional, wild type rHIS-GST-CHFI was, for the first time, identified. The fully functional recombinant protein was verified via developing an inhibition test against FXIIa. The established expression, purification and inhibition assays were used as a fundamental guide to both generating and characterizing mutant proteins of interest that were made on the basis of an appropriate docking model of CHFI-FXIIa interaction. For the first time, the current investigation into the question of specificity of CHFI against FXII revealed that the central Arg34 at the very top of the fully exposed region of CHFI inhibition loop plays a central role in the inhibition function of CHFI toward FXIIa. In addition, this study identified Trp22 at the N-terminus and Arg43 at the C-terminus of the central inhibition loop as two key interaction residues with FXIIa. It was also observed that, in the preinhibition test, CHFI behaves as a noncompetitive inhibitor. In contrast, it acts as a competitive inhibitor in the acute inhibition test, proposing that CHFI is a competitive inhibitor with slow degree of reversibility due to tightness of binding. Reversibility assay showed that CHFI is an inhibitor with slow degree of dissociation. The tight-binding property of CHFI could be due to a non-active site interaction and or numerous hydrogen bonds between the

key interaction residues and their potential targets on FXIIa. With respect to the investigation into FXII function, It was observed that both Cys340-Cys466 and glycosylated peptide fragment of the proline-rich region have a functional role for the full catalytic activity of FXII protease domain. Cumulatively, the current study identified the key important residues on the exposed surface of CHF1 and their potential target residues on the surface of FXIIa that would be highly informative and important factors helping to understand the mechanism of selective and tight binding interaction of CHF1 with FXIIa. This project can be considered as an early, necessary approach to design novel, specific and safe anticoagulants for the treatment of thrombosis and its complications.

Acknowledgments

I should offer my thanks, compliance, and gratitude to **Allah** the greatest from whom I receive guide and help.

First to my supervisor, **Dr. Lodewijk Dekker**, I would like to thank you for establishing this project, taking me on as a student, important guidance you offered throughout the Ph.D. I appreciate all their supervision, encouragement, and huge knowledge that enabled me to understand the subject throughout my Ph.D., and assistance in writing the reports (i.e., 1st year, 2nd year and this thesis).

I would like to express my sincere gratitude to my second supervisor **Prof. Jonas Emley** for giving me the opportunity to carry out research on FXII. I heartily thank him for kind guidance. I also appreciate help with elucidating the results of the mutagenesis and peptide studies.

I also wish to express my thanks to **Monika Pathak** for helping me in performing molecular biology works in C84 lab and providing me with the different protein constructs for the characterization studies. I wish to convey my sincere thanks to **Rosa Manna** for giving me her protein constructs for the kinetic and characterization studies. I would like to thank **Bubacarr Kaira**, **Chan Li** and **Saleem Muhammed** for teaching me fundamental tools to understand and perform molecular biology works. Many thanks also for **Anna Boettiger** for helping me a lot when my time was quite tight and for her kindness and friendship.

My lab colleagues; **Khalid Elfsei, Yidong Liu, Anchala Kuruppu, Tiangong Lu, Vijay Raja, Mohannad Qazzaz and Mohammed Al-Hayali**, you made years of the PhD delightful experience.

Special thanks to my sponsor **HCDP/KRG**. Thanks to **Nottingham University**.

Sincere thanks and gratitude to my wife, **Sarween Abdullah, Mohammed Kareem, Sawan Kareem** and **Mustafa Kareem** for much love encouragement, patience, positivity, belief and general wonderfulness.

I offer my regards, blessings and deepest gratitude to my beloved supportive **parents**, my **sisters** and my **brothers** for their spiritual and physical supports, constant guidance, encouragements and sacrifice. All that I have achieved so far is actually their achievement. The words are insufficient to express my feelings for them.

Table of contents

| | |
|--|-------------|
| Acknowledgments | IV |
| Table of contents | VI |
| List of abbreviations | XII |
| List of Figures..... | XVII |
| List of Tables | XXII |
| Chapter 1: Introduction | 1 |
| 1.1 Hemostasis..... | 1 |
| 1.1.1 Vasoconstriction | 1 |
| 1.1.2 Platelet plug | 2 |
| 1.1.3 Blood coagulation..... | 7 |
| 1.1.4 Fibrin formation..... | 13 |
| 1.1.5 Inhibitors of the coagulation cascade and fibrinolysis system | 14 |
| 1.2 Serine proteases and coagulation FXII..... | 16 |
| 1.3 Catalytic mechanism of serine proteases..... | 17 |
| 1.4 Structure and function of the domains of human coagulation factor XII (Hageman factor)..... | 20 |
| 1.4.1 Heavy chain of Hageman factor (FXII) | 23 |
| 1.4.2 Fibronectin domain..... | 24 |
| 1.4.3 Epidermal growth factor- like domains | 25 |
| 1.4.4 Light chain (catalytic domain) of FXII | 27 |
| 1.5 Activation of FXII | 27 |
| 1.5.1 Activation pathways..... | 27 |
| 1.5.2 Generation of activated forms of FXII..... | 30 |

| | |
|--|-----------|
| 1.5.3 Role of zinc cation in the activation pathways | 30 |
| 1.6 Pathophysiological role of FXII | 32 |
| 1.6.1 Noncoagulation-related role | 32 |
| 1.6.2 Coagulation-related role: history of the role of FXII in physiological coagulation and pathological thrombosis | 35 |
| 1.7 Serine protease inhibitors | 38 |
| 1.8 Corn Hageman factor inhibitor (CHFI) | 39 |
| 1.9 The rationales of development of novel (target and or ligand-based) FXII inhibitors versus the currently available anticoagulants | 42 |
| 1.10 Aims and objectives | 44 |
| Chapter 2: Cloning, expression, purification, and characterization of the recombinant wild type CHFI (rHIS-GST-CHFI) | 48 |
| 2.1 Abstract | 48 |
| 2.2 Introduction | 50 |
| 2.3 Cloning | 52 |
| 2.3.1 Materials | 52 |
| 2.3.2 Method | 62 |
| 2.4 Protein expression and purification | 72 |
| 2.4.1 Materials | 72 |
| 2.4.2 Method | 80 |
| 2.5 Characterization of rHIS-GST-CHFI | 86 |
| 2.5.1 Materials | 86 |
| 2.5.2 Methods | 89 |
| 2.6 Results and discussion | 92 |
| 2.6.1 Cloning | 92 |
| 2.6.2 Expression, purification, and characterization of the inhibitory activity of rHIS-GST-CHFI against FXIIa | 93 |

| | |
|---|-----|
| 2.6.3 Characterization of rHIS-GST-CHFI | 99 |
| 2.7 Conclusion | 106 |
| 3.1 Abstract | 107 |
| 3.2 Introduction | 108 |
| 3.3 Materials and methods | 109 |
| 3.3.1 Materials | 109 |
| 3.3.2 Methods | 111 |
| 3.4 Results and discussion | 116 |
| 3.4.1 Prediction of CHFI-FXII interaction | 116 |
| 3.4.2 Site-directed mutagenesis | 125 |
| 3.4.3 Preparation of the recombinant CHFI mutants- expression and purification | 126 |
| 3.4.4 Inhibitory activity of the mutants against rHIS-GST- CHFI | 128 |
| 3.4.5 Experimental validation of the crucial role of the central Arg34 in the inhibitory function of CHFI | 129 |
| 3.4.6 Inhibitory effect of rHIS-GST-CHFI-L35A, rHIS-GST- CHFI-G30W, and rHIS-GST-CHFI-G32W on FXIIa | 131 |
| 3.4.7 The effect of rHIS-GST-CHFI-R27A, rHIS-GST-CHFI- W37A, rHIS-GST-CHFI-E39A, and rHIS-GST-CHFI-R42A on the inhibition of FXII enzyme | 135 |
| 3.4.8 Experimental verification of the significance of two key interaction residues, Trp22 and Arg43, for the inhibitory activity of CHFI | 139 |
| 3.4.9 Investigation of the inhibitory activity of the synthetic isolated peptides of CHFI central inhibition loop: with relevance to the role of the Cys20-Cys44 in the function/active conformation of the loop | 142 |

| | |
|---|------------|
| 3.4.10 Evaluation of the inhibitory activity of the linear peptide lacking Trp22 and Arg43 | 146 |
| 3.5 Conclusion | 150 |
| Chapter 4: Dual kinetic mechanisms of CHFI: relevance to the hypothesis of tight binding of CHFI to the different forms of human coagulation FXIIa, α-FXIIa, β-FXIIa and MBP-β- FXIIa..... | 152 |
| 4.1 Abstract | 152 |
| 4.2 Introduction | 153 |
| 4.3 Materials and methods..... | 154 |
| 4.3.1 Materials | 154 |
| 4.3.2 Methods..... | 156 |
| 4.4 Results and Discussion | 160 |
| 4.4.1 Dual kinetic actions of CHFI | 160 |
| 4.4.2 Identification of mechanism of inhibition using the relationship between [S-2302] and IC_{50} | 171 |
| 4.4.3 Identification of mechanism of inhibition via examining the effect of inhibition on K_M and k_{cat} and Lineweaver-Burk plot..... | 183 |
| 4.4.4 Tight-binding behaviour of CHFI | 194 |
| 4.5 Conclusion | 199 |
| Chapter 5: Characterization of the different recombinant variants of the human coagulation FXII catalytic domain: relevance to the functional role of both Cys466 and glycosylated peptide fragment from proline-rich region in the full catalytic activity of the protease domain | 200 |
| 5.1 Abstract | 200 |
| 5.2 Introduction | 203 |
| 5.3 Materials and methods..... | 206 |
| 5.3.1 Materials | 206 |

| | |
|--|------------|
| 5.3.2 Methods..... | 214 |
| 5.4 Results and discussion..... | 215 |
| 5.4.1 Amidolytic activity of the commercial forms of FXIIa, α -FXIIa and β -FXIIa..... | 215 |
| 5.4.2 Amidolytic activity of FXII zymogen, FXIIac, and FXIIc in comparison with β -FXIIa and α -FXIIa..... | 222 |
| 5.4.3 Autoactivation of FXII zymogen and the recombinant catalytic domains..... | 227 |
| 5.4.4 Investigation of the activation of FXIIac by NGPLSCGQR / NGPLSCGQRLRKSLSMTR beta stump peptides..... | 232 |
| 5.5.5 Investigation of the role of the remnant peptide bound to the catalytic domain via Cys340-Cys466 in the catalytic activity of the protease domain..... | 234 |
| 5.5.6 Investigation of the functional role of the glycosylated peptide fragment bound to the catalytic domain via Cys340-Cys466..... | 237 |
| 5.5 Conclusion..... | 241 |
| Chapter 6: General discussion, significance of the current project, and future plan..... | 243 |
| 6.1 General discussion..... | 243 |
| 6.2 Significance of this study..... | 252 |
| 6.3 Future plan..... | 253 |
| 6.3.1 Prediction studies of CHFI interaction with other proteases..... | 253 |
| 6.3.2 Generation and inhibitory activity of different CHFI mutants..... | 253 |
| 6.3.3 Point mutations of the potential target residues of CHFI in FXII..... | 254 |

| | |
|--|------------|
| 6.3.4 Inhibitory activity of the different forms of the isolated peptides of CHFI against other proteases that have sequence homology with FXII | 254 |
| 6.3.5 Reversibility assay of CHFI mutants | 255 |
| 6.3.6 Using the CHFI isolated peptide as a template for pharmacophore-based drug design. | 255 |
| 6.3.7 Preclinical studies of candidate peptides | 256 |
| 6.3.7 Point mutations of the potential target residues of the CHFI-FXII model | 256 |
| 6.3.8 Crystallization studies of FXIIa, CHFI-FXII, and the lead peptide generated from pharmacophore-based drug design | 256 |
| References | 257 |
| Appendix | 281 |
| Publication..... | 281 |
| Article: | 281 |
| Conference paper: | 281 |

List of abbreviations

| | |
|---------------------------------|---|
| α-FXII | Activated Coagulation Factor FXII alpha |
| ADP | adenosine diphosphate |
| APC | Activated protein C |
| APTT | Activated partial thromboplastin time |
| Asp | Aspartic acid |
| ATIII | Antithrombin III |
| β-FXII | Activated coagulation Factor XII beta |
| CHFI | Corn Hageman factor inhibitor |
| CK1 | Cytokeratin 1 |
| CTI | Corn trypsin inhibitor |
| Cys | Cysteine |
| DTT | Dithiothreitol |
| EDTA | Ethylenediamine tetraacetic acid |
| EGF | Epidermal growth factor |
| EGFR | Epidermal growth factor receptor |
| EPGR | Epidermal growth factor receptor |
| EPI | Extrinsic pathway inhibitor (EPI) |

| | |
|---------------|--|
| EPRC | endothelial protein C receptor |
| ERK1/2 | Extracellular-signal regulated kinases 1/2 |
| FcγRI | Fragment crystallisable gamma receptor I |
| FDA | Fibrin degradation product |
| FIX | Coagulation factor IX |
| FIXa | Activated coagulation factor IX |
| FV | Coagulation factor V |
| FVa | Activated coagulation Factor V |
| FVII | Coagulation factor VII |
| FVIIa | Activated coagulation factor VII |
| FVIII | Coagulation factor VIII |
| FVIIIa | Activated coagulation factor VIII |
| FX | Coagulation factor X |
| FXa | Activated coagulation factor X |
| FXI | Coagulation factor XI |
| FXIa | Activated coagulation factor XI |
| FXII | Coagulation factor XII |
| FXIIa | Activated coagulation factor XII |
| FXIII | Coagulation factor XIII |

| | |
|-----------------------------|---|
| FXIIIa | Activated coagulation factor XIII |
| gC1q-R | Receptor for the globular heads of C1q |
| GLA | Gamma-carboxyglutamic acid |
| Gla | gamma-carboxyglutamic acid |
| Glu | Glutamic acid |
| GPCRs | G-Protein Coupled Receptors |
| GPIb | Glycoprotein Ib |
| HF | Hageman Factor |
| His | Histidine |
| HK or HMWK | High-molecular-weight kininogen |
| HSP 90 | Heat shock protein 90 |
| HUVEC | Human umbilical vein endothelial cells |
| IC₅₀ | Half maximal inhibitory concentration |
| Ile | Isoleucine |
| kb | Kilobase |
| <i>K_d</i> | Dissociation constant |
| kDa | Kilodalton |
| LACI | Lipoprotein-associated coagulation inhibitor |

| | |
|--------------|------------------------------------|
| LB | Lysogeny Broth |
| Leu | Leucine |
| LMWH | Low molecular weight heparin |
| M | Molar |
| MAPK | Mitogen activated protein kinase |
| MBP | Maltose Binding Protein |
| mg | Milligram |
| mM | Millimolar |
| nm | Nanometer |
| nM | Nanomolar |
| NO | Nitric oxide |
| OD600 | Optical density at 600 nm |
| PAGE | Polyacrylamide gel electrophoresis |
| PARs | protease-activated receptors |
| PBS | Phosphate buffered saline |
| PCR | Polymerase Chain Reaction |
| PE | Phosphatidylethanolamine |
| Phe | Phenylalanine |
| PK | Prekallikrein |

| | |
|--------------|---|
| PLA2 | phospholipase A2 |
| Pro | Proline |
| ProCP | Prolylcarboxypeptidase |
| PT | Prothrombin time |
| RAGE | Receptors for advanced glycation end products |
| SDS | Sodium dodecyl sulphate |
| TFPI | tissue factor pathway inhibitor |
| tPA | tissue plasminogen activator |
| uPA | urokinase plasminogen activator |
| TxA2 | Thromboxane A2 |
| VWF | Von Willebrand factor |

List of Figures

| | Page |
|--------------------|--|
| Figure 1.1 | Stages of platelet aggregation 7 |
| Figure 1.2 | Schematic diagram of the coagulation and fibrinolysis pathway 10 |
| Figure 1.3 | Schematic diagram of the fibrinolysis pathway 14 |
| Figure 1.4 | Functional structures of FXII domains 19 |
| Figure 1.5 | Functional structures of FXII domains 22 |
| Figure 1.6 | Coloured presentation diagrams of α -FXIIa and β -FXIIa 23 |
| Figure 1.7 | Fluid-phase and solid-phase activation pathways of FXII. 29 |
| Figure 1.8 | Pathway of direct and indirect functions of the different forms of Hageman factor 35 |
| Figure 1.9 | Cartoon diagram of CHFI crystal structure. 42 |
| Figure 2.1 | Expression vectors, pCold I and pCold I-GST 57 |
| Figure 2.2 | Schematic representation of the DNA constructs 59 |
| Figure 2.3 | Schematic diagram of principle of the method 90 |
| Figure 2.4 | 1% agarose gel showing insert band after digestion 93 |
| Figure 2.5 | Expression of the fusion protein, rHIS-GST-CHFI... 95 |
| Figure 2.6 | Optimization of induction period 96 |
| Figure 2.7 | Optimization of induction... 96 |
| Figure 2.8 | Optimizing [IPTG] for induction of protein expression in Origami™ 2 97 |
| Figure 2.9 | 15% SDS showing Ni^{2+} column purification of rHIS-GST-CHFI 98 |
| Figure 2.10 | Ni^{2+} column purification of rHIS-GST tag 99 |
| Figure 2.11 | Calibration line and equation between the amount of p-nitroaniline and absorbance unit for the machine with filter system 99 |
| Figure 2.12 | Inhibition assay of rHIS-GST-CHFI versus commercial CHFI 102 |

| | | |
|--------------------|--|------------|
| Figure 3.1 | Prediction of CHF1-FXIIa interaction | 117 |
| Figure 3.2 | Prediction of the central, functional role of Arg34 in the inhibitory activity of CHF1 | 119 |
| Figure 3.3 | Key interaction residues relevant for elucidating specificity of CHF1 toward FXIIa | 121 |
| Figure 3.4 | Residues affecting hydrophobicity and flexibility of the central inhibition loop | 123 |
| Figure 3.5 | Charged residues and hydrophobic-aromatic residue on the surface of CHF1 central inhibition loop | 124 |
| Figure 3.6 | Expression and purification of CHF1 mutants | 127 |
| Figure 3.7 | Experimental verification of the functional role of Arg34 | 131 |
| Figure 3.8 | CHF1 mutants acting as partial inhibitors of FXIIa | 134 |
| Figure 3.9 | Inhibitory activity of the wild type like mutants | 137 |
| Figure 3.10 | Effect of double point mutations on the inhibitory activity of CHF1 | 138 |
| Figure 3.11 | Inhibitory activity of rHIS-GST-CHF1-W22A and rHIS-GST-CHF1-R43A | 141 |
| Figure 3.12 | Inhibitory activity of the synthetic, isolated peptides of the central inhibition loop | 145 |
| Figure 3.13 | Inhibitory activity of Trp22-lacking and Arg43-lacking peptides | 148 |
| Figure 4.1 | Schematic representation of reversibility assay | 158 |
| Figure 4.2 | Time-dependent inhibition of the catalytic breakdown of S-2302 by different [CHF1] | 161 |
| Figure 4.3 | Noncompetitive inhibition behaviour of CHF1 in the preincubation condition | 163 |
| Figure 4.4 | CHF1 follows noncompetitive inhibition model against β -FXIIa in the preincubation assay | 164 |
| Figure 4.5 | CHF1 acts as a noncompetitive inhibitor of MBP- β -FXIIa in the preincubation assay | 165 |
| Figure 4.6 | CHF1 obeys competitive inhibition against α -FXIIa in the coincubation assay. | 167 |

| | | |
|--------------------|---|------------|
| Figure 4.7 | CHFII follows competitive inhibition against β -FXIIa in the coincubation assay | 168 |
| Figure 4.8 | CHFII obeys competitive inhibition toward MBP- β -FXIIa in the coincubation assay. | 169 |
| Figure 4.9 | IC ₅₀ Curves of CHFII at different [S-2302] in the preincubation assay of CHFII- α -FXIIa interaction. | 172 |
| Figure 4.10 | IC ₅₀ Curves of CHFII at different [S-2302] in the coincubation state of CHFII- α -FXIIa interaction. | 173 |
| Figure 4.11 | IC ₅₀ Curves of CHFII at different [S-2302] in the preincubation assay of CHFII- β -FXIIa interaction | 175 |
| Figure 4.12 | IC ₅₀ Curves of CHFII at different [S-2302] in the coincubation state of CHFII- β -FXIIa interaction | 176 |
| Figure 4.13 | IC ₅₀ Curves of CHFII at different [S-2302] in the preincubation state of CHFII- MBP- β -FXIIa interaction | 178 |
| Figure 4.14 | IC ₅₀ Curves of CHFII at different [S-2302] in the coincubation state of CHFII- MBP- β -FXIIa interaction | 179 |
| Figure 4.15 | Relationship between [S]/ K_M and IC ₅₀ / K_i in CHFII- α -FXIIa interaction | 181 |
| Figure 4.16 | Relationship between [S]/ K_M and IC ₅₀ / K_i in CHFII- β -FXIIa interaction | 182 |
| Figure 4.17 | Relationship between [S]/ K_M and IC ₅₀ / K_i in CHFII- MBP β -FXIIa interaction | 183 |
| Figure 4.18 | Michaelis-Menten kinetics of the inhibition of α -FXIIa by CHFII in the preincubation assay | 184 |
| Figure 4.19 | Lineweaver-Burk plots showing non-competitive inhibition of α -FXIIa by CHFII | 185 |
| Figure 4.20 | Michaelis-Menten kinetics of β -FXIIa-CHFII interaction in the preincubation assay | 186 |
| Figure 4.21 | Lineweaver-Burk plots showing non-competitive inhibition of β -FXIIa by CHFII. | 187 |
| Figure 4.22 | Michaelis-Menten kinetics of the inhibition of MBP- β -FXIIa by CHFII in the preincubation assay | 188 |
| Figure 4.23 | Lineweaver-Burk plots showing non-competitive | 189 |

| | | |
|--------------------|--|------------|
| | inhibition of MBP- β -FXIIa by CHFI | |
| Figure 4.24 | Michaelis-Menten kinetics of the inhibition of α -FXIIa by CHFI in the coincubation assay | 190 |
| Figure 4.25 | Lineweaver-Burk plots showing competitive inhibition of α -FXIIa by CHFI | 191 |
| Figure 4.26 | Michaelis-Menten kinetics of the inhibition of β -FXIIa by CHFI in the coincubation assay | 191 |
| Figure 4.27 | Lineweaver-Burk plots showing competitive inhibition of β -FXIIa by CHFI | 192 |
| Figure 4.28 | Michaelis-Menten kinetics of the inhibition of MBP- β -FXIIa by CHFI in the coincubation assay | 193 |
| Figure 4.29 | Lineweaver-Burk plots showing competitive inhibition of MBP- β -FXIIa by CHFI. | 194 |
| Figure 4.30 | Slow recovery of enzyme activity after rapid dilution | 196 |
| Figure 5.1 | The scheme of enzyme-substrate reaction according to Michaelis-Menten model | 203 |
| Figure 5.2 | Schematic representation of the FXIIac | 211 |
| Figure 5.3 | Schematic representation of FXIIc | 211 |
| Figure 5.4 | Cartoon diagram of HISTF- β FXII | 213 |
| Figure 5.5 | Cartoon diagram of MBP- β -FXIIa | 213 |
| Figure 5.6 | α -FXIIa-S-2302 time dependent assays | 216 |
| Figure 5.7 | β -FXIIa-S-2302 time dependent assays | 217 |
| Figure 5.8 | α -FXIIa obeys Michaelis-Menten model | 219 |
| Figure 5.9 | β -FXIIa obeys Michaelis-Menten model | 220 |
| Figure 5.10 | Comparative time dependent assay of the different commercial forms and recombinant variants of FXII | 223 |
| Figure 5.11 | Activity of different forms of FXII | 224 |
| Figure 5.12 | Amidolytic activity of FXIIc | 225 |
| Figure 5.13 | Amidolytic effect of FXIIac | 226 |
| Figure 5.14 | Autoactivation of human FXII zymogen | 229 |
| Figure 5.15 | Autoactivation of the different forms of FXII | 230 |
| Figure 5.16 | Autoactivation of the different forms of FXII | 231 |
| Figure 5.17 | Failure of activation of FXIIac by NGPLSCGQR or | 233 |

NGPLSCGQRLRKSLSSMTR beta stump peptides

| | | |
|--------------------|---|------------|
| Figure 5.18 | Comparative time dependent assays of human FXIIa (α -FXIIa and β -FXIIa) forms and HISTF- β FXII. | 235 |
| Figure 5.19 | Weak amidolytic activity of HISTF- β FXII. | 236 |
| Figure 5.20 | Comparative time dependent assays of human FXIIa (α -FXIIa and β -FXIIa) forms and MBP- β -FXIIa generated in <i>Drosophila Schneider 2 cells</i> | 238 |
| Figure 5.21 | Activity MBP- β -FXIIa in comparison with α -FXIIa and β -FXIIa. | 239 |

List of Tables

| | | Page |
|------------------|--|-------------|
| Table 2.1 | List of the materials and reagents used in the molecular cloning of CHFI | 52 |
| Table 2.2 | List of the materials and reagents required for expression and purification of CHFI | 72 |
| Table 2.3 | Solutions for preparing resolving gels for a 15% SDS-PAGE | 79 |
| Table 2.4 | Solutions for preparing stacking gels for a 15% SDS-PAGE | 79 |
| Table 2.5 | List of the materials used in the characterization study of CHFI | 86 |
| Table 2.6 | Inhibition effectiveness value (IC_{50}) of the recombinant wild type, rHIS-GST-CHFI, in comparison with that of commercial CHFI | 103 |
| Table 2.7 | Effect of different factors on the stability and inhibitory activity of rHIS-GST-CHFI. | 105 |
| Table 3.1 | List and quantity of the materials supplied in the site-directed mutagenesis kit | 109 |
| Table 3.2 | List of the synthetic, isolated peptides | 110 |

| | | |
|-------------------|---|------------|
| Table 3.3 | List of the mutagenic primers used in the PCR site directed mutagenesis. | 112 |
| Table 3.4 | Protocol for PCR site directed mutagenesis | 113 |
| Table 3.5 | Cycling parameters for the reactions of PCR site directed mutagenesis | 114 |
| Table 3.6 | Inhibition effectiveness of the mutants behaving as partial inhibitors. | 135 |
| Table 3.7 | Inhibitory activity of the wild type like mutants. | 139 |
| Table 3.8 | Inhibitory activity of rHIS-GST-CHFI-W22A and rHIS-GST-CHFI-R43A | 142 |
| Table 3.9 | Inhibition activity of the linear peptide, cyclic peptide, and short peptide. | 146 |
| Table 3.10 | Inhibition activity of Trp22-deficient and Arg43-deficient peptide. | 149 |
| Table 4.1 | List of the materials required for the kinetic study of CHFI-FXII interaction | 154 |
| Table 4.2 | Analysis of initial reaction rates in CHFI-FXIIa inhibition interaction | 162 |
| Table 4.3 | Kinetic parameters of the noncompetitive inhibition model of CHFI-FXIIa interaction | 166 |
| Table 4.4 | The kinetic parameters of the competitive inhibition model | 170 |

| | | |
|-------------------|---|------------|
| Table 4.5 | IC ₅₀ values of CHFI at different [S-2302] in the preincubation and coincubation state of CHFI- α -FXIIa interaction. | 174 |
| Table 4.6 | IC ₅₀ values of CHFI at different [S-2302] in the preincubation and coincubation state of CHFI- β -FXIIa interaction | 177 |
| Table 4.7 | IC ₅₀ values of CHFI at different [S-2302] in the preincubation and coincubation state of CHFI- MBP- β -FXIIa interaction. | 180 |
| Table 4.8 | Kinetic parameters of CHFI- α -FXIIa interaction in preincubation condition using Michaelis-Menten kinetics | 185 |
| Table 4.9 | Kinetic parameters of CHFI- β -FXIIa interaction in the preincubation condition using Michaelis-Menten kinetics | 186 |
| Table 4.10 | Kinetic parameters of CHFI-MBP- β -FXIIa interaction in the preincubation condition using Michaelis-Menten kinetics | 188 |
| Table 4.11 | Kinetic parameters of CHFI- α -FXIIa interaction in the coincubation condition using Michaelis-Menten kinetics | 190 |
| Table 4.12 | Kinetic parameters of CHFI- β -FXIIa interaction in the coincubation condition using Michaelis-Menten kinetics | 192 |

| | | |
|-------------------|--|------------|
| Table 4.13 | Kinetic parameters of CHFI-MBP- β -FXIIa interaction in the coincubation condition using Michaelis-Menten kinetics | 193 |
| Table 5.1 | List of materials used in the characterization study of different recombinant variants of FXII | 206 |
| Table 5.2 | Initial reaction rates of the cleavage of the different concentrations of S-2302 by one pmol of the enzyme. | 218 |
| Table 5.3 | Initial reaction rates of the hydrolysis of the different concentrations of S-2302 by one pmol of the enzyme. | 218 |
| Table 5.4 | Estimation of V_{max} , K_M and k_{cat} values of the different forms of human activated Hageman factor | 221 |
| Table 5.5 | Kinetic parameter values of kinetic hydrolysis of S-2302 by MBP- β -FXIIa | 240 |

Chapter 1: Introduction

1.1 Hemostasis

The term hemostasis means prevention of blood loss. Hemostasis is a complicated system keeping blood in balance between bleeding and thrombosis. In a healthy individual, the blood is sustained in a flowing state in the vascular system, but is always ready to quickly produce a hemostatic plug that stops bleeding once a blood vessel is traumatized. When a blood vessel is ruptured, hemostasis is achieved by numerous mechanisms: first, vasoconstriction, second, formation of a platelet plug, third, formation of a blood clot due to blood coagulation (this differs from thrombosis, a process that generates an abnormal clot known as thrombus), and four, eventual growth of fibrous tissue (fibrin mesh) into the blood clot to permanently close the hole in the vessel. Based on the above mechanisms, hemostasis can be divided into two types: primary hemostasis (platelets adhere to the damaged endothelium and form a platelet plug) and secondary hemostasis (stabilization of a platelet plug with a cross linked fibrin i.e. the combination of platelet plug formation and clot formation). If the injury to the blood vessel is minor (actually, numerous small vascular holes are produced throughout the body each day), the injury is often closed by a platelet plug (i.e. primary hemostasis), rather than by a blood clot [1-4].

1.1.1 Vasoconstriction

Once rupture of the blood vessel occurs, the damage to the vessel wall itself triggers contraction of the smooth muscle in the wall (vasoconstriction); this

process rapidly decreases the flow of blood from the traumatized vessel. Local myogenic spasm, nervous reflexes, and blood platelets are the factors causing this contraction. Vasoconstriction that perhaps results from local myogenic contraction of the blood vessels is initiated by direct damage to the vascular wall. Nerve reflex is induced by pain nerve impulses or other sensory impulses driving from the ruptured vessel or adjacent tissues. The platelets cause much of the vasoconstriction in the smaller vessels via the release of a vasoconstrictor substance, thromboxane A₂ (TxA₂). There is a direct relationship between the severity of injury and the degree of vascular spasm i.e. the more harshly a blood vessel is traumatized the higher the degree of contraction of the blood vessel is induced. The vasoconstriction period ranges between many minutes to hours. During this period, the processes of platelet plug formation and blood coagulation can happen [1-5].

1.1.2 Platelet plug

Prior to the vascular injury, platelet activation is inhibited by the endothelial cell-derived inhibitory factors. These include prostaglandin PGI₂ (prostacyclin), nitric oxide (NO), and CD39, an ADPase on the surface of the endothelial cells that can cleave small amounts of ADP (adenosine diphosphate) that might otherwise cause improper platelet activation. Following vascular injury, the formation of a firm platelet plug occurs in three stages: initiation, extension, and stabilization (**Figure 1.1**). Initiation (also known as initiation of platelet activation or adhesion stage) happens upon damage to the endothelial monolayer when Von Willebrand factor (VWF) binds to the exposed collagen of the injury site via A₃ domain and becomes a

strong adhesive substrate. VWF, a multimeric adhesive glycoprotein, is present in plasma and formed in the endothelium cells, platelet α -granules, and connective tissue of the sub-endothelial layer; its function is involvement in hemostasis. As described below in detail, VWF can bind to platelet GPIb (Glycoprotein Ib, or known as CD42, forms a complex with gpV, and gpIX, producing GPIb-V-IX receptor complex on the platelet surface) on the surface of unactivated and activated platelets in the initiation and activation stage respectively. VWF can also bind to glycoprotein IIb/IIIa (GPIIb/IIIa, also known as integrin α IIb β 3) on the surface of activated platelets in the activation stage as mentioned below in detail [5-10].

Two processes generate the adhesion stage. The first is direct binding of GPVI (FcRy) receptor of unactivated platelets to the exposed collagen. The second is interaction between GPIb-V-IX on the platelet surface and the A1 domain of VWF; the exposed collagen helps as a binding site for VWF, and therefore contributes to the adhesion of unactivated platelets through GPIb-V-IX. The interaction of VWF to GPIb-V-IX receptor is also necessary for the firm adhesion of platelets via enabling GPVI to intensely bind to the collagen [9, 11]. Extension, also termed as activation stage or the stage of growth of the thrombus via autocatalytic signaling, occurs beyond the first monolayer of platelets adherent to the collagen/ VWF [10,12]. The addition of the subsequent layers of platelets to the growing thrombus is intensely enhanced by the activity of locally released agonists like TxA2 and ADP, as well as by the activity of the locally formed thrombin. These agonists play an important role in this step and activate platelets via mechanisms related to specific G-Protein Coupled Receptors (GPCRs) on the platelet surface. Upon platelet

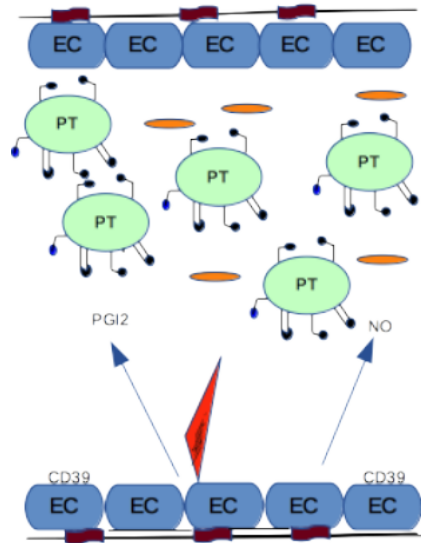
activation, ADP is liberated from the dense granules of platelets attached to the VWF or the exposed collagen. P2Y1 and P2Y12 are the primary receptors for ADP, existing on the surface of platelets likely to be activated [8, 13, 14]. P2Y12 is the target of clopidogrel, the commonly used anti-platelet drug [15]. Following activation of platelets by ADP, Ca^{2+} mobilization activates phospholipase A2 (PLA2), which in turn converts membrane phospholipids to arachidonic acid. TxA2 is synthesized from arachidonic acid by the aspirin sensitive cyclooxygenase (COX-1) enzyme and released from activated platelet membrane phospholipids [16].

TxA2 can diffuse across the membrane and activate adjacent platelets. TxA2 causes Ca^{2+} mobilization, phosphoinositide hydrolysis and protein phosphorylation [17]. The local generation of thrombin (factor IIa) is accelerated by the activated platelets that provide a surface on which clotting factor complexes can be assembled. In addition, thrombin, a potent platelet agonist bound protease-activated receptors (PARs) [18], causes fast mobilization of intracellular Ca^{2+} followed by activation of PLA2 and thromboxane generation [17]. After activation of agonist receptors, downstream intracellular signaling stimulates and activates integrin $\alpha\text{IIb}\beta3$ (GPIIb-IIIa) and $\alpha2\beta1$ (GPIa/IIa) [18]. Activated $\alpha2\beta1$ causes binding of the activated platelets to the exposed collagen. GPIb-V-IX and activated $\alpha\text{IIb}\beta3$ cause interactions between platelets (cohesion interaction or platelet aggregation). Such an interaction can be formed via bridges formed by VWF, fibrinogen, and fibrin.

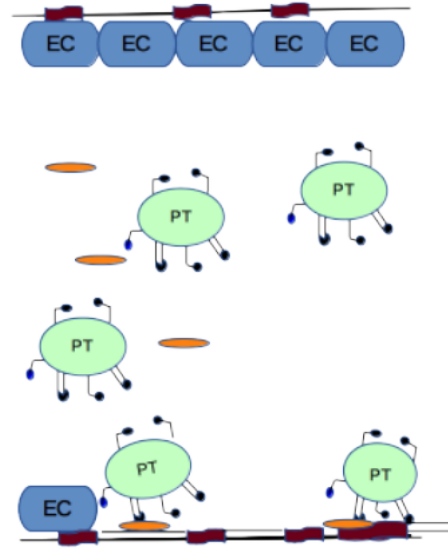
The final stage of platelet aggregation is stabilization. This helps to maintain

the platelet plug and prevents premature disaggregation. This is possibly made by the close communications between platelets that can occur only once platelet aggregation begins. Examples of such a communication include outside-in signaling through integrins. The net product is a hemostatic plug composed of the activated platelets fixed within a cross-linked fibrin mesh that is a structure stable enough to resist the shear forces generated by flowing blood in arterial circulation [8, 13, 14].

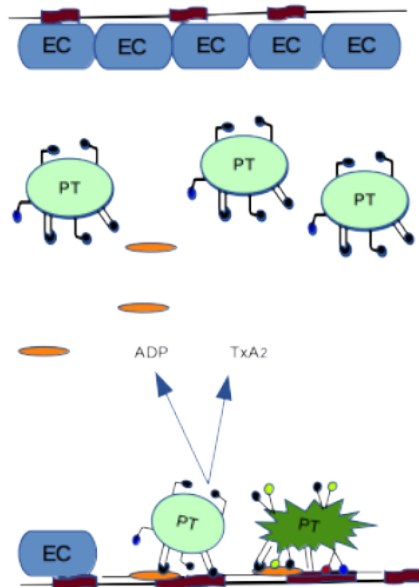
A. Injury



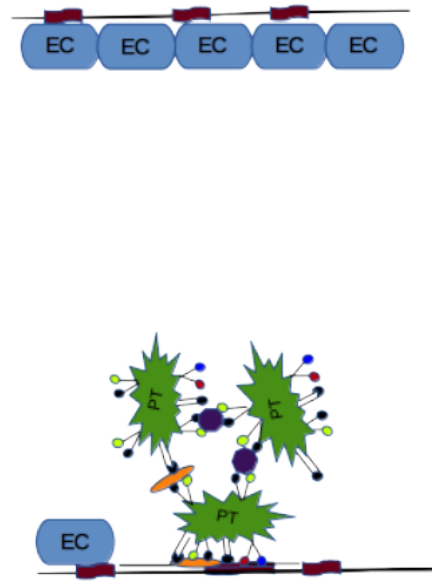
B. Initiation



C. Extension and activation



D. Stabilization



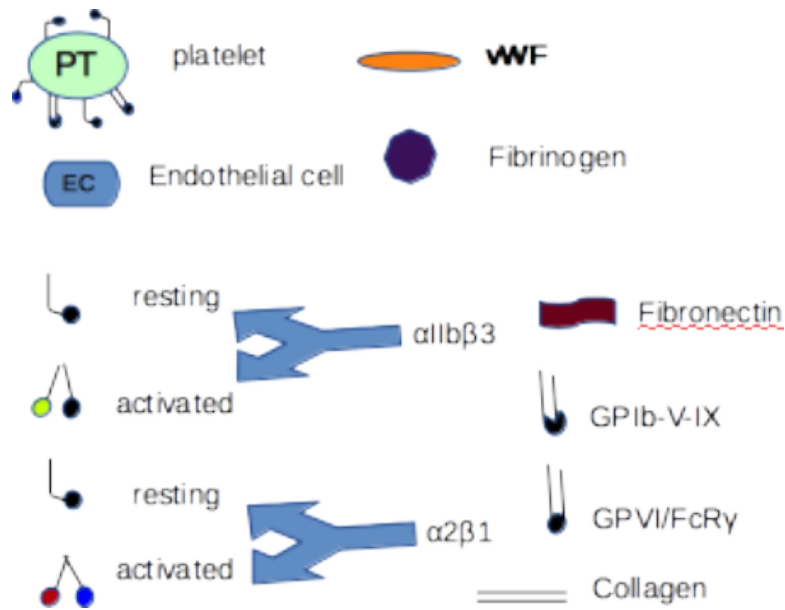


Figure 1.1 Stages of platelet aggregation. (A) Injury: before vascular injury, platelet activation is hindered by endothelial cell-derived inhibitory factors. These include prostaglandin PGI₂ (prostacyclin), nitric oxide (NO), and CD39, an ADPase on the surface of endothelial cells that can cleave trace amounts of ADP that might, if not, cause improper platelet activation. (B) Initiation: the growth of the platelet plug is initiated by the collagen-VWF complex that captures and activates moving platelets. Platelets adhere and spread, forming a monolayer. (C) Extension: the platelet mass is extended when extra platelets are activated via the release or secretion of TxA₂, ADP, and thrombin. Activated platelets stick to each other via bridges formed by fibrinogen, fibrin, or VWF (D) Stabilization: finally, communication between platelets helps to maintain and stabilize the platelet plug.

1.1.3 Blood coagulation

1.1.3.1 Extrinsic pathway

The extrinsic system (tissue factor pathway) plays a fundamental role in the initiation of fibrin formation[4]. The extrinsic pathway can be activated when the traumatized tissue releases a complex factor called tissue factor. Tissue factor (also called factor III, thromboplastin, or CD142) is a glycoprotein

expressed under physiological condition in the vascular tissue, for example, in the smooth muscles of sub-endothelial tissue. Under pathological condition, it can also be synthesized in both non-vascular tissue such as leukocytes or vascular tissue such as endothelial cells [19-25].

When TF becomes exposed to the blood at the site of injury, it has a high affinity for the blood-circulating factor VII (FVII) [19-25]. Factor VII is one of the vitamin K-dependent proteins (including factors IX and X, prothrombin and protein C) that is secreted by hepatocytes and contains a γ -glutamyl carboxyl acid at the N-terminus that allows these molecules to bind to calcium ion and subsequently assemble on a phospholipid surface; this process helps catalytic reaction proceed [26]. TF comes into contact with the circulating activated factor VII (FVIIa), resulting in the TF-FVIIa complex (**Figure 1.2**). Alternatively, TF can bind to inactive factor VII and form the TF-FVII complex, which is converted to TF-FVIIa by FVIIa or previously formed TF-FVIIa [25, 27]. The TF-FVIIa complex activates factor IX, which in turn activates factor X; alternatively, factor X is directly converted to factor Xa by TF-FVIIa [25, 26, 28, 29]. The reaction of the activation of both factor IX and factor X is catalyzed by Ca^{2+} ions. When there is low concentration of TF in the traumatized area, the activation of FX progresses through the activation of factor IX (FIXa) by FXI and factor VIII (FVIIIa) by IIa [30]. Once activated, FXa forms a complex with the activated factor V (FVa) in a reaction catalyzed by Ca^{2+} and phospholipids[31]. This complex, called prothrombinase, is responsible for the conversion of prothrombin to thrombin [32]. In the production of thrombin, FVa contributes as co-enzyme [33]. When thrombin is generated, it can also be a factor in the activation of the coagulation Factor V

[34, 35]. The generation of thrombin is followed by conversion of fibrinogen to fibrin. Thrombin is also involved in the activation of FXIII (FXIIIa), an enzyme responsible for the formation of covalent cross-links between two adjacent fibrin monomers to form a polymerized fibrin mesh. In the presence of Ca^{2+} ions, this coagulation factor can be activated by thrombin [36]. A variety of enzymes including factors IXa, Xa, XIIa, and thrombin have been shown to activate VII and this makes the cascade strongly self-amplifying [37]. Most of these reactions happen in the presence of and Ca^{2+} phospholipids [38]. Due to the presence of several inhibitors, like lipoprotein-associated coagulation inhibitor (LACI) or extrinsic pathway inhibitor (EPI), the extrinsic pathway has short life [20, 39]. In this case, the generation of FXa occurs through FIXa following the stimulation of intrinsic pathway.

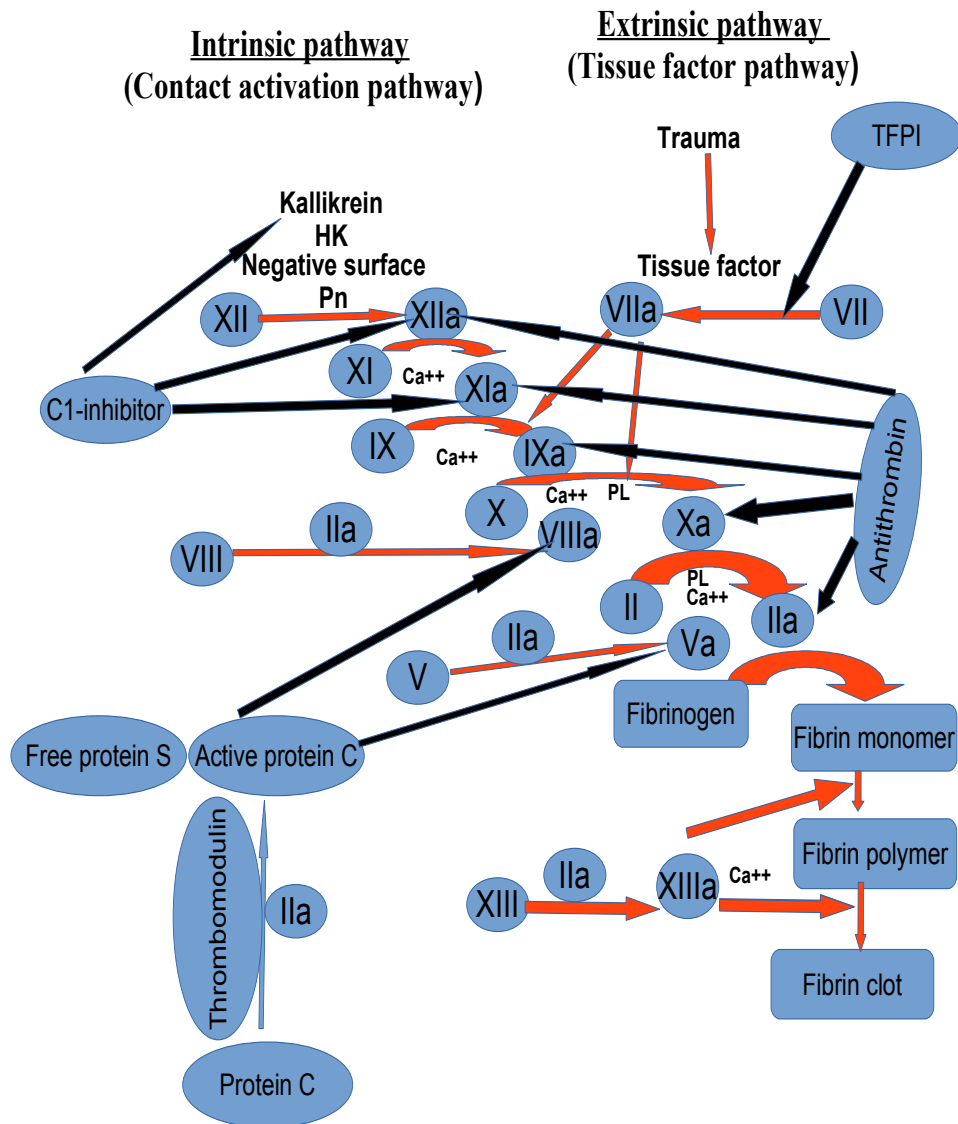


Figure 1.2 Schematic diagram of the coagulation and fibrinolysis pathway. The intrinsic cascade is mostly initiated when contact is made between blood and an exposed negatively charged surface. The extrinsic pathway is initiated upon vascular injury leading to exposure of tissue factor, TF. The two pathways unite at the activation of factor X to Xa that is termed as the common pathway. The final product of the common pathway is fibrin polymer. The red arrows mean activation; the black arrows mean inhibition.

1.1.3.2 Intrinsic pathway and contact activation

The “intrinsic” ability of plasma liquid to solidify when placed in a glass tube or in contact with negative surfaces (glass, clay, kaolin) generates the intrinsic pathway [40]. Under physiological conditions, the intrinsic pathway is much less significant to hemostasis than is the extrinsic pathway. However, abnormal conditions such as bacterial infiltration and hyperlipidemia can cause activation of thrombosis in the intrinsic coagulation cascade [41]. The intrinsic pathway needs the coagulation factors VIII, IX, X, XI, and XII, prekallikrein (PK), high-molecular-weight kininogen (HK or HMWK), Ca^{2+} and phospholipids [1, 42].

This pathway is triggered by the activation of factor XII zymogen upon contact with the endogenous negative surfaces (described in detail in the section of the activation of FXII). The heavy chain of factor XII binds to the surfaces, causing a substantial increase in the local enzyme concentration by autoactivation. Then, FXIIa cause activation of prekallikrein and factor XI. Subsequently, Factor IX is activated by XIa [42-45].

Kallikrein cleaves HK to liberate bradykinin, a potent stimulus forming a link between the coagulation and the inflammatory pathways. Kallikrein can mutually activate factor XII (explained in detail in the section of FXII function) [42].

Intrinsic pathway can occur as a result of the interaction of FXII with the phospholipids (primarily phosphatidylethanolamine, PE) of the circulating lipoproteins such as chylomicrons, VLDLs, and oxidized LDLs. This is the

mechanism of the role of hyperlipidemia in the enhancement of the prothrombotic state and the development of atherosclerosis [41](**Figure 1.2**).

1.1.3.3 The common pathway

The intrinsic and extrinsic pathways generate factor Xa as a final common pathway; then, it is followed by the conversion of prothrombin to thrombin and, subsequently, the conversion of fibrinogen into fibrin [46] (**Figure 1.2**).

Prothrombin is another vitamin K-dependent zymogen that needs calcium to bind to phospholipid surfaces. Following cleavage by Xa, the N-terminus Gamma-carboxyglutamic acid-rich (GLA) domain of prothrombin is detached and thrombin is generated. Thrombin play an important role in the formation of the hemostatic plug and controls both its own formation and destruction by acting on the numerous substrates including fibrinogen, factors V, VIII, XI, platelet receptors, proteins S and C. In comparison to that generated by factor Xa alone, the prothrombinase complex (factors Xa, Va, phospholipid and calcium) can produce 300,000-fold increase in the generation of thrombin from the localized prothrombin [47]. This indicates that factor Va can play an important role in the generation of thrombin. Activated factor V is possibly released from α -granules of the activated platelets [48] . It is proposed by several studies that when there is a deficiency in FXII, thrombin is the main cause of the activation of FXI. [49, 50] (**Figure 1.2**).

1.1.4 Fibrin formation

Following vascular endothelial injury, the local reactions on the surface of the traumatized area stimulate an immediate activation of platelets, which aggregate at the site of trauma. In the same time, the coagulation pathway is locally activated, generating fibrin mesh. Thrombin binding to fibrinogen releases fibrinopeptides A and B, resulting in the formation of fibrin monomer. Factor XIIIa further converts fibrin monomer to fibrin polymer resisting degradation by plasmin [8, 51, 52] (**figure 1.3**). The polymerized fibrin together with platelets forms a hemostatic plug or clot over the injury site [8, 52]. The fibrin net clamps platelets together and connects them to the vessel wall by binding to the platelet receptors, glycoproteins, and by interacting with other adhesive proteins like thrombospondin and fibronectin. VWF also serves as a bridge between the platelets and the subendothelium collagen via platelet membrane GPIb and α IIb β 3 (mentioned in the platelet aggregation section) [9, 53].

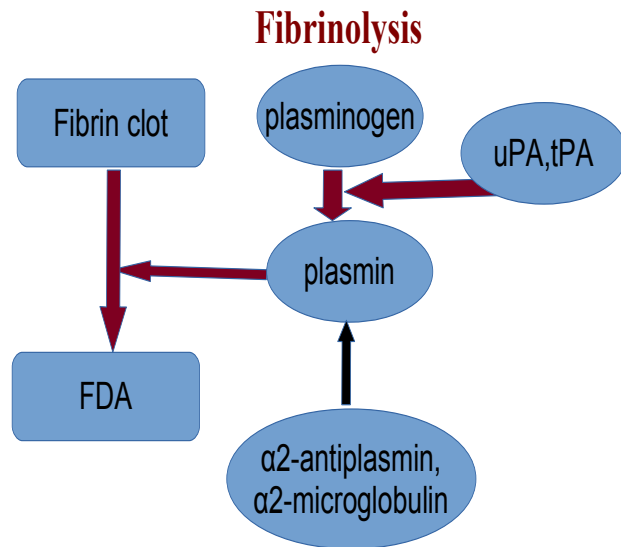


Figure 1.3 Schematic diagram of the fibrinolysis pathway. Following the process of fibrin formation; plasminogen starts to be converted to plasmin dissolving the fibrin clot. HK is high molecular weight kininogen; PK is prekallikrein; PL is phospholipids from activated platelets; Pn is polyphosphate released from the activated platelets. The red arrows mean activation; the black arrow means inhibition.

Numerous mechanisms exist to confine and localize the extent of thrombosis. Firstly, thrombin, in combination with thrombomodulin on the endothelial surface, is a target for protein C. Activated protein C is a potent inhibitor of factor V and factor VIII. Secondly, the shear forces of blood flow tear away the loosely-attached clusters of platelets [54]. Finally, thrombin is efficiently inhibited by the plasma inhibitors like ATIII (antithrombin III) [55] (**Figure 1.2**).

1.1.5 Inhibitors of the coagulation cascade and fibrinolysis system

These are endogenous substances that limit the extent of activation of both coagulation and the fibrinolysis processes; they are also termed as plasma

inhibitors or regulators. The major plasma inhibitors are C1- inhibitor, ATIII and tissue factor pathway inhibitor (TFPI).

C1-inhibitor blocks the autoactivation of FXII zymogen, the capacity of FXIIa to activate prekallikrein and FXI, the activation of HK by kallikrein, and the feedback activation of Factor XII by kallikrein [42, 56].

Antithrombin III (ATIII) is one of the general serine protease inhibitors (serpins) and limits the action of the most active proteases in the coagulation cascade. In particular, ATIII strongly inhibits the action of thrombin [57] and other coagulation factors, like FIXa, FXa, FXIa and FXIIa [4]. The serine of the catalytic triad of thrombin reacts with the arginine of ATIII inhibitory site to form an inactive complex. The affinity of ATIII for thrombin is highly enhanced by binding of ATIII to heparin (a negatively charged sulphated polysaccharide existing on the endothelial surface) [55]. Heparin induces a conformational change in ATIII, thus enhancing the formation of thrombin-ATIII complex. ATIII deficiency is associated with a substantial increase in the risk of thromboembolism [55].

TFPI is mainly produced by the vascular endothelial cells [58]. The endothelial form of TFPI is released into circulation after administration of parenteral heparin or low molecular weight heparin (LMWH) [59, 60] and bound to heparin sulphate, LDL, and platelets. TFPI regulates the function of TF and inhibits TF:FVIIa complex [61].

Plasmin is present in liver cells in the form of its zymogen, plasminogen. When plasminogen binds to blood clots or cell surfaces, it can be converted to

active plasmin by the action of the different enzymes, tissue plasminogen activator (tPA), urokinase plasminogen activator (uPA), kallikrein, and factor XII. Plasmin is a serine protease that dissolves blood clot and splits fibrin polymer into fibrin degradation products [62, 63].

Activated protein C (APC) is a vitamin K-dependent glycoprotein, circulating in the blood as a zymogen. In combination with protein S, APC inactivates FVa and FVIIIa[64]. Protein C is activated by thrombin in the presence of thrombomodulin cofactor, a single chain glycoprotein located on the surface of endothelial cells [65], and this effect is enhanced in the presence of the endothelial protein C receptor (EPRC) [66].

α 2-Macroglobulin is an inhibitor of several coagulation and fibrinolytic enzymes including kallikrein, thrombin, and plasmin [67]. α 2-Antiplasmin is the primary inhibitor of plasmin and serves to limit the fibrinolytic response till completion of the process of wound healing [68]. Protein C inhibitor is a serine protease inhibitor that can inhibit the action of protein C [69].

1.2 Serine proteases and coagulation FXII

Proteases are categorized into the following broad groups: Aspartic (A), Cysteine (C), Glutamic (G), Metallo (M), Asparagine (N), Mixed (P), Serine (S), Threonine (T), and Unknown (U) proteases [70]. Proteolytic enzymes can be classified into clans based on their catalytic mechanism (arrangement of their catalytic site residues) and in to families according to the identity of their amino acid sequence (sequence homology). Serine proteases constitute more than one third of the known proteolytic enzymes. The serine proteases are

classified into 13 clans and 40 families. The family name originates from the nucleophilic serine in the enzyme active site [71]. Clan PA proteases are extremely present in eukaryotes. Peptidases under subclan PA (S) (family S1) contain the catalytic triad His, Asp (or Glu), and Ser. Subfamily S1A proteases are the trypsins mediating a variety of extracellular processes. FXII is one of the serine proteases, clan PA, subclan PA (S), family S1, and subfamily S1A [70, 71].

1.3 Catalytic mechanism of serine proteases

The steps of the catalytic mechanism of action of serine proteases are illustrated in **figure 1.3**. The protease contains a catalytic triad of serine, histidine and arginine. The histidine can act as a base, proton acceptor, abstracting hydrogen from the serine, which is then rendered nucleophilically reactive. In addition, a so-called oxanion hole is present in the catalytic site, playing a role in substrate recognition (and catalysis). A substrate peptide binds to the surface of the serine protease in such a way that the scissile bond at the P1 position becomes juxtaposed to the catalytic triad of the enzyme, with the carbonyl carbon of this bond positioned near the nucleophilic serine. [72, 73]. A transition state tetrahedral intermediate is produced by transfer of the electron pair on the serine oxygen to the carbonyl carbon and by rearrangement of one of the electron pairs of the double bond. The transition state reforms the carbonyl double bond and the electrons of the N-C bond rearrange to bond with the hydrogen atom on the Histidine of the catalytic triad, breaking the peptide bond. Thus one part of the peptide chain breaks free.

In the second step, the deacylation step, the residual (from the acylation step) carbonyl part, still attached to the serine, is removed and the active site is reproduced. This step is essentially the same as the one above except that water fulfils the role of both the serine and the histidine. Ultimately, the C-terminus of the peptide is released [72, 73].

The backbone NHs of the amino acids, Glycine and Serine, contribute to oxyanion hole formation. These atoms form a pocket of positive charge (these amino acids donate backbone hydrogen for hydrogen bonding) that activates the carbonyl of the scissile peptide bond and stabilizes the negatively charged oxyanion of the tetrahedral intermediate (when the tetrahedral intermediate is formed, the negative oxygen ion, having accepted the pair of electrons from the carbonyl double bond fits completely into the oxyanion hole) [72, 73].

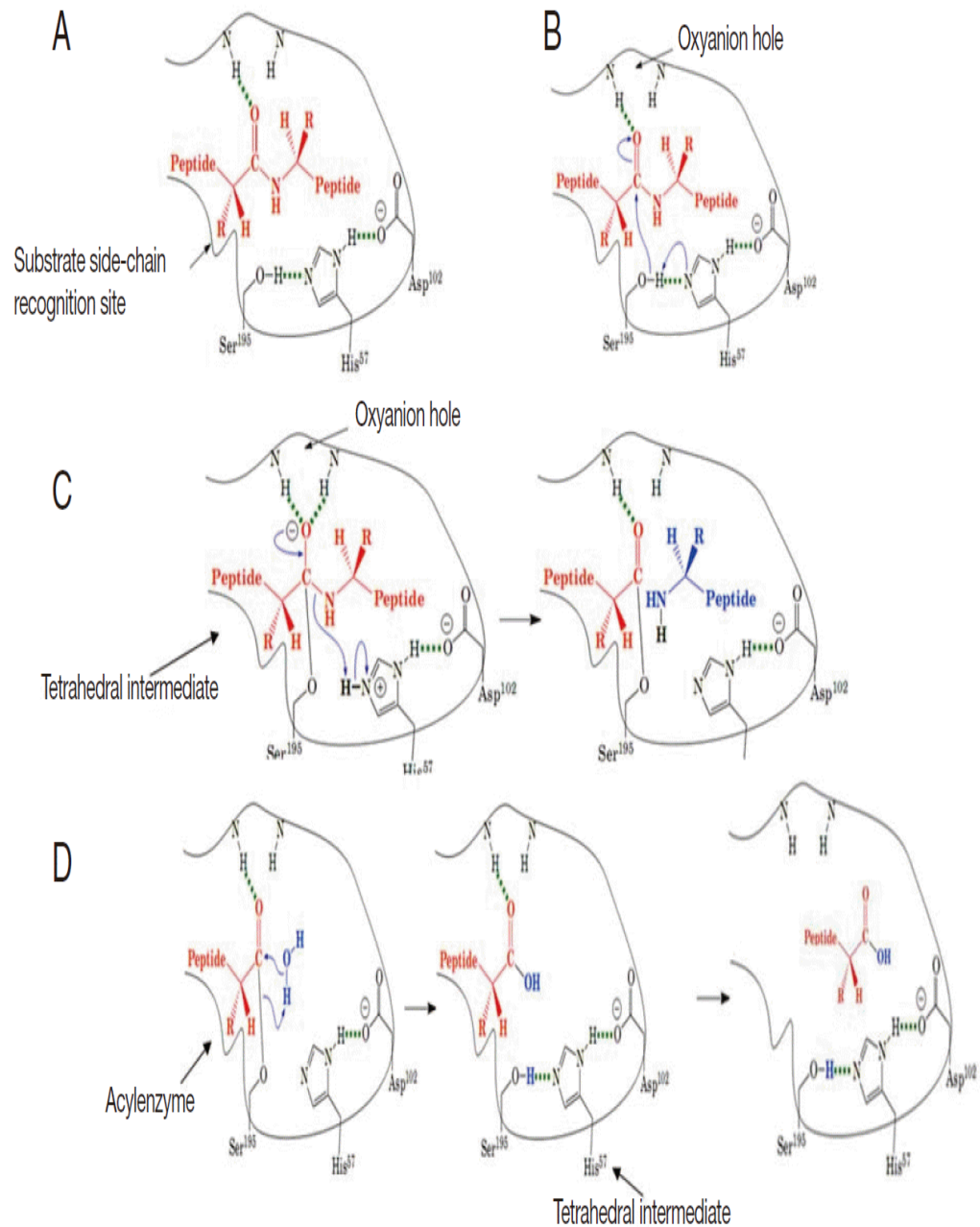


Figure 1.4 A diagram of the general catalytic mechanism for serine proteases. (A) Substrate binding: a substrate binds to the recognition site of the serine protease and exposes the carbonyl of the scissile amide bond. (B) Nucleophilic attack: the His attracts the proton from the hydroxyl group of the Ser and the Ser attacks the carbonyl of the peptide substrate. (C) Protonation: The amide of peptide substrate accepts a proton from the His and dissociates. (D) Deacylation: water molecule attacks the acyl-enzyme complex and catalytic triad is restored. This figure is adapted from Yang et al [72].

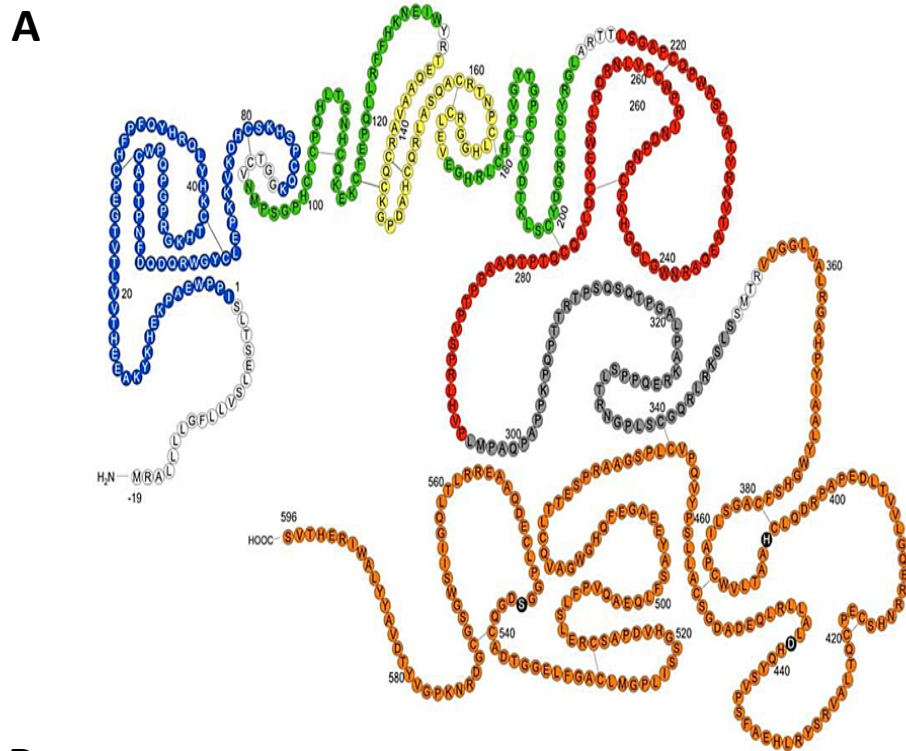
1.4 Structure and function of the domains of human coagulation factor XII (Hageman factor)

Human factor XII (FXII or Hageman factor) is a serine-protease and a coagulation factor originating from a single gene on chromosome 5. Its gene is 12kb and consists of 13 introns and 14 exons. FXII is produced by the liver and circulates in plasma as a single-chain zymogen. It is structurally similar to EGF (epidermal growth factor), single chain urokinase, and tissue plasminogen activator by having two domains homologous to EGF like domain, as described in detail below [74].

FXII zymogen has a molecular weight of 80 kDa and is composed of non-catalytic domains of 353 amino acid residues (Mr 52 kDa) and a catalytic domain of 243 amino acid residues (Mr 28 kDa). The proline-rich domain (the last non-catalytic domain) ends with Arg353 while the catalytic domain starts from Val354 and ends with Ser596. In addition to Arg353-Val354 linkage, the proline-rich domain is connected to the catalytic domain by a disulphide bond located between amino acid residues Cys340 and Cys466 [75-78] (**Figure 1.5**).

α -FXIIa is an activated form of FXII, having the same molecular weight, 80 kDa, as FXII zymogen has. In this active form, the bond between Arg353 and Val354 is broken. Thus, it is composed of two chains, heavy chain (it denotes non-catalytic domains of the zymogen) and light chain (it denotes the catalytic domain) (**Figure 1.5**). β -FXIIa, another activated form of FXII, is also composed of a heavy chain of 28 kDa molecular weight (represents the light chain of the original enzyme, α -FXIIa) and a light chain of 2000 Da molecular

weight (represents 9 amino acids of the proline-rich region, last region of α -FXIIa heavy chain). In addition to a disulphide bond that holds both the L-chain and H-chains together, β XIIa has also six extra internal disulphide bonds within the heavy chain [75-78] (**Figure 1.5 and 1.6**).



B

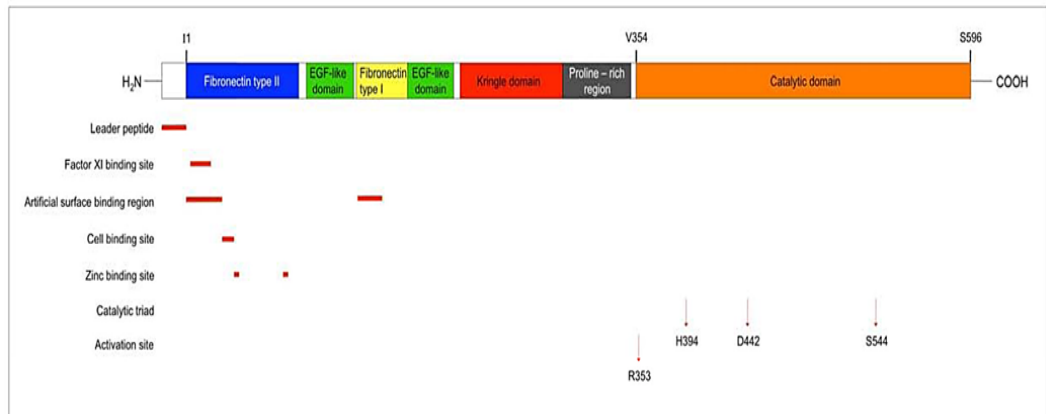


Figure 1.5 Functional structures of FXII domains. **A** is the full-length zymogen composed of 596 residues plus the leader peptide. Amino acids 1–353 represent heavy chain. The different colours of sequences represent the various domains of heavy chain. The longest domain is light chain consisting of residues 354–596. Both light chain and heavy chain are linked by a disulphide bond between Cys340–Cys466. **B** is the linear, coloured diagram indicating each of the regions on the FXII zymogen. This figure is adapted [75-78].

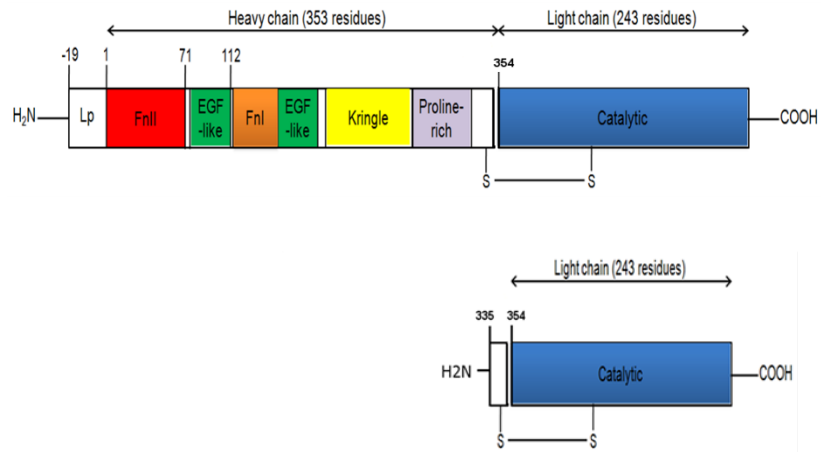


Figure 1.6 Coloured presentation diagrams of α -FXIIa and β -FXIIa. Top linear diagram is α -FXIIa (HFa, factor XIIa, XIIa HMW). It has the same domains and number of residues (Mr 80 kDa) as full-length zymogen has. The bond between Arg353 and Val354 is broken. It exists as a two-chain protein linked by a disulphide bond between Cys340 and Cys466. Bottom linear diagram is β -FXIIa (Hageman factor fragment, HFf, FXIIIf, β -HFa, XIIa LMW). It is composed of the catalytic chain (243 amino acids) and a peptide of 9 amino acids Asn335 -Arg343 of proline-rich region. The disulphide bond is still present between the two regions.

1.4.1 Heavy chain of Hageman factor (FXII)

Heavy chain of FXII consists of numerous domains [76, 77]. From N-terminus to C-terminus, these domains are leader peptide, fibronectin domain type II, epidermal growth factor-like (EGF-like) domain, fibronectin domain type I, EGF-like domain, kringle domain, proline-rich region. Apart from the proline-rich region special to FXII, the domains are analogous with those found in other serine proteases. The N-terminal region of α -FXIIa heavy chain shows strong homology with tissue type plasminogen activator (tPA) as both of them have fibronectin type I, EGF-like and Kringle domains. The leader peptide is the shortest region composed of residues -19 to 1. Other regions are described in detail in the following subsections.

1.4.2 Fibronectin domain

From N-terminus to C-terminus, FXII has two kinds of fibronectin domains; these are fibronectin domains type II and type I. Fibronectin domain type II is composed of residues 1-88 of heavy chain. Structural and functional studies of human FXII by means of recombinant deletion mutants established that the N-terminus of FXII comprises a binding site for negatively charged activating surfaces [74]. The artificial surface-binding properties of factor XII is thought to be due to the collagen-binding site present in the fibronectin type II [79]. A subdomain of residues 1–28 within fibronectin type II domain was further identified as a binding site for negatively charged surfaces [80, 81].

A subdomain of residues 3–19 within the fibronectin type II domain functions as a binding site for coagulation factor XI (FXI) [82]. FXII has also two documented zinc binding sites in this fibronectin type II region, residues 40–44 and 78–82 [83]. FXII can attach to the cell surface via the fibronectin domain only when the local zinc ion concentration is adequately high [84]. It has been established that FXII can interact with platelets, endothelial cells and neutrophils [85, 86].

FXII can bind to the GPIb-V-IX complex present on platelets by means of fibronectin region [85, 86]. In vivo, collagen-activated platelets can appropriately release zinc ions helping the interaction between FXII and the platelets happen [84]. On the endothelial cells, FXII interacts and co-localises with the receptors, cytokeratin 1, uPAR (urokinase plasminogen activator), and gC1q-R (receptor for the globular heads of C1q or p33 or hyaluronan-binding protein); it is also established that these receptors are likely to be HK-

binding targets. [87, 88]. There is a sequence of nine residues (39-47) in the fibronectin type II domain that could interact with both artificial and endothelial cell surfaces [89]. It is found that there is a uPAR-binding area on the cell surface for FXII; this binding region is identical to the one single-chain urokinase, high-molecular-weight kininogen and vitronectin bind. Residues 39–47 on fibronectin type II can bind to human umbilical vein endothelial cells (HUVEC) [84]. The positively charged amino acid sequence, 39–47, in the fibronectin type II domain is responsible for binding of FXII to the negatively charged surfaces [90]. The sequence could be a promising target for hindering the activation of FXII. Contribution of zinc, as a divalent cation, to FXII activation is due to its role in binding of FXII to the cell surface that causes conformational change of FXII [74, 83, 91].

Fibronectin type I domain composed of residues 133–173. Although its particular function is unknown, but it possesses a subdomain of amino acids 134–153, which has been considered to contribute to surface binding. [92, 93]. Besides, the domain owns a binding sequence for both heparin and fibrin [79].

1.4.3 Epidermal growth factor- like domains

EGF (or epidermal growth factor) regulates growth, proliferation and differentiation in the mammalian cells by binding to EGFR and stimulating DNA and protein synthesis [94]. The mechanism of EGF action is phosphorylation of the tyrosine residues in the intracellular proteins [95]. FXII has two domains homologous to the EGF-like sequence recognized in many proteins such as tissue plasminogen activator (tPA), single chain uPA, transforming growth factor type 1 and a number of coagulation factors [96].

These two domains are EGF-like region 1 and EGF-like region 2 that are composed of residues 94–131 and 174-210 respectively. EGF-like region 1 can behave as a zinc-binding site whereas a subdomain and residues 146-174 within EGF-like region 2 can possibly act as an artificial surface binding site and zinc-binding site respectively [74, 83, 91].

1.4.4 Kringle and proline-rich region

The Kringle domain is found in the proteases, FXII and urokinase plasminogen activator. The kringle domain of the latter has been shown to mediate binding of plasminogen activator to dextran sulphate therefore the kringle domain of FXII may similarly act as an artificial surface binding region [74, 91]. Furthermore, the kringle domain of FXII has 80 amino acid residues and has a subdomain of residues 193–276 that may enhance susceptibility to cleavage by kallikrein [97].

The last peptide sequence in the heavy chain of FXII is proline-rich domain, which consists of residues 296–349; 25% of the residues composed of amino acid proline. This domain is unique to FXII as it is not present in the other serine proteases. Its function is undefined [74, 91],[76].

1.4.4 Light chain (catalytic domain) of FXII

As mentioned above, FXII in the activated state i.e. α -FXIIa has two main chains namely heavy chain (represents the non-catalytic domains of FXII zymogen) and light chain (represents the catalytic domain of FXII zymogen). The light chain is the catalytic domain consisting of 243 amino acids (residues 354–596) and has a molecular weight of 28 kDa [76]. It has residues His394, Asp442, and Ser544 that act as catalytic triad of the active site of FXII.

1.5 Activation of FXII

1.5.1 Activation pathways

Activated FXII, FXIIa, is produced by different pathways. The first way is proteolytic cleavage of FXII zymogen through activation by plasma proteinases such as plasma kallikrein, trypsin and plasmin on cell membranes. In this case, the activation is known as fluid-phase activation or endothelial cell-activation pathway. The second is autoactivation (autoproteolysis, autocatalysis) on the physiological (biological) and non-physiological (artificial) surfaces possessing a negatively charged property. In this condition, the activation of FXII is termed as solid-phase activation [98-101]. The mechanism for FXII autoproteolysis is not completely recognized. There could be a change in the structure of FXII during attaching to the negative surface agents. Nevertheless, crystallographic studies would be the only method to determine the molecular basis for FXII autocatalysis [76]. A study shows that bacteria can elicit both proteolysis and autoactivation of FXII by means of releasing enzymes and negative surface agents (such as endotoxin) [102].

Artificial or non-physiological negatively charged surfaces that cause FXII autoactivation include kaolin, ellagic acid, silicone, sulfatides, dextran sulphate with high molecular weight, bismuth subgallate, dacron, polyethylene and polymers. Biological or physiological materials that stimulate FXII autoactivation include heparins, chondroitin sulphate, phosphatidylserine, phosphatidylglycerol, phosphatidylinositol, phosphatidic acid, fatty acids, endotoxin, sodium urate crystals, calcium pyrophosphate, L-homocysteine, haematin and protoporphyrins [98-101].

Numerous biologic substances, associated with emerging thrombosis, have been shown recently to cause FXII autoactivation [103-105]. These substances include polyphosphates secreted from platelets during platelet activation process, extracellular RNA, misfolded proteins and exposed collagen of blood vessels.

Activation of FXII by kallikrein enhances the rate of kallikrein formation via FXII-PK reciprocal activation loop [87]. Kallikrein is generated by proteolytic cleavage of prekallikrein (PK, Fletcher Factor) by the activated form of FXII, FXIIa. High molecular weight kininogen (HK), heat shock protein 90 (HSP90), and prolylcarboxypeptidase (ProCP) contribute to prekallikrein (PK) activation. PK is usually bound to HK on the cell surface. HK and FXII zymogen interacts and co-localized with the receptors, cytokeratin 1, urokinase plasminogen activator, and gC1q-R (receptor for the globular heads of C1q or p33 or hyaluronan-binding protein) [87], [90] [103-105].

Generation of both fluid-phase activation and solid-phase activation can stimulate each other because in contact activation system, polyphosphates (Pn) released from the intense granules of activated platelets binds to and activate factor XII (FXII) by autoprotolytic mechanism including a conformational change in FXII and production of α -FXIIa. Subsequently, the generated FXIIa can trigger FXII-PK activation loop through stimulation of prekallikrein [90] (Figure 1.7).

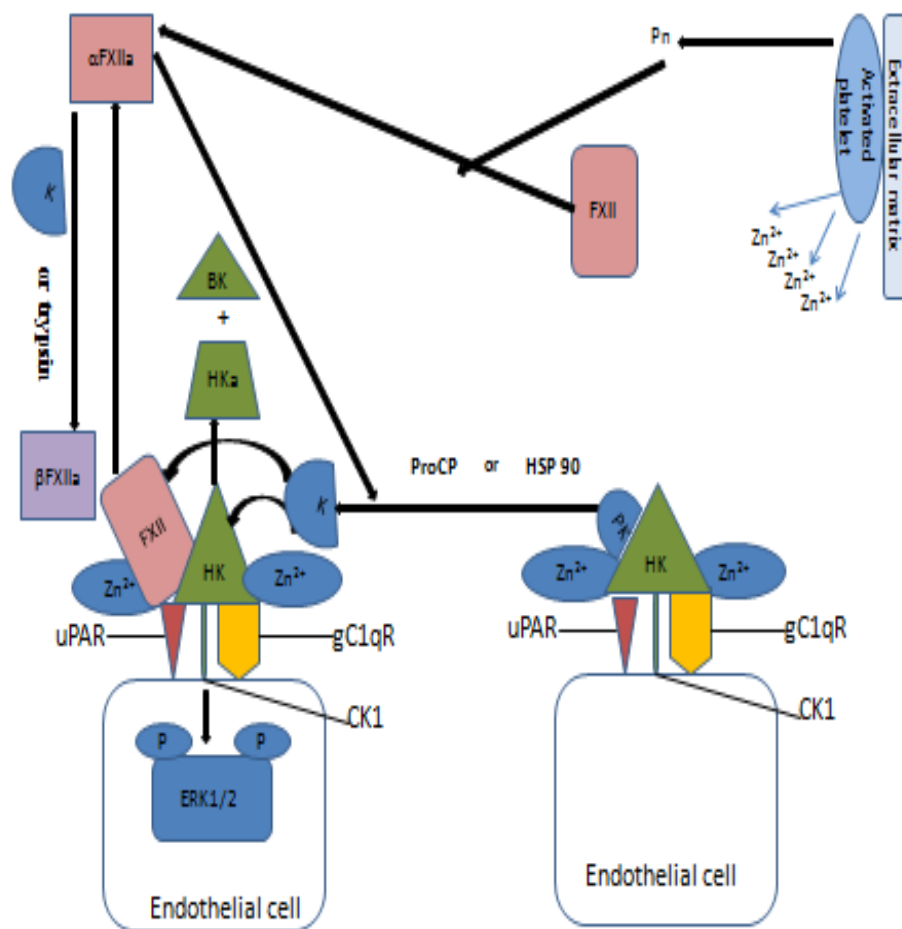


Figure 1.7 Fluid-phase and solid-phase activation pathways of FXII.

1.5.2 Generation of activated forms of FXII

α -FXIIa (variously referred to as HFa, factor XIIa, XIIa HMW) and β -FXIIa (Hageman factor fragment, Hff, FXIIf, β -HFa, XIIa LMW) are activated forms of FXII zymogen. The former is produced after proteolytic cleavage of Arg353-Val354 bond that leads to conversion of the single chain zymogen to the double chain α -FXIIa. The process of proteolytic breakdown is triggered by interaction of FXII zymogen with the negatively charged surfaces (either artificial or biological cleavage), kallikrein, plasmin, FXIa, FXIIa, and trypsin. Cleavage of α -FXIIa is produced by kallikrein or trypsin at Arg 334 and Arg 343, generating β -FXIIa enzymatically much more active than α -FXIIa. β -FXIIa is unlikely to react with the negatively charged surfaces [76, 106].

1.5.3 Role of zinc cation in the activation pathways

There is much to be said for the role of the divalent metals in FXII activation. The effect of Zn^{2+} on Hageman factor is attributable to the cooperative binding of, at least, four Zn^{2+} to FXII. The proenzyme of FXII contains four Zn^{2+} binding sites; α -FXIIa has only three and β -FXIIa has none. These sites are either composed of two His residues plus one Asp/Glu residue or composed of two His residues only. Modification of Asp/Glu residues results in the loss of one and two Zn^{2+} binding sites in α -FXIIa and the zymogen respectively, proposing that two of the four Zn^{2+} binding sites in FXII consist of two His residues only. The remaining two regions comprise two His residues and one Asp/Glu residue. One of these binding sites is lost when factor FXII zymogen is activated to α -FXIIa and all are lost when α -FXIIa is converted to β -FXIIa.

In addition, Alteration of the His amino acids leads to complete loss of four Zn^{2+} binding sites. Two of the sites are anticipated to be located at positions His40-His44 and His78-His82 [83]·[107].

Regarding its function in the autoactivation process, Zn^{2+} is expected to be necessary for modulation or conformational change of FXII [108]. This indicates that the autoproteolysis of FXII on the negatively charged surfaces, for instance phospholipids and sulphates, needs Zn^{2+} as cofactor. Hence, a specific Zn^{2+} chelator might be a promising pharmacologic approach to regulate phospholipid-mediated FXII activation. However, the interaction between FXII zymogen and sulfatides is independent of this divalent cation. [90].

Zn^{2+} also plays an indirect, important function in the fluid-phase activation (or endothelial cell activation pathway). The mechanism of this action is that ProCP and HSP 90 cause hydrolysis of PK attached to the endothelial cells in a Zn^{2+} -HK dependent manner [90]. The result of this proteolysis is generation of kallikrein. It is then followed by kallikrein- dependent FXII zymogen activation. This process also occurs in the presence and co-localization of the cofactors, HK and Zn^{2+} , when FXII is bound to the cell membrane. It is found that FXII can attach to the cell membrane (involving endothelial cells) only when the local Zn^{2+} concentration is sufficiently high. The source of this cation is collagen-activated platelets [84]. FXII binding to the endothelial cell membrane is highly regulated by the plasma concentration of HK and Zn^{2+} . Once bound, FXII can stimulate ERK1/2 (extracellular-

signal-regulated kinases 1/2) phosphorylation and thymidine uptake as well (Figure 1.7). [109]

1.6 Pathophysiological role of FXII

1.6.1 Noncoagulation-related role

Activated form of FXII, α -FXIIa, has multiple functions through generation of kallikrein from prekallikrein in the presence of high molecular weight kininogen (HK) as illustrated in (Figure 1.8). Kallikrein has certain substrates helping various physiological and biochemical functions take place. First of all, cleavage of HK by kallikrein causes liberation of a short-lived nonapeptide, bradykinin. Bradykinin, a potent inflammatory mediator, can cause angiogenesis, inflammation, increased vascular permeability and inherited angioedema. The mechanism of induction of vasodilatation, vascular leakage, and pain sensations is activation of bradykinin B2 receptor, which is a G-protein coupled receptor. In addition, bradykinin can generate tissue plasminogen activator (tPA) that causes fibrinolysis [98]. Profibrinolytic activity of FXIIa has been reported via direct activation of plasminogen [110].

Another peptide generated from breakdown of HK by kallikrein is activated HK (HKa). HKa exerts converse effects; it has anti-infection, anti-angiogenesis, and anti-kallikrein-kinin system (KKS) properties. Both BK and HKa protect injured/dysfunctional tissues in a cooperative mode, allowing the wounded tissues to repair [111].

A study shows that FXII zymogen also stimulates angiogenesis independent of autoactivation and formation of FXIIa [109]. The mechanism of its angiogenic effect on the endothelial cells is explained as below. FXII zymogen reacts with a domain (domain2) of uPAR on the human umbilical vein endothelial cells (HUVEC) membranes. Following stimulation of uPAR by FXII zymogen, the message of cell activation / angiogenesis of uPAR to the cell through β -integrin receptor is initiated. EGFR is also involved in the cell activation through uPAR and β -integrin. These mechanisms elicit ERK1/2 and Akt phosphorylation. Communication between ERK1/2 and Akt occurs. These pathways trigger cell proliferation and angiogenesis. Due to its proliferative effect, FXII may become a pharmacological target to promote cell repair after injury [109].

Moreover, kallikrein by itself activates major components of the complement system, C3 and C5, that can then activate both conventional and alternative complement activation pathways [98].

FXIIa has been shown to cause neutrophil accumulation and release of elastase by degranulation process of these cells. The catalytic activity of FXIIa is necessary for this effect. FXIIa active site inhibitors, D-Pro-Phe-Arg-CH₂Cl and corn Hageman factor inhibitor, have been shown to eliminate this effect. FXIIa controls the expression of Fc γ RI (fragment crystallisable gamma receptor I, CD64, IgG receptor) of the monocyte by down regulation of these receptors without disturbing its affinity. This effect could impair the clearance of the immune complexes. The site on FXIIa responsible for the reduction in Fc γ RI may be within the N-terminal 18 amino acids. This indicates that this

reaction necessitates the heavy chain but not the catalytic device, meaning that it differs from the effect of FXIIa on the polymorphonuclear leukocytes that needs the catalytic triad [110]. Monocyte synthesis and secretion of IL-1 and IL-6 can be induced by factor XII [110]. Lipopolysaccharide-stimulated discharge of these interleukins is also potentiated by FXII. FXII zymogen and its activated form, α -FXIIa, are mitogenic in human liver carcinoma cells (HepG2, hepatocellular carcinoma) [112, 113]. FXII stimulates MAP kinase in fibroblasts and Hep G2 cells [113, 114].

β -FXIIa, liberated from α -FXIIa by the action of kallikrein or trypsin, can elevate blood pressure, heart rate and cardiac tonicity by activation of the sympathoadrenal system in the presence of bradykinin or kininogen [98]. β -FXIIa is a positive inotropic agent; it can raise systolic blood pressure more than diastolic with associated increase in heart rate [115]. β -FXIIa can contribute to complement activation by converting the macromolecular C1qrs complex to enzymatically active C1r and C1s [98]. β -FXIIa liberated from α -FXIIa can trigger fluid phase activation of both PK and C1-complex (first complement protein composed of 1 molecule of C1q, 2 molecules of C1r and 2 molecules of C1s) [116, 117].

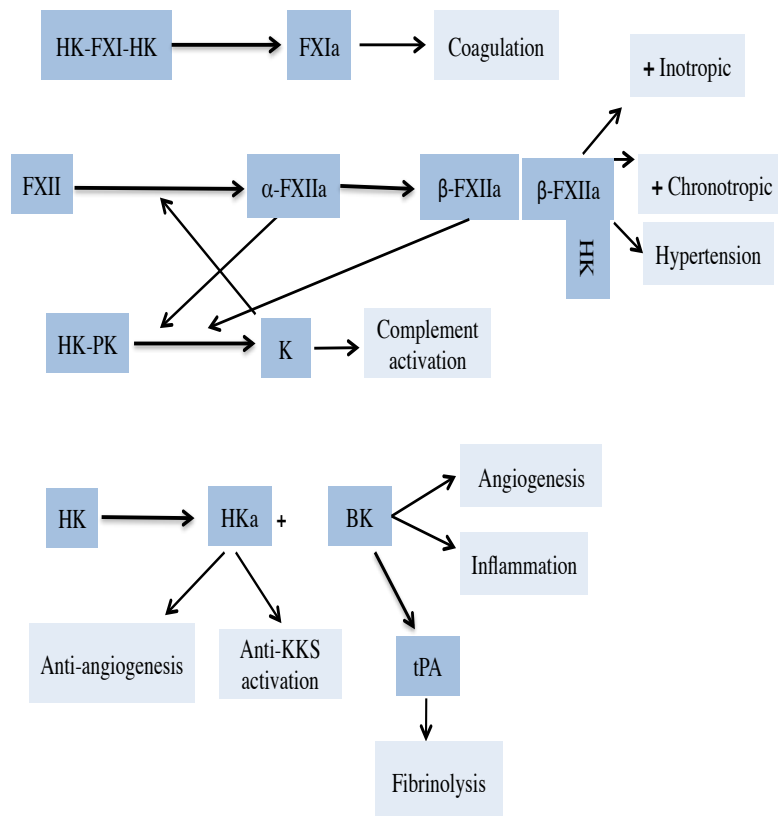


Figure 1.8 Pathway of direct and indirect functions of the different forms of FXII [98].

1.6.2 Coagulation-related role: history of the role of FXII in physiological coagulation and pathological thrombosis

Numerous studies showed that FXIIa activates plasma prekallikrein (PK) to Kallikrein (K), which, then, converts FXII zymogen α -FXIIa in FXII-Kallikrein loop (**Figure 1.8**). In the presence of high molecular weight kininogen (HK), α -FXIIa triggers activation of FXI (FXIa) leading to thrombin generation through a series of reactions (as described in detail in **section 1.1.3**). Without the contribution of FXII, thrombin can independently

activate FXI. FXIa generated through this pathway yields further thrombin, causing a more quickly and stable formation of thrombus. β -FXIIa can stimulate fluid phase activation of coagulation factor VII known as serum prothrombin conversion accelerator [116, 117].

When FXII was discovered by Rantoff and Colopy in 1955, the role of FXII in the process of coagulation and thrombosis has been subject of enormous debate [118]. Hereditary deficiency of factor XII in animals is not associated with bleeding signs and symptoms [119, 120]; for example, vertebrates such as birds or fish have a closed circulatory system and although they lack FXII they do not show bleeding [119, 120]. These findings may suggest that FXII is dispensable for physiological blood coagulation and haemostasis. [90, 121].

The first knockout of FXII was developed in 2004. The study showed that, consistent with their human counterparts, FXII^{-/-} mice have a normal hemostasis. Nevertheless, thrombus formation in FXII^{-/-} mice is largely defective, and the animals are protected from experimental cerebral ischemia and pulmonary embolism [122]. In 2005, Renné et al used the same model to study the contributions of FXII to thrombosis *vivo*. They found that FXII-deficient mice are protected against collagen-induced thromboembolism and thromboembolism induced by a lethal dose of epinephrine whilst not showing extemporaneous or extreme injury-related bleeding [123]. This model created new interest in FXII as a therapeutic target in anti coagulation therapies [121].

There are reports suggesting that FXII deficiency in humans may predispose to thrombosis [125]. Interestingly, hereditary deficiency of factor XII in humans is not associated with clinically relevant bleeding: persons with partial or severe FXII deficiency do not bleed extremely from sites of injury despite an obvious prolongation of the APTT [118, 126].

A study on human carotid thrombi showed that FXII (a) coexist with fibrin(ogen) [127]. Compared to α -FXIIa or FXII zymogen, β -FXIIa has 20-40 times lower affinity for fibrin and /or fibrinogen. α -C-region of fibrinogen has a group of negatively charged amino acids that could serve as a binding site for FXII and α -FXIIa [127]. Both α -FXIIa and FXII zymogen bind to fibrin (ogen) in the same manner, but modifications in fibrin clot structure were only noticed with α -FXIIa. This indicates that both binding and enzymatic activity are involved in α -FXIIa-induced changes in fibrin clot structure. The synergistic combination of direct (via interaction with fibrinogen) and indirect (through enhanced thrombin generation) effects may underlie the action of FXIIa on fibrin structure and function. Thus inhibition of FXIIa-induced solid fibrin clot could be a useful treatment of thrombosis [75-78].

In 2015, a study of population-based cohorts established that FXII single-nucleotide polymorphisms were correlated with lower thrombin generation (TG). Thrombin generation is linked with an increased risk of ischemic stroke. These results of the study support the significance of contact activation pathway-dependent TG as a risk factor for ischemic stroke, and indicate the importance of FXII for TG in this process [128].

Overall blocking of FXII may be a promising and an interesting pharmacological strategy to manage thrombosis; this inhibition is not expected to cause bleeding side effects [90],[129],[130],[131, 132].

1.7 Serine protease inhibitors

The most profoundly studied complex models of protein-protein recognition are serine proteases and their natural protein inhibitors [71, 133-136]. Serine protease inhibitors can be classified into three categories according to their mechanism of action: canonical (standard mechanism), non-canonical inhibitors, and serpins [71, 135, 136].

Canonical inhibitors are composed of 14 to about 200 amino acid residues. They block enzymes based on the standard mechanism of inhibition [137]. Although loops similar to canonical structure exist rarely in non-canonical inhibitors, there is doubt that they can inhibit proteases according to the standard mechanism [138].

Standard mechanism is a non-covalent interaction and substrate-like binding manner between an enzyme and an inhibitor that can occur as a hydrolysis / resynthesis reaction of the P1-P1 prime reactive-site peptide bond [139-142]. The standard mechanism denotes that canonical inhibitors behave as atypical protein substrates, which have a reactive site P1-P1 prime scissile peptide bond situated in the outermost region of the protease-binding loop. The corresponding sub-sites on the protease represent as S1-S1 prime [143]. The part responsible for protease inhibition, the protease-binding loop, in all the recognized structures of this kind of inhibitor, has possibly a similar conformation [135]. The extended, solvent-exposed and convex loop is

complementary to and interacts with the concave, active site of the cognate enzyme; this interaction resembles enzyme-substrate Michaelis complex [135, 142, 143]. However, the complex EI is much more stable than the Michaelis-ES complex; standard inhibition constant (K_i) values 10⁶-10⁹ times lower than K_M values. During interaction, the protease-binding loop of canonical inhibitors is kept in a well-organized conformation [133, 134].

1.8 Corn Hageman factor inhibitor (CHFI)

CHFI is also known as corn trypsin inhibitor (CTI) or popcorn inhibitor. It is a bifunctional serine protease/ α -amylase inhibitor protein of 13.6-kDa molecular weight and 127 residues [144-149]. It was discovered and isolated from corn in 1970 and shown to have inhibitory activity against trypsin [147, 149-151]. Subsequently, in 1980, CHFI was described as an inhibitor against coagulation FXIIa ($K_i = 24$ nM) and for this reason it is also termed as CHFI [145, 146, 152-154]. It is substantiated that CHFI is selective toward FXIIa without interfering the function of FXa, thrombin, and kallikrein. Since then, CHFI has been used as a selective inhibitor of FXIIa to prevent intrinsic pathway (contact activation) in ex vivo plasma studies of prothrombin time (PT), activated partial thromboplastin time (APTT) and thrombin time [152, 153, 155]. From clinical point of view, it is also found that CHFI-coated catheter attenuates catheter-induced clotting in both in vitro and in vivo experiments using rabbits. This finding supports the concept that the prothrombotic activity of catheters reflects their ability to activate FXII; this study identified CHFI coating as a novel approach for making catheters and other blood-contacting medical devices less thrombogenic [149]. In 1984, it

was identified that CHFI mature protein consists of 127 amino acids and has a scissile bond between Arg34 and Leu35. This bond is predicted to involve in the interactions with both trypsin and, presumably, with activated coagulation factor XII (FXIIa) [156]. With reference to the same study, the reactive site has numerous proline residues. Occurrence of proline is rare in the active site regions of serine protease inhibitors. The existence of the proline residues would significantly limit the chain's flexibility. The prolines probably help to conserve the reactive site region in a conformation that is mainly fit for inhibiting the catalytic triad of trypsin (and possibly of factor XIIa). Thereafter, in 1992, a mutagenesis study established that CHFI acts as an inhibitor toward insect α -amylase [157]. Hence, it is better described as bifunctional CHFI because of its capacity for blocking different subgroups of hydrolase enzymes, trypsin and FXII (serine proteases /trypsin family) and α -amylase (α -glucosidases family), through two independent active sites. According to this study, deletion of 11 residues of N-terminus resulted in loss of inhibitory activity, indicating that the N-terminal region of the inhibitor binds to α -amylase. This region, located on the opposite side of the reactive, central inhibition loop, is supposed to interact with the serine proteases, trypsin and possibly FXIIa [145, 146]. For the first time, expression and purification of CHFI was reported in *Escherichia coli* of BL21 (DE3) cells in insoluble form¹³¹. However, the refolded protein was indistinguishable from CHFI isolated from corn in the inhibition of FXII. Afterwards, in 1999, antifungal activities have been reported for CHFI [158-160].

In 1998, the crystal structure of CHFI revealed that the inhibitor has an inhibition loop or central reaction loop (serine protease binding loop

compromising residues 31-38). It also possesses helix A, B, C and D consisting of residues 18-29, 37-49, 56-65 and 88-95 respectively. In addition, residues 66-79 constitute the finger loop. Five disulphide bridges support the stabilization of its structure. A disulphide bond located between Cys20 and Cys55 closes the inhibition loop. This study suggests that the protease-binding loop has a canonical characteristic; the selective inhibitory activity of CHFI for factor XIIa is not due to the specific, atypical conformation of its protease inhibitory site. Arg34-Leu35 contains the scissile bond. Arg34 at the scissile bond is fully exposed and projects away from the body of the protein. As mentioned above, the importance of Arg34 was confirmed in the interaction with trypsin. It was hypothesized that the Arg is also involved in the inhibitory activity against coagulation factor XIIa (FXIIa) (**Figure 1.9**). [136, 156]

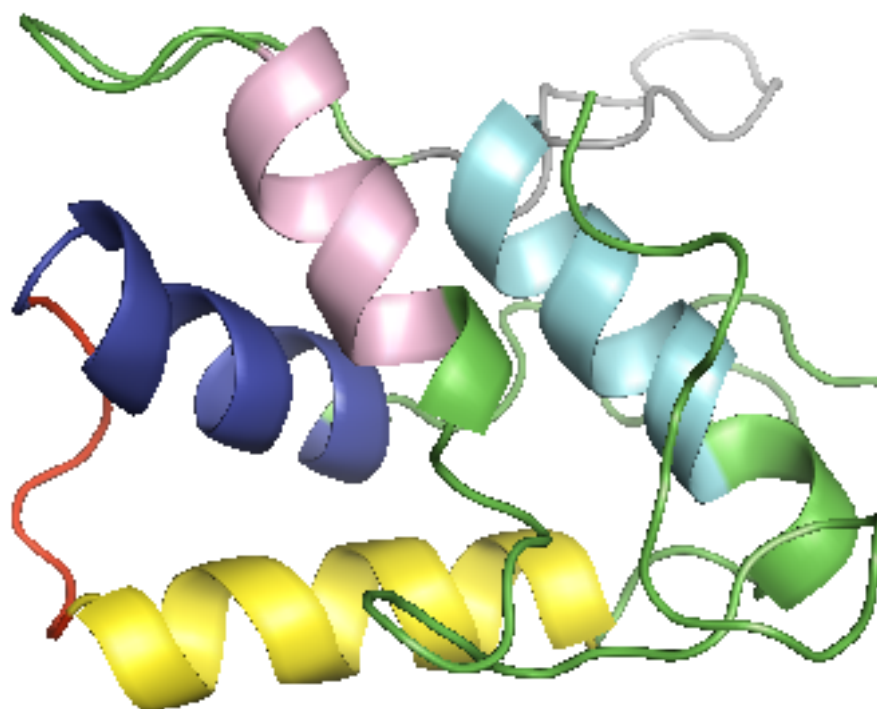


Figure 1.9 Ribbon structure of CHFI crystal structure. The protease inhibition loop (residues 31-38, 8 residues), helix A (residues 18-29, 11 residues), helix B (residues 37-49, 13 residues), helix C (residues 56-65, 10 residues), helix D (residues 88-95, 7 residues), and the finger loop (residues 66-79, 14 residues) are marked with red, blue, yellow, cyan, pink, and grey colours respectively.

1.9 The rationales of development of novel (target and/ or ligand-based) FXII inhibitors versus the currently available anticoagulants

The ideal anticoagulant is suggested to be administered orally, with wide therapeutic window, and a predictable dose response, without the requirement for monitoring of anticoagulant effects, and without bleeding side effects. Arguably, such an anticoagulant does not exist. All the currently existing anticoagulants have some problems associated with them [60].

The conventional anticoagulants, warfarin and heparin, even though effective, need monitoring, dose adjustment, and are unsuitable for long-lasting therapy

due to bleeding side effects. The side effects are due to their broad spectrum of inhibition effect. Thrombin and FXa are inhibited by heparin, whilst vitamin K-dependent clotting factors, factors II, VII, IX and X are inhibited by warfarin [161-165]. Importantly, vitamin K and protamine sulphate are antidotes available for warfarin and heparin, respectively, to be used when excessive bleeding occurs when taking these anticoagulants [166]. More recently, direct thrombin and FXa inhibitors such as dabigatran, apixaban, rivaroxaban, and edoxaban have hemorrhagic side effects, but less so than the classical anticoagulants [167-170]. Compared to the classical anticoagulants, they have another disadvantage in that there are no known antidotes available counteracting their side effects [166]. Hemorrhage most likely to occur due to anticoagulants can be life threatening. Therefore, the necessity for an anticoagulant with no or less bleeding side effects is of particular interest [171].

The development of a specific small molecule FXIIa inhibitor would have numerous advantages. It is proposed to be convenient for chronic administration without the necessity for close monitoring and dose adjustment due to that it will have least or no bleeding side effects compared to the anticoagulants currently available. Hence the development of such a more selective FXII-inhibitor is expected to have an extensive therapeutic index and will improve the efficacy of anticoagulants.

1.10 Aims and objectives

The studies on factor XII-deficient animal models elucidated that this protein is a risk factor for generating stable thrombus triggering obstruction of blood vessels and then loss of blood supply to the brain, which is termed as ischemic stroke. Contrary to other blood coagulation factors, deficiency in FXII is not related to abnormal bleeding in patients or in animals [172],[124] . These findings propose that specific inhibition of FXII could be an attractive medicine and a new method of anticoagulation to treat or prevent pathological thrombosis that could have a lower risk for haemorrhage and a safer anticoagulation profile than the currently available non-selective, broad-spectrum anticoagulants, such as warfarin, or novel direct thrombin and FXa inhibitors [129],[130],[131, 132], [167-170].

Specific inhibition of FXIIa can be mainly achieved from answering the question of the molecular mechanism of selective inhibition of the enzyme by CHF1 and or the molecular mechanism of activation and activity of FXII. This information can be achieved from the structure of CHF1-FXIIa complex and or FXIIa. Unfortunately, both of them have not been recognized yet. Compared to that of the other serine protease inhibitors lacking inhibitory activity against FXIIa, the crystal structure of CHF1 suggested that the protein has no particular, atypical conformation. Lack of information on FXIIa and or CHF1-FXIIa complex created an obstacle in the approach of studies trying to rationalize the reason of selective inhibition of FXIIa by CHF1 and to understand the mechanism of FXIIa function.

Hence, the overall aim of the current PhD work was to pharmacologically investigate into the mechanism of FXII-CHFI interaction and FXIIa function through the following rational directions:

The objective of chapter two was firstly to perform molecular cloning of CHFI, and then, to establish an effective expression and purification system for generating soluble and functional recombinant wild type CHFI, rHIS-GST-CHFI, using BL21 (DE3), origamiTM2 (DE3) cells (*Escherichia coli*) and pCOLD I-GST vector. Lastly, to characterize the construct, its inhibitory activity against FXIIa was evaluated. Numerous rationales were behind performing inhibitory activity assay of rHIS-GST-CHFI in comparison to the commercially available CHFI extracted from corn. The first purpose was to validate proper function and inhibition effectiveness of the protein construct using commercial CHFI as a reference. The second was to validate that the expression and purification is efficient system for generating native type and CHFI mutants (described in the next chapter) in their correctly folded conformation and to substantiate that the storage condition was appropriate for preserving them. The third aim was to ascertain a fundamental inhibition assay that was used as a guide to testing inhibition effectiveness of the CHFI mutants made on the basis of a proper docking model essential for CHFI-FXIIa interaction study.

The objective of chapter three was to investigate into CHFI-FXIIa interaction through the following directions. Guided by the established, efficient expression and single-step purification system for generating soluble and functional recombinant rHIS-GST-CHFI (explained in chapter 2), the first

objective was to generate different recombinant variants of CHF1 with the desired point mutations made on the basis of a proper prediction study for CHF1-FXIIa interaction. The second objective was characterization of the inhibitory activity of the mutant proteins of interest using the established, fundamental inhibition assay of rHIS-GST-CHF1 as a guide. The prediction study of CHF1-FXII interaction was conducted by M Pathak (a research assistant in the structural biology group/ Emsley group) using the following tools: first, the published crystal structure of CHF1 [136,156], second, the crystal structure of FXII zymogen- like protease domain [173], and third, HGFA homology modelling.

The objective of chapter four was to evaluate the pharmacological mechanisms of CHF1 binding to the different forms of human coagulation FXIIa with relevance to the tight-binding assumption. The study structure included different assay strategies comprising preincubation, coincubation and reversibility experiments. Numerous methods for analysis of the kinetic data were also used to validate the results.

In order to investigate into FXII function, the objective of chapter 5 was to examine the effect of Cys466 and the glycosylated peptide fragment of the proline-rich region on the catalytic activity of the protease domain by characterizing the amidolytic activity of the different recombinant variants (FXIIc and FXIIac were generated by M Pathak, a research assistant in the structural biology group/ Emsley group; HISTF- β FXII and MBP- β -FXIIa were generated by R Manna, a PhD student in the structural biology group/ Emsley group) of the protease domain of human coagulation factor FXII.

FXIIc and FXIIac are composed of the catalytic domain having Cys466 substituted by Ser, lacking the peptide fragment of the proline-rich region. At N-terminus, FXIIc has the additional residues, an Arg followed by a Ser. The first goal behind amidolytic activity of these proteins was to evaluate the impact of the deficiency in both Cys466 and the peptide fragment on the function of the protease domain and to examine if they have enzyme-like or zymogen-like behaviour.

The second goal was to examine the autoactivation of these recombinant forms. The third goal was to evaluate the effect of the extra residues at N-terminus on the amidolytic activity of the catalytic domain.

The objective behind the amidolytic activity of HISTF- β FXII and MBP- β -FXIIa was to evaluate the influence of the presence of Cys466 in combination with either the glycosylated or non-glycosylated peptide fragment of the proline-rich region on the catalytic activity of the protease domain. The glycosylated peptide would be existent in MBP- β -FXIIa due to its generation in *Drosophila Schneider S2 cells* whereas it would be absent in HISTF- β FXII as a result of its generation in bacteria.

Chapter 2: Cloning, expression, purification, and characterization of the recombinant wild type CHF1 (rHIS-GST-CHF1)

2.1 Abstract

Corn Hageman factor inhibitor (CHF1) is a bifunctional serine protease / α -amylase inhibitor protein having a molecular weight of 13.6-kDa and 127 residues. It was found that CHF1 is selective toward FXIIa without affecting the function of the other coagulation factors. The aim of this chapter was firstly to perform molecular cloning of CHF1, and then, to ascertain an efficient expression and purification system for generating soluble and functional recombinant wild type CHF1. The last objective was to evaluate the inhibitory activity of the recombinant protein against FXIIa in comparison to the commercially available CHF1.

In the present study, the gene of interest of CHF1 was cloned into the expression vector successfully. The resulting fusion gene encodes a fusion protein having 6xHis tag, factor Xa site, GST tag, HRV3C protease site and CHF1 from N-terminus to C-terminus. An efficient protocol for soluble expression and single step purification of the recombinant CHF1 was identified. rHIS-GST tag as a negative control did not show inhibitory activity whereas the recombinant wild type CHF1 (rHIS-GST-CHF1) showed full inhibitory activity against FXIIa; this confirms that the recombinant protein is as active inhibitor as commercial CHF1 and is properly folded following expression, purification and storage. This also verifies that rHIS-GST tag does not interfere with the molecular interaction between CHF1 and FXIIa and the inhibition effect is completely due to CHF1. Lastly, this assay was used as a

leading assay and a reference guide for the analysis of the inhibitory activity of the mutants against FXIIa in the characterization study of CHFI-FXIIa interaction as explained later in the next chapter.

2.2 Introduction

Corn Hageman factor inhibitor (CHFIs, corn trypsin inhibitor, CTI, or popcorn inhibitor), is a bifunctional serine protease/ α -amylase inhibitor protein having a molecular weight of 13.6 kDa and 127 residues [144-149]. It was discovered and isolated from corn in 1970 and shown to have inhibitory activity against trypsin [147,149-151]. Subsequently, in 1980, CTI was described as an inhibitor against coagulation FXIIa ($K_i = 24$ nM) and for this reason it is also named as CHFIs [145, 146, 152-154]. It is substantiated that CHFIs is selective toward FXIIa without interfering the function of FXa, thrombin and kallikrein. Since then CHFIs has been used as a selective inhibitor of FXIIa to prevent intrinsic pathway. A study in 1998 first reported a protocol for expression of CHFIs in BL21 (DE3) cells of *Escherichia coli*. However, the protein (which included 7 amino acids derived from the vector linker) was insoluble. A refolding procedure was developed and the inhibitory activity of the refolded protein toward FXIIa was indistinguishable from that of the native type CHFIs commercially available [144-149].

The overall aim in this chapter and the next chapter (chapter four) was to investigate into the molecular interaction between CHFIs and human coagulation FXII, which was essential to elucidate selective inhibitory activity of CHFIs against FXII. The aim of this chapter was firstly to perform molecular cloning of CHFIs, and then, to develop an efficient expression and purification system for producing soluble and functional recombinant wild type CHFIs, rHIS-GST-CHFIs, using BL21 (DE3), origami™2 (DE3) cells (*Escherichia coli*) and pCOLD I-GST vector. Lastly, to characterize the construct, its

inhibitory activity against FXIIa was evaluated. There were several rationales behind performing inhibitory activity assay of rHIS-GST-CHFI in comparison to the commercially available CHFI extracted from corn. The first purpose was to confirm appropriate function and inhibition effectiveness of the construct using commercial CHFI as a reference. The second was to verify that the expression and purification is effective system for generating wild type and CHFI mutants (described in the next chapter) in their correctly folded conformation and to verify that the storage condition was appropriate for maintaining them. The third aim was to establish a principal inhibition assay used as a guide to testing inhibition effectiveness of the CHFI mutants made on the basis of a docking model important for CHFI-FXIIa interaction study as described fully in the next chapter.

2.3 Cloning

2.3.1 Materials

2.3.1.1 List of reagents

Almost all the ingredients listed below (**Table 2.1**) were ordered by our structural biology group and stored at appropriate temperature in C84 Lab.

Table 2.1 List of the materials and reagents used in the molecular cloning of CHFI.

| Reagents | Description/uses | Storage T | Provider | or Lab. Prep. |
|--------------------|---|-----------|---------------|------------------|
| Digestion set | Restriction enzymes (NdeI and XbaI), buffer 4, and BSA/ligation | -20 °C | NEB | |
| Quick ligation kit | Ligase buffer | -20 °C | NEB | |
| Luria Broth powder | Tryptone (pancreatic digest of casein) 10 g/, Yeast extract 5 g/L, NaCl 10 g/L. | Lab T | Sigma Aldrich | |
| Agar powder | Gum agar, Agar-agar. Preparation of LB-Agar-ampicillin plate. | Lab T | Sigma Aldrich | |
| Ampicillin powder | Detection of ampicillin resistance | 4°C | | |
| EDTA | Ethylene diaminetetraacetic acid, | Lab T | Sigma Aldrich | |

| | | | |
|------------------------|--|--------|---------------|
| | preparation of TAE buffer | | |
| 1kb DNA ladder | Marker | -20 °C | NEB |
| DNA loading dye | Used to make DNA be visualized. | -20 °C | NEB |
| Sodium acetate 3M | DNA precipitation | Lab T | Sigma Aldrich |
| Isopropanol 100% | DNA precipitation | Lab T | Sigma Aldrich |
| 70% ethanol | DNA precipitation, sterilization | Lab T | Sigma Aldrich |
| SYBR® Green I | Used to stain DNA | -20 °C | Sigma Aldrich |
| Nucleic Acid Gel Stain | | | |
| Tris Base | Tris (hydroxymethyl) aminomethane or 2-Amino-2-(hydroxymethyl)-1,3-propanediol, used for TAE buffer | Lab T | Sigma Aldrich |
| Agarose | Used for analysis of nucleic acids by gel electrophoresis or blotting (Northern or Southern) and is also suitable for protein applications such as Ouchterlony and radial immunodiffusion. | Lab T | Sigma Aldrich |

| | | | |
|-----------------------------|---|-------|---------------|
| 50 TEA (TAE) | Tris base 242 g, Na-acetate 136 g, Na ₂ EDTA 18.6 g, H ₂ O, Adjusting pH to 8.2 with glacial acetic acid, Bringing final volume to 1 L, Filter (optional), used for preparation of agarose gel and running agarose gel electrophoresis. | Lab T | Lab. Prep |
| Sodium acetate 3M | Used for DNA precipitation | Lab T | Sigma Aldrich |
| GenElute™ Extraction Kit | Gel Column preparation solution, Gel Solubilisation Solution, Wash Solution Concentrate G, Elution Solution (10 mM Tris-HCl, pH 9.0), GenElute Binding ColumnG, Collection Tubes, 2 ml | Lab T | Sigma Aldrich |

| | | | | |
|---------------------------|---------|---|--------------|---------------|
| GenElute™ Miniprep Kit | Plasmid | RNase A Solution Solution ,Neutralization/ inding Solution ,Column PreparationSolution ,Opti onal Wash Solution Wash Solution Concentrate , Elution Solution (10 mMTris-HCl, 1 mM, EDTA, pH approx.8.0), GenEluteMiniprep. Binding Columns,2ml Collection Tubes Resuspension solution and neutralization solution | Lysis Lab. T | Sigma Aldrich |
|---------------------------|---------|---|--------------|---------------|

4°C

| | | | | |
|---------------------------|---------|---|--------|---------------|
| GenElute™ Maxiprep Kit | Plasmid | Column Preparation Solution, RNase A Solution, Resuspension Solution, Lysis Solution, Neutralization Solution, Binding Solution, Wash Solution 1, Wash Solution 2 Elution Buffer (10 mMTris-HCl, pH 8.5) GenElute HP Maxiprep Filter Syringe GenElute | Lab. T | Sigma Aldrich |
|---------------------------|---------|---|--------|---------------|

4°C

HP Maxiprep Binding
Column Collection Tubes,
50 mL conical
Resuspension Solution,
Lysis Solution ,
Neutralization Solution

2.3.1.2 pCOLD I-GST subcloning vector (expression vector)

pCold I cold-shock vector is a vector for high-level expression and purification of soluble proteins in *E. coli*. The vector is modified to include a glutathione S-transferase (GST) tag (**Figure 2.1**) [174].

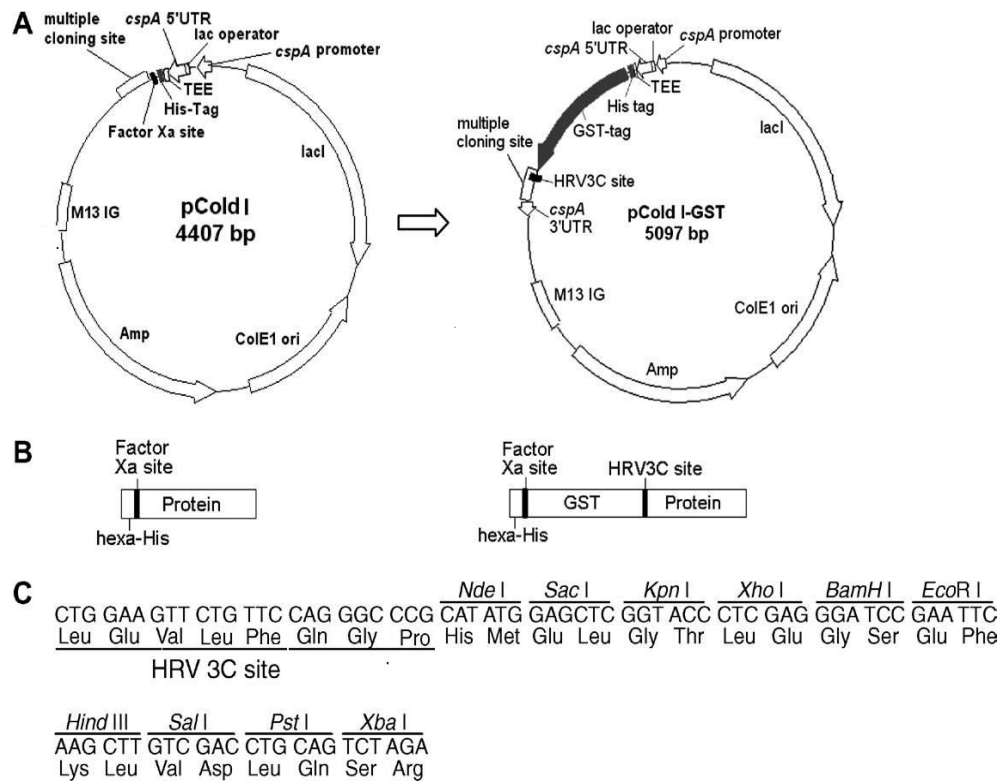


Figure 2.1 Expression vectors, pCold I and pCold I-GST. The restriction sites, CAT ATG and TCT AGA of the restriction enzymes, *Nde* I and *Xba* I respectively, were selected for digestion. Following digestion, the gene of interest (insert, CHFI gene) was subcloned into the vector designed for protein expression (expression vector) [174].

2.3.1.3 NCBI software

This was used to get genetic frame and the sequence of the amino acids of corn Hageman factor inhibitor as illustrated below.

1. CHFI gene sequence analysis

```
AGCGCCGGGACCTCCTGCGTGCCGGGGTGGGCCATCCCGCACAACCCGCTCCCGAGCTGCCGC
TGGTACGTGACCAGCCGGACCTGCGGCATCGGGCCGCGCCTCCCGTGGCCGGAGCTGAAGAGG
AGATGCTGCCGGGAGCTGGCGGACATCCCGGCGTACTGCCGGTGCACGGCGCTGAGCATCCTC
ATGGACGGCGCGATCCCGCCGGGCCCGGACGCGCAGCTGGAGGGCCGCTAGAGGACCTGCCG
GGCTGCCCCGGGAGGTGCAGAGGGGATTCGCCGCCACCCTCGTCACGGAGGCCGAGTGCAAC
CTGGCCACCATCAGCGGCGTCGCCGAATGCCCTGGATTCTCGGCGGCGGAACGATGCCCTCC
AAGTAA
```

2. CHFI amino acid sequence

```
SAGTSCVPGWAIIPHNLPLSCRWYVTSRTCGIGPRLPWPELKRRCRELADIPAYCRCTALSIL
MDGAIPPGPDAQLEGRLEDLPGCPREVQRF AATLVTEAECNLATISGVAECPWILGGGTMP
K
```

2.3.1.4 CHFI gene

GenScript Company synthesised and did codon optimization of the sequence for bacterial expression first and put NdeI (CATATG) and XbaI (TCTAGA) restriction site at two ends of the sequence respectively. Then, the company inserted it into the cloning vector pUC57, and the product was pUC57-CHFI. To be able to clone the gene of interest (CHFI insert) into the expression vector, both cloning vector and expression vectors were treated with the two restriction enzymes (NdeI and XbaI), creating compatible ends (**Figure 2.2**).



Figure 2.2 Schematic representation of the DNA fragments encoding 6xHis tag, factor Xa site, GST tag, HRV3C protease site, and CHFI from N-terminus to C-terminus respectively.

2.3.1.5 Competent cells

E. coli competent cells (NovaBlue, aliquots of 100 µl/ Eppendorf), prepared stored in -80° freezer, were used for bacterial transformation.

2.3.1.6 Luria Broth (LB) media

LB powder (20 g), composed of tryptone, yeast extract and NaCl, was weighed and dissolved in 800 ml of distilled water in a 1000ml cylinder using magnetic stirrer. Then the volume was completed to one litre. The solution was divided to four fractions of 250 ml volume in 250 ml bottles (or the preparation was divided to the fractions of 100 ml depending on the purpose of use). The bottles, loosely covered and labelled with autoclave tape, were sterilized by autoclave and stored at laboratory temperature. When required, they were used for bacterial transformation, inoculation and preparation of cultural media.

2.3.1.7 LB-agar ampicillin plate

LB and agar (8 and 6 g respectively) were dissolved in 350 ml distilled water in a 500 ml flask; then, the volume was completed to 400 ml by the same solvent. The flask was covered with the aluminium foil and labelled with the autoclave tape. Then, it was autoclaved for 30-45 minutes. When the agar had

been autoclaved, it was allowed to cool until the bottle can be held with bare hands because too much heat can destroy the antibacterial. Ampicillin 400 µl at 1:1000 (1000X stock, 1g / ml) stock concentration was added to the solution mixed thoroughly by inverting. When pouring plates, the bench area was kept sterile by working near a flame. Then the mixture (20 mL) was carefully poured out into each sterile plastic petri dish. The plates were allowed to cool for 30-60 minutes (until solidified), inverted, and let sit for several more hours or overnight. The bottom of the plates were labelled with the antibiotic and date; then, the plates were stored in a fridge at 4°C until use for bacterial transformation.

2.3.1.8 Agarose gel

Agarose (1 g) was measured out and dissolved in a flask containing 100 ml of 1 TAE. The solution was heated in the microwave to dissolve the agarose until all the beads in the solution had completely disappeared. A sponge plug was placed over the top of the flask to prevent boiling over. While letting agarose solution cool down for 5 min at room temperature, the two dams were put into the slots on each side of the gel plate or tray. The melted agarose was poured into a gel tray with the comb (well–marker) in place slowly to avoid bubbles, which could intrude the gel. Any bubbles were removed from the well comb or moved towards the sides/edges of the gel with a pipette tip. The comb with the larger teeth (10 teeth) was used for eight or fewer samples whereas the comb with smaller teeth (15 teeth) was used when having up to 14 samples. The plate gel was let cool to room temperature for 20-30 minutes until it had completely solidified. Once solidified, the dams and the comb were removed

and the agarose gel was placed into the gel box (electrophoresis unit). For the large wells, 10 μ l samples were prepared and for the smaller wells, 7 μ l samples were prepared at least. Loading dye and SYBR® Green dye (2 μ l and 1 μ l respectively) were added to the samples (digest and PCR samples) and 7 μ l 1kb ladder (marker) was dispensed into the first lane. Loading buffer or loading dye serves two purposes: first, it provides a visible dye that helps with gel loading and will also help to estimate how far the gel or how "fast" the gel has run and second it contains a high glycerol %, so after adding it, the sample is heavier than water and will settle to the bottom of the gel well, instead of diffusing in the buffer. The gel box was filled with 1TAE until the gel was covered. Samples were loaded into the additional wells of the gel. The gel was run at 80-150V until the dye line was approximately 75-80% of the way down the gel. (It was noticed that black is negative; red is positive; the DNA is negatively charged and will run towards the positive electrode; a typical run time is about 1-1.5 hours, depending on the gel concentration and voltage). Power was turned off, the electrodes were disconnected from the power source, and then carefully the gel was taken away from the gel box. DNA fragments were visualized using UV light-camera. When purifying the DNA was needed for later use, the DNA was exposed to the light for as short period of time as possible to diminish DNA damage, the fragments of DNA are usually referred to as 'bands' due to their appearance on the gel.

2.3.2 Method

2.3.2.1 Bacterial transformation

Competent cells of *E. coli* (NovaBlue, aliquots of 100 μ l/ Eppendorf), taken out of -80°C , were thawed on ice (that took 5-10 min). Agar plates containing ampicillin were taken out of fridge to warm up to room temperature. DNA 2 μ l, 20 ng (usually 1 to 5 μ l, 10 pg to 100 ng can be used) was mixed with the competent cells in the eppendorf (20 μ l-100 μ l can be used, 50 μ L on one plate and the rest on a second plate). Once DNA added, mixing was produced by gentle flicking the bottom of the tube with finger a few times. The mixture of the competent cell/DNA was left on ice for 20-30 min. to make bacterial cells take up plasmid DNA, each transformation tube was then heat shocked for 30-60 seconds (45 sec was usually ideal) by placing the bottom 1/2 to 2/3 of the tube into the holes of the heat block previously heated to 42°C (Purpose of heat shock: The heat shock causes the bacterial cells to take up the plasmid with the new DNA because the heat expands the pores on the cell membrane and the plasmid can enter the cell easily). The tubes were put back on ice for 2 min. LB media 900 μ l (250-900 μ l media volume can be used), without antibiotic, was added to bacteria grown in a 37°C shaking incubator for 45 min (it is usually for 30-60 min). This step was important for antibiotic resistance (this outgrowth step gives the bacteria time to generate the antibiotic resistance proteins encoded on the plasmid backbone so that they will be able to grow once plated on the antibiotic-containing agar plate). Some of the transformation, for example, 200 μ l, was plated onto LB agar plate containing the appropriate antibiotic (Ampicillin). Plates were incubated at

37°C overnight. This procedure was performed for bacterial transformation with the plasmids (pUC57 carrying CHFI gene or pUC57-CHFI, pCOLD I-GST vector and recombinant pCOLD I-GST-CHFI). In the case of pCOLD I-GST-CHFI, after shaking incubation for 45 min, it was centrifuged for 2 min, 12000xg then 200ml was placed on LB agar plate.

2.3.2.2 Bacterial plasmid culture (inoculation)

To grow bacteria that contain a specific DNA plasmid, which will be used in other experiments and to prepare E.coli cell with the same plasmid DNA, bacterial plasmid culture was carried out. For DNA miniprep, LB media (5 ml), Ampicillin (5 µl) and a single colony of bacteria were added to a sterile falcon tube in a sterile condition using Bunsen burner. Then the mixture was incubated for overnight (12-18hr) 37°C. For DNA maxiprep, LB media (5 ml), Ampicillin (5 µl) and a single colony of bacteria were added to a sterile falcon tube in a sterile condition using Bunsen burner. Then, the media was incubated for 4 hrs at 37°C. After that, the media was poured into an autoclaved flask of 150ml LB media then incubated for overnight at 37°C. This was performed after bacterial transformation with the plasmids, pUC57-CHFI, pCOLD I-GST, and recombinant pCOLD I-GST-CHFI.

2.3.2.3 DNA preparation

DNA preparation after bacterial plasmid culture (inoculation) was conducted using the recipes of Gen Elute™ Plasmid Miniprep Kit and GenElute™ Plasmid Maxiprep Kit of Sigma Company as described below. All steps are carried out at room temperature.

2.3.2.3.1 Miniprep (low scale DNA preparation)

An overnight recombinant *E. coli* culture (5 ml) was harvested by centrifugation, at $\geq 12000xg$, for one minute (2 ml Eppendorf was used, every time 1ml was harvested x5 times). The supernatant was discarded. The bacterial pellet was resuspended completely with 200 μ l of the resuspension solution. Scraping the bottoms of the microcentrifuge tubes back and forth 5 times across the surface of a polypropylene microcentrifuge tube storage rack (or doing vortex or pipette up and down) was done to resuspend the cells thoroughly until homogeneous. The resuspended cells were lysed by adding 200 μ l of the lysis solution. Immediately the contents were mixed by gentle inversion (6–8 times) until the mixture had become clear and viscous (doing vortex and harsh mixing could shear genomic DNA, resulting in chromosomal DNA contamination in the final recovered plasmid DNA). Lysis reaction was not allowed to exceed 5 minutes (prolonged alkaline lysis may permanently denature supercoiled plasmid DNA that may cause to be unsuitable for most applications). The cell debris was precipitated by adding 350 μ l of the neutralization solution. The tube was gently inverted 4–6 times. The sample was centrifuged at $\geq 12000 \times g$ or maximum speed for 10 minutes to pellet the cell debris, proteins, lipids, SDS, and chromosomal DNA as a cloudy, viscous precipitate. (If the supernatant contained a large amount of floating particulates after centrifugation, the supernatant, before proceeding to the next step, was recentrifuged). A GenElute Miniprep binding column was inserted into a provided microcentrifuge tube. The column preparation solution (500 μ l) was added to each miniprep column and centrifuged at $\geq 12000 \times g$ for 1 minute. The flow-through liquid was decanted (The column preparation

solution maximized binding of DNA to the membrane resulting in more consistent yields). The cleared lysate (from step 3) was transferred to the column prepared in step 4 and centrifuged at $\geq 12000 \times g$ for 1 minute. The flow-through liquid poured out.

The diluted wash solution (750 μ l) was added to the column. It was centrifuged at $\geq 12000 \times g$ for 1 minute (The column wash step got rid of residual salt and other contaminants introduced during the column load). The flow-through liquid was discarded. Then, it was centrifuged again at maximum speed (17000 $\times g$) for 2 minutes without any additional Wash Solution to remove excess ethanol (that is usually present in diluted wash solution). The column was transferred to a fresh collection tube. To which, elution solution (50 μ l) was added. It was centrifuged at 17000 $\times g$ for 2 minutes. Sodium acetate buffer solution (3.0 M, pH 5.2, 0.1 volumes = 5 μ l), and isopropanol (0.7 volumes = 35 μ l) were added to the recovered plasmid. The tube was mixed well by inversion and centrifugation at $\geq 15000 \times g$ at 4°C for 45 minutes. The supernatant was decanted without disturbing the pellet. The DNA pellet was rinsed with 1.5 mL of 70% (v/v) ethanol and centrifuged as before for 10 minutes. The supernatant was poured out carefully and the pellet was air-dried for 15 min to allow residual ethanol to evaporate. The DNA pellet was resuspended in 20 μ l of elution solution. This recipe was used for preparation of the three types of plasmid DNA (pUC57-CHFI, pCOLD I-GST vector and recombinant pCOLD I-GST-CHFI).

2.3.2.3.2 Maxiprep (large scale DNA preparation)

An overnight culture (150 mL) was added to a falcon tube (50 ml) and harvested by centrifugation at 4500xg for 20 minutes and the supernatant was discarded (the process was done 3 times each time 50 ml). Resuspension/RNaseA Solution (12 ml) was added to the bacterial pellet; it was completely resuspended by pipetting up and down, or vortex. Lysis solution (12 ml) was used to lyse the resuspended cells, and the contents were immediately mixed by gently inverting 6 to 8 times. The mixture was allowed to sit for 3 to 5 minutes until it had become clear and viscous. Lysis was not allowed to proceed longer than 5 minutes. (Prolonged alkaline lysis may permanently denature the supercoiled plasmid DNA and may render it unsuitable for use in downstream applications.). A filter syringe was prepared by removing the plunger and placing the barrel in a rack in order to allow the syringe barrel to be upright. The lysed cells from step 3 were neutralized by adding 12 ml of the neutralization solution to the mixture and gently inverted 4 to 6 times. A white aggregate (cell debris, proteins, lipids, SDS, and chromosomal DNA) was formed. Binding solution (9 mL) was added and inverted 2 times. The tube content was immediately poured into the barrel of the filter syringe (the cell lysate didn't pass through the filter until the plunger was inserted into the syringe). The lysate was let sit for 5 minutes. The white aggregate floated to the top. GenElute HP Maxiprep binding column was placed into a 50 mL collection tube provided. The column preparation solution (12 mL) was added to the column and centrifuged at 3000 xg for 2 minutes. The eluate was discarded. The filter syringe barrel was held over the binding column and pressure was gently applied to the plunger to expel half of the

cleared lysate into the column; the lysate was allowed to pass through the column. The plunger was pulled back slightly to stop flow of the remaining lysate. It was spun 3000xg for 2 minutes then the eluate was discarded. This procedure was applied for the second half of the cleared lysate. Wash solution 1 (12 ml) was added to the column. Then, it was centrifuged at 3000xg for 5 minutes; the eluate was discarded. Wash solution 2 (12 ml) was added to the column. Then, it was centrifuged at 3000 x g for 5 minutes, and the eluate was discarded. The binding column was transferred to a clean 50 mL collection tube provided. Then, it was centrifuged 3000xg for 5 minutes. Elution solution (5 ml) was added; after that, the collection tube was centrifuged at 3000xg for 5 minutes. In order to concentrate the DNA prepared, sodium acetate buffer solution (3.0 M, pH 5.2, 0.1 volumes = 500 μ l), and isopropanol (0.7 volumes = 3500 μ l) were added to the recovered plasmid. The tube was mixed well by inversion and centrifugation at ≥ 15000 x g at 4°C for 45 minutes. The supernatant was decanted without disturbing the pellet. The DNA pellet was rinsed with 1.5 mL of 70% (v/v) ethanol and centrifuged as before for 10 minutes. The supernatant was poured out carefully, and the pellet was air-dried for 15 min to allow residual ethanol to evaporate. The DNA pellet was resuspended in 20 μ l of elution solution. This procedure was used for preparation of three types of plasmid DNA (pUC57-CHFI, pCOLD I-GST vector and recombinant pCOLD I-GST-CHFI) in large scale.

2.3.2.4 Measuring DNA concentration with the Nanodrop Spectrophotometer

The accurate measurement of a substance is based on its absorbance. It is necessary to know the wavelength of light that a substance maximally absorbs. In the case of nucleic acid (DNA and RNA), the maximal absorbance is at 260nm. A NanoDrop, a very small spectrophotometer, can accurately read DNA concentration in as little as 1 μ l. The extinction coefficient is usually used to convert absorbance unit to the absolute amount of (nucleic acid) unit. The extinction coefficient value is as follows, RNA 40, DNA (double-stranded, for example our DNA types, pUC57-CHFI, pCOLD I-GST and recombinant pCOLD I-GST-CHFI) 50, DNA (single-stranded) 33.

Before measurement, the samples were centrifuged to cause unwanted, damaged materials to gather on the bottom of the sample tubes (this step was mainly used for recombinant protein measurement to remove unfolded protein). The protocol steps were carried out as below. Lower (sensor) pedestal and the upper (lid) pedestal was washed with distilled water spray bottle, and then both pedestals were cleaned with a Kimwipe. To initiate the machine, 2 μ l of millipore-filtered water (or nucleic acid water) was added to pedestal then the arm was lowered ; the water volume was read by clicking on "proceed". When finished, top and bottom measurement pedestal surfaces cleaned with a Kimwipe tissue. Two microlitre of elution buffer (whatever DNA was eluted with in the miniprep and maxiprep) was loaded as blank on the pedestal and the top arm was placed. The blank measurement was run by clicking the "BLANK" button. When finished, the pedestal (top and bottom)

were cleaned with a Kimwipe. Sample1 (2 μ l) was loaded on the lower pedestal, the arm was placed. The sample name was entered in the window provided. Measurement was done by clicking on the “Measure” button (the display shows the spectrum and the calculated concentration). The same steps were repeated for other samples; cleaning was done between sample measurements with a Kimwipe. When finished, the report could be saved or printed after clicking “show report”. Finally, the pedestals were cleaned and closed. The abovementioned procedure used to measure the DNA samples; pUC57-CHFI, pCOLD I-GST and pCOLD I -GST-CHFI.

2.3.2.5 Restriction Enzyme Digestion

The plasmids, pUC57-CHFI, pCOLD I-GST and pCOLD I-GST-CHFI, were digested with the appropriate restriction enzymes, XbaI and NdeI. The restriction enzyme digestion was carried out in a reaction volume of 20 μ L containing 0.2-1.5 μ g of DNA, 10 u/ μ L (0.5 μ L) of each restriction enzyme, 100XBSA (0.2 μ L bovine serum albumin) and 10 μ L of 10XBuffer 4 (50 mM potassium acetate, 20 mM Tris-HCl, 10 mM MgCl₂, 1 mM Dithiothreitol, pH 7.9). The digestion mixture was incubated at 37°C overnight. The linearized DNA samples were then analysed and purified as mentioned below.

2.3.2.6 Analysing DNA

After preparation of agarose gel (as mentioned above), one kb DNA ladder as marker (7 μ l) in combination with SYBR Green (1 μ l) was loaded in the first lane as a guide (the size of each band based on manufacturer's instruction). A mixture of 7-10 μ l samples, 1-2 μ l of each of SYBRGreen and DNA loading

dye was loaded in the remaining lanes. The gel was photographed with camera provided with a UV filter. The resulting DNA bands were interpreted. A few simple ways to increase the resolution (crispness) of DNA bands were carried out that include: running the gel at a lower voltage for a longer period of time, using a wider gel comb or loading less DNA into well.

2.3.2.7 Purification of DNA (Gel extraction)

For purification of DNA, Gel extraction Kit protocol of Sigma Company was used as summarized below. The DNA fragment of interest from the agarose gel was excised with a clean, sharp blade. Excess gel was trimmed away to minimize the amount of agarose. The gel slice was weighed in a falcon tube. Three gel volumes of the gel solubilization solution were added to the gel slice (for every 100 mg of agarose gel, 300 mL of Gel solubilization solution was added). The gel mixture was incubated at 50-60 °C using heat block for 10 minutes, or until the gel slice had completely dissolved. To help dissolve the gel, brief shaking or (vortex) every 2-3 minutes during incubation was done. Isopropanol (100%, 1 gel volume) was added and mixed until homogenous. GenElute binding column G was inserted into the provided 2 ml collection tubes. Column preparation solution (500 µl) was added to the binding column. Centrifugation at 12000xg was performed for 1 minute. Flow-through liquid was discarded. The solubilized gel solution (700 mL fractions) was loaded into the binding column. It was spun for 1 minute after loading each volume portion. The flow through liquid was discarded. Wash solution (700 mL) was added to the binding column. Afterwards, it was centrifuged at 12000xg for 1 minute. The binding column was taken away from the collection tube and the

flow-through liquid was discarded. The binding column was placed back into the collection tube and centrifuged again at 12000xg for 1 minute without any additional wash solution to remove excess ethanol. The binding column was transferred to a fresh collection tube. Elution solution (50 mL) was added to the center of the membrane and incubated for 1 minute. Then, it was centrifuged at 12000xg for 1 minute. In order to precipitate the DNA extracted, the DNA concentration was performed as described in maxiprep. This procedure was used for purification of the insert and vector (CHF1 gene, pCOLD I-GST) after digestion of pUC57-CHF1, pCOLD I-GST and pCOLD I-GST-CHF1. Then, their concentration was measured using Nanodrop/spectrophotometer.

2.3.2.8 Ligation

The insert (CHF1 gene) and the linearized vector (pCOLD I-GST) were ligated accordingly using the “Quick Ligation Kit” protocol (NEB). An amount of 50 ng pCOLD I-GST vector was combined with 150 ng insert (3-fold molar excess of insert, insert: vector ratio 3:1), and the volume was adjusted to 10 μ l with distilled water. Then, 2Xquick ligation reaction buffer (10 μ l) was added and mixed. Quick T4 DNA Ligase (1 μ l) was added and mixed thoroughly. The mixture was centrifuged briefly and incubated at room temperature for 5 min. after that, the expected ligation product (pCOLD I-GST-CHF1) was subjected to the restriction enzyme digestion (as explained above).

2.4 Protein expression and purification

2.4.1 Materials

2.4.1.1 Material list

The ingredients listed below (**Table 2.2**) were ordered by the structural biology (C84 Lab.) group and were stored at appropriate temperature.

Table 2.2 List of the materials and reagents required for expression and purification of CHFI.

| Reagents | Description/uses | Storage T | Supplier or Lab prep. |
|---------------------------------------|--|-----------|-----------------------|
| NaH ₂ PO ₄ 1M | used for preparation of Sodium phosphate buffer | Lab. T | Sigma |
| Na ₂ HPO ₄ 1M | used for preparation of Sodium phosphate buffer | Lab. T | Sigma |
| NaH ₂ PO ₄ 1M | NaH ₂ PO ₄ 69g in 500ml D.W. | Lab. T | Sigma |
| Na ₂ HPO ₄ 1M | Na ₂ HPO ₄ 71g in 500ml D.W. | Lab. T | Sigma |
| Sodium phosphate buffer pH 7.4, 0.1 M | NaH ₂ PO ₄ (1M) 22.6 ml, Na ₂ HPO ₄ (1M) 77.4 ml, D.W. QS 1000 ml. | Lab. T | Sigma |
| Sodium phosphate buffer pH 8, 0.1 M | NaH ₂ PO ₄ (1M) 6.8 ml, Na ₂ HPO ₄ (1M) 93.2 ml, D.W. QS 1000 ml | Lab. T | Lab. Prep. |
| NaCl | used for preparation of SOB media and different types of buffer solution | Lab. T | Sigma |

| | | | |
|----------------|--|--------|----------------------------|
| NaCl (4M) | 116.88 g NaCl in 500 ml D.W. | Lab T | Prepared by C62 Lab staff. |
| glycerol | Preparation of lysis buffer | Lab. T | Thermo scientific |
| Lysis buffer | NaH ₂ PO ₄ (1M) 2.26 ml, Na ₂ HPO ₄ (1M) 7.74 ml (sodium phosphate buffer 100 mM, pH 7.4) +NaCl (1M) 30 ml (300 mM), glycerol 8 ml (10%)+ D.W. QS 100 ml | Lab. T | Lab. Prep. |
| Imidazole | used for preparation of buffers used in Ni ²⁺ column purification | Lab. T | Sigma |
| Imidazole 1M | 68.07 g Imidazole in 1L D.W. | 4°C | Lab. Prep. |
| Binding buffer | Sodium phosphate buffer pH 7.4, 0.1 M 200ml (20 mM) + NaCl 4M 125 ml (500mM) + Imidazole 1M 20 ml (20 mM) D.W. QS 1000 ml pH adjusted to 7.4 by HCl 14 M | 4°C | Lab. Prep. |
| washing buffer | Sodium phosphate buffer pH 7.4, 0.1 M 200ml (20 mM) + NaCl 4M 125 ml (500mM) + Imidazole 1M 40 ml (40 mM) D.W. QS 1000 ml pH adjusted to 7.4 by HCl 14 M | 4°C | Lab. Prep. |
| Elution buffer | Sodium phosphate buffer pH 7.4, 0.1 M 200ml (20 mM) + | 4°C | Lab. Prep. |

| | | | |
|-----------------------------------|---|--------|------------|
| | NaCl 4M 125 ml (500mM) + Imidazole 1M 500 ml (500 mM) D.W. QS 1000 ml pH adjusted to 7.4 by HCl 14 M | | |
| Tris HCl | Tris (hydroxymethyl) aminomethane hydrochloride, Tris base used for preparation of buffers. | Lab. T | Sigma |
| Tris HCl (1M) | Tris HCl 121.14 g in 1 L D.W. pH 7.4 | Lab. T | Lab. Prep. |
| TBS | 50mM Tris base pH 7.4, 150 mM NaCl | Lab. T | Lab. Prep. |
| SDS | Sodium dodecyl sulphate, Used to solubilize and denature proteins for denaturing-PAGE | Lab. T | Sigma |
| SDS 10% | 10 g of SDS in 80 ml of H ₂ O then H ₂ O was added to 100 mL | Lab. T | Lab. Prep. |
| Bromophenol blue | used for preparation of non- reducing and reducing SDS dye preparation. | Lab. T | Sigma |
| Bromophenol blue 0.5% (w/v) | 0.1g bromophenol blue was dissolved in 20ml D.W. | 4°C | Lab. Prep. |
| β-mercaptoetha nol | used to reduce disulphide bonds | Lab. T | Sigma |
| SDS non- reducing dye | D.W. (3.55 ml), 0.5M Tris HCl, pH 6.8 (1.25ml), | 4°C | Lab. Prep. |

| | | | | |
|---------------------------------|---|--------|------------|--|
| (sample buffer, loading buffer) | glycerol (2.5ml), 10% (w/v) SDS 2.0 ml, 0.5% (w/v) bromophenol blue (200 µl) | | | |
| SDS reducing dye | 950µl of SDS non reducing dye + β-mercaptoethanol 50 µl | 4°C | Lab. Prep. | |
| IPTG (1M) | Isopropyl β-D-1-thiogalactopyranoside, inducer of protein expression | -20° | Sigma | |
| 30% Acrylamide | used in protein electrophoresis , protein separation | 4°C | Sigma | |
| APS | 10% (w/v) used as a catalyst for the copolymerization of acrylamide gels | Lab. T | Sigma | |
| 10% APS | Ammonium persulphate 1g was dissolved in 10 mL of H ₂ O and stored at 4°C, Ammonium persulphate decays slowly in solution, so the stock solution was replaced every 2-3 wk | -20° | Lab. Prep. | |
| Urea buffer | 100mM(2.76 g) NaH ₂ PO ₄ , 10mM(0.24g) Tris base, 8M (96.1g) urea in 150 ml D.W., pH was adjusted to 8 by NaOH then completed to 200ml D.W. | Lab. T | Lab. Prep. | |
| 10XSDS PAGE Running | – Glycine (288g), Tris base (60.4g), SDS (20g) in 1.8 L | Lab. T | Lab. Prep. | |

| | | | |
|---------------------------|---|--------|------------|
| Buffer | D.W. | | |
| Glutathione agarose beads | used for GST-pull down purification | 4°C | Sigma |
| Glutathion powder | used for GST-pull down purification | Lab. T | Sigma |
| Glutathion 5mM | 76 mg was dissolved in 1ml TBS pH 8 (250mM). From which 5mM was prepared. | -20°C | Lab. Prep. |
| Coomassie blue | used to visualize protein when running SDS-PAGE | Lab. T | |
| Destaining solution | to remove Coomassie blue from gel | Lab. T | |

2.4.1.2 LB-agar ampicillin-tetracycline plate

LB and agar (8 and 6 g respectively) were dissolved in 350 ml distilled water in a 500 ml flask; then, the volume was completed to 400 ml by the same solvent. The flask was covered with aluminium foil and labelled with autoclave tape. Then, it was autoclaved for 30-45 minutes. When the agar had been autoclaved, it was allowed to cool until the bottle can be held with bare hands because too much heat can destroy the antibacterial. Ampicillin and tetracycline (400 µl, 1000 X antibiotic stocks) was added to the solution and mixed thoroughly by inverting. When pouring plates, bench area was kept sterile by working near Bunsen burner. Then the mixture (20 mL) was carefully poured out into each sterile plastic petri dish. The plates were allowed to cool for 30-60 minutes (until solidified), inverted, and let sit for several more hours or overnight. The bottom of plates was labelled with

antibiotic and date and stored at 4°C. They were used for bacterial transformation of origami™2 (DE3) competent cells using recombinant vector (pCOLD I-GST-CHFI) as this bacteria resists tetracycline and the recombinant vector is ampicillin resistant.

2.4.1.3 LB-agar ampicillin-chloramphenicol plate

The previous procedure was used, but instead of ampicillin and tetracycline, Ampicillin and chloramphenicol (400 µl, 1000X antibiotic stocks) was added to LB-Agar solution. They were used for bacterial transformation of BL21 (DE3) competent cells using recombinant vector (pCOLD I-GST-CHFI); this bacteria resists chloramphenicol and the recombinant vector is ampicillin resistant.

2.4.1.4 Preparation of supra optimal broth (SOB) media

Distilled water (800 ml) was prepared in one litre glass beaker. Tryptone (20 g), yeast extract (5 g), and NaCl (0.5g) were added and dissolved using magnetic stirring. KCl (10 ml, 250 mM) was added (this solution was made by dissolving 1.86 g KCl in 100 ml distilled water). pH was adjusted to 7 (if required, NaOH was added). The volume was adjusted to 1L and autoclaved. Just before using the media, MgCl₂ was added (this solution was made by dissolving 19 g MgCl₂ in 90 ml distilled water; the volume was adjusted to 100ml with distilled water and sterilized by autoclaving).

2.4.1.5 Preparation of SDS-PAGE gel

The casting frames were set (two glass plates in the casting frames were clamped) on the casting stands. Resolving gel or separating gel was prepared according to the recipes described below (**Table 2.3 and 2.4**) in a separate small beaker. Appropriate amount of separating gel solution was dispensed into the gap between the glass plates. To make the top of the separating gel be horizontal, the gap was filled with isopropanol until overflow. Then, it was allowed (20-30min) to polymerize. After that, the isopropanol was thrown away. The line of resolving gel was noticed. Then stacking gel was prepared and added until overflow. The well-forming comb was inserted without trapping air under the teeth. It was allowed (20-30 min) to set.

Table 2.3 Solutions for preparing resolving gels for a 15% SDS-PAGE

| Resolving gel | |
|--|--------------------|
| Chemical components | Volume (mL) |
| H ₂ O | 1.8 |
| Acrylamide/Bis-acrylamide (30%/0.8%w/v) | 4 |
| 1.5 M TrisHCl pH 8.8 | 2 |
| 10% (w/v) SDS | 0.08 |
| 10% (w/v) APS | 0.08 |
| TEMED | 8×10^{-3} |

Table 2.4 Solutions for preparing stacking gels for a 15% SDS-PAGE

| Stacking gel | |
|--|--------------------|
| Chemical components | Volume (mL) |
| H ₂ O | 2.6 |
| Acrylamide/Bis-acrylamide (30%/0.8%w/v) | 1 |
| 0.5 M TrisHCl pH 6.8 | 1.25 |
| 10% (w/v) SDS | 0.05 |
| 10% (w/v) APS | 0.05 |
| TEMED | 5×10^{-3} |

2.4.2 Method

2.4.2.1 Bacterial transformation

The same recipe of bacterial transformation (as reported in the cloning section) was used, but, here, ampicillin-tetracyclin plates were used for origami™2 (DE3) and ampicillin-chloramphenicol –plate were used for BL21 (DE3) competent cells. Both competent cells were transformed with pCOLD I-GST-CHFI.

2.4.2.2 Bacterial plasmid culture (inoculation)

The same procedure of bacterial plasmid culture, as explained in the cloning section, was used for protein expression. Ampicillin and tetracyclin were used for origami™2 (DE3) culture whilst ampicillin and chloramphenicol were used for BL21 (DE3) competent cells. The culture volume was 5-15 ml.

2.4.2.3 Bacterial culture, optical density measurement and induction

Overnight inoculation culture (1-10) ml was prepared. After that, culture media (100-1000 mL of SOB) was prepared for protein expression. The antibiotics, Ampicillin and tetracyclin for origami™2 (DE3), ampicillin and chloramphenicol for BL21 (DE3), were added to SOB at 100 mg/ml final concentration. Then, the prepared overnight culture was added to the media then grown and incubated in a shaker (250 rpm) at 37° C until the required OD (0.6 for BL21 and 0.9 for origami™2 (DE3)). Then the culture was induced by the addition of IPTG (isopropylthiogalactoside) at 500µM (final concentration) for overnight with shaking at 10°C (Once IPTG added, the

culture was transferred to another shaker with 10°C temperature). After induction, the bacterial culture was centrifuged in 500 ml plastic bottles at 4500 x g, 4° C, for 20 min. After induction, lysis was performed as shown below.

2.4.2.4 Lysis and sonication of the bacteria

Following induction, centrifugation of bacteria was performed in 500 ml bottles in the rotor at 4500-7000xg rpm, 4° C until all the culture was spun down saving the cell pastes each time. Lysis buffer (as mentioned above) 5-25 ml (generally the volume of lysis buffer is 1/20 to 1/50 the volume of the bacterial culture) was added with the protease inhibitor tab (it is a mixture of several protease inhibitors used for the inhibition of serine, cysteine, but not metalloproteases; it is ordered from Roche company). The suspension was let incubate for 20 minutes at room temperature until the suspension became turbid and viscous due to release of the bacteria's genomic DNA. In order to get rid of the extreme turbidity of the suspension, sonication of the suspension was done to shear the DNA until the turbidity was similar to that of a normal protein solution. The solution was centrifuged at 7000 x g for 30 minutes at 4° C. The pellet and the supernatant were separated.

2.4.2.5 Treating pellet with urea buffer

The pellet was treated with 5 ml of urea buffer (the formula was explained above). This buffer causes protein unfolding and makes them seen on SDS-PAGE. The pellet and urea buffer were gently mixed by pipetting up and down without making foam. The solution was left at Lab. temperature for 1hr.

It was spun down at 7000 x g for 30 minutes at 4° C. The supernatant was analysed by SDS-PAGE as explained below. This procedure was used for 100 ml bacterial culture.

2.4.2.6 GST-pull down purification (GST -pull down affinity chromatography) of supernatant.

The supernatant was purified by GST-pull down. Lysis buffer (1 ml for 100ml culture of bacteria) was mixed with glutathion agarose beads (50 µl for 100 ml bacterial culture). The mixture was spun down at ≥ 6000 x g and the supernatant was discarded. Then, it was resuspended with lysis buffer (50 µl). The supernatant of the lysed bacterial cells or lysate (1 ml of 100 ml bacterial culture) was added and immobilized for 1 hr at 4° C (during this period, recombinant rHIS-GST-CHFI binds to the glutathione agarose beads and other unspecific proteins remain in the solution). Then it was spun down at ≥ 6000 xg for 10 min at 4° C and the supernatant was poured out. It was washed with lysis buffer (500 µl) then spun down at ≥ 6000 x g for 2 min at 4° C; the supernatant was discarded. Then glutathione 5 mM (50 µl for 1 ml lysate) was added. Centrifugation of the solution was done at ≥ 6000 x g for 10 min at 4° C. (glutathione binds agarose beads and replaces rHIS-GST-CHFI. Hence, the recombinant protein goes into solution, but agarose beads with glutathion and unspecific proteins remain at bottom). The supernatant (eluate) was either taken for SDS-PAGE electrophoresis or further purified using Ni²⁺-column affinity chromatography then the eluate was analysed by running SDS-PAGE.

2.4.2.7 Ni²⁺ column purification (Ni²⁺ column affinity chromatography)

The recombinant fusion protein, rHIS-GST-CHFI, has also 6His-tag or polyhistidine-tag used for Ni²⁺ column affinity chromatography. Flow pump system was assembled. To wash the system, filtered water (50 ml), ethanol (50 ml, 20% (v/v)) and filtered water again (50ml) were flowed through the machine respectively (lower inlet pipe in a 50 ml beaker sucks and upper outlet pipe in another beaker discharges). Ni²⁺ column (1 ml volume) was set up and adapted using stand adapters. Bottom and upper part of the column unscrewed. The outlet connected with the upper part. Air was removed from the column by flushing with water. Filtered water and binding buffer (50 ml each that is equal to 50 volumes) were passed through the Ni²⁺ column respectively. The supernatant (from lysate or GST purification) was diluted to 50 ml using binding buffer in 50 ml falcon tube and filtered using filter-syringe. Then it was flowed through the Ni²⁺ column system for 1 hr duration (inlet and outlet were in the supernatant falcon tube for recycling flow, 6 His-tag of rHIS-GST-CHFI attaches to Ni²⁺ by chelation interaction; flow through is composed of waste and unspecific protein).

2.4.2.8 Collection of rHIS-GST-CHFI bound to Ni²⁺ column using ACTA purifier collection system

The system was switched on. It was washed using filtered water (flow rate 10 ml/min, 50 ml) and binding buffer or buffer A (flow rate 2 ml/min, pressure 0.3 psk). During flow of washing buffer, Ni²⁺ column (to which rHIS-GST-CHFI was expected to be bound) connected to the system and the washing buffer flow was shifted to flow rate 2 ml/min, pressure 0.3 psk, fraction size 2

ml/fraction and 20 ml volume. Elution buffer or buffer B flow program was set up as follows: flow rate 2 ml/min, pressure 0.3 psk, fraction size 2 ml/fraction, B% [imidazole] = 100%. (Imidazole at high concentration was able to chelate Ni^{2+} and replace 6His-tag of rHIS-GST-CHFI. The recombinant protein then went into solution). The eluate was collected into fraction tubes. Then, the samples of the fractions were checked by running SDS-PAGE as explained below.

2.4.2.9 One-step purification from crude lysate to >95% pure protein

The supernatant was filtered through a 0.22 μm syringe filter for large-scale purification. Ni^{2+} -NTA agarose bead was resuspended by gently shaking the bottle several times. Resin slurry (2ml) was transferred from the bottle into 50 ml falcon tube. Then it was sediment by centrifugation at $2500\times g$ for 5 min; the supernatant was discarded. To remove excess ethanol, it was replaced with distilled water, mixed gently by pipetting up and down, and centrifuged at $2500\times g$ for 5 min; the supernatant was discarded. The bead was resuspended with 10 ml binding buffer (contained 20 mM imidazole), centrifuged at $2500\times g$ for 5 min, and the supernatant was decanted (the purpose of this step was to remove unspecific proteins when the bead was reused). The bead was resuspended again with 5 ml binding buffer and the filtered lysate was added; the mixture was incubated at 4°C in the fridge for overnight. It was then centrifuged, and the supernatant was removed using a plastic pipette and saved as one fraction. The bead was resuspended with 5 ml binding buffer; the mixture was transferred to a plastic column with the bottom closed; the bead was allowed to settle. The bottom was opened and

collection volume was kept as one fraction. Then, the bead was washed extensively with (4-5X5) mL washing buffer (contains 40 mM imidazole) and each time the collection was kept for SDS analysis. After that, the protein was eluted with 7.5 ml elution buffer (contained 500 mM imidazole) as 1.5 ml fractions. The samples were analysed by SDS.

2.4.2.10 Running SDS-Page

The separation degree and the purity of the protein were verified by Sodium Dodecyl Sulphate–Poly Acrylamide Gel Electrophoresis (SDS-PAGE) in reducing conditions and non-reducing condition. Every sample (20-40uL) was mixed with (10-20) μ l of SDS sample buffer containing β -mercaptoethanol (sapmls anlyesed in non reducing condition did not contain β -mercaptoethanol) ; then the mixture was incubated at 95°C for 5 min in order to induce the denaturation of the protein and then run on a 15% SDS-PAGE for 1 h at 180V voltage. After 1h, the gel was stained with Coomassie blue and shaken at room temperature for 30 min. The staining solution was poured off; the gel washed with destaining solution containing 10% (v/v) acetic acid and 10% (v/v) isopropanol and then left on the shaker at room temperature for 1h. All the materials and methods, described above for rHIS-GST-CHFI expression and purification, were also used for expression and purification of rHIS-GST.

2.5 Characterization of rHIS-GST-CHFI

2.5.1 Materials

The list of materials required for inhibitory activity of the recombinant protein is illustrated below (**Table 2.5**).

Table 2.5 List of the materials used in the characterization study of CHFI

| Reagents | Description/Uses | Storage | Provider | or |
|-------------------------------|---|---------|------------------------------|----|
| | | T | Lab. | |
| α -FXIIa (alpha FXIIa) | Human coagulation Factor XIIa alpha, concentration 1.85 mg/mL (23.14 μ M) (before lyophilisation), aliquot of 1 x 0.50 mg and a volume/ aliquot 0.270 mL, stock is 23.14 μ M | -80°C | Enzyme Research Laboratories | |
| S-2302 | Chromogenic substrate for FXII. Chemical name: H-D-Prolyl-L-phenylalanyl-L-arginine-p-nitroaniline dihydrochloride (H-D-Pro-Phe-Arg-pNA·2HCl or S-2302). Stock is 25mg/4 ml D.W (10mM). | -20 °C | Chromogenix, | |
| CHFI | A selective and potent | -80 °C | Enzyme Research | |

| | | | |
|----------------|---|--------|-------------------|
| | inhibitor of human factor XIIa, concentration 1.73 mg/mL (123.58 μ M) (before lyophilisation), aliquot of 1 x 1 mg and volume / aliquot 0.578 mL, stock is 30 μ M (1mg in 2.38). | | Laboratories |
| p-nitroaniline | p-nitroaniline (Mr: 138.12) yellow crystalline powder 13.8 mg was dissolved in 10 ml hot water in a falcon tube to prepare 10 mM stock solution. From the stock, a set of working concentrations was prepared (0.4 mM, 1 mM, 2 mM, 3 mM, 4 mM and 6 mM) and used for calibration assay. | -20 °C | Sigma |
| 96 -well plate | Ninety-six well plates used for colorimetric assay. The plate is marked vertically with alphabetical letter (A-H for 8 wells) and horizontally with numbers (1-12 for 12 wells). | -20 °C | Thermo scientific |

Buffer solution The buffer media used for Lab T. C62 Lab
all the experiments was
phosphate buffer saline
(PBS). Its pH was always
checked using pH meter.

2.5.2 Methods

2.5.2.1 Principle of amidolytic assay

The method for the determination of enzyme activity is based on the difference in absorbance (optical density) between the pNA formed and the original substrate. The rate of pNA formation, i.e. the increase in absorbance per second at 405 nm, is proportional to the enzymatic activity and is conveniently determined with a spectrophotometer. The basic absorbance equation used for determination of the amount of product formed is $A = \epsilon bc$ (A: absorbance, ϵ : molar absorptivity or extinction coefficient which is constant, c: concentration of compound in solution, b: is the path length of the cuvette in which the sample is contained) (**Figure 2.3**).

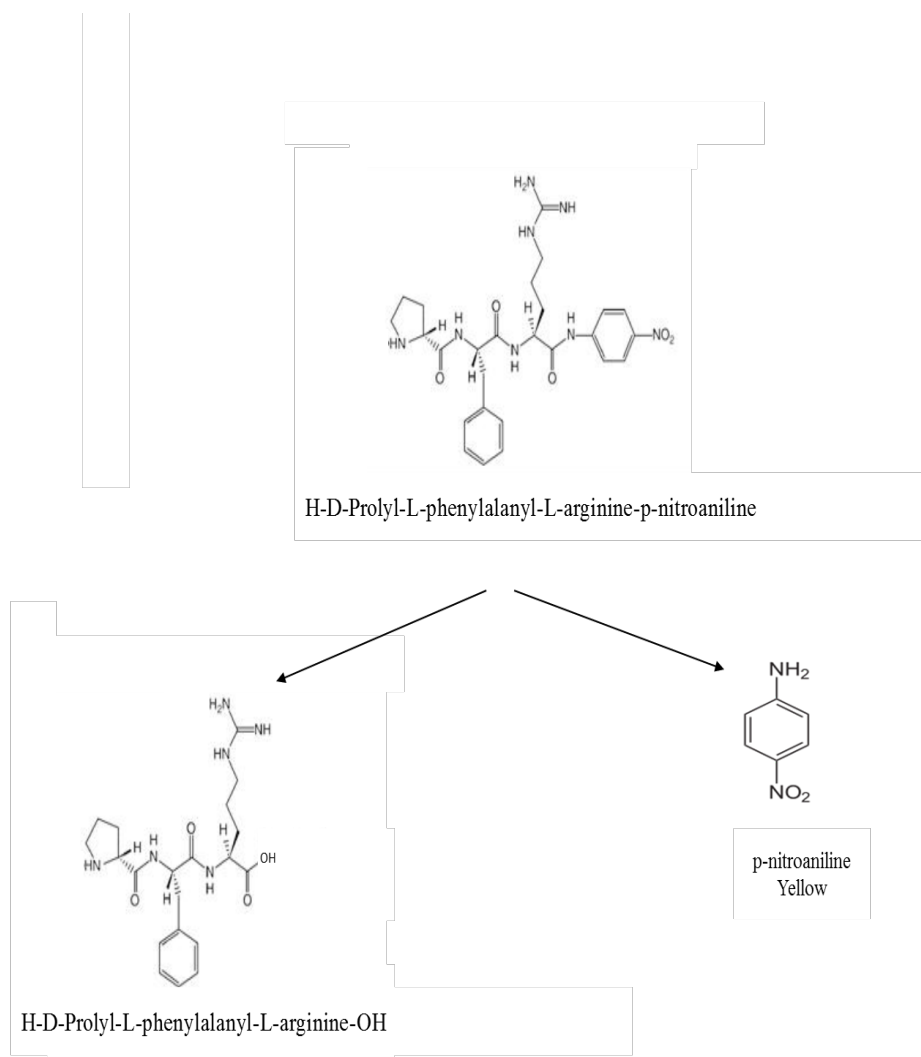


Figure 2.3 Schematic diagram of principle of the colorimetric assay using S-2302.

2.5.2.2 Calibration assay

In order to find a relationship between absorbance and the absolute amount of the yellow product (chromophore, pNA) released from S-2302 breakdown by the proteases, calibration assay was performed. A 96-well plate was prepared for the experiment. 1-6 wells were selected for a series of p-nitroaniline concentrations, 0.4 mM, 1 mM, 2 mM, 3 mM, 4 mM and 6 mM horizontally. Four wells were vertically used for each concentration while 6 wells were

selected as control composed of 100 μ l PBS. To the test wells, 10 μ l of each of p-nitroaniline concentration plus 90 μ l PBS were added. Then, the plate was transferred to the plate reader machine for reading. The temperature of the machine was set up to 33°C and its absorbance wave length to 405nm. This assay was performed for both spectrophotometers in C62 Lab (Perkin Elmer Wallac Envision Plate reader)

2.5.2.3 Inhibition assay of rHIS-GST-CHFI

The aim of this assay was to characterize rHIS-GST-CHFI using commercial CHFI as a positive control and rHIS-GST as a negative control. A 96-well plate marked horizontally (1-12) and vertically (letter: A-H), was used for the assay. The wells were divided properly to four groups of experiments. The wells, (A, B, 1-7), (C, D, 1-7), (E, F, 1-7), (G, H, 1-7) respectively, were selected for testing commercial CHFI, rHIS-GST-CHFI, rHIS-GST and different controls. First, regarding the test wells, to each duplicate well, PBS was added. Then, fixed substrate concentration (0.2 mM S-2302) and different concentrations (0, 10, 30, 60, 100, 300, 600, 1000 nM) of each of rHIS-GST, commercial CHFI, and rHIS-GST-CHFI were added; after that, a fixed α -FXIIa concentration (10 nM) was added to the mixture. Various controls were used: S-2302+CHFI+PBS, S-2302+PBS, CHFI+PBS, α -FXIIa +PBS, and PBS alone. The reaction volume was 100 μ l. Once was ready, the plate was transferred to the plate reader for monitoring amidolytic activity of the enzyme at 33°C and 405nm wave length for 30 min with 5 min time intervals.

2.6 Results and discussion

2.6.1 Cloning

In order to express recombinant native type CHF1, the gene sequence encoding the inhibitor was cloned into the expression vector, pCOLD I-GST vector. The vector improves expression and purification of the proteins with numerous disulphide bonds [174]. pCOLD I-GST-CHF1 was digested with the appropriate restriction enzymes (XbaI and NdeI) successfully. The ligation of the insert into the proper vector was verified by running the digestion mixture on a 1% Agarose gel (**Figure 2.4**). The cloning was further confirmed via DNA sequencing. The resulting fusion gene was 6xHis tag, factor Xa site, GST tag, HRV3C protease site and CHF1 from N-terminus to C-terminus.

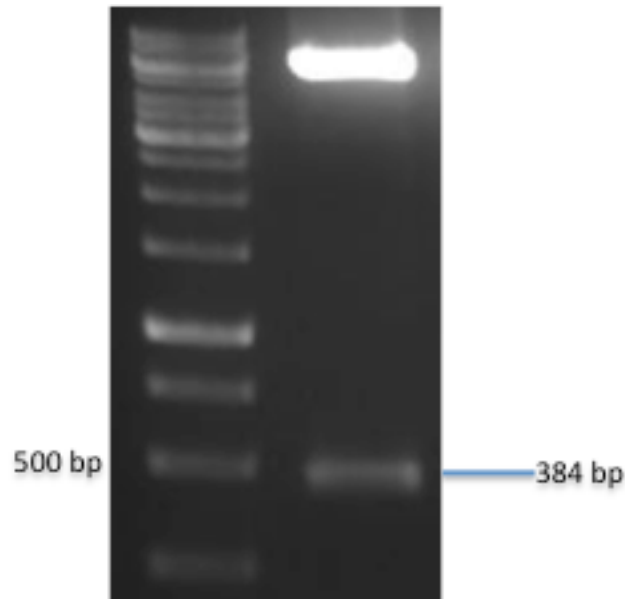


Figure 2.4 1% agarose gel showing insert band after digestion. The recombinant plasmid (pCOLD I-GST-CHFI, 5400 bp) was composed of pCOLD I-GST vector having a size of 5097 bp and of rCHFI gene, having 384 bp, being cloned. Following digestion of the recombinant plasmid, two fragments, the vector of 5097 bp and rCHFI of 384 bp, were released.

2.6.2 Expression, purification, and characterization of the inhibitory activity of rHIS-GST-CHFI against FXIIa

2.6.2.1 Expression of rHIS-GST-CHFI

The recombinant protein (rHISGSTCHFI) with a 6xHis tag, factor Xa site, GST tag, HRV3C protease site and CHFI from N-terminus to C-terminus was expressed successfully in Origami™ 2 and BL21 DE3 as a fusion engineered protein using pCOLD I-GST-CHFI expression vector. Initially, expression and purification was performed at low scale (qualitative analysis) for optimization purpose. Following cell-lysis, sonication and spinning, the supernatant was purified and the pellet (insoluble form of protein might be in inclusion body or pellet) was treated with urea buffer for the purpose of denaturation (**Figure**

2.5). The degree of purification and the right size of the fusion protein (40 kDa) was analyzed using SDS electrophoresis.

Soluble expression of rHIS-GST-CHFI was optimized by manipulating induction period and [IPTG] and their effect on the expression level was evaluated. There was no significant difference between an overnight incubation and the induction periods, 1, 2, 3, 4 and 5 hours, in the amount of the recombinant protein produced in supernatant (**Figure 2.6 and 2.7**) using BL21 DE3 and Origami™ 2 cells . The concentrations of IPTG (100, 500 and 1000 μ M) showed the same influence on the efficiency of expression (**Figure 2.8**) using Origami™ 2 cells.

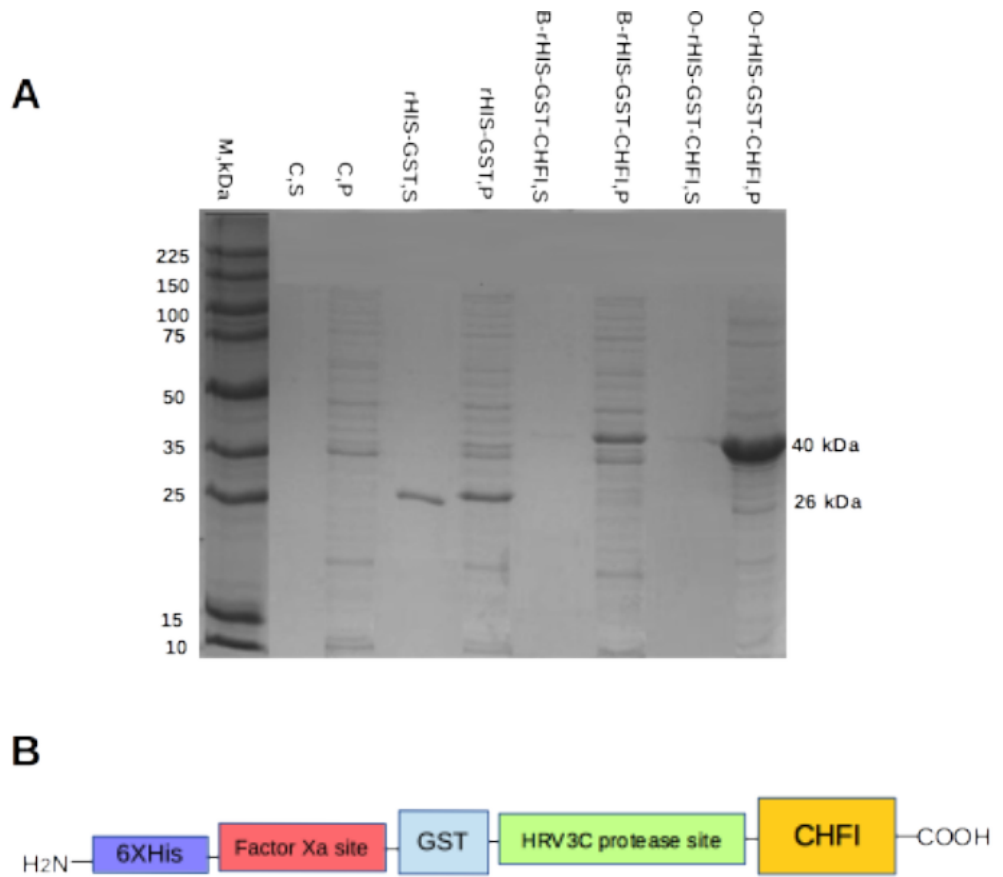


Figure 2.5 Expression of rHIS-GST-CHFI. **Figure A:** Expression of the fusion protein in bacteria using 500 μ M IPTG, an overnight incubation, and GST pull-down affinity chromatography. S is supernatant, P is pellet, C is control, O is origami, and B is BL21 DE3. **Figure B:** the fusion protein has 6xHis-GST tag, factor Xa site, GST tag, HRV3C protease site and CHFI from N-terminus to C-terminus.

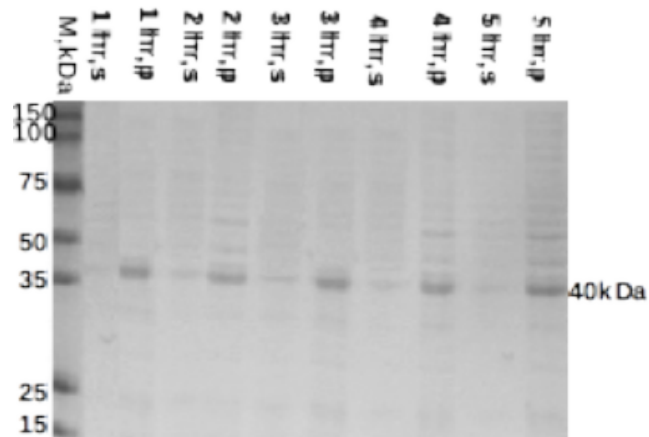


Figure 2.6 Optimization of induction period. There is no significant difference in the effect of different induction periods (1, 2, 3, 4 and 5 hours) on the level of expression of rHIS-GST-CHF1 in Origami™ 2 cells. S (supernatant), p (pellet), hr. (hour).

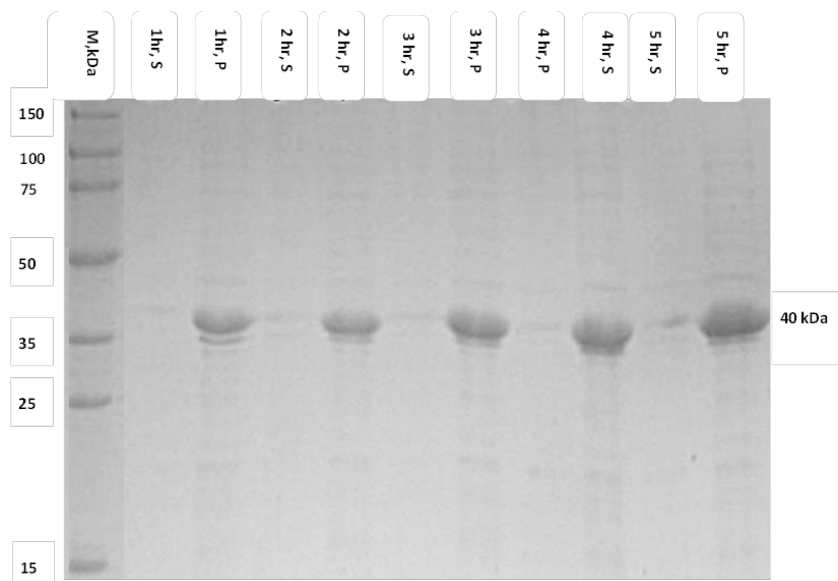


Figure 2.7 Optimization of induction using different time periods. There is no significant difference in the effect of different induction periods (1, 2, 3, 4 and 5 hr.) on the level of expression of rHIS-GST-CHF1 in BL21 DE3 cells. S (supernatant), p (pellet), hr. (hour).

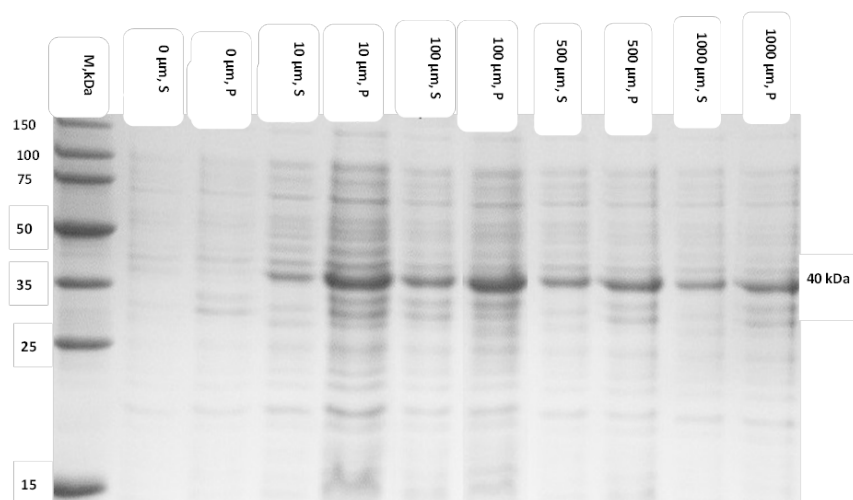


Figure 2.8 Optimizing [IPTG] for induction of protein expression in Origami™ 2. S (supernatant), P (pellet). The concentrations of IPTG (100, 500 and 1000 μM) showed the same influence on the protein expression.

2.6.2.2 Purification of rHIS-GST-CHFI

In the present study, the first simple protocol for soluble expression and single step purification of the recombinant CHFI was successfully identified using Origami™ 2 and BL21 DE3 expression system. A research group, in 1998, faced difficulties and found recombinant CHFI in insoluble form. To overcome this problem, they performed denaturation and renaturation. Herein single step purification was first optimized in order to get a purified amount of wild type CHFI protein in supernatant. Although the protein was poorly expressed, 0.5-1 mg protein was produced out of 3 L culture, it was sufficient to show full inhibition against FXIIa. In this chapter, the protein of interest, fused with HIS-GST tag, was purified via Ni^{2+} column affinity chromatography at large scale. The Ni^{2+} bead was extensively washed with the high concentration imidazole (40 mM) to allow efficient removal of the non-specifically binding proteins. The desired protein was eluted by adding 500

mM imidazole (as a competitor). The fractions were then analysed by 15% (w/v) SDS-PAGE gel under reducing and non-reducing condition to confirm the size of the protein and to verify its degree of purity. The analysis of the gel indicates that the protein was successfully purified with the right size 40 kDa. The linker between recombinant CHF1 and HIS-GST is HRV3C protease site (Leu-Phe-Gln-Gly-Pro). The fusion tag was not substantially removed from the protein by the action of HRV3C protease; the reason may be steric effect or steric hindrance due to CHF1 and HIS-GST being too close together. As an alternative strategy, HIS-GST, expressed and purified in the same fashion as CHF1, was used as a negative control in the inhibition assay of rHIS-GST-CHF1 vs. commercial CHF1 (**Figure 2.9 and 2.10**).

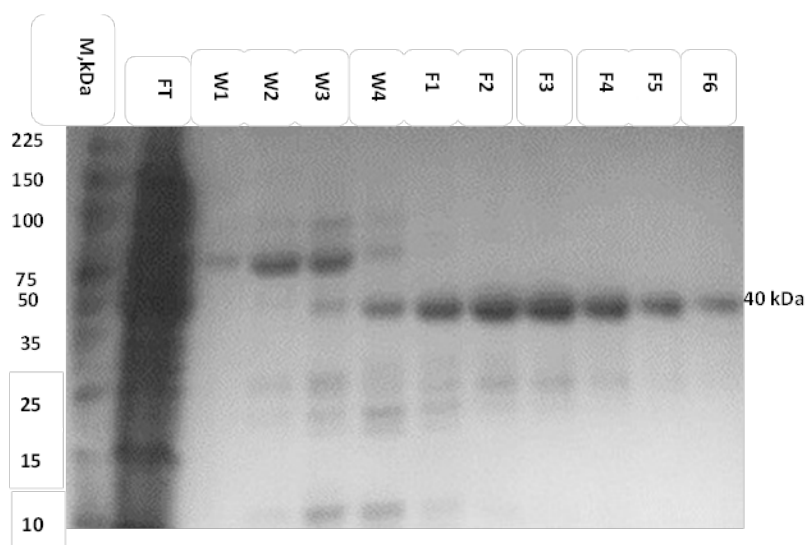


Figure 2.9 15% SDS showing Ni^{2+} column purification of rHIS-GST-CHF1. F1, F2, F3, F4, F5 and F6 are fractions 1, 2, 3, 4, 5, and 6; W is wash sample, FT is flow through column sample, and L is load sample. M is protein marker

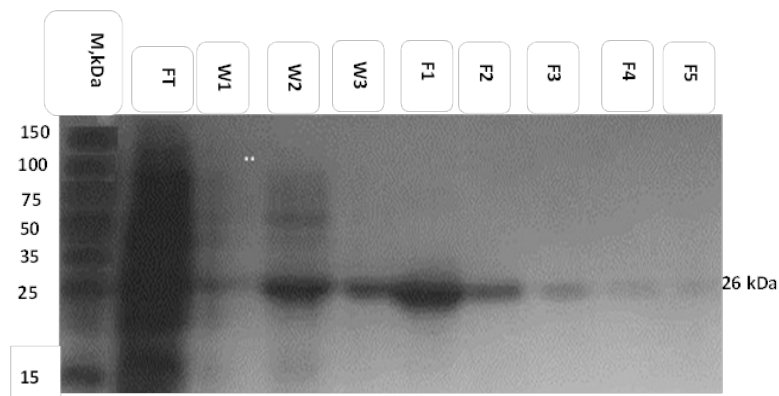


Figure 2.10 Ni^{2+} column purification of rHIS-GST tag. F1, F2, F3, F4 and F5 are fractions 1, 2, 3, 4 and 5; W is wash sample, FT is flow through column sample, M is protein marker.

2.6.3 Characterization of rHIS-GST-CHFI

2.6.3.1 Relationship between absorbance unit and the product generated

In order to calculate the molar absorptivity of the pNA chromogen in the spectrophotometers used in this study, the absorbance of different concentrations of pNA was measured. The molar absorptivity of the chromogen was 7.2×10^6 /mole (**Figure 2.11**)

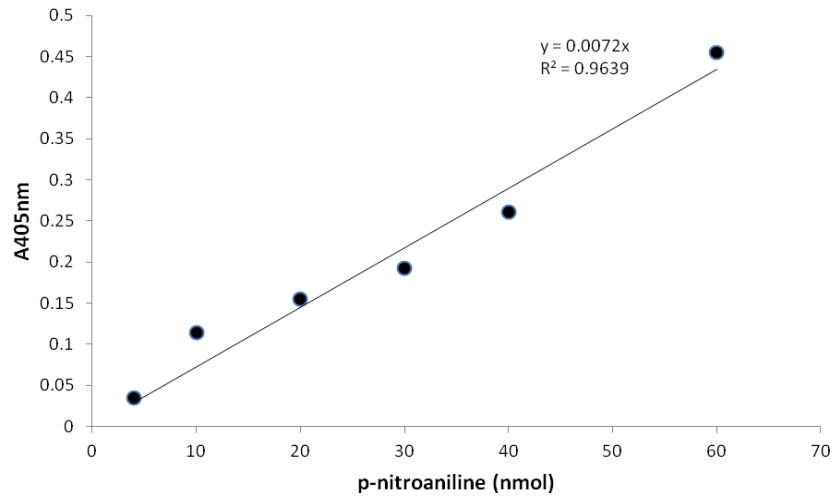


Figure 2.11 Calibration line and equation between the amount of p-nitroaniline and absorbance unit for the machine with filter system. Relationship between amount of p-nitroaniline and absorbance signal for the spectrophotometer is explained by the equation $y=0.0072x$ (y =absorbance, x = amount of p-nitroaniline).

3.6.3.2 Inhibitory activity of rHIS-GST-CHFI versus commercial CHFI against FXIIa

Inhibitory activity, reflecting inhibition effect of CHFI different forms on the catalytic activity of FXIIa enzyme, was measured by the effect of the rHIS-GST-CHFI, rHISGST and commercial CHFI on the amount of pNA released from substrate (S-2032) by FXIIa. To analyse IC_{50} , nonlinear regression was used.

There were several objectives behind conducting an inhibition assay for recombinant CHFI and commercial CHFI. First was to examine the efficiency of the expression and purification system in generating properly folded protein with correct disulphide bridges; the protein originally has 5 disulphide bonds, which play an essential role in maintaining its three-dimensional structure and

function. The second was to examine whether the storage and purification conditions are suitable for conserving correct protein folding. The last was to establish an inhibitory activity assay for the recombinant wild type CHF1, which then can be used as a master assay for studying CHF1-FXIIa characterization, chapter 3.

HIS-GST as a negative control has no inhibitory activity at all, whereas recombinant wild type CHF1 (rHIS-GST-CHF1) shows remarkable inhibition (**Figure 2.12**). The protein construct and commercial CHF1 (as a positive control) have a similar kinetic behaviour when inhibiting FXIIa and show almost the same strength of binding (**Figure 2.12**). This is interesting, substantiating the following points. Firstly, the wild type protein construct has complete inhibitory activity and is as active an inhibitor as commercial CHF1. IC_{50} values for rHIS-GST-CHF1 and commercial CHF1 are 109 ± 20 , 110 ± 20 , using both ordinary fit 107 ± 11 and 109 ± 12 (nM) using constraining fit analysis. This indicates that the protein is properly folded following expression, purification and storage. Secondly, the rHIS-GST tag does not interfere with the molecular interaction between CHF1 and FXIIa and the inhibition effect of rHIS-GST-CHF1 is therefore entirely due to CHF1. Lastly, rHIS-GST-CHF1 can be used as a principal assay to investigate inhibitory activity of the mutants against FXIIa as described in the next chapter (**Figure 2.12**).

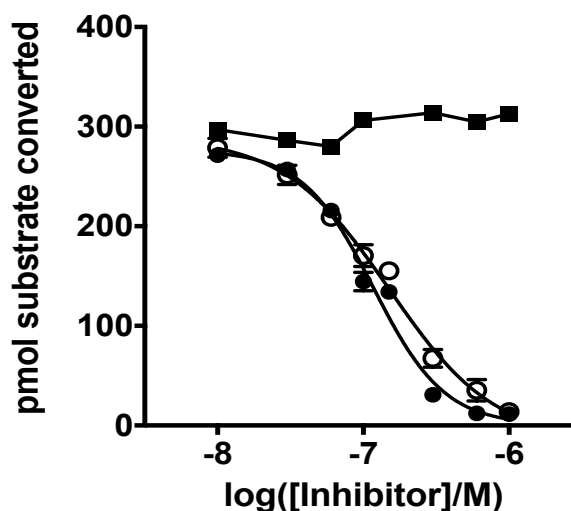


Figure 2.12 Inhibition assay of rHIS-GST-CHFI versus commercial CHFI. Absorbance unit was converted to the amount of the yellow product (chromophore) generated using calibration equation. Activity of FXIIa treated with CHFI represents as (pmol of product/pmol of enzyme/sec). The assay was performed with different concentrations (10, 30, 60, 100, 300, 600, and 1000 nM) of commercial CHFI, rHIS-GST-CHFI and rHIS-GST co-incubated with 0.2 mM S-2302, and then the mixture was supplemented with 10 nM FXIIa; the substrate cleavage was monitored at 405 nm wave length at 33 °C for 30 min time (5 minutes time interval). Commercial CHFI and rHIS-GST-CHFI behave similarly and have same inhibition effectiveness (**Table 2.6**) whereas the tag did not show any inhibitory activity. The result is average of ten independent experiments. The error bar is standard error of all independent experiments. The symbols (\square , \bullet , \circ) denote commercial CHFI, rHIS-GST-CHFI and rHIS-GST respectively.

Table 2.6 Inhibition effectiveness value (IC_{50}) of the recombinant wild type, rHIS-GST-CHFI, in comparison with that of commercial CHFI. The error bar is standard error of the mean of ten independent experiments. In every experiment a duplicate was used for each single concentration of the inhibitors. Average of the duplicate results was taken.

| Different forms | IC_{50} (nM) | |
|-----------------|-------------------|--------------------------|
| | Constraining fit* | Ordinary (floating) fit+ |
| rHIS-GST-CHFI | 110±20 | 109±20 |
| Commercial CHFI | 109 ±12 | 107 ±11 |

* IC_{50} can be calculated in such a way that basal non-inhibition gaps are subtracted away. This means that inhibition (Y) at very high concentrations of an inhibitor (X) has to be zero.

+ IC_{50} is calculated ordinarily as inhibition (Y) at very high concentrations of an inhibitor (X) is approximately zero. in such a case, basal non-inhibition gaps are absent.

2.6.3.3 Optimization of storage condition in relation to inhibitory activity

In order to test the stability of the recombinant protein and find an optimal condition required for maintaining the activity of the protein, its percentage of inhibition versus commercial CHFI was observed in relation to the following factors: storage temperature of the protein, imidazole concentration of the protein solution/elution buffer, detection of precipitation in the protein solution/elution buffer, pH of protein storage buffer, presence of glycerol in the protein storage buffer, and period between isolation and inhibition assay.

It was noticed that the recombinant protein behaves appropriately in the following conditions explained below. First, testing for inhibition activity, once rHIS-GST-CHFI was isolated; in this condition the protein construct was in 500 mM imidazole buffer at pH 7.2. Second, the activity test was performed

one day after isolation; the protein was in a buffer solution of 15 times diluted concentration of imidazole (rHIS-GST-CHFI was in TBS buffer with 0.01 mM imidazole at pH 7.2 using protein concentration and buffer exchange procedures). Third, the protein was tested after one week storage at -20 °C in TBS buffer containing diluted imidazole at pH 7.2.

The storage of protein in the elution buffer (500 mM imidazole and pH 7.2 at -20°C) showed massive precipitation with no inhibition effect. One month storage in TBS buffer (with diluted imidazole and pH 7.2) at two different temperatures, -20 °C and -80 °C, showed a substantial and a slight reduction in the inhibition activity respectively. Storage for ≥ 1 month in TBS buffer (pH 8.2, 0.01 mM imidazole+25 % glycerol (v/v) , -80 °C) showed an inhibition almost similar to that of the commercial CHFI as shown in (**Table 2.7**). Hence, this condition was selected for long-term storage in order to maintain proper behaviour of the recombinant wild protein and the mutants expressed as explained in the next chapter.

Table 2.7 Effect of different factors on the stability and inhibitory activity of rHIS-GST-CHFI.

| pH | T(°C) | [Imidazole] (mM) | precipitation | The period (day) | Inhibition% | |
|-----|-------|---------------------|-------------------|------------------|-----------------------------|--------------------------------|
| | | | | | between Isolation and IA | compared to commercial CHFI |
| 7.2 | -20 | 500 | No | No | Almost equal | |
| 7.2 | | 500 | Yes/massive | 30 | Null | |
| 7.2 | -20 | 0.01 | No | 1 | Almost equal | |
| 7.2 | | 0.01 | No | 7 | Almost equal | |
| 7.2 | -20 | 0.01 | Yes/slight | 30 | Decreased by 66% | |
| 7.2 | -80 | 0.01 | No/cloudy sol. | 30 | A slight reduction | |
| 8.2 | -80 | 0.01 | No | ≥ 30 | Almost equal | |

2.7 Conclusion

The gene of interest (CHF1 gene) was cloned into the expression vector, pCOLD I-GST vector, successfully. The resulting fusion gene encoding a fusion protein composed of 6xHis tag, factor Xa site, GST tag, HRV3C protease site and CHF1 from N-terminus to C-terminus. An effective protocol for soluble expression and single step purification of recombinant CHF1 was first recognized using pCOLD I-GST vector and the bacterial expression systems, BL21 DE3 and origami™ 2 (DE3). It was observed that the molar absorptivity of the pNA chromogen is 7.2×10^6 /mole. The inhibitory activity, meaning inhibition effect of the CHF1 different forms on the catalytic activity of FXIIa enzyme, was measured by the influence of rHIS-GST-CHF1, rHIS-GST and commercial CHF1 on the amount of pNA generated from amidolytic breakdown of the chromogenic substrate by the enzyme. rHIS-GST tag as a negative control did not show inhibitory activity at all while the recombinant wild type CHF1 (rHIS-GST-CHF1) displayed tremendous and complete inhibitory activity against FXIIa; this ascertains the following points. First, the recombinant protein is as active inhibitor as commercial CHF1 and is properly folded after expression, purification and storage. Second, rHIS-GST tag cannot interfere with the molecular interaction between CHF1 and FXIIa and the inhibition effect is entirely due to recombinant CHF1 bound to rHIS-GST tag through HRV3C protease linker. This assay can be used as a principal assay and a reference guide for evaluation of the inhibitory activity of the mutants against FXIIa in the characterization study of CHF1-FXIIa interaction as described in the next chapter.

Chapter 3: Molecular pharmacological investigation into CHF1-FXII interaction

3.1 Abstract

The Lack of information on CHF1-FXIIa or FXIIa structure created an obstacle in the approach of the studies trying to rationalize the reason of selectivity of CHF1 toward FXIIa. CHF1-FXII interaction study can be extremely informative in designing low molecular weight inhibitors for the treatment of pathological thrombosis and its complications related to FXII. The aim of this chapter was to investigate CHF1-FXIIa interaction through the following objectives: first, using the expression and single-step purification system for generating soluble and functional recombinant rHIS-GST-CHF1 explained in chapter 2, to generate different recombinant variants of CHF1 with the desired point mutations guided by a proper prediction study designed for CHF1-FXIIa interaction. The second objective was to characterize the inhibitory activity of the mutant proteins of interest using the developed, principal inhibition assay of rHIS-GST-CHF1 as a reference. The current investigation into the question of specificity of CHF1 against FXII first identified that the central Arg34 at the very top of the fully exposed region of CHF1 inhibition loop plays a fundamental role in the inhibition function of CHF1 toward FXIIa. For the first time, this study revealed that Trp22 at the N-terminus and Arg43 at the C-terminus of the central inhibition loop are the two key interaction residues with FXIIa. They would help to further investigate if there is an additional factor elucidating specificity of the key interaction residues with the potential target residues on FXIIa.

3.2 Introduction

The CHF1-FXII interaction study can be extremely informative in understanding the molecular mechanism of specific inhibition of FXIIa by CHF1 and has the potential to provide templates for drug discovery to design low molecular weight inhibitors for the treatment of pathological thrombosis and its complications related to FXII, which is explained by recent studies of novel insights into thrombosis[129][130][131, 132]. Lack of information on CHF1-FXIIa complex or FXIIa structure created an obstacle in the way of studies trying to rationalize the reason of selectivity of CHF1. Crystal structure of FXIIa and co-crystallization of CHF1-FXIIa complex have not been solved yet. With reference to a study carried out in 1984, a scissile bond exists between Arg34 and Leu35 in the exposed region of CHF1; this bond was expected to involve in the interactions with both trypsin and, presumably, with activated coagulation factor XII (FXIIa) [136, 156]. In 1998, the crystal structure of CHF1 suggested that the inhibition selectivity of CHF1 for factor XIIa is not due to specific, atypical conformation of its protease inhibitory site. It also proposed that Arg34-Leu35 contains the scissile bond [136, 156].

The aim of this chapter was to investigate the CHF1-FXIIa interaction via the following objectives. The first objective was to generate different recombinant variants of CHF1 with the desired point mutations made on the basis of a proper prediction study for CHF1-FXIIa interaction. The second objective was characterization of the inhibitory activity of the mutant proteins of interest using the developed, principal inhibition assay of rHIS-GST-CHF1 as a template.

3.3 Materials and methods

3.3.1 Materials

3.3.1.1 Software and online tools

In order to design mutagenic primers, www.agilent.com/genomics/qcpd tool was used. Graph pad prism was used to analyse inhibition effectiveness of the mutants.

3.3.1.2 Site-directed mutagenesis kit

The kit was ordered from Stratagene European. It contained a list of materials required for performing PCR site-directed mutagenesis as described in detail in the (Table 3.1

Table 3.1 List and quantity of the materials supplied in the site-directed mutagenesis kit

| Materials provided | Quantity |
|---|-----------------|
| PfuUltra™ High Fidelity DNA polymerase (2.5 U/μl) | 25 U |
| 10× reaction buffer | 500 μl |
| Dpn I restriction enzyme (10 U/ μl) | 100 U |
| QuikSolution™ reagent | 500 μl |
| dNTP mix | 10 μl |
| XL10-Gold® ultracompetent cellsd (yellow tubes) | 4 × 135 μl |
| XL10-Gold® β-mercaptoethanol mix (β-ME) | 50 μl |

XL10-Gold® Ultra competent cells, XL10-Gold® β-ME, and pUC18 control plasmid were stored at –80°, but all other components at –20°C. The dNTP mix was thawed once, single-use aliquots were prepared and stored at –20°C in order to avoid multiple freeze-thaw cycles.

3.3.1.3 Peptides

The peptides listed below (**Table 3.2**) were ordered from GenScript. Their solubility was tested by the company. The quantity of the peptides was 1-4 mg and their purity was >95%.

Table 3.2 List of the synthetic, isolated peptides

| Different peptides | Description |
|----------------------------|------------------------------|
| CRWYVTSRTAGIGPRLPWPELKRRRC | Cyclic peptide |
| –RWYVTSRTAGIGPRLPWPELKRR– | Linear peptide |
| ---YVTSRTAGIGPRLPWPELKRR | Linear peptide lacking Trp22 |
| –RWYVTSRTAGIGPRLPWPELKR– | Linear peptide lacking Arg43 |
| -----IGPRLPWP----- | P4P3P2P1-P1’P2’P3’P4’ region |
| GISTAGPWRRRPPELLKVTY | Scrambled peptide |

3.3.1.4 Other materials

Almost all the materials described in chapter 2 (cloning and expression), required for bacterial transformation, DNA preparation, protein expression, protein purification and analysis, were used for generation of the recombinant mutant proteins of rHIS-GST-CHF1 in this chapter.

3.3.2 Methods

3.3.2.1 Prediction of CHF1-FXII interaction

In order to investigate the specific inhibitory activity of CHF1 toward human coagulation FXII, an appropriate docking study was designed by M.Pathak (a research assistant in the structural biology group/ Emsley group) based on three fundamental tools: first, the available crystal structure of CHF1[136, 156], second, the crystal structure of FXII protease domain solved by M Pathak (a research assistant in the structural biology group/ Emsley group)[173], and third, HGFA modelling, constructing a model of FXII from the three-dimensional structure of the related homologous protein, HGFA as a template.

3.3.2.2 Design of mutagenic primers

A forward and reverse primer pair for each of the ten point mutations and two double point mutations (leading to the substitution of Trp22, Arg27, Gly30, Gly32, Arg34, Leu35, Trp37, Glu39, Arg42, Arg43, Arg27Glu39A and Arg27Arg42 in CHF1) was designed using the www.agilent.com/genomics/

qcpd tool (**Table 3.3**). The primers were typically between 25-45 base pairs in length and had melting temperatures between 75-85°C, having GC-content between 40 and 60%. The primers were ordered from Eurofins MWG.

Table 3.3 List of the mutagenic primers used in the PCR site directed mutagenesis. The red codons encoding the point sites of interest

| Point mutations | Forward Primers (5' to 3') | Reverse Primers (5' to 3') |
|-----------------|------------------------------------|------------------------------------|
| Trp22Ala | ctgccgtcctgtcgcgctatgtcacctcacg | cgtgaggtgacatacgcgcgacaggacggcag |
| Arg27Ala | ctggtatgtcacctcagccacctgtggcattggt | accaatgccacaggtggctgaggtgacataccag |
| Gly30Trp | cctcacgcacctgttggattgtccgcgtct | agacgcgaccacaaatccaacaggtgcgtgagg |
| Gly32Trp | ctcacgcacctgtggcattggccgcgtctgc | gcagacgcgcccaaatgccacaggtgcgtgag |
| Arg34Ala | tggcattgtccggctctgccgtggccg | cggccacggcagagccggaccaatgccac |
| Leu35Ala | gtggcattgtccgcgtgcgacctggcc | ggccacggcgacgcggaccaatgccac |
| Trp37Ala | gtccgcgtctgccggccggaactgaaac | gtttcagttccggcgccggcagacgaggac |
| Glu39Ala | ctgccgtggccggactgaaacgtcgc | gcgacgttcagtcggccacggcag |
| Arg42Ala | gccgtggccggaactgaaagctcgctgctgt | acagcagcagctttcagttccggccacggc |
| Arg43Ala | gccggaactgaaagctcctgctgtcgtgaaactg | cagttcacgacagcaggcagctttcagttccggc |
| Arg27Ala | ctggtatgtcacctcagccacctgtggcattggt | accaatgccacaggtggctgaggtgacataccag |
| Glu39Ala | | |
| Arg27Ala | ctggtatgtcacctcagccacctgtggcattggt | accaatgccacaggtggctgaggtgacataccag |
| Arg42Ala | | |

3.3.2.3 PCR site-directed mutagenesis

The bacterial expression vector, pCOLD I-GST expression vector, carrying the target gene of the wild type CHFI (rHIS-GST-CHFI), was used as a

template for the mutagenesis reactions of almost all the point mutations, except for the double point mutations wherein the vector carrying the mutated gene (rHIS-GST-CHFI-R27A, in which Arg27 was replaced by Ala) was used as a template. The mutagenesis was carried out following the manufacturer's instructions using site directed mutagenesis Kit (Catalog # 200521). The supercoiled double-stranded DNA (dsDNA) vector with the gene of interest to be mutated at a desired point was amplified by polymerase chain reaction (PCR) using a specific pair of the forward and reverse primers and polymerase, PfuUltra™ High Fidelity DNA polymerase. The mixture of the reagents and thermal cycles for performing PCR site directed mutagenesis were described (**Table 3.4 and 3.5**).

Table 3.4 Protocol for PCR site directed mutagenesis

| Reagent | Volume | Final concentration |
|--------------------------|-----------------------------------|----------------------------|
| 5 µl | 10× reaction buffer | - |
| X µl | dsDNA template | 10–100 ng |
| X µl | forward oligonucleotide primer | 125 ng |
| X µl | reverse oligonucleotide primer | 125 ng |
| 1.5 µl | dNTP mix | 0.2 mM |
| 1.5 µl | QuikSolution reagent | - |
| Final volume of 50 µl | ddH ₂ O | - |

Table 3.5 Cycling parameters for the reactions of PCR site directed mutagenesis

| Segment | Cycles | Temperature | Time |
|---------|--------|-------------|--------------------------------|
| 1 | 1 | 95°C | 1 min |
| | | 95°C | 50 s |
| 2 | 18 | 60°C | 50 s |
| | | 68°C | 1 min /kb of plasmid length |
| 3 | 1 | 68°C | 7 min |

PCR amplified DNA plasmids were selected by digesting parental methylated and hemi-methylated DNA plasmids with DpnI enzyme at 37 °C for 1-2 hrs. DpnI digested PCR products were then used to transform chemically competent *E. coli* XL10-Gold ultra-competent cells (the same protocol of bacterial transformation, explained in chapter 2, was used). The transformation mixtures were spread on LB agar plates containing the appropriate antibiotic selection and grown overnight at 37°C. A single colony was selected and grown overnight in 10 ml LB medium containing the appropriate antibiotic selection. Then, DNA extraction was performed (the detailed procedures of DNA miniprep was mentioned in the previous chapter). In order to validate the proper size of the DNA, an amount of the prepared DNA was treated with the appropriate restriction enzymes (XbaI and NdeI).

The restriction enzyme digestion was carried out in a reaction volume of 20 μL containing 0.2-1.5 μg of DNA, 10u / μL (0.5 μL) of each restriction enzyme, 100XBSA (0.2 μL bovine serum albumin) and 10 μL of 10XBuffer 4 (50mM Potassium Acetate, 20 mM Tris-HCl, 10 mM MgCl_2 , 1mM Dithiothreitol, pH 7.9). The digestion mixture was incubated at 37°C overnight. The linearized DNA samples were then analysed by running 1% (w/v) agarose gel using wild type DNA plasmid as a reference. Following the analysis verifying appropriate size of the fusion gene of interest, the DNA was sent for sequencing to analyse whether the desired point mutation is present.

3.3.2.4 Expression and purification of the mutant proteins of rHIS-GST-CHFI

All the methods described in detail in chapter two (bacterial transformation, protein expression, protein purification and concentration, protein analysis and measurement), were also used as a template for the recombinant formation of the mutants.

3.4 Results and discussion

3.4.1 Prediction of CHF1-FXII interaction

In order to understand the selective inhibitory of CHF1, a prediction study of CHF1-FXIIa interaction was conducted by M Pathak (a research assistant in the structural biology group/ Emsley group) based on the following tools: first, the published crystal structure of CHF1 [136,156], second, the crystal structure of FXII zymogen-like protease domain[173] , and third, HGFA homology modelling. The prediction study showed that the residues of interest exist on the surface of the central inhibition loop projecting away from the body of CHF1 (**Figure 3.1**).

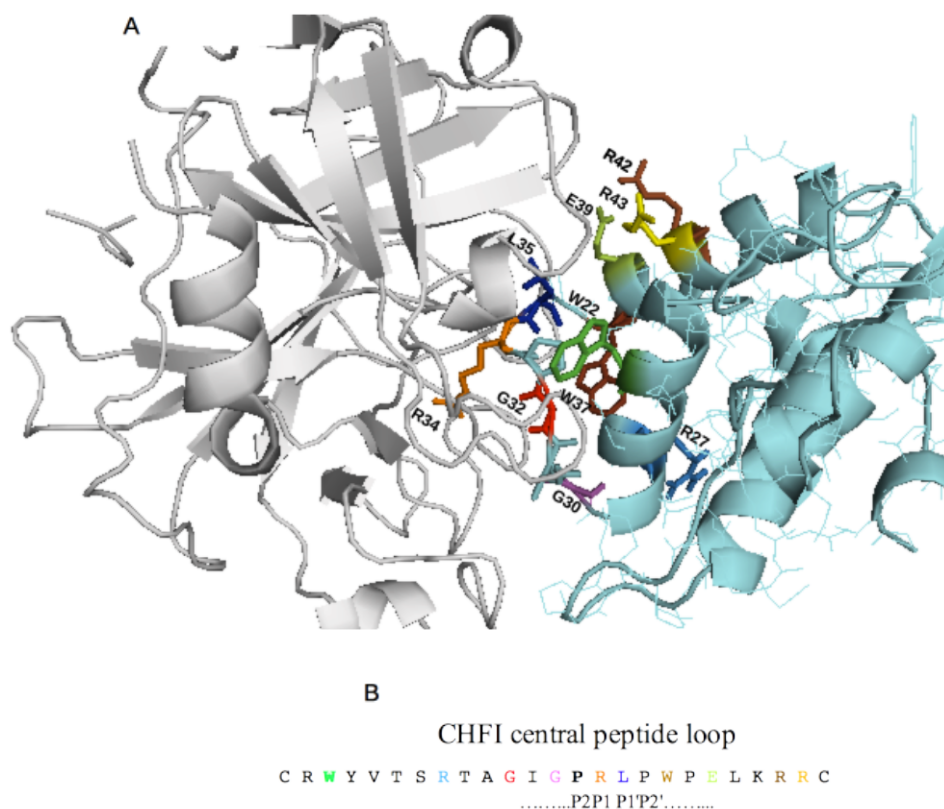


Figure 3.1 Prediction of CHFI-FXIIa interaction. The cyan cartoon on the right side is CHFI; the white grey on the left side is human coagulation FXII catalytic domain. The residues of interest are accumulated within the cluster of the central inhibition loop. The colours, green, sky blue, pink, red, orange, blue, chocolate, yellow-green, brown and yellow, represents Trp22, Arg27, Gly30, Gly32, Arg34, Leu35, Trp37, Glu39, Arg42, Arg43 at positions, P13, P8, P5, P3, P1, P1', P3', P5', P8' and P9' respectively.

It was anticipated that the fully exposed Arg34 projecting away from the body of the protein may have a central role in the inhibition of FXIIa. Arg34 at P1 substrate position was likely to extend into S1 pocket of FXII catalytic domain and bind to a potential target residue, Asp592. It was proposed that one nitrogen atom of the guanidinium group of Arg34 forms a hydrogen bond of 2.7 Å with Asp592 of FXII whereas the other nitrogen atom forms a hydrogen

bond of 2.4 Å with Gly621 in FXII. The carbonyl oxygen of Arg34 was anticipated to be located in the oxyanion hole, interacting with hydroxyl group of Ser598 of the catalytic triad and producing Michaelis complex. The catalytic triad is composed of Ser598, His447, and Asp597. Gly596 could also contribute to the catalytic reaction generated by the catalytic triad. Hence, Arg34 was expected to fill the space of S1 pocket and make a primary contribution to the affinity for the CHF1 inhibition of FXII protease domain (**Figure 3.2**).

This result is consistent with what has been hypothesized in the studies performed on trypsin, for instance, with reference to a study carried out in 1984, it was explained that the scissile bond exists between Arg34 and Leu35 of the exposed region of CHF1; this bond was predicted to be important for interaction with both trypsin and, presumably, with activated coagulation factor XII (FXIIa) [136, 156].

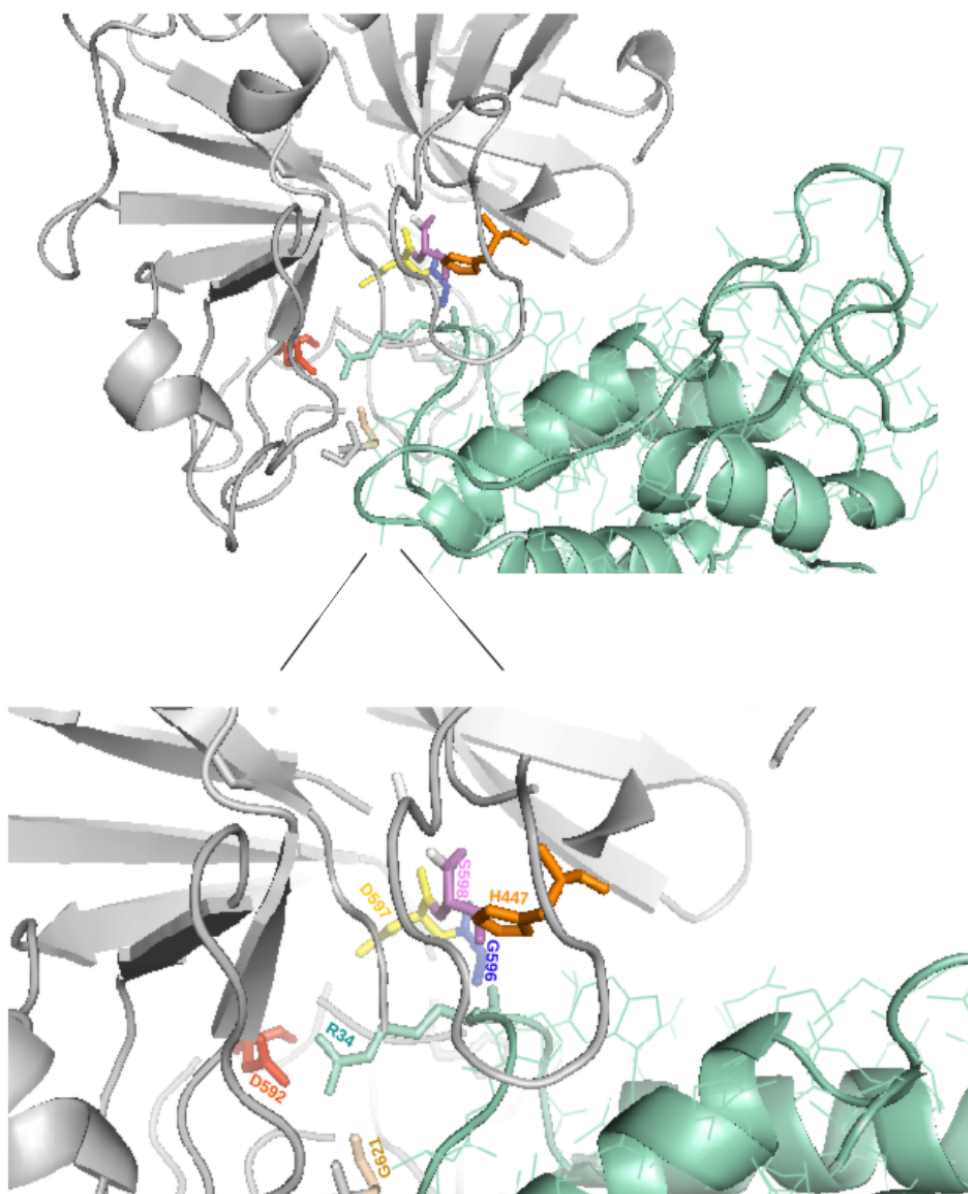


Figure 3.2 Prediction of the central, functional role of Arg34 in the inhibitory activity of CHF1. Arg34 at P1 position of the central inhibition loop of CHF1 was anticipated to interact with the Asp592 at S1 position of the catalytic domain of human coagulation FXIIa. Arg34 could form a hydrogen bond with Asp592 and Gly621 of FXIIa. The carbonyl oxygen of Arg34 is expected to interact with the catalytic triad composed of Ser598, His447, and Asp597. Gly596 of FXIIa could also contribute to this reaction.

Trp22 and Arg43 located at either ends of the central inhibition loop i.e. N-terminus and C-terminus respectively were predicted to be key residues for inhibition of FXIIa. These key residues would be important factors helping to elucidate specificity of CHF1 toward FXIIa. It was anticipated that a pocket can be created by loop 99 of FXII catalytic domain into which Trp22 inserts. Within the pocket, Gln450 at position S13 of FXIIa is likely to interact with Trp22 at position P13 of CHF1 by forming a hydrogen bond. Arg43 at position P9' of CHF1 is expected to form a salt bridge with Asp452 at S9' on the exposed surface of FXIIa; Asp452 can probably function as an exosite for substrate cleavage as well as function as a binding site for CHF1 (**Figure 3.3**)

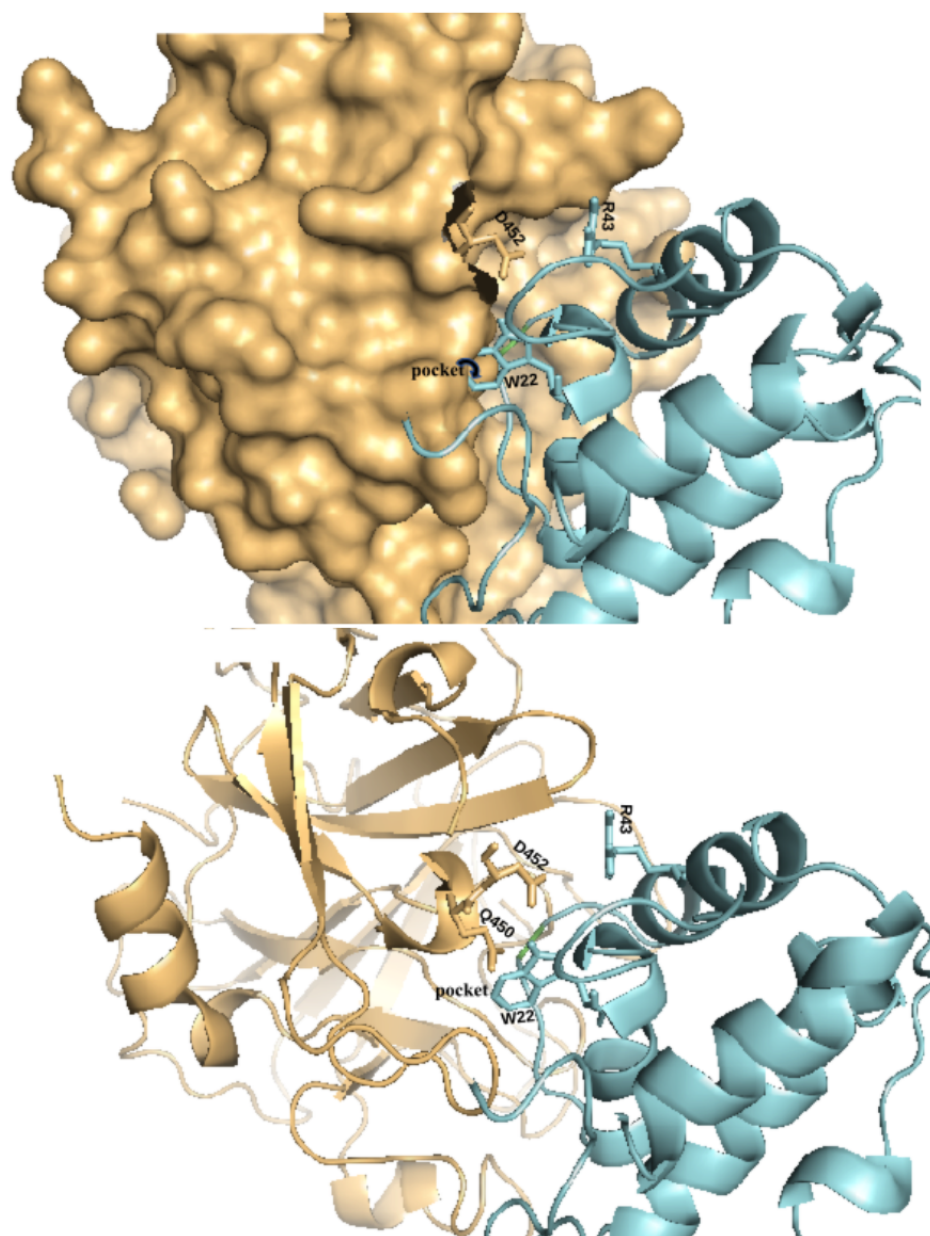


Figure 3.3 Key interaction residues relevant for elucidating specificity of CHF1 toward FXIIa. The cyan color picture on the right side is CHF1; the brown one on the left side is the protease domain of human coagulation FXIIa. The key residues were expected to be Trp22 and Arg43 at positions P13 and P9' respectively. A pocket is likely to be created by loop 99 of FXII into which Trp22 inserts; within the pocket, Gln450 of FXII could interact with Trp22 of CHF1 by forming a hydrogen bond. Arg43 is predicted to interact with Asp452 by forming a salt bridge.

Gly30, Ile31, Gly32, Pro33, Leu35, Pro36 and Pro38 at positions P5, P4, P3, P2, P1', P2' and p4' were predicted to be accumulated at the very top of the convex-shaped, exposed region of the central inhibition loop of CHF1, surrounding the central Arg34. The existence of the proline residues could maintain the rigidity of the loop whereas glycine residues can provide flexibility to the exposed surface. It was expected that Pro33 and Pro38 of CHF1 interact with Tyr493 and Glu548 of FXIIa respectively. Gly30 and Gly32 of CHF1 were anticipated to hydrogen bond with Trp618 and Gly619 of the cognate enzyme respectively. These residues are also present in the other protease inhibitor having sequence identity with CHF1. Leu35 could be important to maintain hydrophobic interaction of the inhibition loop (**Figure 3.4**).

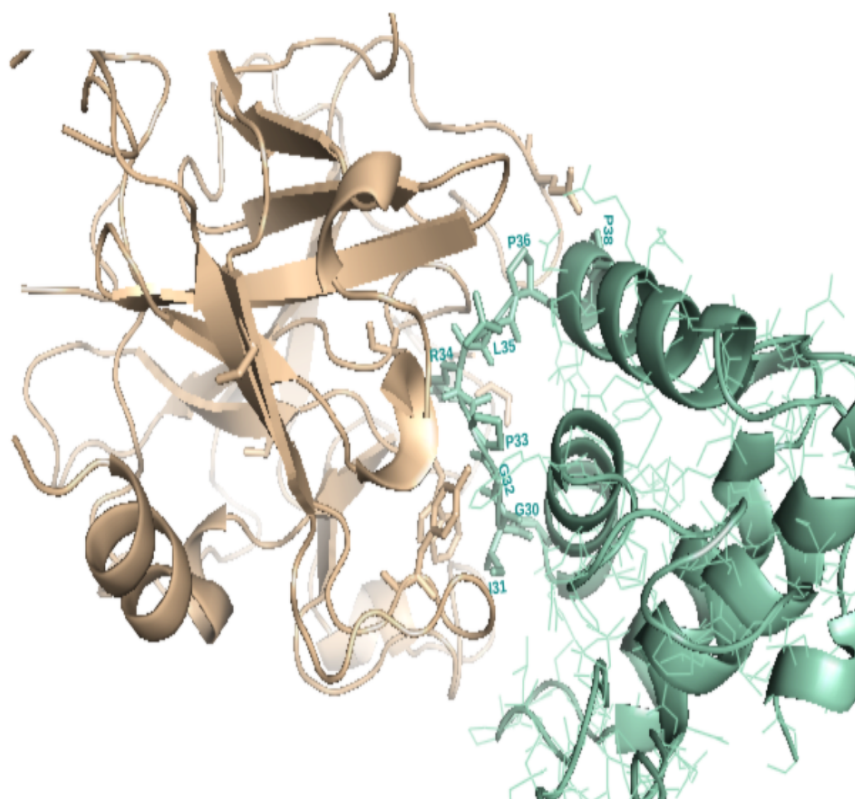


Figure 3.4 Residues affecting hydrophobicity and flexibility of the central inhibition loop. Gly30, Ile31, Gly32, Pro33, Leu35, Pro36 and Pro38 at positions P5, P4, P3, P2, P1', P2' and p4' were predicted to be accumulated at the very top of the exposed region of the inhibition loop of CHF1. These residues, surrounding the central Arg34, could be important for the function of Arg34.

At positions, P8, P5' and P8' of CHF1, the charged residues, Arg27, Glu39 and Arg42, are present. It was predicted that both Arg42 and Glu39 can hydrogen bond with His429 of the enzyme, and they also tend to form a hydrogen bond with each other on the surface of the central inhibition loop as they are close to each other. An aromatic, hydrophobic Trp37 may hydrogen bond with Glu545, existing at P3'. Arg27 was expected to be far away from the surface of FXIIa catalytic domain (**Figure 3.5**).

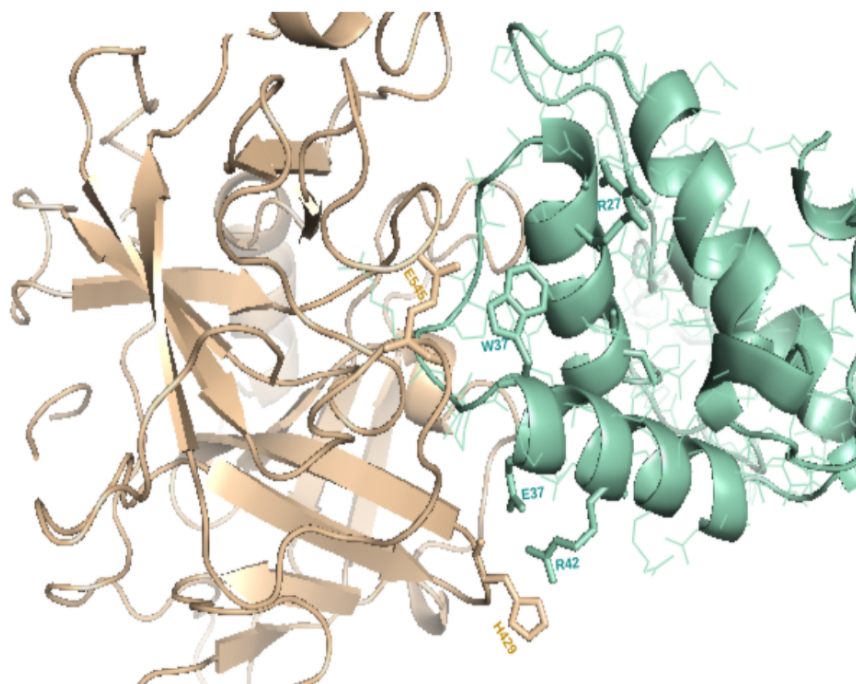


Figure 3.5 Charged residues and a hydrophobic-aromatic residue on the surface of CHFI central inhibition loop. The cyan colour picture on the right side is CHFI; the brown one on the left side is the protease domain of human coagulation FXII. Arg27, Trp37, Glu39 and Arg42 at positions P8, P3', P5' and P8' were expected to be present on the CHFI interaction surface. It was expected that Arg27 has no contribution to CHFI affinity whereas Glu39 and Arg42 may bind to His429 of the target enzyme via hydrogen bonds. Trp37 of CHFI is expected to bind to Glu545 of the enzyme.

On the basis of these observed interactions, the central residue, Arg34, and the two key interaction residues, Trp22 and Arg43, were chosen for point mutation. It is hypothesized that Arg34 would play a main, fundamental role in the function of CHFI. Trp22 and Arg43 would behave as two key interaction residues helping Arg34 function. In addition, Lue35, Gly30, Gly32, Glu39, Arg42, Arg27, and Trp37 were also selected for mutation. It is postulated that the replacement of Leu35 with Ala would affect the inhibition

of FXII due to the fact that Leu35 could retain hydrophobic interaction of the central inhibition loop. Furthermore, since this residue is adjacent to Arg34, any substitution mutation of this residue could cause a tremendous effect on the function of Arg34. The mutation of Gly30 and Gly32 would affect the flexibility of the loop. Replacement of Arg27 by Ala is likely to have no impact on the inhibition of FXII enzyme. The mutation of the charged residues, Glu39 and Arg42, and the hydrophobic residue, Trp37, is anticipated to have an effect on the inhibition activity of CHF1. Generation of these mutants and evaluation of their inhibition activity will be explained in detail in the following sections below.

3.4.2 Site-directed mutagenesis

Site-directed mutagenesis for all the twelve point mutations was performed using the protocol of Quik Change XL Site-Directed Mutagenesis Kit. Following DNA preparation from the positive colonies grown and DNA digestion, the appropriate size of the gene of interest (CHF1 gene) with a desired point mutation was analysed via 1% (w/v) Agarose gel prior to sequencing. Then, the mutations were all confirmed by DNA sequencing.

3.4.3 Preparation of the recombinant CHF1 mutants-expression and purification

In order to understand CHF1-FXIIa interaction, the validity of the interaction model was checked experimentally by generating different recombinant variants of CHF1 with the amino acid exchanges in the sequence positions assumed to be important (i.e. Trp22, Arg27, Gly30, Gly32, Arg34, Leu35, Trp37, Glu39, Arg42 and Arg43). Expression and purification of the different recombinant variants of CHF1 (rHIS-GST-CHF1-W22A, rHIS-GST-CHF1-R27A, rHIS-GST-CHF1-G30W, rHIS-GST-CHF1-G32W, rHIS-GST-CHF1-R34A, rHIS-GST-CHF1-L35A, rHIS-GST-CHF1-W37A, rHIS-GST-CHF1-E39A, rHIS-GST-CHF1-R42A, rHIS-GST-CHF1-R43A, rHIS-GST-CHF1-R27A-E39A and rHIS-GST-CHF1-R27A-R42A) were performed by means of the same template protocol used for soluble expression and single step purification of the properly folded recombinant wild type CHF1, rHIS-GST-CHF1, described in chapter two.

The proteins were quantified using the Lowry method and quantification was confirmed by SDS-PAGE, which then further validated accurate inhibitory concentrations used for characterization of the inhibitory activity of the twelve mutants elucidated below (**Figure 3.6**).



Figure 3.6 Expression and purification of CHFI mutants. 15% (w/v) SDS showed successful expression and Ni^{2+} column purification of the different recombinant variants of CHFI. The bands almost have the same thickness and intensification. This indicates that the same amount of the recombinant proteins were loaded, verifying that the concentration of the different proteins was accurately measured. The lanes 1, 2, 3...14 are protein marker, rHIS-GST-CHFI-W22A, rHIS-GST-CHFI-R27A, rHIS-GST-CHFI-G30W, rHIS-GST-CHFI-G32W, rHIS-GST-CHFI-R34A, rHIS-GST-CHFI-L35A, rHIS-GST-CHFI-W37A, rHIS-GST-CHFI-E39A, rHIS-GST-CHFI-R42A, rHIS-GST-CHFI-R43A, rHIS-GST-CHFI-R27A-E39A and rHIS-GST-CHFI-R27A-R42A respectively.

3.4.4 Inhibitory activity of the mutants against rHIS-GST-CHF1

Inhibitory activity assays were performed for all the recombinant CHF1 mutants and compared to that of the recombinant wild type. Inhibitory activity, representing inhibition effect of CHF1 different forms on the catalytic activity of FXIIa enzyme, was measured by the effect of the recombinant wild type (rHIS-GST-CHF1) and the different mutants on the amount of the chromophore released from amidolytic breakdown of the chromogenic substrate (S-2032) by FXIIa using the established colorimetric assay elucidated in detail in chapter two. The inhibitory assay of rHIS-GST-CHF1, as a positive control, was used as a reference guide for the analysis of the inhibitory activity of the mutants. According to their inhibitory activity, the recombinant variants of CHF1 were classified into two main categories: wild type like mutants and non-wild type like mutants. The former would refer to those mutants behaving like rHIS-GST-CHF1 and having no influence on binding whereas the latter would be defined as the mutants having a significant effect on binding. The latter can be further subdivided into two groups according to their affinity, the mutants displaying complete loss of binding and those having partial loss of binding.

3.4.5 Experimental validation of the crucial role of the central Arg34 in the inhibitory function of CHF1

In the current study, it was predicted that the fully exposed Arg34 has a central role in the inhibition of FXIIa. To experimentally verify this prediction, the inhibitory activity of the rHIS-GST-CHF1-R34A was performed using the inhibition assay of rHIS-GST-CHF1 as a positive control. Substitution of the positively charged Arg34 at P1 substrate site with hydrophobic Ala34 caused complete loss of affinity of the inhibitor and didn't show any inhibition effect on the catalytic activity of FXIIa. Even at high concentration, the mutant was not able to produce any inhibition. This finding indicates that Arg34 plays a fundamental role in the binding of CHF1 to FXIIa. Hence, substitution of this residue with Ala completely obliterates the inhibition; this verified the appropriateness of the docking model described in the current study. In addition, this finding is consistent with what has been hypothesized in the studies performed on trypsin, for instance, with reference to a study carried out in 1984, it was identified that the scissile bond exists between Arg34 and Leu35; the study postulated that this bond is involved in the interaction with both trypsin and, presumably, with activated coagulation factor XII (FXIIa) [136,156].

Arg34 at P1 substrate position is expected to extend into S1 pocket of FXII catalytic domain and bind to a potential target residue, Asp592, by hydrogen bond. Arg34 may also form a hydrogen bond with Gly621 of the target enzyme. The carbonyl oxygen of Arg34 is expected to interact with the hydroxyl group of Ser598 in the catalytic triad cave of FXIIa. This would

suggest that Arg34 occupy the space of S1 pocket and make a crucial contribution to the inhibition of FXII protease domain by CHF1 (**Figure 3.7**). However, Arg34 is not enough to justify selectivity of CHF1 toward FXIIa due to two reasons. The first, with reference to the present docking model, is that there would be key residues expected to participate in the CHF1 binding to FXIIa. The second is Arg34 at a similar position, P1, of the central inhibition loop was also previously found in the other protease inhibitors lacking inhibitory effect on FXIIa, for example, RATI. This protease inhibitor has sequence identity with CHF1.

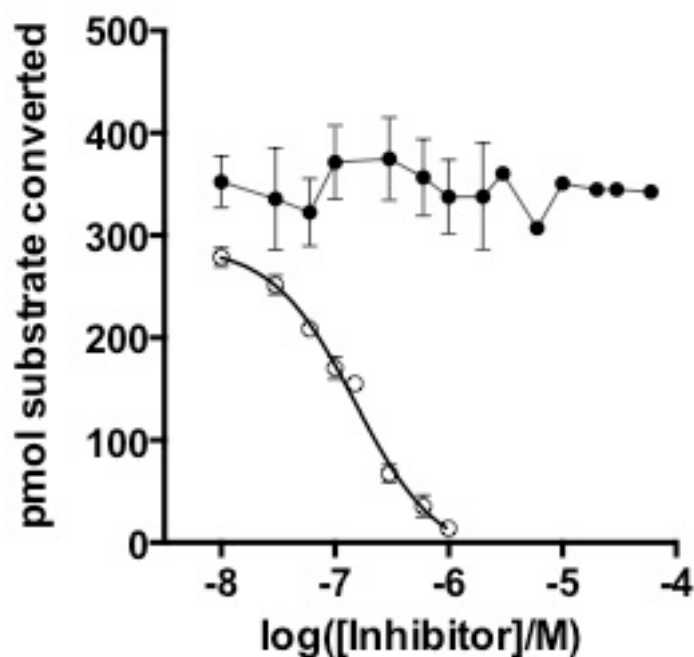


Figure 3.7 Experimental verification of the functional role of Arg34. Substitution of this residue with Ala completely abolished the inhibition of FXIIa. Even at higher concentration of rHIS-GST-CHFI-R34A (2, 3, 6, 10, 20, 30, 60 μM), the mutant didn't inhibit the enzyme. The positive control showed significant inhibition. The markers (\square and \bullet) represent rHIS-GST-CHFI and rHIS-GST-CHFI-R34A respectively. The error bar is standard error of the mean of three independent experiments. In each experiment, a duplicate was used for testing every single concentration of the different recombinant variants of CHFI. Average of the duplicate results was taken.

3.4.6 Inhibitory effect of rHIS-GST-CHFI-L35A, rHIS-GST-CHFI-G30W, and rHIS-GST-CHFI-G32W on FXIIa

With the purpose of evaluating the contribution of Leu35, Gly30 and Gly32 to the function of CHFI, substitutions with Ala35, Trp30 and Trp32 were introduced and the inhibitory activity of rHIS-GST-CHFI-L35A, rHIS-GST-CHFI-G30W, and rHIS-GST-CHFI-G32W was conducted. None of these were able to inhibit FXIIa at low concentrations, but they did at higher

concentration (**Figure 3.8**). They would be described as partial inhibitors. The inhibition effectiveness of rHIS-GST-CHF1-G30W was approximately 3 times less potent than that of the wild type, rHIS-GST-CHF1 (Table 3.6). The minimum concentration values of rHIS-GST-CHF1-L35A and rHIS-GST-CHF1-G32W at which 50% inhibition is achieved are 5 μ M and 23 μ M respectively. There may be the following reasons behind this observation. With respect to Gly30 and Gly32, replacement of these residues with any other amino acids means the addition of new bulky group side chain; this is due to the fact that glycine is unique as it contains just hydrogen as its 'side chain'. In addition, glycine is generally often found at the surface of proteins, often within loops, providing high conformational flexibility to these regions. The flexibility is due to absence of a carbon side chain. Gly30 and Gly32 of CHF1 are expected to form hydrogen bonds with Trp618 and Gly619 of the cognate enzyme respectively. Compared to Gly30, Gly32 resulted in a decrease in the inhibition effect; the reason for that would be explained below. Gly32 position is nearer to the top of the convex-extended protease binding loop and central Arg34; hence, the impact of the reduction in flexibility on the inhibition effect could be higher. Replacement of Gly32 with Trp would affect the rigidity of Pro33 existing adjacent to Arg34 (proline has the opposite effect, providing rigidity to the protein structure as its side chain is connected to the protein backbone twice, forming a five-membered ring). This would then affect the rigidity of the loop and then the function of Arg34. With respect to the point mutation of Leu35, the first reason of the obliteration of the inhibition would be that Leu35 is $C\gamma$ branched. This means that there is a lot more bulkiness near to the protein backbone (N-terminus). This would affect

its hydrophobic interaction when substituted by an Ala having no a branched carbon in its side chain. The second reason would be that Leu35 at position P1' is adjacent to Arg34; hence, any point mutation of it could cause a dramatic change in the inhibition function. Compared to rHIS-GST-CHFI-G32W, the slightly higher inhibition effect of rHIS-GST-CHFI-L35A could be resulted from that, to some extent, Ala could retain hydrophobic interaction property of Leu 35 and the central inhibition loop whereas replacement of Gly32 with hydrophobic Trp would substantially affect the rigidity and hydrophobicity of the loop. However, these residues cannot explain the specificity of CHFI due to three reasons; the first reason is Gly has hydrogen as its side chain (as mentioned above) and Leu side chain is very non-reactive. The second reason would be that the synthetic peptide (heptapeptide, IGPRLPWP, described below in **3.4.9 section**) of the convex region of the central inhibition loop did not show any inhibition effect toward FXIIa. The last, these three residues with the central Arg34 are present in the same position of the inhibition loop of the protease inhibitor, RATI, lacking inhibitory activity against FXIIa. The experimental observation of behaviour of these three mutants is in agreement with the prediction model of the current CHFI-FXIIa interaction study; this would further verify that the central inhibition loop region would be responsible for the inhibition function against CHFI.

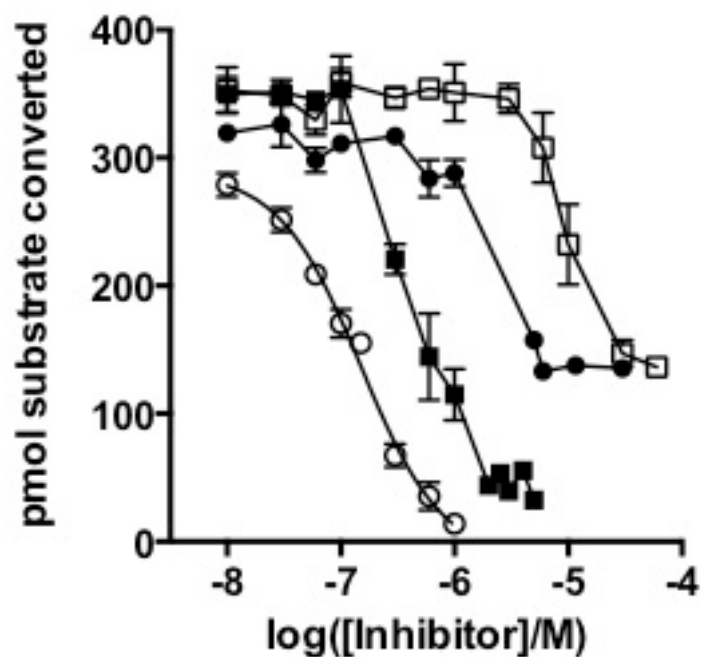


Figure 3.8 CHFI mutants acting as partial inhibitors of FXIIa. Substitution of Gly30 and Gly32 with Trp and substitution of Leu34 with Ala reduced the inhibitory activity using the inhibition effect of the recombinant wild type, rHIS-GST-CHFI, as a reference. The amidolytic activity of FXIIa blocked by the different recombinant variants of CHFI reflects pmol of S-2302 converted /pmol of enzyme/sec. The error bar is standard error of the mean of three independent experiments. In each experiment a duplicate was used for testing every single concentration of the different forms of CHFI. Average of the duplicate results was taken. The symbols (●, □, ■ and ○) indicate rHIS-GST-CHFI-L35A, rHIS-GST-CHFI-G32W, rHIS-GST-CHFI-G30W, and rHIS-GST-CHFI respectively.

Table 3.6 Inhibition effectiveness of the mutants behaving as partial inhibitors. The value of IC_{50} of the different recombinant variants (mutants) of CHF1 was analysed using the recombinant wild type, rHIS-GST-CHF1, as a positive control. The error bar is standard error of the mean of three independent experiments. In every experiment, a duplicate was used for each single concentration of the inhibitors. Average of the duplicate results was taken.

| Different recombinant variants | IC_{50} (μ M) | |
|--------------------------------|----------------------|-------------------------|
| | Constraining fit | Ordinary (floating) fit |
| rHIS-GST-CHF1 | 0.11±0.02 | 0.11±0.02 |
| rHIS-GST-CHF1-G30W | 0.30±0.003 | 0.35±0.02 |
| rHIS-GST-CHF1-G32W* | 23 | 23 |
| rHIS-GST-CHF1-L35A* | 5 | 5 |

* The inhibition effectiveness of the mutants is defined as the minimum concentration value at which 50% inhibition is achieved.

3.4.7 The effect of rHIS-GST-CHF1-R27A, rHIS-GST-CHF1-W37A, rHIS-GST-CHF1-E39A, and rHIS-GST-CHF1-R42A on the inhibition of FXII enzyme

With reference to the prediction study of CHF1-FXIIa interaction, the aim of this section was to evaluate the influence of the point mutations, R27A, W37A, E39A, and R42A on the function of CHF1. The mutants, rHIS-GST-CHF1-R27A, rHIS-GST-CHF1-W37A, rHIS-GST-CHF1-E39A, and rHIS-GST-CHF1-R42A, did not show an effect on the inhibitory activity and behaved like the recombinant wild type CHF1, rHIS-GST-CHF1 (**Figure 3.9**). Their potency of inhibition was comparable to that of rHIS-GST-CHF1. The

values of IC_{50} for rHIS-GST-CHFI, rHIS-GST-CHFI-R27A, rHIS-GST-CHFI-W37A, rHIS-GST-CHFI-E39A, and rHIS-GST-CHFI-R42A are 109 ± 20 , 117.05 ± 6 , 105 ± 5 , 118 ± 8 and 126 ± 20 nM (using ordinary fit analysis), and 110 ± 20 , 123 ± 7 , 101 ± 3 , 127 ± 12 , and 130 ± 18 (nM) (using constraining fit analysis) respectively (**Table 3.7**). This indicates that when substituting Arg27, Trp37, Glu39, and Arg42 with Ala, the affinity of Arg34 of the central inhibition loop kept unaffected, suggesting that they would not be essential for the inhibition function of CHFI toward α -FXIIa. To further analyse their potential effect in the form of combination, the mutants with two point mutations, rHIS-GST-CHFI-R27A-E39A and rHIS-GST-CHFI-R27A-R42A, were generated and then tested against α -FXIIa. These mutants did not show an influence on the binding of CHFI to FXIIa either (**Figure 3.10**). The values of IC_{50} of rHIS-GST-CHFI-R27A-E39A and rHIS-GST-CHFI-R27A-R42A are 142 ± 28 and 117 ± 13 nM (using ordinary fit) and 157 ± 26 and 130 ± 16 nM (using constraining fit) respectively (**Table 3.7**). With respect to the substitution of Arg27 by Ala, lack of alteration in the inhibition effect is consistent with the prediction study as this residue is far away from the exposed surface of α -FXIIa catalytic domain. When substituting Trp37, Glu39, and Arg42 by Ala, the reason of the absence of modification in the inhibitory activity would be that Ala could form hydrogen bond having about the same strength as that formed by Glu39 and Arg42 with His429 and as that formed by Trp37 with Glu595 on the enzyme surface. In addition, in the case of Trp37, the hydrogen bond predicted to be formed between this residue and Gln595 could be very weak as the length of the bond is 4.6 Å.

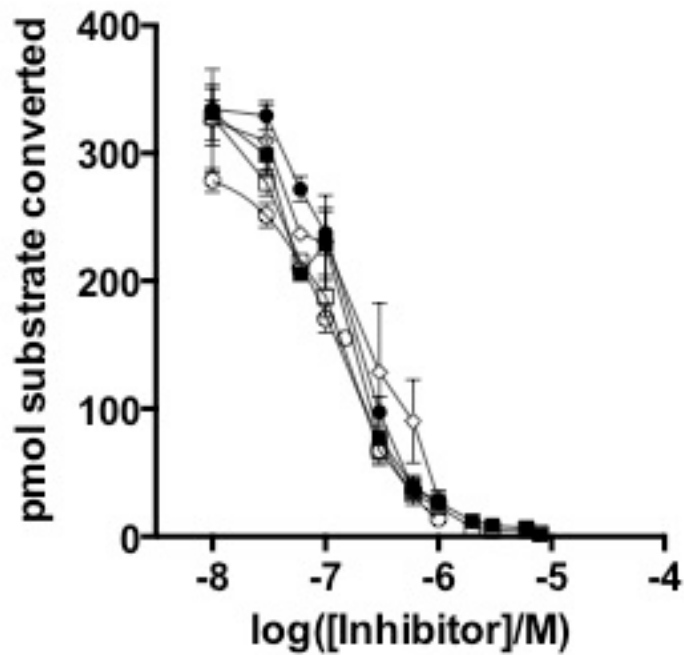


Figure 3.9 Inhibitory activity of the wild type like mutants. The inhibitory activity of the mutants, rHIS-GST-CHFI-R27A ●, rHIS-GST-CHFI-W37A □, rHIS-GST-CHFI-E39A ■ and rHIS-GST-CHFI-R42A ◇ resembles that of the wild type, rHIS-GST-CHFI ○, which was used as a positive control. Hydrolytic activity of α -FXIIa treated with the different recombinant variants of CHFI reflects pmol of S-2302 converted /pmol of enzyme/sec. The error bar is standard error of the mean of three independent experiments. In each experiment a duplicate was used for each concentration of CHFI various forms. Average of the duplicate results was taken.

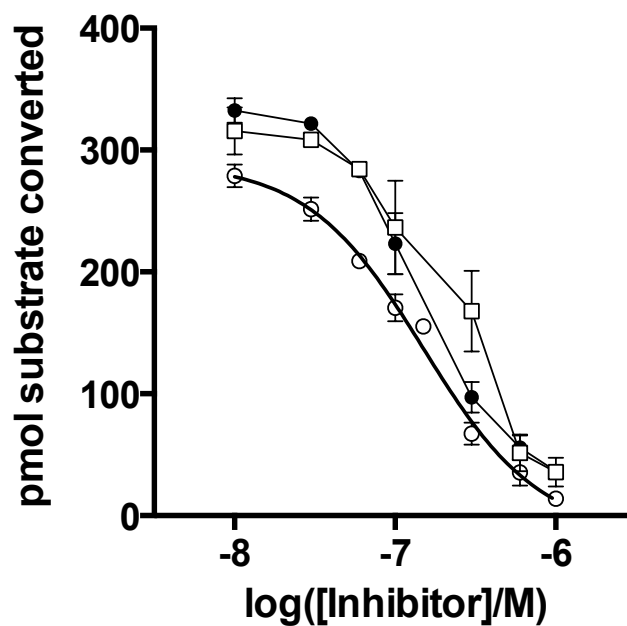


Figure 3.10 Effect of double point mutations on the inhibitory activity of CHFI. rHIS-GST-CHFI-R27AR42A \bullet and rHIS-GST-CHFI-R27AE39A \square resemble rHIS-GST-CHFI \circ in the inhibitory activity. Amidolytic activity of α -FXIIa treated with the different recombinant variants of CHFI reflects pmol of S-2302 converted /pmol of enzyme/sec. The error bar is standard error of the mean of three independent experiments. In each experiment a duplicate was used for each concentration of CHFI various forms. Average of the duplicate results was taken.

Table 3.7 Inhibitory activity of the wild type like mutants. Inhibition effectiveness value (IC_{50}) of the wild type-like mutants in comparison with that of the recombinant wild type, rHIS-GST-CHF1, was evaluated. The error is standard error of the mean of three independent experiments. In every experiment a duplicate was used for each single concentration of the inhibitors. Average of the duplicate results was taken.

| Different recombinant variants | IC_{50} (nM) | |
|--------------------------------|------------------|-------------------------|
| | Constraining fit | Ordinary (floating) fit |
| rHIS-GST-CHF1 | 110±20 | 109±20 |
| rHIS-GST-CHF1-R27A | 123 ±7 | 117.05 ±6 |
| rHIS-GST-CHF1-W37A | 101±3 | 105 ±5 |
| rHIS-GST-CHF1-E39A | 127±12 | 118±8 |
| rHIS-GST-CHF1-R42A | 130±18 | 126±20 |
| rHIS-GST-CHF1-R27A-E39A | 157±26 | 142 ±28 |
| rHIS-GST-CHF1-R27A-R42A | 130±16 | 117±13 |

3.4.8 Experimental verification of the significance of two key interaction residues, Trp22 and Arg43, for the inhibitory activity of CHF1

The aim in this section was to experimentally verify the relevance of the predicted key residues Trp22 and Arg43, demonstrated in the docking study, in explicating the specific inhibitory activity of CHF1 toward FXIIa. The protein mutants, rHIS-GST-CHF1-W22A and rHIS-GST-CHF1-R43A, were

assayed for inhibitory activity. These two mutants did not obliterate the catalytic activity of α -FXIIa at low concentration (10, 30, 60, 100, 300, 600, 1000 nM), but they started to inhibit at higher concentrations (2, 3, 4, 5, 6000, 10, 20, 30, 60 μ M) (**Figure 3.11**).

They would be known as partial inhibitors. Hence, in the current study, the two key residues (Trp22 and Arg43) were first identified, which would be important factors for explaining the question of specificity of CHF1 against α -FXIIa, having been under investigations for many years. The minimum concentration value of rHIS-GST-CHF1-W22A and rHIS-GST-CHF1-R43A at which 50% inhibition is achieved is 20 μ M and 17 μ M respectively (Table 3.8). This finding further verifies the appropriateness of the docking study. In correlation with the prediction model, it would be suggested that loop 99 in FXIIa may create a pocket into which Trp22 inserts and this pocket could not be found in the other coagulation proteases. In the space of this pocket, Gln450 of FXIIa could interact with Trp22 of CHF1 by forming a hydrogen bond. The key interaction residue, Arg43, would be expected to form a salt bridge with the aspartic acid (Asp452) on the exposed surface of FXIIa; Asp452 can function as an exosite for substrate cleavage as well as function as a binding site for CHF1.

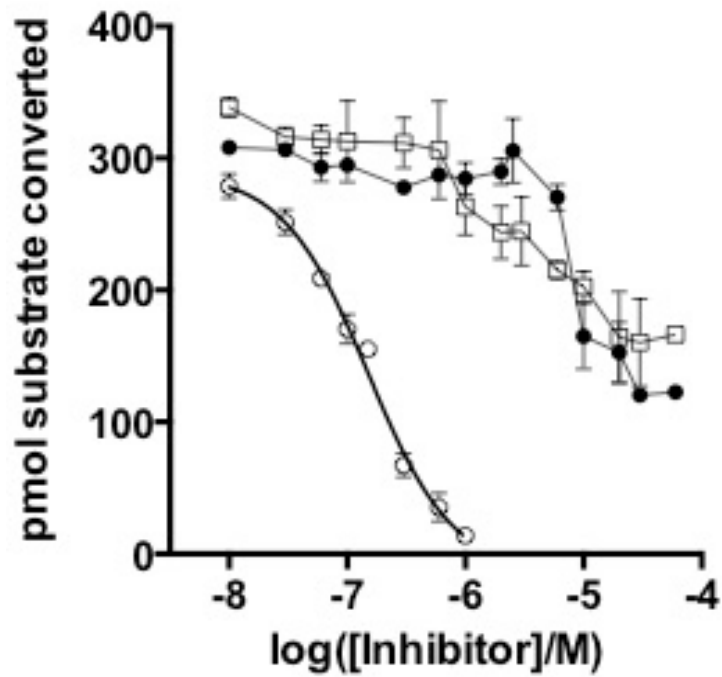


Figure 3.11 Inhibitory activity of rHIS-GST-CHFI-W22A and rHIS-GST-CHFI-R43A. The experimental validation of the key interaction residues relevant for elucidating septicity of CHFI toward FXIIa was examined. At high concentration, the mutants, rHIS-GST-CHFI-W22A \square and rHIS-GST-CHFI-R43A \bullet , partially blocked the cognate enzyme using rHIS-GST-CHFI \circ as a positive control. The Error bar is standard error of the mean of three independent experiments. In each experiment a duplicate was used for every concentration of CHFI. Average of the duplicate results was taken.

Table 3.8 Inhibitory activity of rHIS-GST-CHFI-W22A and rHIS-GST-CHFI-R43A. Inhibition effectiveness value (IC_{50}) of the mutants lacking the key residues was analysed using the recombinant wild type, rHIS-GST-CHFI, as a reference. The error is standard error of the mean of three independent experiments. In every experiment a duplicate was used for each single concentration of the inhibitors. Average of the duplicate results was taken.

| | | IC_{50} (μ M) | |
|---------------------|-------------|----------------------|-------------------------|
| Different variants | recombinant | Constraining fit | Ordinary (floating) fit |
| rHIS-GST-CHFI | | 0.11±0.02 | 0.11±0.02 |
| rHIS-GST-CHFI-W22A* | | 20 | 20 |
| rHIS-GST-CHFI-R43A* | | 17 | 17 |

* The inhibition effectiveness of the mutants is defined as the minimum concentration value at which 50% inhibition is achieved.

3.4.9 Investigation of the inhibitory activity of the synthetic isolated peptides of CHFI central inhibition loop: with relevance to the role of the Cys20-Cys44 in the function/active conformation of the loop

With reference to the outcome of the prediction study and experimental validation via point mutation, the central inhibition loop would be responsible for the function of CHFI. The two key interaction residues with FXIIa would be present at N-terminus and C-terminus of the central loop peptide. The purpose of the peptide assay is, firstly, to evaluate the relevance of the central inhibition loop peptide in the inhibitory activity of CHFI, secondly, to investigate the necessity of Cys20-Cys44 disulphide-coupled peptide folding

of the inhibition loop for the function of the key residues, and lastly, to further validate the importance of Arg34, Trp22, and Arg43 for elucidating function and specificity of CHF1 toward coagulation FXIIa. To do so, different peptides were designed (explained in the section of materials and methods). It was observed that the scrambled peptide, as a negative control, and the heptapeptide, the short peptide having only eight residues at the very top of the exposed region, did not have any inhibitory activity (**Figure 3.12**). This finding would be explained as follows: the scrambled peptide usually does not have effect due to derangement of the amino acid residues. The short peptide lacks peptide folding important for enabling Arg34 to have the fundamental function in the inhibition of FXIIa; this could be resulting from the absence of both key residues, Trp22 and Arg43; to further analyse these possible postulations, the inhibitory activity of the other peptide forms was analysed. The linear peptide - the non-cyclic peptide lacking the two Cys residues existing usually at the either ends of the peptide inhibited the coagulation protease at IC_{50} 321 ± 0.00 and 452 ± 51 (μ M) using floating fit and constraining fit respectively (**Table 3.9**). The peptide is 3×10^3 - 4.5×10^3 -fold less potent an inhibitor than the original recombinant wild type, rHIS-GST-CHF1

For the purpose of understanding the functional role of Cys20-Cys44 disulphide bridge, the cyclic peptide was also tested for inhibitory activity. Compared to that of the linear peptide, the peptide displayed the same inhibition effectiveness with IC_{50} 293 ± 15 and 346 ± 58 (μ M) using floating and constraining fit respectively (**Table 3.9**). This finding is perhaps due to that the key interaction residues that would explain the inhibitory activity of CHF1 against FXIIa are at either ends of the peptide i.e. Trp22 at N-terminus and

Arg43 at C-terminus of the inhibition loop. These two interaction residues may help the peptide fold around and negate the dependence on the Cys20-Cys44 disulphide bridge. To further verify this conclusion, the inhibitory activity of the non-cyclic peptide lacking the key residues was evaluated, explained below in detail.

Weak inhibition activity of the isolated peptides compared to the intact protein was expected because the active conformation of three-dimensional structure (geometric shape) of the whole CHF1 protein could give rise to such a rigidity / flexibility of the central inhibition loop bringing about a proper, fully functional folding of the loop helping the key residues of interaction with FXIIa have full affinity for their potential target residues on the exposed surface of FXIIa. The angle between two α -helices is likely to play an important role in the rigidity of the loop and tight interaction with FXIIa. However, in the case of the isolated peptides, such a rigidity/felxibility of the loop couldn't happen; hence, the key residues would have less affinity for their targets.

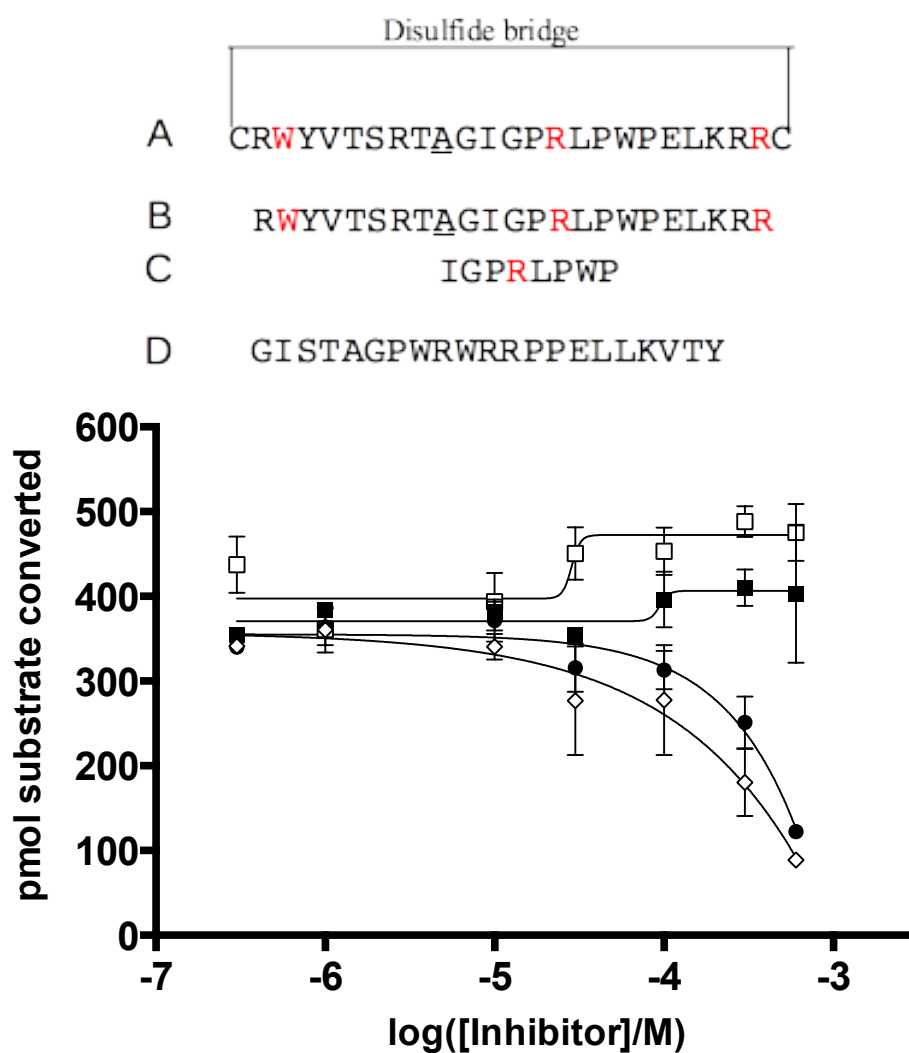


Figure 3.12 Inhibitory activity of the synthetic, isolated peptides of the central inhibition loop. A is the cyclic peptide \diamond ; B is the linear peptide \bullet ; C is the eight residues at the very top of the convex-shaped central inhibition loop \blacksquare ; D is the scrambled peptide \square , Error bar represents the standard error of the mean of three independent experiments. In each experiment a duplicate was used for testing every concentration of the different forms of the peptides. Average the duplicate result was taken.

Table 3.9 Inhibition activity of the linear peptide, cyclic peptide, and short peptide. Inhibition effectiveness value (IC_{50}) of the different peptide forms of the central inhibition loop of CHF1 in comparison with the recombinant wild type CHF1 was analysed using the scrambled peptide as a negative control. The error is standard error of the mean of the three independent experiments. In every experiment a duplicate was used for testing each concentration of the different forms. Average of the duplicate results was taken.

| Different forms | IC_{50} (μM) | |
|-------------------|-----------------------|-------------------------|
| | Constraining fit | Ordinary (floating) fit |
| rHIS-GST-CHF1 | 0.11±0.02 | 0.11±0.02 |
| Linear peptide | 452±51 | 321±0.00 |
| Cyclic peptide | 346±58 | 293±15 |
| heptapeptide | - | - |
| Scrambled peptide | - | - |

3.4.10 Evaluation of the inhibitory activity of the linear peptide lacking Trp22 and Arg43

The aim of this assay was to investigate the assumption that the key residues at N-terminus and C-terminus of the linear peptide would help the peptide fold around. The omission of Trp22 abolished the binding with inhibition effectiveness values $1985 \pm 0.00 \mu M$ (floating fit) and $1121 \pm 26 \mu M$ (constraining fit) (**Table 3.10**). Hence, this would additionally verify the following points: Trp22 appears to be an important residue for interaction with

FXIIa; this is consistent with the result of the characterization study of CHFI mutants. The linear peptide would negate the dependence on the disulphide bridge as both Trp22 and Arg43 can help the peptide fold around. However, the peptide missing Arg43 retained the inhibitory activity with IC_{50} 201 ± 10 and 148 ± 14 μ M using ordinary and constraining fit respectively. The reason behind this behaviour would be that Arg42 at C-terminus could substitute for Arg43 in the interaction with FXIIa (**Figure 3.13**).

A study reported that CHFI has weak inhibitory activity against FXIa and plasmin146. This finding in combination with the results of the current study would propose that prediction studies of CHFI interaction with other coagulation-fibrinolysis proteases and inhibitory activity of CHFI isolated peptides against these proteases would be necessary. This would be important for identifying if there is an extra factor elucidating specificity of the key interaction residues for the potential targets on FXIIa, for example, initiation of steric effect when CHFI molecule comes close to the molecules of the other coagulation proteases whereas absence of such an effect during CHFI-FXIIa interaction. 172

A YVTSRTAGIGPRLPWPELKRR
 B RWYVTSRTAGIGPRLPWPELKR
 C GISTAGPWRWRRPPELLKVTY

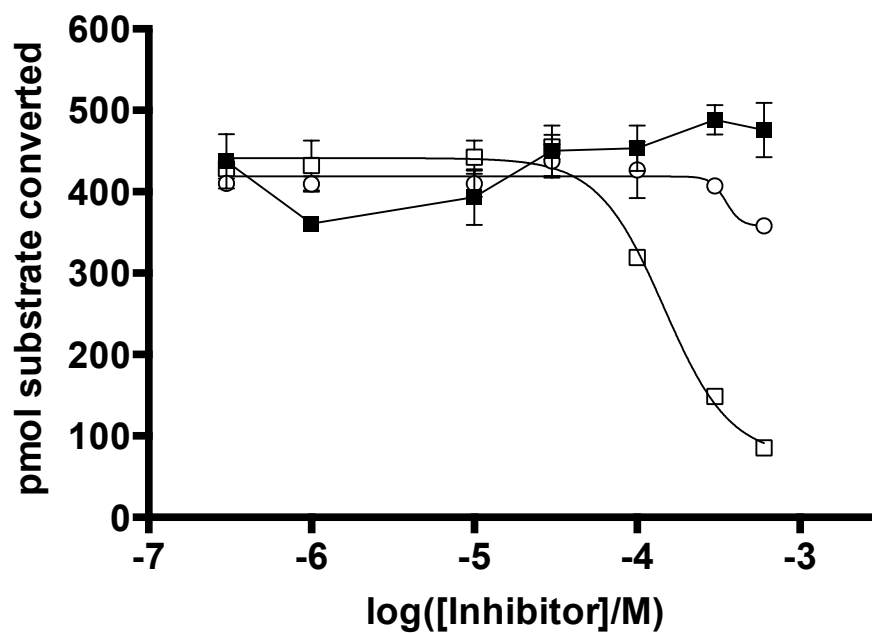


Figure 3.13 Inhibitory activity of Trp22-lacking and Arg43-lacking peptides. A \diamond is non-cyclic peptide lacking the key residue, Trp22; B \square is non-cyclic peptide lacking the key residue, Arg43; C \blacksquare is the scrambled peptide. The error bar is standard error of the mean of three independent experiments. In each experiment a duplicate was used for testing every concentration of the different forms of the peptides. Average of the duplicate results was taken.

Table 3.10 Inhibition activity of Trp22-deficient and Arg43-deficient peptide. Inhibition effectiveness value (IC_{50}) of the different peptide forms of the central inhibition loop of CHF1 in comparison with the recombinant wild type CHF1 was shown using the scrambled peptide as a negative control. The error is standard error of the mean of the three independent experiments. In every experiment, a duplicate was used for testing each concentration of the different forms of the peptide. Average of the duplicate results was taken.

| Different forms | IC_{50} (μM) | |
|------------------------------|-----------------------|-------------------------|
| | Constraining fit | Ordinary (floating) fit |
| rHISGSTCHF1 | 0.11±0.02 | 0.11±0.02 |
| Linear peptide lacking Trp22 | 1121 ±26 | 1985 ±0.00 |
| Linear peptide lacking Arg43 | 148±14 | 201 ±10 |
| Scrambled peptide | - | - |

3.5 Conclusion

Site directed mutagenesis was used successfully for twelve mutants with the desired point mutations. Guided by the established, effective expression and single-step purification system for generating soluble and functional recombinant rHIS-GST-CHFI explained in chapter 2, soluble expression and purification of the different recombinant variants of CHFI, rHIS-GST-CHFI-W22A, rHIS-GST-CHFI-R27A, rHIS-GST-CHFI-G30W, rHIS-GST-CHFI-G32W, rHIS-GST-CHFI-R34A, rHIS-GST-CHFI-L35A, rHIS-GST-CHFI-W37A, rHIS-GST-CHFI-E39A, rHIS-GST-CHFI-R42A, rHIS-GST-CHFI-R43A, rHIS-GST-CHFI-R27A-R42A and rHIS-GST-CHFI-R27A-R42A were performed successfully. Characterization of the inhibitory activity of the mutant proteins of interest was performed using the developed, principal inhibition assay of rHIS-GST-CHFI as a template. The central Arg34 at the very top of the fully exposed region of the CHFI inhibition loop plays a crucial role in the inhibition function of CHFI against human coagulation FXIIa. Trp22 at the N-terminus and Arg43 at the C-terminus of the central inhibition loop are two key residues for interaction of CHFI with FXIIa. They can be speculated to be two factors important for elucidating the question of specific inhibitory activity of CHFI toward the cognate enzyme. Cyclic and no-cyclic forms of the synthetic isolated peptide of CHFI central inhibition loop showed the same inhibition effectiveness, suggesting that Cys20-Cys44 disulphide bridge would be irrelevant for the inhibitory activity of the isolated peptide. The reason may be that the two key residues at the either ends of the peptide would help the peptide fold around and negate the dependence on the Cys20-Cys44 disulphide bond. Further studies, for example, prediction studies of

CHFI interaction with other coagulation proteases and inhibition activity of the isolated peptides toward other coagulation enzymes, for example, FXa would be required. This would be important for finding if there is an additional factor explicating specificity of the key interaction residues for the potential targets on FXIIa, for example, induction of steric hindrance when CHFI molecule comes in contact with the target molecules of the other coagulation factors like FX and FXI is assumed to happen while such an influence is impossible to take place during CHFI-FXIIa interaction.

Chapter 4: Dual kinetic mechanisms of CHF1: relevance to the hypothesis of tight binding of CHF1 to the different forms of human coagulation FXIIa, α -FXIIa, β -FXIIa and MBP- β - FXIIa

4.1 Abstract

Reversible inhibitors usually form noncovalent interactions with the enzyme surface, which can be rapidly reversed by dilution or dialysis. Irreversible inhibitors usually interact with the different functional groups on the enzyme surface by forming covalent bonds that often persist even during complete protein breakdown. The last type of inhibitors is a typical group known as tight-binding inhibitors, which usually bind tightly to the enzyme in a noncovalent interaction and remain bound for some time, but ultimately dissociate from enzyme. The current study aimed pharmacologically at examining the mechanisms of inhibition of the different forms of human coagulation FXIIa by CHF1 with relevance to the postulation of the tight-binding characteristics of CHF1. This investigation included the different experimental strategies, for instance, preincubation, coincubation and reversibility assays, and different analyses of the kinetic data.

It was observed that, when preincubated with enzyme, CHF1 behaves as a noncompetitive inhibitor of the commercial forms and the recombinant variant of FXIIa. In contrast, it acts as a competitive inhibitor when assayed 'acutely'. This proposes that CHF1 is a competitive inhibitor either with slow degree of reversibility or irreversible property due to tightness of binding. Reversibility assay validated that CHF1 is an inhibitor with slow degree of dissociation.

4.2 Introduction

Compounds affecting the rates of enzyme-catalysed reactions are known as modulators, moderators, or modifiers[175]. Usually, the influence is to reduce the rate, and this is called inhibition [176]. Inhibitors are usually divided into three groups, reversible, irreversible, and slow, tight-binding inhibitors [175] [177] [178] [179] [180]. Reversible inhibitors form noncovalent interactions with various parts of the enzyme surface, which can be easily and rapidly reversed by dilution or dialysis. Irreversible inhibitors usually interact with different functional groups on the enzyme surface by forming covalent bonds that often persist even during complete protein breakdown. Tight-binding inhibitors usually bind tightly to the enzyme in a noncovalent interaction and remain bound for some time, but eventually dissociate from the enzyme [177][178]. Quantitative investigation of tight-binding inhibition is complicated by the fact that a substantial reduction in the concentration of unbound inhibitor could occur following addition of the inhibitor to enzyme. If appreciable inhibition at a concentration resembling that of the enzyme present happens, tight-binding inhibition should be suspected[180]. However, upon dialysis or dilution, slow recovery of enzyme activity can be noticed in a time-dependent manner [180][178]. Competitive and noncompetitive inhibition depends on the time-dependent state of the enzyme-inhibitor complex. Investigation of such a system is complex and may require a combination of numerous methods [180],[181] ,[182].

A structural study suggested that the CHFI inhibition loop looks like a canonical inhibitor loop, hypothesizing that CHFI would probably follow standard mechanism of inhibition[136, 156]. Based on the standard mechanism of action of the canonical inhibitors, it can be postulated that CHFI would have tightly binding properties when inhibiting FXIIa. Hence, the current study aimed at examining the pharmacological mechanisms of CHFI binding to human coagulation FXIIa with relevance to the tight-binding assumption. The study scheme included different assay strategies comprising preincubation, coincubation and reversibility experiments. Several methods for analysis of the kinetic data were also used to validate the conclusion of the results.

4.3 Materials and methods

4.3.1 Materials

All the materials required to perform this study are listed below (**Table 4.1**).

Table 4.1 List of the materials required for the kinetic study of CHFI-FXII interaction

| Reagents | Description/Uses | Storage T | Provider or preparation | Lab. |
|-------------------------------------|---|-----------|-------------------------|----------|
| α -FXIIa (alpha FXIIa) | Human coagulation Factor XIIa alpha. It is described in detail in chapter 2 and 5 | -80°C | Enzyme Laboratories | Research |
| S-2302 | Chromogenic substrate for FXII, it | -20°C | Chromogenix, | |

| | | | |
|-----------------|--|-------|---------------------------------|
| | is described in detail in chapter 2 | | |
| CHFI | A selective and potent inhibitor of human factor XIIa. it is described in detail in chapter 2 | -80°C | Enzyme Research Laboratories |
| β-FXIIa | Human coagulation Factor XIIa beta. It is described in detail in chapter 5 | -80°C | Enzyme Research Laboratories |
| MBP-β- FXIIa | A recombinant variant of human coagulation Factor XIIa. It is described in detail in chapter 5 | -80°C | Generated by R Manna. |

4.3.2 Methods

4.3.2.1 Identification of the mechanism of action of CHFI

The aim of this assay was to analyse the kinetic mechanism of inhibition of FXII when it was pretreated with CHFI. In this assay, CHFI- α -FXIIa inhibition assay, a 96-well plate was used. The plate was marked horizontally (No: 1-12) and vertically (letter: A-H) for different [S-2302] (0.04, 0.1, 0.2, 0.3, 0.4, 0.6 mM), and different [CHFI] (0, 10, 30, 60, 100, 300, 600, 1000 nM) respectively. To each duplicate well, PBS, different [CHFI] and fixed [α -FXIIa] (14 nM) were added and preincubated at 37°C for 30 min. Then, the mixture was tested on different [S-2302]. Various controls were used as follows: S-2302+CHF+PBS, S-2302+PBS, CHF+PBS, FXII enzyme+PBS, and PBS alone. The reaction volume was 100 μ l. Once ready, the plate was transferred to the plate reader for monitoring amidolytic activity of the enzyme at 33°C and 405nm wave length for 10 min with 5 min time intervals. Three independent experiments were carried out.

4.3.2.2 Differentiation between noncompetitive allosteric site and active site inhibition

The aim of this assay was, firstly, to investigate whether CHFI has a noncompetitive behaviour when it acutely blocks FXIIa and, secondly, to differentiate between the two possible mechanisms that CHFI may follow, which are either noncompetitive allosteric site or noncompetitive active site inhibition. Herein, the enzyme was not pretreated with the inhibitor. To each duplicate well, various [CHF] (0, 10, 30, 60, 100, 200, 300, 600, 1000 nM)

and [S-2302] (0.04, 0.1, 0.2, 0.3, 0.4, 0.6 mM) were dispensed and coincubated at 37°C for 10 min. Then, α -FXIIa was added; the plate was transferred to the plate reader for observation of hydrolytic cleavage of the chromogenic substrate. The reaction volume was 100 μ l. various controls were used as follows: S-2302+CHFI+PBS, S-2302+PBS, CHFI+PBS, FXII enzyme+PBS, and PBS alone. Three independent experiments were performed.

4.3.2.3 Validation of tight-binding property of CHFI

The purpose of this assay was to investigate into the slow degree of reversibility of CHFI due to tight binding. This investigation was carried out using different experiments. First was reversibility test; in which 100 nM α -FXIIa was in complex with CHFI at concentration of IC_{50} (200 nM). The complex was preincubated for 10 min at 37°C. Then, it was diluted 1:10 ([CHFI] was likely to be reduced to 10-fold below IC_{50} i.e. the final assay concentrations was anticipated to be 20 nM CHFI and 10 nM α -FXIIa). Second was negative control test that had the same experimental design described before, but CHFI was excluded. Thirdly, a concentration of 10-fold below IC_{50} of CHFI was in an acute assay condition (20 nM CHFI + 10nM α -FXIIa)[178][177]. Finally, a high concentration of CHFI (i.e. at [IC_{50}]) was in an acute assay condition (200 nM CHFI + 10 nM α -FXIIa). The reaction volume was 100 μ l. The plate was transferred to the plate reader for an overnight monitoring of amidolytic cleavage of S-2302 and releases of the chromophore every 15 min time intervals at 33°C and 405nm wave length (**Figure 4.1**).

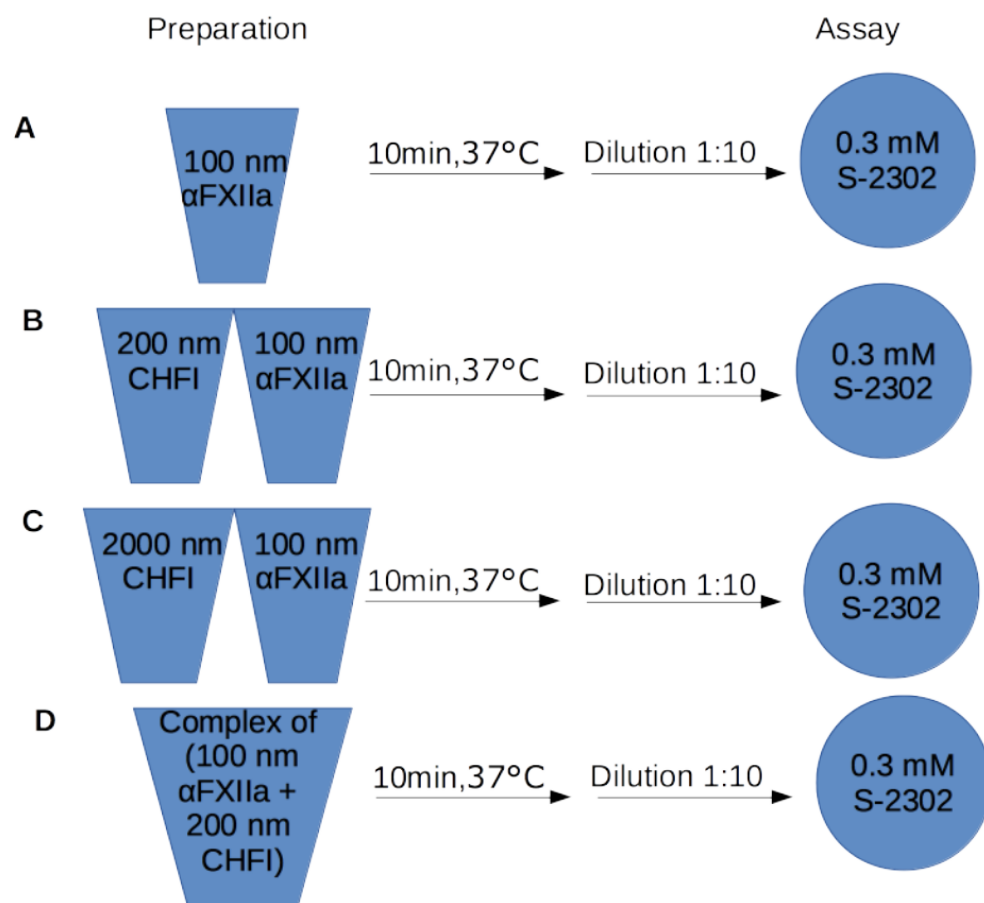


Figure 4.1 Schematic representation of reversibility assay. **A** represents the negative control sample that was pre-incubated and diluted in the absence of inhibitor. **B** is an acute assay of the low concentration inhibitor. **C** is the reversibility assay of CHFI in complex with FXII (CHFI- α FXII complex) at a concentration of the inhibitor equal to $[IC_{50}]$. **D** is an acute assay of the high concentration inhibitor.

4.3.4.4 Statistical analysis of the kinetic data

Absorbance unit was converted to the absolute amount of pNA (p-nitroaniline) generated using the calibration curve. Initial velocities were calculated by taking time points within the linear window of the initial reaction of the time

course assays . Statistical analyses were performed using linear regression and non-linear regression for the following purposes: first, to perform curve-fitting analyses required for detecting the model of inhibition, second, as a second approach, to perform Michaelis-Menten kinetic to describe the kinetic parameters informative for evaluating inhibition mechanisms to further validate the model of inhibition, and third, to find IC_{50} values important for examining the correlation between inhibition effectiveness of CHF1 and [S-2302] that was essential for identifying and further confirming the model of inhibition . With respect of curve-fitting analysis, to compare the goodness-of-fit of the model found with alternative nested models, the extra-sum-of squares F test was analysed using Graphpad Prism; thereby, the resulting model was further verified.

4.4 Results and Discussion

4.4.1 Dual kinetic actions of CHF1

The present study aimed to evaluate CHF1 inhibitory mechanism against human coagulation FXIIa with relevance to the tight-binding assumption. The experimental design included different assay strategies to identify kinetic inhibition of different activated forms of FXII by CHF1; this includes preincubation, coincubation and reversibility assays.

In the preincubation assay, time-dependent assays of the catalytic activity of α FXII preincubated with the different CHF1 concentrations were performed at different chromogenic substrate (S-2302) concentrations. The activity of amidolytic breakdown of 0.6mM S-2302 by FXII enzyme pre-treated with the different CHF1 concentrations versus time was monitored every 5 min for 30 min duration (**Figure 4.2**).

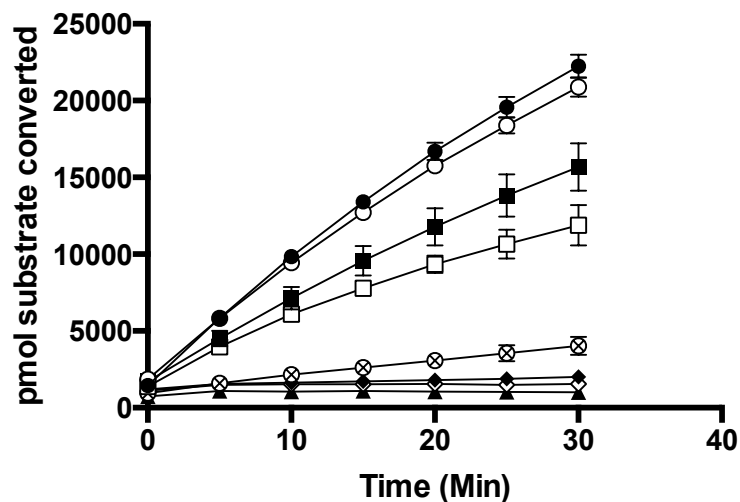


Figure 4.2 Time-dependent inhibition of the catalytic breakdown of S-2302 by different [CHF1]. The amount of product (pmol per pmol of α -FXIIa) produced by hydrolytic breakdown of 0.6 mM chromogenic substrate in the presence of different amounts of CHF1 is plotted versus time. Average of duplicate observations of 3 independent experiments was used; Error bars represent standard error of the mean of the independent experiments. The following symbols are different [CHF1]: (0 nM, ●), (10nM, ○), (30 nM, ■), (60 nM, □), (200 nM, ◆), (300, ◇), (600, ⊗), (1000 nM, ▲).

The initial velocities of hydrolytic breakdown of the different concentrations of S-2302 by the enzyme inhibited by different concentrations of CHF1 were analysed by taking two time points within the window of the linear initial reaction (**Table 4.2**).

Table 4.2 Analysis of initial reaction rates in CHFI-FXIIa inhibition interaction. Initial velocities (pmol/sec) of catalytic cleavage of the different [S-2302] by one pmol of α FXII inhibited by the different [CHFI]. The value of each initial reaction rate is an average of three independent experiments. In every single experiment two duplicate measurements were taken and the average of them was calculated. The error is standard error of the mean of all the independent experiments.

| | [S-2302] (mM) | | | | | |
|----------------------------|----------------------|------------------|------------------|------------------|------------------|------------------|
| [CHFI] | 0.04 | 0.1 | 0.2 | 0.3 | 0.4 | 0.6 |
| (μM) | | | | | | |
| 0.00 | 3.00 \pm 0.15 | 6.72 \pm 0.25 | 8.96 \pm 0.16 | 10.79 \pm 0.27 | 11.44 \pm 0.55 | 11.68 \pm 0.37 |
| 0.01 | 2.26 \pm 0.44 | 4.53 \pm 0.91 | 6.88 \pm 1.22 | 8.61 \pm 0.67 | 9.1 \pm 10.35 | 10.57 \pm 0.1 |
| 0.03 | 1.6 \pm 0.31 | 3.36 \pm 0.5 | 4.94 \pm 0.22 | 6.14 \pm 0.73 | 6.83 \pm 0.46 | 7.24 \pm 0.42 |
| 0.06 | 0.82 \pm 0.41 | 1.81 \pm 0.84 | 2.12 \pm 0.65 | 2.75 \pm 0.65 | 3.54 \pm 0.91 | 4.61 \pm 0.86 |
| 0.2 | 0.25 \pm 0.12 | 0.62 \pm 0.31 | 0.83 \pm 0.18 | 0.97 \pm 0.129 | 1.41 \pm 0.18 | 1.63 \pm 0.27 |
| 0.3 | 0.33 \pm 0.36 | 0.75 \pm 0.65 | 1.18 \pm 0.87 | 0.12 \pm 0.1 | 0.22 \pm 0.12 | 0.22 \pm 0.11 |
| 0.6 | -0.12 \pm 0.04 | 0.03 \pm 0.07 | 0.00 \pm 0.05 | -0.06 \pm 0.02 | 0.04 \pm 0.08 | -0.07 \pm 0.05 |
| 1 | -0.03 \pm 0.10 | -0.01 \pm 0.02 | -0.06 \pm 0.04 | 0 \pm 0 | -0.08 \pm 0.04 | -0.04 \pm 0.01 |

To define the kinetic behaviour of CHFI in the preincubation assay, the experimental values obtained were examined by the different methods of the enzyme kinetic data analysis as explained below.

The first method was curve-fitting model; this was performed by using nonlinear regression via two steps: first, to consider fitting to the anticipated curves of an inhibition model, and second, to compare the goodness-of-fit of the appropriate model with that of other alternative models using extra-sum-of-squares F test and thereby to indicate the possible mechanism of action. CHF1, when preincubated with α -FXIIa, would behave as a noncompetitive inhibitor (Figure 4.3).

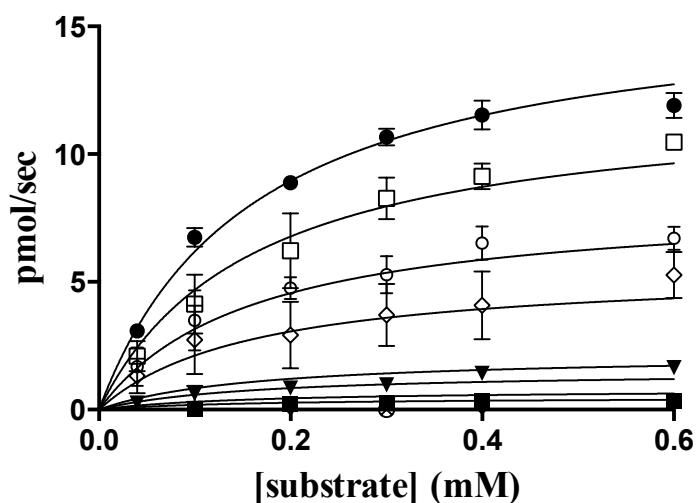


Figure 4.3 Noncompetitive inhibition behaviour of CHF1 in the preincubation condition. Velocities per pmol of α -FXIIa versus different concentration of S-2302 exemplify the inhibition reactions in which α -FXIIa was pretreated with CHF1. Observed activity dots fit with the predicted lines of noncompetitive model of inhibition. In each experiment a duplicate was used for different [CHF1] versus different [S-2302]. Average of the duplicate values was taken. The error bar is standard error of the mean of three independent experiments. The following symbols are different [CHF1]: (0 nM, \bullet), (10 nM, \square), (30 nM, \circ), (60 nM, \diamond), (200 nM, \blacktriangle), (300 nM, \blacksquare), (600 nM, \blacklozenge), (1000 nM, \circ).

Similar procedures and analysis were performed for the inhibition of the other forms of FXIIa, β -FXIIa and MBP- β -FXIIa; it was observed that CHF1 would behave as a noncompetitive behaviour in the preincubation state (**Figure 4.4 and 4.5**).

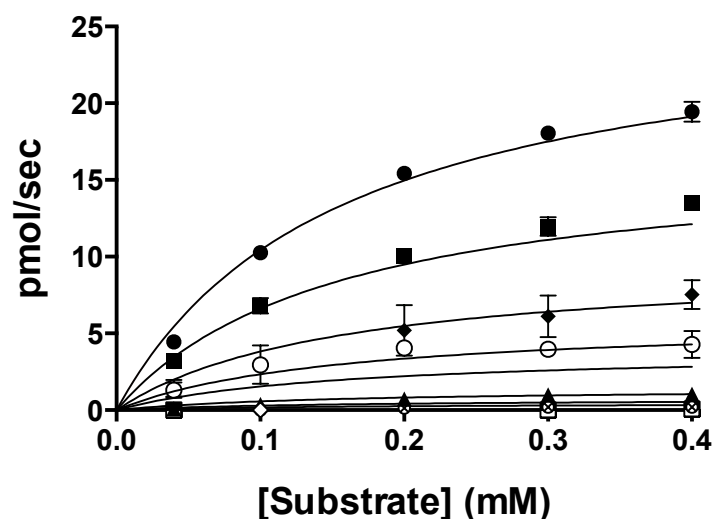


Figure 4.4 CHF1 follows noncompetitive inhibition model against β -FXIIa in the preincubation assay. Activity points (pmol of product /sec/ pmol of enzyme) of β -FXIIa, pretreated with CHF1 versus different [S2302] in the inhibition reaction assays, are fit for noncompetitive model of inhibition. In every experiment a duplicate was used for different [CHF1] against different [S-2302], each vs. each. Average of the duplicate was taken. The error bar is standard error of the mean of three independent experiments. The symbols are different [CHF1] as follows: (0 nM, ●), (10 nM, ■), (30 nM, ◆), (60 nM, ○), (100 nM, ◇), (300 nM, △), (600 nM, ◼).

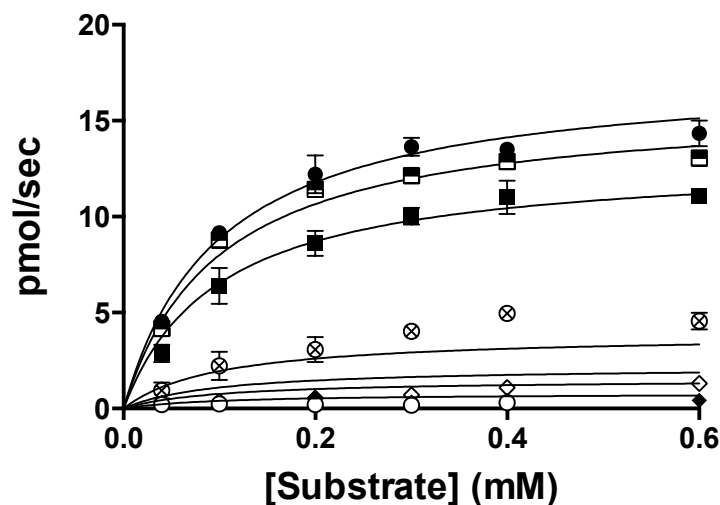


Figure 4.5 CHFI acts as a noncompetitive inhibitor of MBP- β -FXIIa in the preincubation assay. The observed activity dots are fit for the predicted lines of the noncompetitive model of inhibition. In each experiment a duplicate was used for different [CHF] versus different [S-2302]. Average of the duplicate values was taken. The error bar is standard error of the mean of three individual experiments. The following symbols are different [CHF]: (0 nM, \bullet), (3 nM, \square), (10 nM, \blacksquare), (100nM, \diamond), (200 nM, \circ), (300 nM, \blacklozenge), (600nM, \circ).

The inhibition constant value from this curve-fitting analysis is consistent with what has been previously found. A study showed that CHFI inhibits β -FXIIa with $K_i = 24$ nM[145, 146, 152-154]. With reference to the current investigation, K_i for CHFI against β -FXIIa is 17.34 ± 0.88 (nM). This further verifies that the experiments and the kinetic data analysis are appropriate.

The k_{cat} values for β -FXIIa, α -FXIIa, and MBP- β -FXIIa are 26.5 ± 0.84 , 16.15 ± 0.71 and 17.6 ± 0.5 (s^{-1}) respectively; their K_M values are 0.15 ± 0.01 , 0.16 ± 0.01 , and 0.1 ± 0.0 respectively (**Table 4.3**). With respect to the curve-fitting

analysis, the activity and affinity parameters are considered in the absence of the effect of inhibitors[178].

Table 4.3 Kinetic parameters of the noncompetitive inhibition model of CHFI-FXIIa interaction

| Kinetic parameters | β-FXIIa | α-FXIIa | MBP-β-FXIIa |
|--|---------------------------------|----------------------------------|-------------------------------------|
| K_i (nM) | 17.34±0.88 | 31.17±2.32 | 28.94± 2 |
| K_M (mM) | 0.15±0.01 | 0.16±0.01 | 0.1±0.0 |
| k_{cat} (s ⁻¹) | 26.5±0.84 | 16.15±0.71 | 17.6±0.5 |
| k_{cat} / K_M (L mol ⁻¹ s ⁻¹) | 176666 | 100937 | 176000 |

There are two possible mechanisms that could explain the noncompetitive inhibition behaviour of CHFI in the preincubation experiment. First, CHFI binds to an allosteric site of FXIIa and causes a conformational change of the catalytic triad of these enzymes; in this case, the inhibitor would be known as noncompetitive allosteric site inhibitor (or absolute noncompetitive inhibitor). The second possible mechanism would be that CHFI is actually a competitive inhibitor, but intensely binds to the enzyme, and it has a slow dissociation rate or a slow degree of reversibility, or it doesn't dissociate at all; in this case it would be termed as noncompetitive active site inhibitor. Therefore, to test this hypothesis and to discriminate these two possibilities, and to detect the mechanism that appropriately explains CHFI behaviour, an 'acute' assay (or coincubation assay) was carried out. The reason of conducting this assay is that noncompetitive inhibition (i.e. noncompetitive allosteric site inhibition) can only be completely recognized in a coincubation experiment wherein

CHFI and S-2302 are concurrently added to the preparation of the target protein (FXIIa) to be inhibited or vice versa. The reason behind that is the inhibitor would bind to an allosteric site far away from the active site.

In the acute assay, [CHFI] and [S-2302] were added to the wells and coincubated; then α FXII, β -FXIIa, and MBP- β -FXIIa were tested for time-dependent enzymatic activity. The initial reaction rates were analyzed using the same steps described before. With reference to the curve-fitting analysis and the extra-sum-of squares F test, CHFI behaves as competitive behaviour (Figure 4.6-4.8).

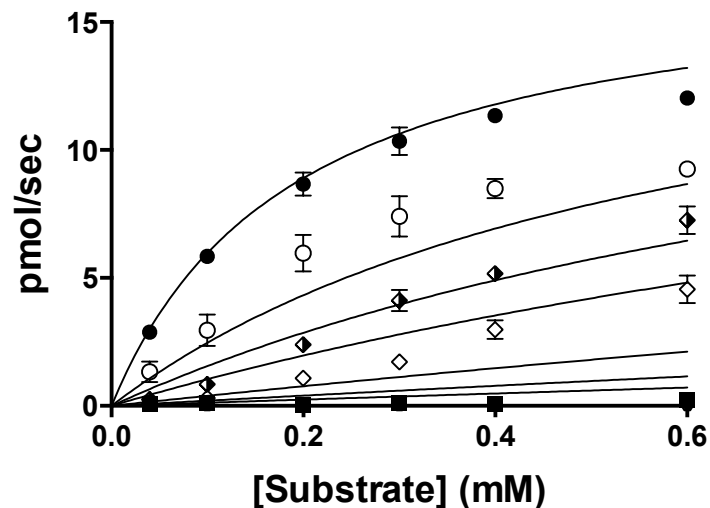


Figure 4.6 CHFI obeys competitive inhibition against α -FXIIa in the coincubation assay. Activity (pmol of product /sec/ pmol of enzyme) of α -FXIIa versus different concentrations of the substrate illustrates the inhibition model. Activity points display competitive model of inhibition when S-2302 and CHFI were coincubated. In every experiment a duplicate was used for different [CHFI] vs. various [S-2302], each vs. each. Average of the duplicate values was taken. The error bar is standard error of the mean of three independent experiments. The symbols are different [CHFI] as follows: (0 nM, ●), (30 nM, ○), (60 nM, ◊), (100 nM, ◐), (300 nM, ◑), (600 nM, ◒) and (1000 nM, ◓).

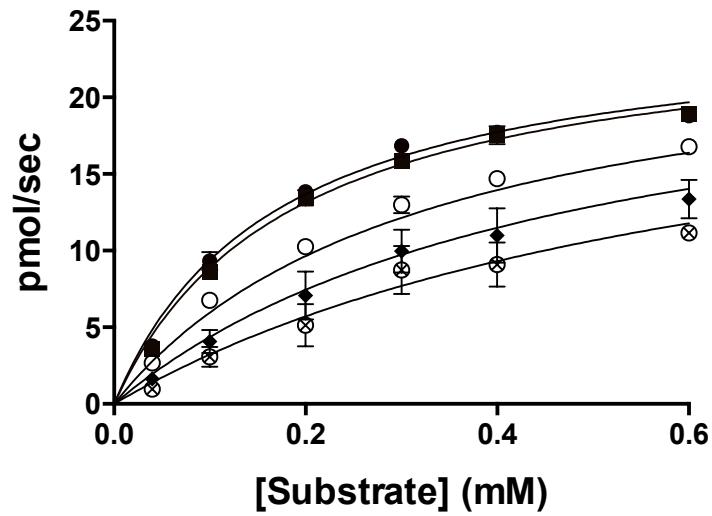


Figure 4.7 CHFI follows competitive inhibition against β -FXIIa in the coincubation assay. Activity (pmol of product /sec/ pmol of enzyme) of β -FXIIa versus different concentrations of the substrate demonstrates the inhibition model. Activity dots are fit for competitive model of inhibition when S-2302 and CHFI were coincubated. In every experiment a duplicate was used for every [CHF] against each [S-2302], each vs. each. Average of the duplicate values was taken. The error bar is standard error of the mean of three independent experiments. The symbols are different [CHF] as follows: (0 nM, ●), (30nM, ◻), (3 nM, ■), (60 nM, ◆) (100 nM, ○).

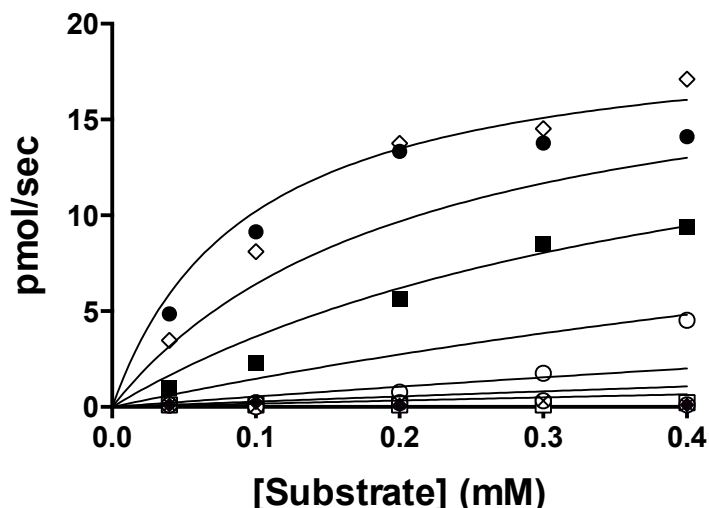


Figure 4.8 CHFI obeys competitive inhibition toward MBP- β -FXIIa in the coincubation assay. Activity (pmol of product / sec / pmol of enzyme) of MBP- β -FXIIa versus different concentrations of the substrate determines the inhibition model. When S-2302 and CHFI were coincubated, activity points are fit for competitive model of inhibition. In every experiment a duplicate was used for every [CHFI] against each [S-2302], each vs. each. Average of the duplicate values was taken. The symbols are different [CHFI] as follows: (0 nM, ●), (10 nM, ◇), (30 nM, ■), (100nM, □), (300 nM, ○), (600 nM, ◆) and (1000 nM, ◻).

The value of K_i of CHFI for inhibition of β -FXIIa, α -FXIIa, and MBP- β -FXIIa is 32.7 ± 3.2 , 13.85 ± 1.72 and 7.35 ± 1.44 (nM) respectively. The values of K_M of β -FXIIa, α -FXIIa, and MBP- β -FXIIa are 0.16 ± 0.01 , 0.19 ± 0.03 and 0.09 ± 0.02 (mM) respectively; the k_{cat} of the enzymes are 25.19 ± 0.93 , 17.43 ± 1.36 and 18.4 ± 1.2 (s^{-1}) respectively (**Table 4.4**). Both affinity and activity of the enzymes in the preincubation condition are similar to that in the coincubation state. This would be due to that the curve-fitting analysis negates the effect of CHFI on K_M and k_{cat} values [178].

The Inhibition constant values propose that CHFI has tight-binding property due to two reasons. First is K_i values of CHFI are around 1×10^{-9} M, which is likely to be described as tight binding inhibitor with respect to the general definition of slow, tight binding-binding inhibitors. The second reason would be that a structural study suggested that CHFI inhibition loop looks like a canonical inhibitor loop, hypothesizing that CHFI is expected to follow the mechanism of canonical inhibitors[136, 156]; with respect to this mechanism, the complex of EI is much more stable than the Michaelis ES complex; the ratio of standard inhibition constant (K_i) values to K_M values is equal or greater than 100, meaning that the inhibitor has high affinity [133, 134]. In the current investigation, according to curve-fitting analysis, the ratio of K_i value is a 1000-fold greater than K_M . This probably supports the hypothesis of tight-binding behaviour of CHFI. In addition to curve-fitting analysis, several other kinetic analyses were performed to further validate the dual kinetic action of CHFI that would reflect tight-binding property.

Table 4.4 The kinetic parameters of the competitive inhibition model

| Kinetic parameters | β -FXIIa | α -FXIIa | MBP- β -FXIIa |
|--|------------------|------------------|---------------------|
| K_i (nM) | 32.7 \pm 3.2 | 13.85 \pm 1.72 | 7.35 \pm 1.44 |
| K_M (mM) | 0.16 \pm 0.01 | 0.19 \pm 0.03 | 0.09 \pm 0.02 |
| k_{cat} (s ⁻¹) | 25.19 \pm 0.93 | 17.43 \pm 1.36 | 18.4 \pm 1.2 |
| k_{cat} / K_M (L mol ⁻¹ s ⁻¹) | 157437 | 91736 | 204444 |

4.4.2 Identification of mechanism of inhibition using the relationship between [S-2302] and IC_{50}

To further verify the model of inhibition based on the relationship between IC_{50} values of CHF1 and different concentrations of S-2302, [substrate]- IC_{50} relationship analysis was performed for the kinetic data of both preincubation and coincubation tests together [183][178]. Inhibition effectiveness curves (Figure 4.9-4.14) and IC_{50} values (Table 4.5-4.7) were first analysed then divided by mean of K_i values of both conditions. Then, the resulting values were plotted versus different S-2302 concentrations divided by mean of K_M values of both conditions (Table 4.3 and 4.4). With respect to the kinetic data of the coincubation assay, it was found that the ratio of IC_{50}/K_i is directly proportional to the ratio of $[S-2302]/K_M$, meaning that in the coincubation test CHF1 would follow competitive model of inhibition. The data of the preincubation test showed that IC_{50}/K_i ratio doesn't change with the increase in $[S-2302]/K_M$ ratio, suggesting that CHF1 obeys noncompetitive model of inhibition in the preincubation assay (Figure 4.15-4.17). The flat curves of noncompetitive model indicate that the findings are consistent with the results found from the abovementioned curve-fitting analysis. In addition, this results further validates that the noncompetitive behaviour of CHF1 is nonallosteric inhibition because the value of cooperativity of interaction (α) would be zero ($\alpha=0$).

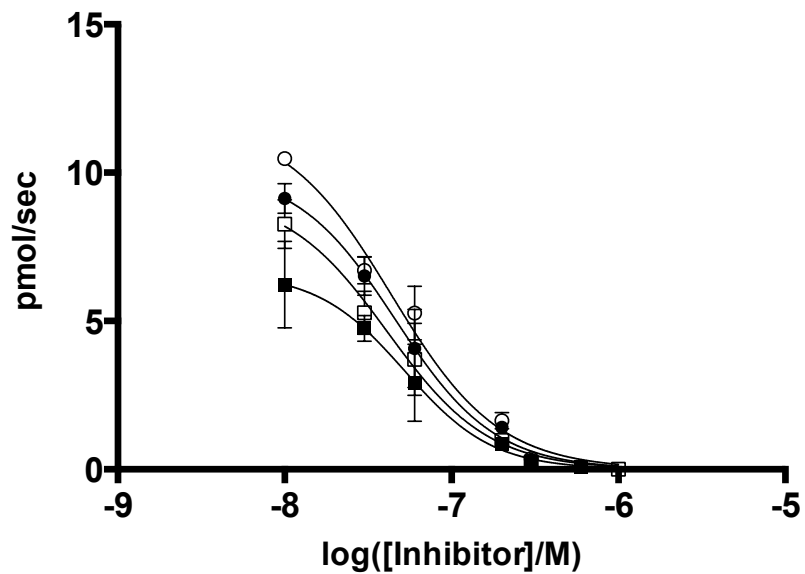


Figure 4.9 IC_{50} Curves of CHF1 at different [S-2302] in the preincubation state of CHF1- α -FXIIa interaction. The unit pmol/sec/ per each pmol of the enzyme reflects the initial reaction rates of S-2302 conversion. The error bar is standard error of the mean of three independent experiments. In each experiment a duplicate was used for testing different [CHF1]. Average of the duplicate results was taken. The symbols are different [S-2302] as follows: (0.1mM, \blacksquare), (0.2mM, \square), (0.4mM, \bullet), (0.6 mM, \circ)

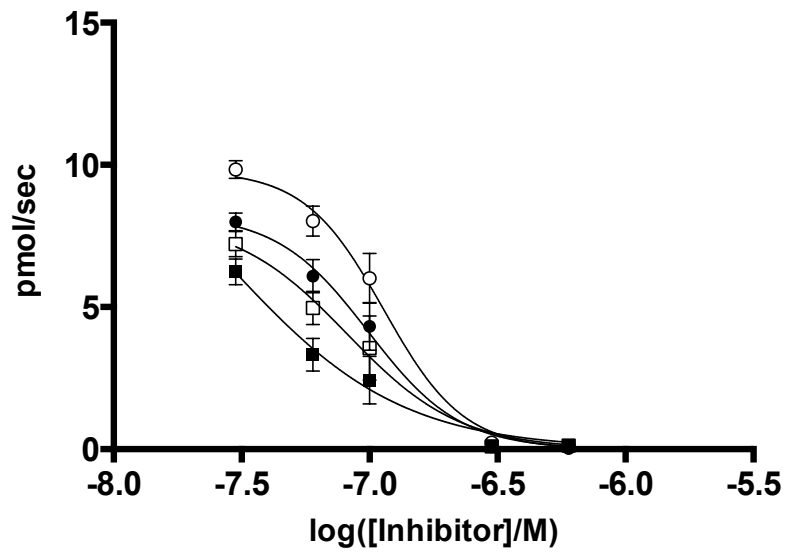


Figure 4.10 IC_{50} Curves of CHFI at different [S-2302] in the coincubation state of CHFI- α -FXIIa interaction. The unit pmol/sec/ per each pmol of the enzyme reflects the initial velocities of S-2302 conversion. The error bar is standard error of the mean of three independent experiments. In each experiment a duplicate was used for testing different [CHFI]. Average of the duplicate results was taken. The symbols are different [S-2302] as follows: (0.1mM, \blacksquare), (0.2mM, \square), (0.4mM, \bullet), (0.6 mM, \circ)

Table 4.5 IC_{50} values of CHFI at different [S-2302] in the preincubation and coincubation state of CHFI- α -FXIIa interaction. The unit pmol/sec/ per each pmol of the enzyme reflects initial reaction rates of S-2302 conversion. The error is standard error of the mean of the three independent experiments. In each experiment a duplicate was used for testing every single concentration of the different forms of CHFI. Average of the duplicate results was taken

| | [S-2302] (mM) | | | |
|----------------|----------------------|------------|------------|------------|
| | 0.1 | 0.2 | 0.4 | 0.6 |
| Preincubation | 52±0.15 | 41±13 | 46 ±0.08 | 44±0.07 |
| IC_{50} (nM) | | | | |
| Coincubation | 28±1 | 81±0.13 | 98±0.06 | 114±0.04 |
| IC_{50} (nM) | | | | |

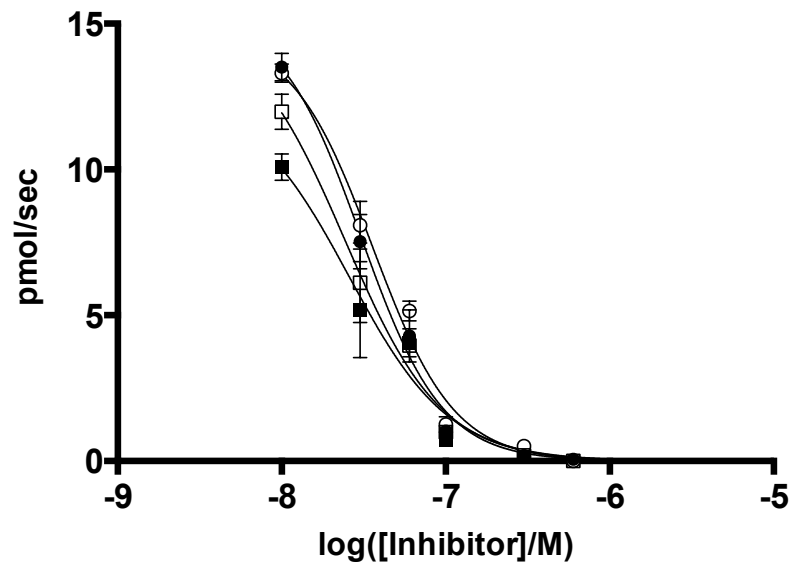


Figure 4.11 IC_{50} Curves of CHFI at different [S-2302] in the preincubation state of CHFI- β -FXIIa interaction. The unit pmol/sec/ per each pmol of the enzyme reflects the initial reaction rates of S-2302 conversion. The error bar is standard error of the mean of three independent experiments. In each experiment a duplicate was used for testing different [CHFI]. Average of the duplicate results was taken. The symbols are different [S-2302] as follows: (0.1mM, \blacksquare), (0.2mM, \square), (0.4mM, \bullet), (0.6 mM, \circ)

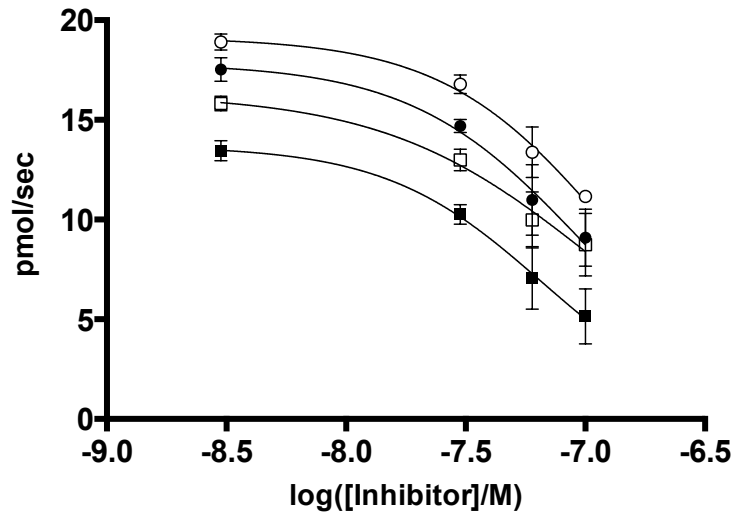


Figure 4.12 IC_{50} Curves of CHFI at different [S-2302] in the coincubation state of CHFI- β -FXIIa interaction. The unit pmol/sec/ per each pmol of the enzyme reflects the initial velocities of S-2302 conversion. The error bar is standard error of the mean of three independent experiments. In each experiment a duplicate was used for testing different [CHFI]. Average of the duplicate results was taken. The symbols are different [S-2302] as follows: (0.1mM, \blacksquare), (0.2mM, \square), (0.4mM, \bullet), (0.6 mM, \circ)

Table 4.6 IC₅₀ values of CHF1 at different [S-2302] in the preincubation and coincubation state of CHF1- β-FXIIa interaction. The unit pmol/sec/ per each pmol of the enzyme reflects initial reaction rates of S-2302 conversion. The error is standard error of the mean of the three independent experiments. In each experiment a duplicate was used for testing every single concentration of the different forms of CHF1. Average of the duplicate results was taken

| | [S-2302] (mM) | | | |
|-----------------------|----------------------|------------|------------|------------|
| | 0.1 | 0.2 | 0.4 | 0.6 |
| Preincubation | 25±0.2 | 24±0.1 | 30 ±0.08 | 35±0.06 |
| IC ₅₀ (nM) | | | | |
| Coincubation | 66±1 | 106±0.1 | 100±1 | 125±1 |
| IC ₅₀ (nM) | | | | |

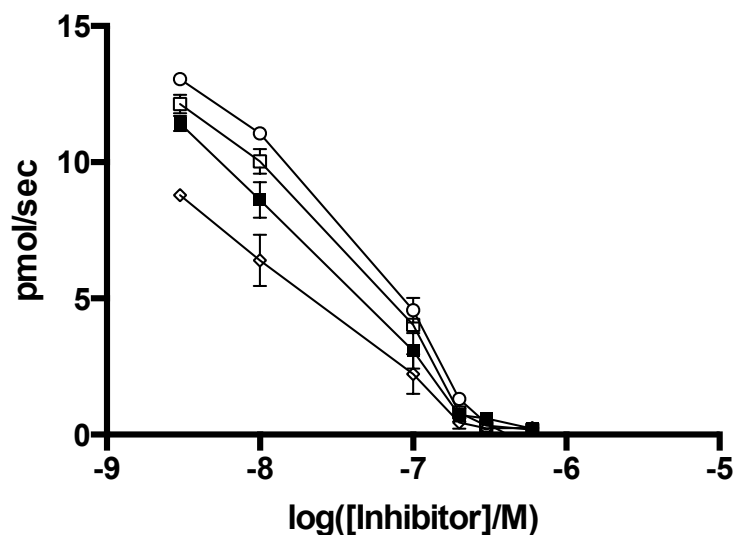


Figure 4.13 IC_{50} Curves of CHF1 at different [S-2302] in the preincubation state of CHF1-MBP- β -FXIIa interaction. The unit pmol/sec/ per each pmol of the enzyme reflects the initial reaction rates of S-2302 conversion. The error bar is standard error of the mean of three independent experiments. In each experiment a duplicate was used for testing different [CHF1]. Average of the duplicate results was taken. The symbols are different [S-2302] as follows: (0.1mM, \blacksquare), (0.2mM, \square), (0.3mM, \bullet), (0.6 mM, \circ)

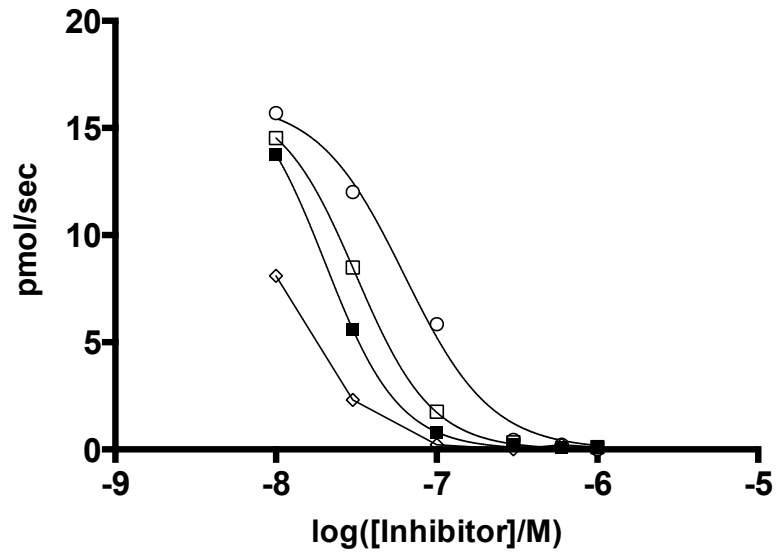


Figure 4.14 IC_{50} Curves of CHFI at different [S-2302] in the coincubation state of CHFI-MBP- β -FXIIa interaction. The unit pmol/sec/ per each pmol of the enzyme reflects the initial velocities of S-2302 conversion. The error bar is standard error of the mean of three independent experiments. In each experiment a duplicate was used for testing different [CHFI]. Average of the duplicate results was taken. The symbols are different [S-2302] as follows: (0.1mM, ■), (0.2mM, □), (0.3mM, ●), (0.6 mM, ○).

Table 4.7 IC₅₀ values of CHF1 at different [S-2302] in the preincubation and coincubation state of CHF1-MBP-β-FXIIa interaction. The unit pmol/sec/ per each pmol of the enzyme reflects initial reaction rates of S-2302 conversion. The error is standard error of the mean of the three independent experiments. In each experiment a duplicate was used for testing every single concentration of the different forms of CHF1. Average of the duplicate results was taken.

| | [S-2302] (mM) | | | |
|-----------------------|----------------------|------------|------------|------------|
| | 0.1 | 0.2 | 0.3 | 0.6 |
| Preincubation | 19±0.1 | 22±1 | 28 ±0.07 | 32±0.08 |
| IC ₅₀ (nM) | | | | |
| Coincubation | 15.5±0.15 | 20.3±0.02 | 31.5±0.03 | 63±0.06 |
| IC ₅₀ (nM) | | | | |

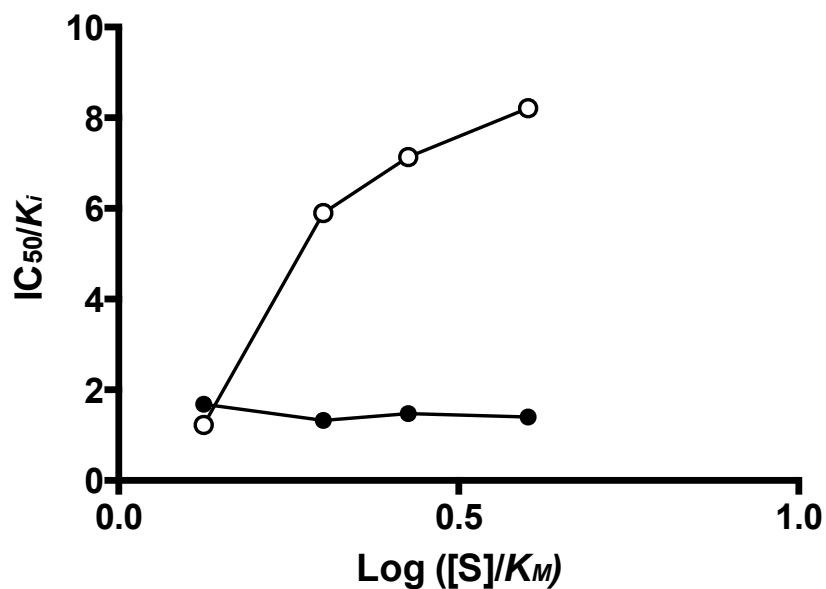


Figure 4.15 Relationship between $[S] / K_M$ and IC_{50} / K_i in CHF1- α -FXIIa interaction. The figure displays the effect of $[S]$ on the IC_{50} value. This correlation shows competitive inhibition in the coincubation interaction whereas it shows noncompetitive inhibition in the preincubation interaction. The curve dot ● represents the correlation in the preincubation state whereas the curve dot ○ represents the correlation in the coincubation state.

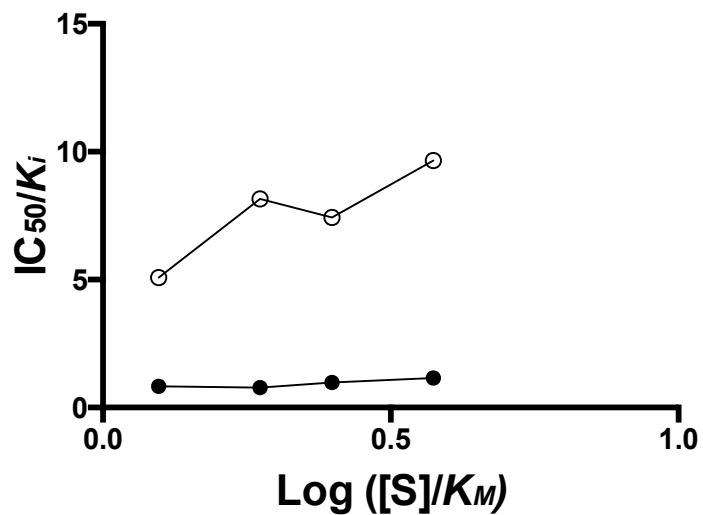


Figure 4.16 Relationship between $[S]/K_M$ and IC_{50}/K_i in CHF1- β -FXIIa interaction. The effect of $[S]$ on the IC_{50} value displays competitive inhibition in the coincubation condition whereas it shows noncompetitive inhibition in the preincubation interaction. The curve dot ● represents the correlation in the preincubation state whereas the curve dot ○ represents the correlation in the coincubation state.

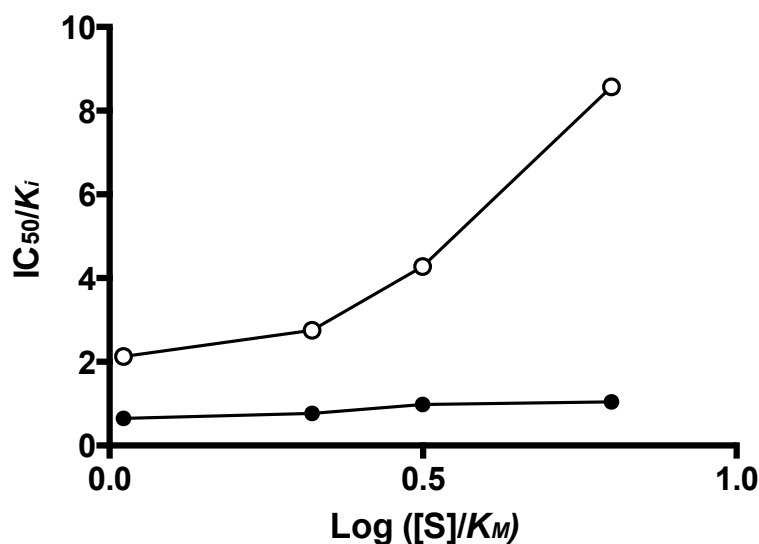


Figure 4.17 Relationship between $[S] / K_M$ and IC_{50} / K_i in CHF1-MBP β -FXIIa interaction. The effect of $[S]$ on the IC_{50} value displays competitive inhibition in the coincubation interaction whereas it shows noncompetitive inhibition in the preincubation interaction. The curve dot ● represents the correlation in the preincubation state whereas the curve dot ○ represents the correlation in the coincubation state.

4.4.3 Identification of mechanism of inhibition via examining the effect of inhibition on K_M and k_{cat} and Lineweaver-Burk plot

To examine the effect of CHF1 on the catalytic activity and affinity of FXII enzymes, Michaelis-Menten model and Lineweaver-Burk plot were used to analyse the kinetic data (Figure 4.18-4.23). This was used to further validate the noncompetitive behaviour of CHF1 in the preincubation assay. It was observed that the increase in the concentration of CHF1 did not affect (or slightly decreased) the values of K_M whereas it caused a reduction in the

values of k_{cat} . Toward the increase in the [CHF1], from the left to the right side of the panels (Table 4.8-4.10), and with respect to Lineweaver-Burk plot analyses (Figure 4.19, 4.21, and 4.23), the k_{cat} values for α -FXIIa, β -FXIIa, and MBP- β -FXIIa decreases whereas the K_M values are either kept unchanged or slightly affected. This would also verify the noncompetitive behaviour of CHF1 in the preincubation test.

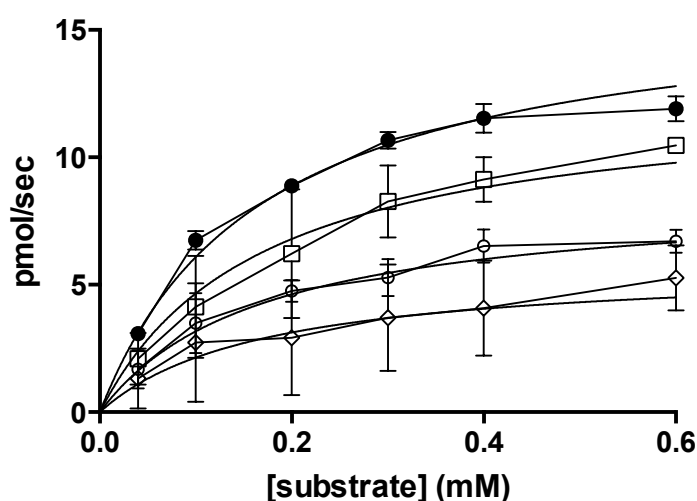


Figure 4.18 Michaelis-Menten kinetics of the inhibition of α -FXIIa by CHF1 in the preincubation assay. The initial reaction rates (pmol of product /sec/ pmol of enzyme) of α -FXIIa vs. different concentration of S-2302 used to describe the kinetic parameters. In every experiment, a duplicate was used for every [CHF1] used alongside with the different [S-2302], each versus each. Average of the duplicate values was taken. The error bar is the standard error of the mean of all independent experiments. The symbols are different [CHF1] as follows: (0 nM, ●), (10 nM, □), (30nM, ○), (60 nM, ◇).

Table 4.8 Kinetic parameters of CHFI- α -FXIIa interaction in preincubation condition using Michaelis-Menten kinetics

| Kinetic parameters | [CHFI] (nM) | | | |
|--|-----------------|-----------------|-----------------|-----------------|
| | 0 | 10 | 30 | 60 |
| K_M (mM) | 0.13 \pm 0.01 | 0.15 \pm 0.03 | 0.15 \pm 0.05 | 0.15 \pm 0.14 |
| k_{cat} (s ⁻¹) | 15 \pm 0.61 | 13.2 \pm 0.9 | 8.54 \pm 1.12 | 5.98 \pm 0.15 |
| k_{cat} / K_M (L mol ⁻¹ s ⁻¹) | 115384 | 86666 | 56933 | 39866 |

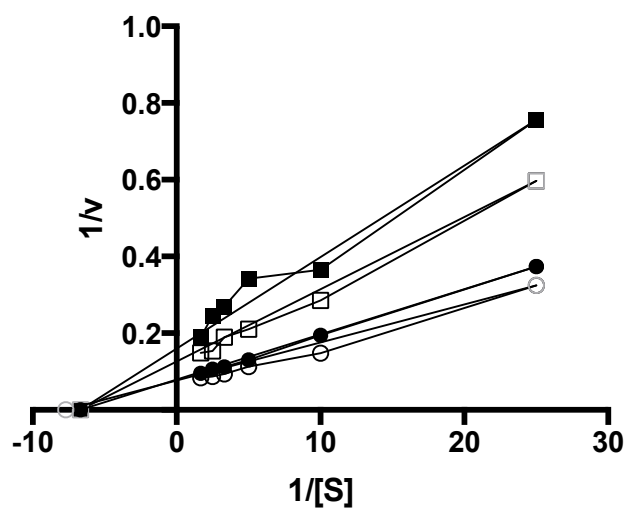


Figure 4.19 Lineweaver-Burk plots showing non-competitive inhibition of α -FXIIa by CHFI. X-axis is $1/[S2302]$, mM^{-1} ; Y-axis is $1/V$, $(\text{pmol}/\text{sec})^{-1}$. The symbols are different [CHFI] as follows: (0 nM, \bullet), (10 nM, \square), (30 nM, \square), (60 nM, \blacksquare).

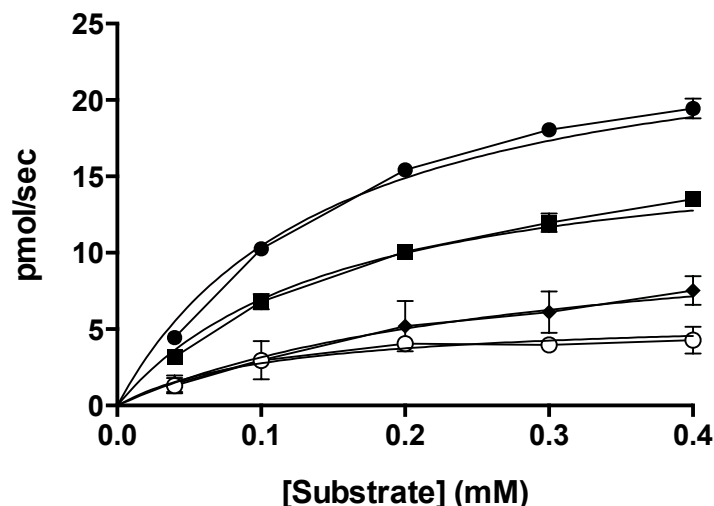


Figure 4.20 Michaelis-Menten kinetics of β -FXIIa-CHFI interaction in the preincubation assay. The initial velocities (pmol of product /sec/ pmol of enzyme) of α -FXIIa vs. different concentrations of S-2302 used to describe the kinetic parameters. In every experiment, a duplicate was used for every [CHFI] used alongside with the different [S-2302], each versus each. Average of the duplicate values was taken. The error bar is the standard error of the mean of all independent experiments. The symbols are different [CHFI] as follows: (0 nM, \bullet), (10 nM, \blacksquare), (30 nM, \blacklozenge) (60nM, \square).

Table 4.9 Kinetic parameters of CHFI- β -FXIIa interaction in the preincubation condition using Michaelis-Menten kinetics

| Kinetic parameters | [CHFI] (nM) | | | |
|---|------------------|-----------------|------------------|-----------------|
| | 0 | 10 | 30 | 60 |
| K_M (mM) | 0.14 \pm 0.01 | 0.15 \pm 0.02 | 0.18 \pm 0.05 | 0.11 \pm 0.04 |
| k_{cat} (s^{-1}) | 25.86 \pm 0.92 | 17.73 \pm 0.9 | 11.89 \pm 1.32 | 5.8 \pm 0.66 |
| k_{cat} / K_M ($L_{mol}^{-1} s^{-1}$) | 184714 | 118200 | 42517 | 52727 |

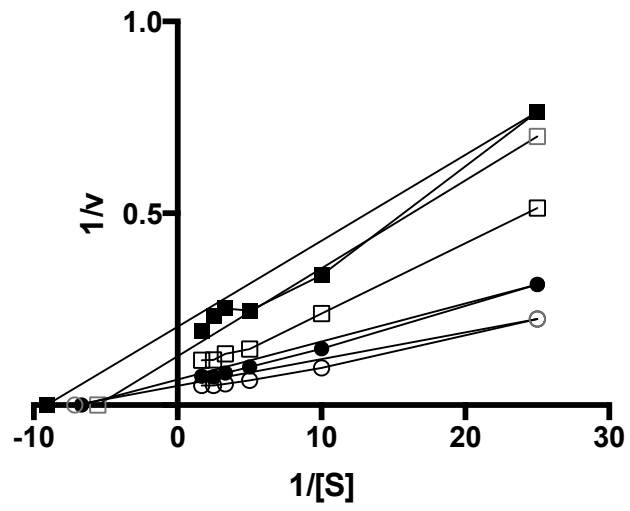


Figure 4.21 Lineweaver-Burk plots showing non-competitive inhibition of β -FXIIa by CHFI. X-axis is $1/[S2302]$, mM^{-1} ; Y-axis is $1/V$, $(\text{pmol}/\text{sec})^{-1}$. The symbols are different $[CHFI]$ as follows: (0 nM, \circ), (10 nM, \bullet), (30 nM, \square), (60 nM, \blacksquare).

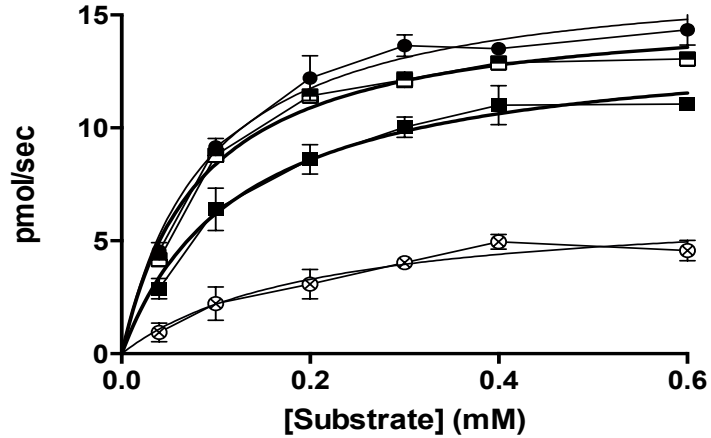


Figure 4.22 Michaelis-Menten kinetics of the inhibition of MBP- β -FXIIa by CHFI in the preincubation assay. The initial reaction rates (pmol of product /sec/ pmol of enzyme) of α -FXIIa vs. different concentrations of S-2302 used to find the kinetic parameters, K_M and k_{cat} . In every experiment, a duplicate was used for every [CHFI] used alongside with the different [S-2302], each versus each. Average of the duplicate values was taken. The error bar is the standard error of the mean of all independent experiments. The symbols are different [CHFI] as follows: (0 nM, \bullet), (3 nM, \square), (10 nM, \blacksquare), (100 nM, \circ).

Table 4.10 Kinetic parameters of CHFI-MBP- β -FXIIa interaction in the preincubation condition using Michaelis-Menten kinetics

| | [CHFI] (nM) | | | |
|---|------------------|------------------|----------------|-----------------|
| Kinetic parameters | 0 | 3 | 10 | 100 |
| K_M (mM) | 0.09 \pm 0.01 | 0.084 \pm 0.01 | 0.1 \pm 0.02 | 0.08 \pm 0.02 |
| k_{cat} (s^{-1}) | 17.02 \pm 0.77 | 15.47 \pm 0.48 | 13.5 \pm 1 | 5.2 \pm 0.3 |
| k_{cat} / K_M ($L \cdot mol^{-1} \cdot s^{-1}$) | 188888 | 184166 | 135000 | 65000 |

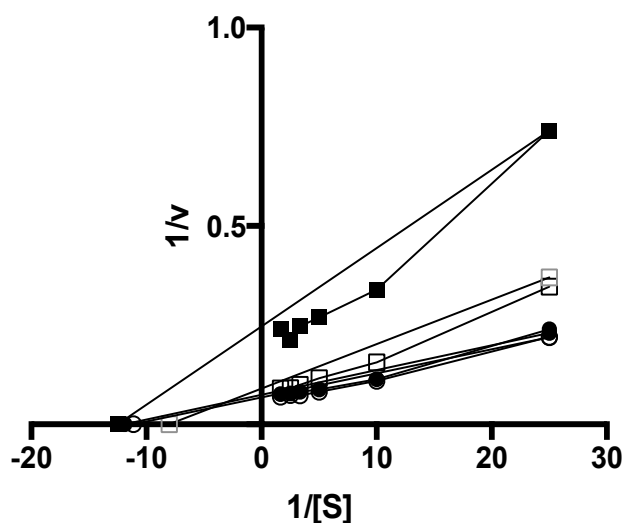


Figure 4.23 Lineweaver-Burk plots showing non-competitive inhibition of MBP- β -FXIIa by CHF1. X-axis is $1/[S2302]$, mM^{-1} ; Y-axis is $1/V$, $(\text{pmol}/\text{sec})^{-1}$. The symbols are different $[\text{CHF1}]$ as follows: (0 nM, \bullet), (3 nM, \square), (10 nM, \square), (30 nM, \blacksquare).

To elucidate the catalytic activity and affinity of FXII enzymes in the presence of CHF1, Michaelis-Menten kinetic analysis and Lineweaver-Burk plot were used to analyse the kinetic data (**Figure 4.24-4.29**). This is also used to verify the competitive behaviour of CHF1 in the coincubation assay. It was noticed that the values of K_M increase with the increase in the concentration of CHF1 whereas k_{cat} values are either kept unchanged or slightly increased (**Figure 4.25, 4.27 and, 4.29**), (**Table 4.11-4.13**). In the presence of high concentration of CHF1, the K_M values for α -FXIIa, β -FXIIa, and MBP- β -FXIIa are 8, 3, and 11 times higher than that in the absence of the inhibitor (**Table 4.11-4.13**).

This finding would further validate the competitive behaviour of CHFI in the coincubation experiment.

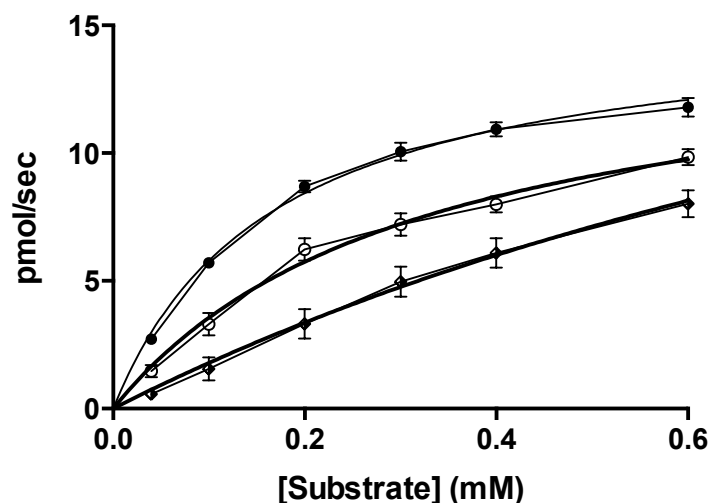


Figure 4.24 Michaelis-Menten kinetics of the inhibition of α -FXIIa by CHFI in the coincubation assay. The initial reaction rates (pmol of product /sec/ pmol of enzyme) of α -FXIIa versus different concentration of S-2302 used to analyze the inhibition effect. In every experiment, a duplicate was used for every [CHFII] alongside with different [S-2302], each vs. each. Average of the duplicate values was taken. The error bar is the standard error of the mean of all independent experiments. The symbols are different [CHFII] as follows: (0 nM, \bullet), (30 nM, \square), (60nM, \blacklozenge)

Table 4.11 Kinetic parameters of CHFII- α -FXIIa interaction in the coincubation condition using Michaelis-Menten kinetics

| Kinetic parameters | [CHFII] (nM) | | |
|--|------------------|-----------------|-----------------|
| | 0 | 30 | 60 |
| K_M (mM) | 0.16 \pm 0.01 | 0.32 \pm 0.06 | 1.3 \pm 0.8 |
| k_{cat} (s $^{-1}$) | 15.43 \pm 0.52 | 15 \pm 1.54 | 25.8 \pm 13.5 |
| k_{cat} / K_M (L mol $^{-1}$ s $^{-1}$) | 96437 | 46875 | 19846 |

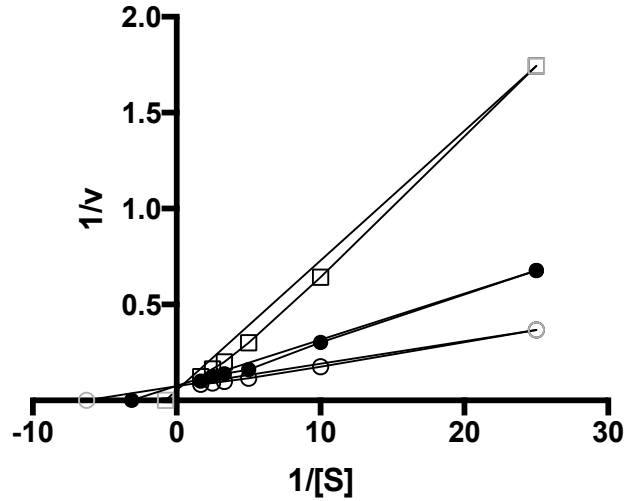


Figure 4.25 Lineweaver-Burk plots showing competitive inhibition of α -FXIIa by CHFI. X-axis is $1/[S_{2302}]$, mM^{-1} ; Y-axis is $1/V$, $(\text{pmol}/\text{sec})^{-1}$. The symbols are different [CHFI] as follows: (0 nM, \circ), (30 nM, \bullet), (60 nM, \square).

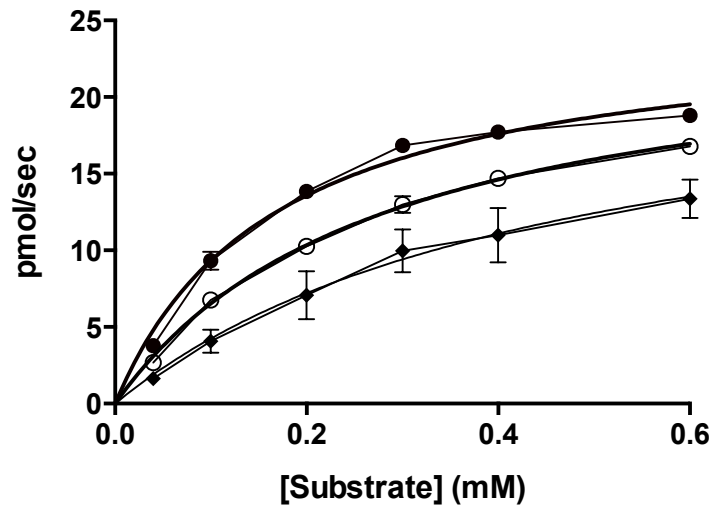


Figure 4.26 Michaelis-Menten kinetics of the inhibition of β -FXIIa by CHFI in the coincubation assay. The initial reaction rates (pmol of product /sec/ pmol of enzyme) versus different concentrations of S-2302 used to describe the inhibition β -FXIIa. In every experiment, a duplicate was used for every [CHFI] against different [S-2302], each vs each. Average of the duplicate values was taken. The error bar is the standard error of the mean of all independent experiments. The symbols are different [CHFI] as follows: (0 nM, \bullet), (30 nM, \circ), (60 nM, \blacklozenge).

Table 4.12 Kinetic parameters of CHF1- β -FXIIa interaction in the coincubation condition using Michaelis-Menten kinetics

| Kinetic parameters | [CHF1](nM) | | |
|--|-----------------|----------------|----------------|
| | 0 | 30 | 60 |
| K_M (mM) | 0.16 \pm 0.01 | 0.3 \pm 0.02 | 0.5 \pm 0.22 |
| k_{cat} (s ⁻¹) | 25 \pm 0.1 | 24.9 \pm 1.2 | 24 \pm 6 |
| k_{cat} / K_M (L mol ⁻¹ s ⁻¹) | 156250 | 83000 | 48000 |

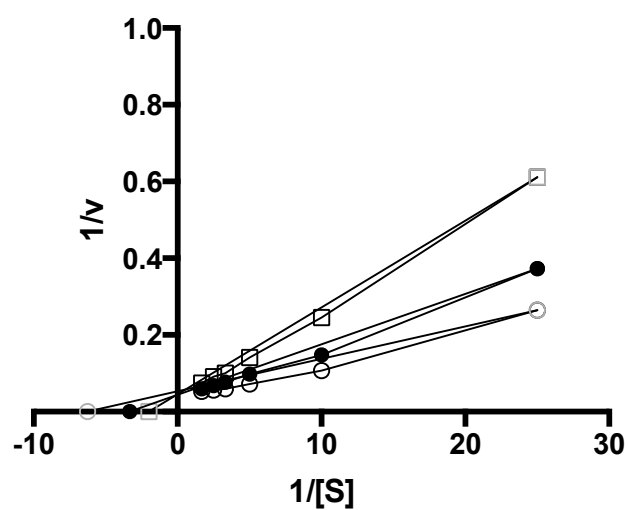


Figure 4.27 Lineweaver-Burk plots showing competitive inhibition of β -FXIIa by CHF1. X-axis is $1/[S2302]$, mM⁻¹; Y-axis is $1/V$, (pmol/sec)⁻¹. The symbols are different [CHF1] as follows: (0 nM, \circ), (30 nM, \bullet), (60 nM, \square).

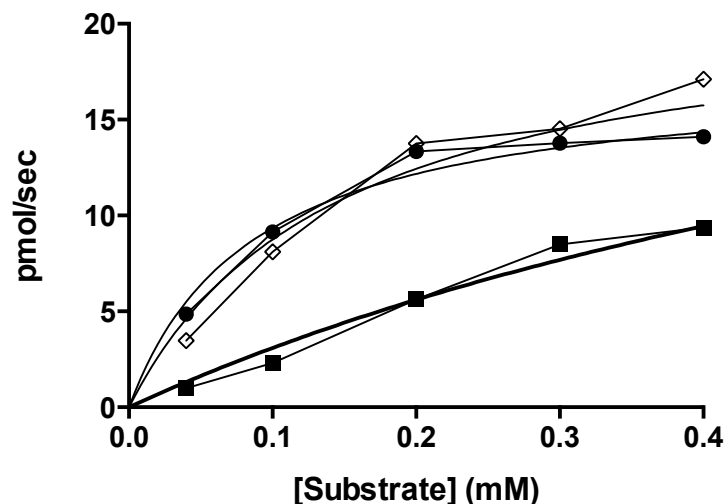


Figure 4.28 Michaelis-Menten kinetics of the inhibition of MBP- β -FXIIa by CHFI in the coincubation assay. The initial reaction rates (pmol of product /sec/ pmol of enzyme) versus different concentrations of S-2302 used to explain the inhibition interaction. In every experiment, a duplicate was used for every [CHFI] against every [S-2302], each versus each. Average of the duplicate values was taken. The error bar is the standard error of the mean of all independent experiments. The symbols are different [CHFI] as follows: (0 nM, \bullet), (10 nM, \diamond) (30 nM, \blacksquare).

Table 4.13 Kinetic parameters of CHFI-MBP- β -FXIIa interaction in the coincubation condition using Michaelis-Menten kinetics

| Kinetic parameters | [CHFI](nM) | | |
|--|------------------|-----------------|-----------------|
| | 0 | 10 | 30 |
| K_M (mM) | 0.08 \pm 0.01 | 0.14 \pm 0.04 | 0.86 \pm 0.3 |
| k_{cat} (s $^{-1}$) | 17.44 \pm 0.93 | 21.5 \pm 2.5 | 29.97 \pm 7.5 |
| k_{cat} / K_M (L mol $^{-1}$ s $^{-1}$) | 218000 | 153571 | 34848 |

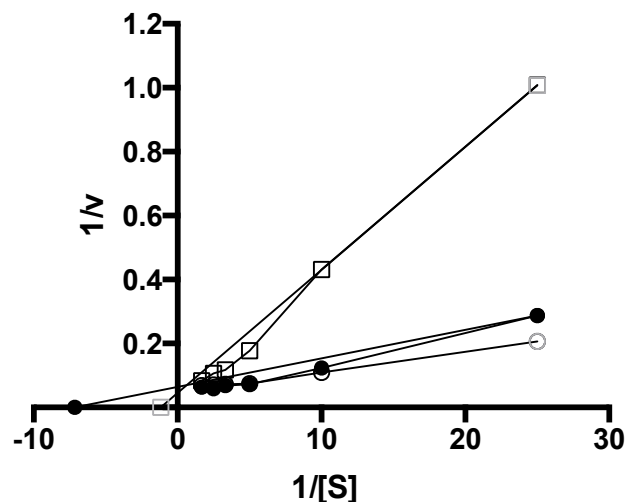


Figure 4.29 Lineweaver-Burk plots showing competitive inhibition of MBP- β -FXIIa by CHFI. X-axis is $1/[S2302]$, mM^{-1} ; Y-axis is $1/V$, $(\text{pmol}/\text{sec})^{-1}$. The symbols are different $[CHFI]$ as follows: (0 nM, \circ), (10 nM, \bullet), (30 nM, \square).

Hence, from these results explained above, it can be proposed that CHFI is a competitive inhibitor with tight-binding property, meaning that it has a slow degree of reversibility or irreversibility.

4.4.4 Tight-binding behaviour of CHFI

To further understand dissociation property of CHFI, reversibility assay was carried out. The objective behind this assay was to investigate that to what degree or how rapidly CHFI can dissociate from FXII enzyme. The second purpose was to validate the postulation that CHFI would tightly binds to FXII enzyme; this property would be responsible for the noncompetitive behaviour of CHFI in the preincubation assay. As explained in (**Figure 4.30**), there is a slow recovery of the enzyme catalytic activity from inhibition after rapid dilution. At 15 min point the amidolytic activity of the chronically inhibited FXII, the acutely inhibited FXII, and the uninhibited FXII is 1280, 3700, and

8000 pmol respectively. The amidolytic activity of the acutely inhibited FXII at high [CHFI] was kept unchanged (flat line of zero catalytic activity). Following approximately 15 min of rapid dilution, the inhibitor thus started to go from IC_{50} concentration (200 nM) to 10-fold below IC_{50} (20 nM), and α FXII from 100nM to 10nM. During this period the inhibitor would behave as a noncompetitive inhibitor and beyond this limit it would behave as a competitive inhibitor. Before 15 min, the dissociation constant (K_d) of CHFI is about zero due to tight binding of the inhibitor to the enzyme. Then, the enzyme dissociated and got maximum activity after 330 min. at this point, (15000) pmol of pNA is a reflection of K_d of CHFI at $[IC_{50}]$ (**Figure 4.30**).

Hence, from these investigations, it can be concluded that CHFI acts as a competitive inhibitor against α FXII with a slow degree of reversibility. This is in agreement with the abovementioned hypothesis and would further support the kinetic behaviour of CHFI in the preincubation state.

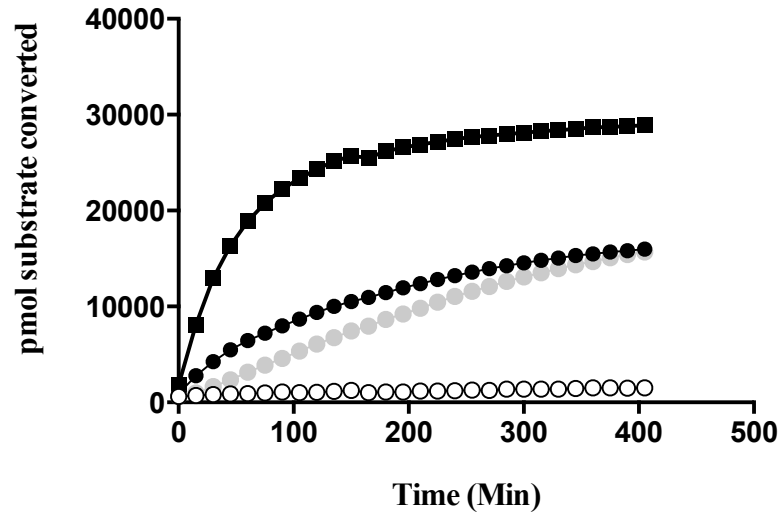


Figure 4.30 Slow recovery of enzyme activity after rapid dilution. The curve symbol (■) represents the behaviour of the negative control sample that was pre-incubated and diluted in the absence of inhibitor. The curve (●) is an acute assay of the low concentration inhibitor. The curve (○) is an acute assay of the high concentration inhibitor. The line with the symbol (●) is the behaviour of CHFI in complex with FXII (CHFI- α FXII complex) at a concentration of the inhibitor equal to 200 nM and of α FXII equal to 100 nM. At 15 min point, the amidolytic activity of the pre-inhibited FXII, acutely inhibited FXII at low [CHFI], and the uninhibited FXII is 1280, 3700, and 8000 pmol respectively. The amidolytic activity of the acutely inhibited FXII at high [CHFI] was kept constant (flat line of zero amidolytic activity). Following approximately 15 min of rapid dilution, the inhibitor concentration starts to go from $[IC_{50}]$ to 10-fold below $[IC_{50}]$ (20 nM). Throughout this period the inhibitor would behave as a non-competitive inhibitor and beyond this point it would behave as competitive inhibitor. Before 15 min the dissociation constant (K_d) of CHFI is about zero. Then, the enzyme becomes reversible and gets saturated after 330 min. at this point, (15000) pmol of the product is a reflection of K_d of CHFI at $[IC_{50}]$.

The competitive inhibition behaviour of CHFI could be due to the following possible mechanisms. The first could be that Arg43 (as described in the chapter 4) of CHFI inhibition loop and the Arg of the tri-peptide Pro-Phe-Arg, S-2302, compete for binding to the negatively charged target, Asp452, located on the surface of FXIIa (as described in chapter 5 in detail); this would function as a non-active site interaction surfaces, or an exosite, on the surface of FXIIa. This site would probably be required to recognize and cleave both S-2302 and CHFI with high specificity. The second possible mechanism would be that Arg34 at the very top of the exposed region of CHFI loop and Arg of the tripeptide substrate compete for binding to the active site of FXIIa. The negatively charged S1 pocket of FXII would accommodate the positively charged side chain of Arg34 of CHFI (as described in chapter 2), enabling the central residue to compete with the Arg of chromogenic substrate for binding to the catalytic triad of FXII. Thus, both CHFI and S-2302 could undergo hydrolytic breakdown resulting in the generation of the chromophore, p-nitroaniline, from S-2302 and cleavage of Arg34-Leu35 located on the surface of CHFI inhibition loop. Hence, there would be a similarity in the site of interaction of S-2302 and CHFI on FXII enzyme and this phenomenon is considered as a characteristic feature of competitive inhibition. Noncompetitive behaviour of CHFI could be due slow degree of dissociation rate as a result of noncovalent, tight binding of CHFI inhibition loop to FXIIa that leads to a more stable E-I (enzyme-inhibitor) complex. This effect would be due to the interaction of Arg43 of CHFI with the potential target residue, Asp452, expected to function as a non-active site interaction surface, or an exosite, on the surface of FXIIa (as described in chapter 5). Numerous

hydrogen bonds could be made between the interaction key residues of CHF1 and the other potential target residues on FXII enzyme that would also contribute to a more E-I complex. As described comprehensively in chapter 2, Arg34 could possibly hydrogen bond to both Asp592 and Gly621 in the S1 pocket of FXII. Trp22 and Gly32 of CHF1 could also form hydrogen bond with Gln450 and Trp618 of FXII respectively. Noncovalent, tight binding is a characteristic feature of the standard mechanism of the canonical inhibitors. With respect to this mechanism, both the intact inhibitor (CHF1) and its ligated product (regenerated CHF1) can impede the active site ^{[141],[136, 156]}. For the purpose of understanding the potential role of hydrogen bonds and non-active site surface salt bridge in the slow dissociation property of CHF1, reversibility assay for CHF1 recombinant variants having the desired point mutations would be required.

4.5 Conclusion

CHF1 behaves as a non-competitive inhibitor of the commercial forms and a recombinant variant of FXIIa when the enzymes were pretreated with the inhibitor. In contrast, it acts as a competitive inhibitor in the acute state. This proposes that CHF1 is a competitive inhibitor either with slow degree of reversibility or irreversible property due to tightness of binding. Reversibility assay validates that CHF1 is an inhibitor with slow degree of dissociation. The tight-binding property of CHF1 could be due to a non-active site interaction and or numerous hydrogen bonds between the key interaction residues and their potential targets on FXIIa

Chapter 5: Characterization of the different recombinant variants of the human coagulation FXII catalytic domain: relevance to the functional role of both Cys466 and glycosylated peptide fragment from proline-rich region in the full catalytic activity of the protease domain

5.1 Abstract

Michaelis-Menten model is extensively used in the studies of enzyme kinetics. The key parameters (k_{cat} and K_M) of a Michaelis-Menten reaction can experimentally be determined, which are useful for comparing different enzymes against each other. Human factor XII (FXII or Hageman factor) is a coagulation factor produced by liver and circulates in plasma as a single-chain zymogen having a molecular weight of 80 kDa and composed of non-catalytic domains (heavy chain) and a catalytic domain (light chain), which are separated by Arg353–Val354 bond. The bond is either cleaved by kallikrein or via surfactants that generates α FXIIa having a heavy chain of 50 kDa connected to a light chain of 28 kDa by Cys340-Cys466 disulphide bridge. Cleavage of α FXIIa causes loss of the heavy chain and production of the isolated protease domain known as β -FXIIa, which contains only a nine amino acid peptide fragment of the proline rich region disulphide bonded to the protease domain.

The aim in this chapter was to investigate into the function of FXII by examining the effect of Cys 466 and glycosylated peptide remnant from the proline-rich region on the function or the full catalytic activity of the protease domain through the following rational directions. Both FXIIc and FXIIac are composed of the catalytic domain having a point mutation at Cys 466 replaced

by Ser. Having N-terminus extra residues, an Arg followed by a Ser, FXIIc is different from FXIIac. These proteins were assayed for amidolytic activity to evaluate the effect of nonexistence of both Cys466 and the peptide fragment of the proline-rich region on the full catalytic activity of FXIIa and to examine whether they have enzyme-like or zymogen-like behaviour. The goal behind the activity test of HISTF- β FXII and MBP- β -FXIIa was to analyse the combined effect of Cys466 and the glycosylated/non-glycosylated) peptide fragment on the function of the catalytic domain. The glycosylated peptide would be existent in MBP- β -FXIIa due to its production in *Drosophila Schneider 2 cells* whereas it would be absent in HISTF- β FXII due to its generation in bacteria.

It was observed that FXIIc, FXIIac, and HISTF- β FXII didn't show any amidolytic activity in comparison with human β -FXIIa and α -FXIIa. However, at high concentration of both S-2302 and these recombinant forms, extremely weak amidolytic activity was noticed; this would propose that they would have zymogen-like behaviour. As far as activity assay is concerned, the zymogen-like behaviour of both FXIIc and FXIIac was used as a preliminary attempt to further develop assays characterizing these proteins in relation to their crystal structures[173]. Failure of autoactivation of FXIIc and FXIIac suggests that the catalytic domain would not have binding sites for the activators.

Compared to FXIIc and FXIIac, the higher amidolytic activity of HISTF- β FXII would be due to the presence of the peptide fragment bound to the catalytic domain of HISTF- β FXII by Cys340-Cys466. The lower amidolytic

activity of FXIIc in comparison with FXIIac would be due the presence of the extra residues at N-terminus of the former recombinant form. MBP- β -FXIIa behaved as β -FXIIa and α -FXIIa. The full amidolytic activity of MBP- β -FXIIa would be due to the existence of the glycosylated form of the peptide fragment likely to be present in MBP- β -FXIIa as a result of its expression in *Drosophila Schneider 2 cells* whereas it would be absent in HISTF- β FXII due to its expression in bacteria.

5.2 Introduction

The majority of the biochemical reactions need catalytic molecules (enzymes), which increase the rate of a certain reaction. In enzymatic reactions, the molecules at the beginning of the process are known as substrates (S); the enzymes (E) selectively convert them into products (P) (**Figure 5.1**). The kinetic explanation of such systems was stated by L. Michaelis and M.L. Menten. The resulting equation of their findings (referred to as Michaelis-Menten kinetics) is widely used in enzymology [184] [185] [186].

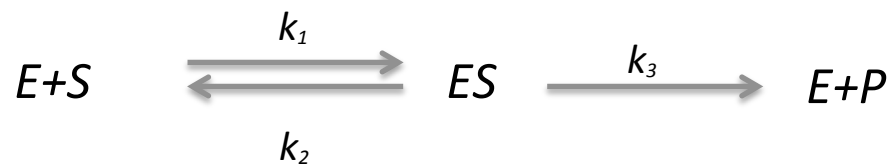


Figure 5.1 The scheme of enzyme-substrate reaction according Michaelis-Menten model. The reaction usually has one substrate, one active site of enzyme, and one product. k_1 is forward reaction constant; k_2 is reverse reaction constant; k_3 is product formation constant (k_{cat}); E is enzyme; S is substrate; ES is enzyme- substrate complex.

Generation of product or reduction of substrate over a certain period of time is experimentally used to determine reaction rates proportional to both of these quantities. The measured data can be analysed through nonlinear regression methods or by linear graphical representations. The key parameters (k_{cat} and K_M) of a Michaelis-Menten reaction can be determined, which are useful for comparing different enzymes against each other. k_{cat} reflects the constant of

product formation (k_3 or k_p) whereas K_M reflects k_2/k_1 (k_r/k_f). Catalytic efficiency of an enzyme depends on both k_{cat} and K_M [185],[186],[183],[178].

Human factor XII (FXII or Hageman factor) is a coagulation factor produced by liver and circulates in plasma as a single-chain zymogen having a molecular weight of 80 kDa and composed of non-catalytic domains (heavy chain) and a catalytic domain (light chain), which are separated by Arg353–Val354 bond [75-78, 98]. Cleavage of Arg353–Val354 peptide bond is caused either via proteolytic cleavage (kallikrein) or via autoactivation (surfactants), generating α FXIIa having a heavy chain of 50 kDa connected to a light chain of 28 kDa by the Cys340-Cys467 disulphide bridge. Cleavage of α FXIIa leads to loss of the heavy chain and generation of the isolated protease domain known as β -FXIIa, which contains only a nine amino acid peptide fragment of the proline rich region disulphide bonded to the protease domain [75-78].

A study showed that r β -FXII is not able to hydrolyse the chromogenic substrate, S-2302 or S2222, as expected of a zymogen. Following activation by kallikrein, it was noticed that compared to human β -FXIIa, r β -FXIIa shows reduced amidolytic activity, proposing that absence of the glycosylated Asn335 of the remnant peptide of the proline rich region or the presence of 39 amino acid residues (T7 promoter, an N-polyhistidine tag, a thrombin restriction site) at the N-terminus would be responsible for loss of activity of r β -FXIIa [75-78, 187, 188].

The aim in this chapter was to study enzyme kinetics of the different recombinant variants (FXIIc and FXIIac were generated by M Pathak, a research assistant in the structural biology group/ Emsley group; HISTF- β FXII

and MBP- β -FXIIa were generated by R Manna, a PhD student in the structural biology group/ Emsley group) of the protease domain of the human coagulation factor FXII in order to investigate into the function of FXII by examining the influence of Cys466 and glycosylated peptide fragment of the proline-rich region on the function of the protease domain.

FXIIc and FXIIac are composed of the catalytic domain having Cys466 substituted by Ser, lacking the peptide fragment remnant from proline-rich region. At N-terminus, FXIIc has extra residues, an Arg followed by a Ser. The first objective behind the amidolytic activity of these proteins was to evaluate the influence of absence of both Cys466 and the peptide fragment of the proline-rich region on the catalytic activity of the protease domain and to examine whether they have enzyme-like or zymogen-like behaviour. The second objective was to examine the autoactivation of these recombinant forms. The third aim was to evaluate the effect of the extra residues at N-terminus on the amidolytic activity of the catalytic domain.

The purpose behind the amidolytic activity of HISTF- β FXII and MBP- β -FXIIa was to examine the impact of the presence of Cys466 in combination with either the glycosylated or the non-glycosylated peptide fragment of the proline-rich region on the full catalytic activity of the protease domain. The glycosylated peptide would be existent in MBP- β -FXIIa due to its generation in *Drosophila Schneider 2 cells* whereas it would be absent in HISTF- β FXII due to its generation in bacteria.

5.3 Materials and methods

5.3.1 Materials

5.3.1.1 List of materials

The materials ordered or previously available in C62 and C84 lab were listed below (**Table 5.1**).

Table 5.1 List of materials used in the characterization study of different recombinant variants of FXII

| Product | Description/Uses | Storage T | Provider |
|-------------------------------|--|-----------|------------------------------|
| FXII (FXII zymogen) | Human coagulation Factor XII, concentration 1.35 mg /mL, 16.89 μ M before lyophilisation, volume/ aliquot, 0.370 mL. The total enzyme protein was 0.5 mg, stock is 25.33 μ M (0.5mg/247 μ l) | -80°C | Enzyme Research Laboratories |
| α -FXIIa (alpha FXIIa) | Human coagulation Factor XIIa alpha, concentration 1.85 mg/mL (23.14 μ M) (before lyophilisation), aliquot of 1 x 0.50 mg | -80°C | Enzyme Research Laboratories |

| | | | |
|---------------------------|--|--|------------------------------|
| | | and volume/ aliquot 0.270 mL, stock is 23.14 μ M | |
| FXIIab FXIIaF, FXIIaP) | (β -FXIIa, Human Factor XIIa beta, | -80°C | Enzyme Research Laboratories |
| | concentration 2.2 mg/mL (74.07 μ M), (before lyophilisation), aliquot of 1 x 0.1 mg and volume/ aliquot 0.045 mL, stock is 16.67 μ M (0.1mg/200 μ l) | | |
| NGPLSCGQR | A peptide of 9 amino acid residues (335-343) of proline-rich region, the peptide (29.1 mg, white lyophilized powder) was dissolved in 14 ml gradually, i.e. first, 5 ml was added, after shaking, another 5 ml was added, finally 4 ml to a concentration of 2.08 mg/ml, (2.23) mM | -20°C | GenScript /custom peptide |
| NGPLSCGQRLRKSL SMTR | A peptide of 19 amino acids, (335-353) of the proline region of FXII. The peptide was supplied as white lyophilized powder | -20°C | GenScript /custom peptide |
| | The peptide (29.2 mg) was dissolved in 14 ml | | |

step by step, i.e. first, 5 ml was added; after shaking, extra 5 ml was added, finally, 4 ml to a concentration of 2.078 mg/ml, 997.95 μ M

| | | | |
|--------------|--|-------------------------|--------------|
| S-2302 | Chromogenic substrate | -20°C | Chromogenix, |
| | <p>for FXII. Chemical name: H-D-Prolyl-L-phenylalanyl-L-arginine-p-nitroaniline dihydrochloride (H-D-Pro-Phe-Arg-pNA·2HCl or S-2302). Stock is 25mg/4 ml D.W (10mM). Various concentrations, 6 mM, 5 mM, 3 mM, 2 mM, 1 mM, and 0.4mM were prepared from the stock.</p> | | |
| Zinc | sulphate | Activator for FXII. Mr: | -20°C |
| heptahydrate | (ZnSO ₄ ·7H ₂ O) | 287.54g/mole, | SIGMA |
| | <p>hygroscopic. 0.29g was dissolved in 10 ml D.W to prepare 100mM: 10ml stock. 10μl was diluted to 10 ml to prepare a working concentration of 100μM: 10ml</p> | | |

| | | | |
|------------------------------|---|--------|---------------|
| Kaolin powder | A negative surface agent activating FXII. An amount of 2.5g as white powder was dissolved in 250 ml D.W to produce a solution of 10mg/ml; manual stirring for 30 minutes was required. | -20°C | SIGMA |
| Poly P | Polyphosphate P is a negative surface agent activating FXII. 0.1g dissolved in 10 ml D.W to produce a solution of 10mg/ml | -20°C | Sigma Aldrich |
| Dextran sulphate sodium salt | A negative surface agent activating FXII. An amount of 0.025 g dissolved in 1 ml D.W. 100 µl was taken and completed to 1ml to get a solution of 2.5mg/ml. to prepare a working concentration of 1mg/10 ml, 400 µl of the solution was added to 15ml falcon tube then completed to 10ml using D.W | -20 °C | Sigma Aldrich |

5.3.1.2 Recombinant FXII enzyme

5.3.1.2.1 FXIIac and FXIIc

FXIIac and FXIIc were generated by M Pathak (a research assistant in the structural biology group/ Emsley group) in *Drosophila Schneider S2 cells*. FXIIac is similar to the human coagulation FXII catalytic domain (Mr 28 kDa), but it has a cysteine residue (Cys466) replaced by a serine using mutagenesis (**Figure 5.2**). A volume of 50 μL of 0.6329 mg/ml (22.60 μM) was used as a stock in the amidolytic assay. A fraction of 10 μL was completed to 1000 μL by PBS to get a working concentration of 0.2260 μM .

FXIIc is similar to FXIIac, but the extra residues, an arginine followed by a serine, are present at N terminus (**Figure 5.3**); its molecular weight is 28.22 kDa. A volume of 50 μl of 23.4 mg/ml (836.07 μM) batch and 30 μl of 55.518 mg/ml (1.9827 mM) batch of the protein were used as stock. When required, for the purpose of evaluation of amidolytic assay, a volume of 10 μl of each stock was diluted to 1000 μl using PBS to get working solutions having the concentrations, 8.36 μM , and 19.83 μM respectively. A volume of 30 μl of the 8.36 μM solution was further diluted to 1000 μl to make a working concentration (0.25 μM) used for the analysis of autoactivation of FXIIc. There were several points behind testing these protein constructs: first, to examine the impact of deficiency of both Cys466 and the peptide fragment of the proline-rich region on the catalytic activity of the protease domain and to examine whether they have enzyme-like or zymogen-like behaviour, second, to evaluate whether the catalytic domain can be autoactivated, third, to analyse the effect of the extra residues at N-terminus on the amidolytic activity of the

catalytic domain, and fourth, from activity side, to preliminarily define the enzymatic behaviour of these forms of FXII enzymes in correlation with their crystal structure [173]

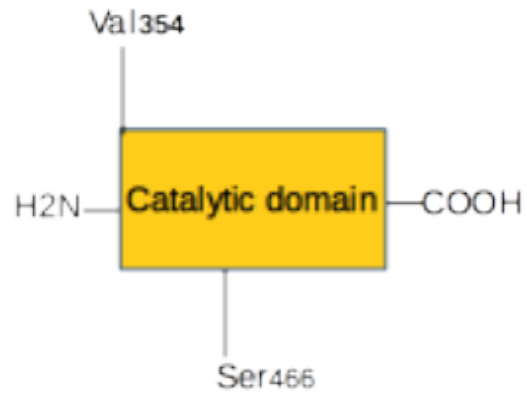


Figure 5.2 Schematic representation of the FXIIac. The protein construct is composed of the catalytic domain with a point mutation; Cys 466 is replaced by Ser 466.

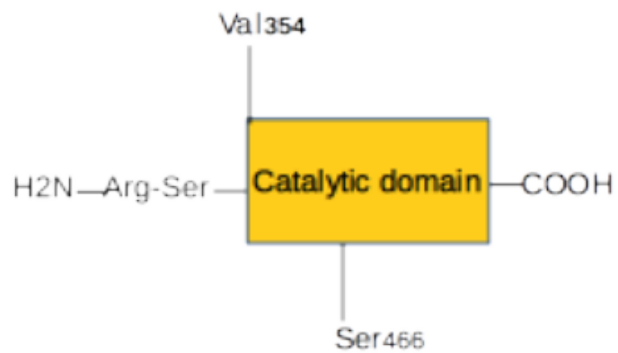


Figure 5.3 Schematic representation of FXIIc. The protein construct is similar to FXIIac, but it has extra N-terminus residues, an Arg followed by a Ser.

5.3.1.2.2 HISTF- β FXII and MBP- β -FXIIa

Both HISTF- β FXII (in bacteria) and MBP- β -FXIIa (in *Drosophila Schneider S2 cells*) were generated by R Manna, a PhD student in the structural biology group/ Emsley group. From N-terminus to C-terminus, HISTF- β FXII consists of His tag, TF (trigger factor), a cleavage site (linker), NGPLSCGQRLRKSLSSMTR (the peptide fragment disulphide bonding to the catalytic domain), and the protease domain. The peptide has the same amino acid sequence as that of human β -FXIIa, but in HISTF- β FXII the peptide is nonglycosylated. The molecular weight of the fusion protein is 78 kDa (**Figure 5.4**).

From N-terminus to C-terminus, MBP- β -FXIIa consists of MBP Tag, AAAAS linker, glycosylated NGPLSCGQRLRKSLSSMTR and the protease domain. The glycosylated peptide has the same amino acid sequence as that of human β -FXIIa. The molecular weight of the construct is 75.6 kDa. The significance of testing these proteins was to evaluate the importance of the glycosylated peptide for the full catalytic activity of β -FXIIa (**Figure 5.5**).

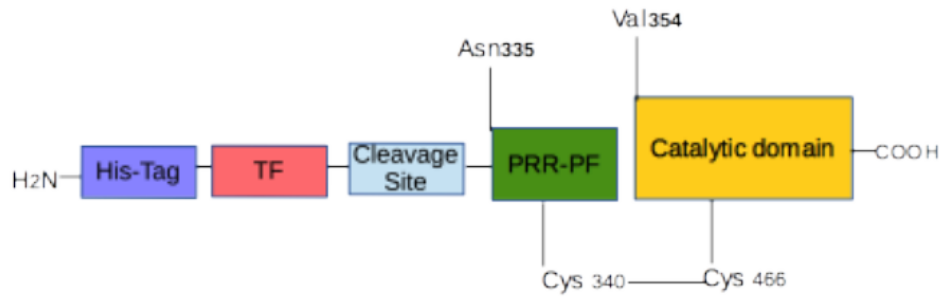


Figure 5.4 Cartoon diagram of HISTF-βFXII. From N-terminus to C-terminus, the construct has His Tag, TF, the cleavage sites (thrombin and HRV3C protease sites), a nonglycosylated (NGPLSCGQRLR_KSLSSMTR) peptide, and the catalytic domain. The peptide is bound to the protease domain via Cys466-Cys340 disulphide bond. TF is trigger factor and PRR-PF means proline-rich region peptide fragment.

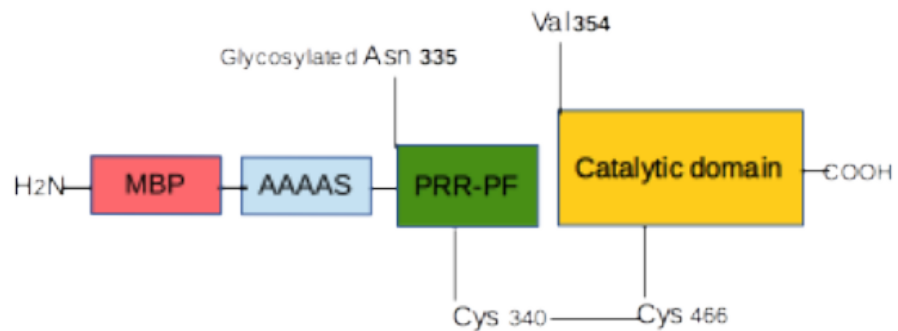


Figure 5.5 Cartoon diagram of MBP-βFXIIa. From N-terminus to C-terminus, the construct has MBP Tag, AAAAS linker, a glycosylated-NGPLSCGQRLR_KSLSSMTR peptide, and the catalytic domain. The peptide is bound to the protease domain via Cys466-Cys340 disulphide bond. PRR-PF means proline-rich region peptide fragment.

5.3.2 Methods

5.3.2.1 Calibration

In order to convert absorbance unit to the absolute amount of the coloured product released, calibration assay was performed using p-nitroaniline as described fully in chapter 1.

5.3.2.2 Amidolytic activity

This assay was performed to test amidolytic activity of the FXII commercial forms. Then, this was used as a guide to enzymology of the FXII recombinant forms. A series of the diluted working solutions of S-2302 was prepared from the stock solution (10 mM: 100 μ l) as follow: 6 mM, 4 mM, 3 mM, 2 mM, 1 mM, 0.4mM (i.e. 0.6 mM, 0.4 mM, 0.3 mM, 0.2 mM, 0.1 mM, 0.04 mM for the assay respectively). Different forms of FXII (0.025 μ M FXII zymogen, 0.023 μ M α -FXIIa, 0.016 μ M β -FXIIa, 0.022 μ M FXIIac and 1.982 μ M FXIIc) were tested on the different concentrations of the S-2302 for amidolytic activity. The plate was marked from 1 to 6 wells with the series of assay [substrate] horizontally. Two duplicates (4 wells) used for each concentration; the assay volume was 100 μ l. PBS alone, PBS with S-2302 and PBS with FXII were used as different controls. Once the plate was prepared, it was transferred to the shaker to mix the contents properly for 20 seconds and then transferred to the plate reader used to detect absorbance due to substrate cleavage each 5 min at 405nm and 37°C for 55-60 min duration.

In FXII-activation assays (The aim of this assay was to evaluate the effect of the negative surface agents and the remnant peptide on the catalytic activity of FXII different forms), the same experimental procedures were performed as described above in detail, but in the activation assays, following pretreatment of the enzymes with the different types of activators, FXII different forms were tested on the different concentrations of S-2032.

5.4 Results and discussion

5.4.1 Amidolytic activity of the commercial forms of FXIIa, α -FXIIa and β -FXIIa

A time course assay of the catalytic activity of α -FXIIa and β -FXIIa was performed at different S-2302 concentrations. There is a clear direct relationship between various substrate concentrations and the amount of product generated. The speed of the linear reaction to reach a saturation state depends on the concentration of the chromogenic substrate when concentration of the enzyme, temperature and duration of the FXII-S-2302 reaction are kept constant (**Figure 5.6 and 5.7**).

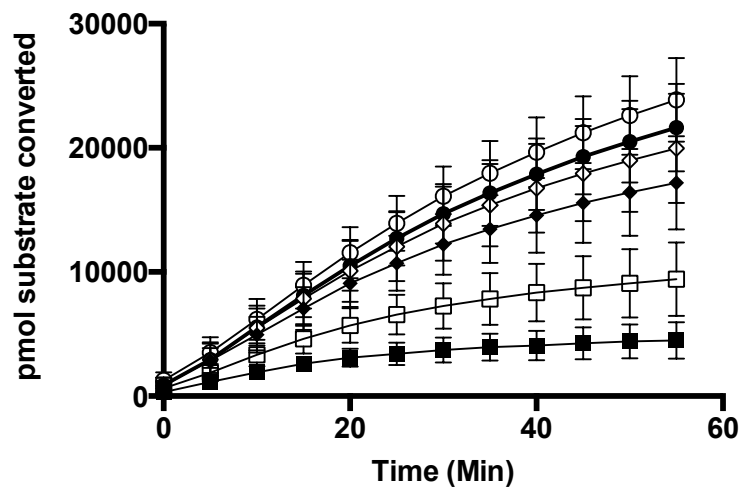


Figure 5.6 α -FXIIa-S-2302 time dependent assays. Number of picomoles of product (per pmol of α -FXIIa) was generated by amidolytic breakdown of the different concentrations of S-2302 versus time. picomoles of product / pmol of the protease is average of 12 independent experiments. In each experiment a duplicate was used for every [substrate]; average of the duplicate values was taken. The error bar is standard error of the mean of all the independent experiments. The following symbols indicate different S-2302 concentrations: (0.04 mM, ■), (0.1 mM, □), (0.2 mM, ●), (0.3 mM, ◇), (0.4 mM, ●), (0.6 mM, ○).

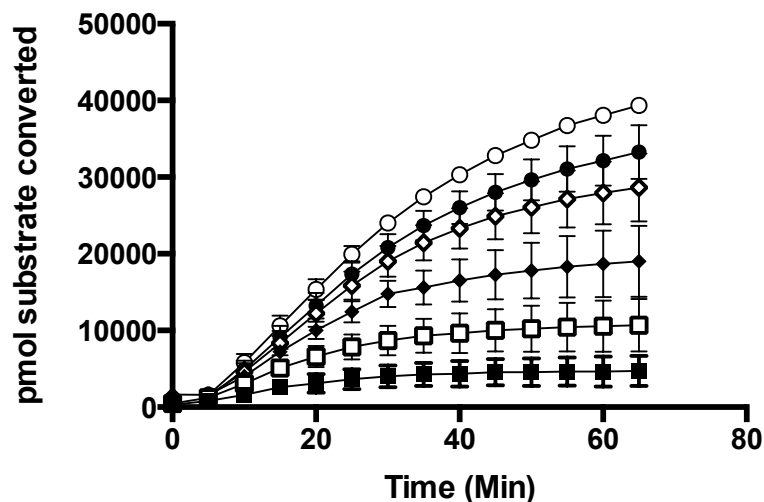


Figure 5.7 β -FXIIa-S-2302 time dependent assays. Number of picomoles of the product (per pmol of β -FXIIa) was produced by hydrolytic breakdown of the different concentrations of chromogenic substrate versus time. Picomoles of product / pmol of the protease was average of 12 independent experiments. In each experiment a duplicate was used for each [substrate]. Average of the duplicate results was taken. The error bar is standard error of the mean of all the independent experiments. The following symbols indicate different S-2302 concentrations: (0.04 mM, ■), (0.1 mM, □), (0.2 mM, ◆), (0.3 mM, ◇), (0.4 mM, ●), (0.6 mM, ○).

The initial rate was then calculated by taking two time points within the window of linear initial reaction (**Table 5.2 and Table 5.3**).

Table 5.2 Initial reaction rates of the cleavage of the different concentrations of S-2302 by one pmol of the enzyme. The value of each initial reaction rate is average of twelve independent experiments. In every single experiment two wells were used as a duplicate. Then, average of the duplicate results was calculated. The error is standard error of the mean of all the independent experiments.

| [Substrate] (mM) | (pmol /s/pmol α-FXIIa) |
|-------------------------|--|
| 0.04 | 2.62±0.20 |
| 0.1 | 5.33±0.33 |
| 0.2 | 8.46±0.24 |
| 0.3 | 9.73±0.43 |
| 0.4 | 11.09±0.48 |
| 0.6 | 11.57±0.33 |

Table 5.3 Initial reaction rates of the hydrolysis of the different concentrations of S-2302 by one pmol of the enzyme. The value of each initial reaction rate is average of twelve independent experiments. In every single experiment two wells were used as a duplicate. Then, average of the duplicate results was calculated. The error is standard error of the mean of all the independent experiments.

| [Substrate] (mM) | (pmol/s/pmol β-XIIa) |
|-------------------------|---|
| 0.04 | 2.82±0.55 |
| 0.1 | 7.02±1.01 |
| 0.2 | 11.05±0.97 |
| 0.3 | 14.41±0.91 |
| 0.4 | 15.49±0.77 |
| 0.6 | 17.43±0.56 |

By plotting the initial rates of product formation against different concentrations of the substrate, the enzymatic behaviour of α -FXIIa and β -FXIIa proteases was shown to follow Michaelis Menten kinetics in respect of the chromogenic substrate (S-2302) (**Figure 5.8 and 5.9**).

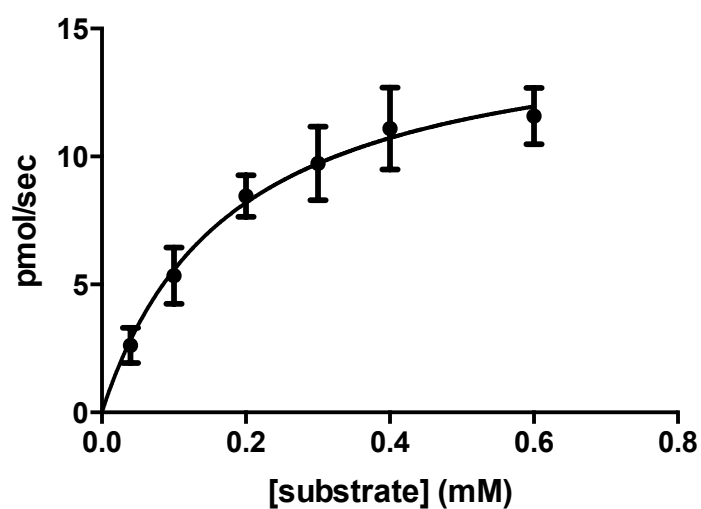


Figure 5.8 α -FXIIa obeys Michaelis-Menten model. Nonlinear regression analysis of the initial velocities per pmol of α -FXIIa versus different concentrations of the substrate was used to define catalytic mechanism of the enzyme. Twelve experiments were performed. In each experiment a duplicate was used for every [substrate]; average of the duplicate values was taken. The error bar is standard error of the mean of all the independent experiments.

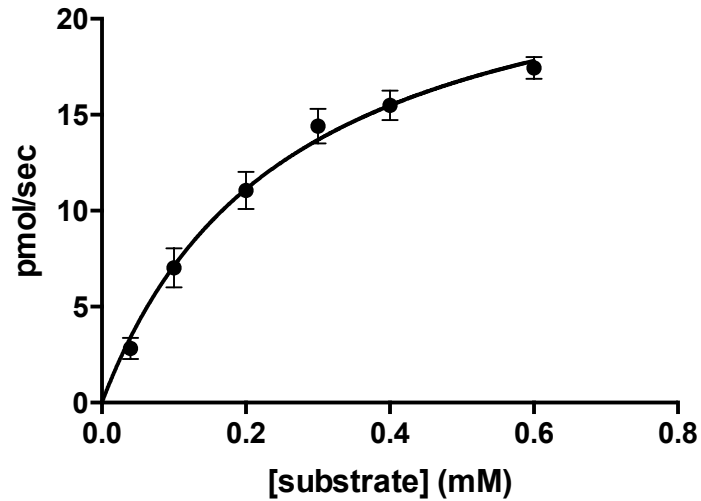


Figure 5.9 β -FXIIa obeys Michaelis Menten model. Nonlinear regression analysis of the initial velocities per pmol of β -FXIIa against different concentrations of the substrate was used to describe catalytic mechanism of the enzyme. Twelve experiments were performed. In each experiment a duplicate was used for every [substrate]; average of the duplicate values was taken. The error bar is standard error of the mean of all the independent experiments.

This model was used to determine enzyme kinetic parameters and explain catalytic activity of these enzymes and all other forms of FXII as explained below (**Table 5.4**).

Table 5.4 Estimation of V_{max} , K_M and k_{cat} values of the different forms of human activated FXII using average of twelve experiments for each of α -FXIIa and β -FXIIa assay. In every single experiment two wells was used as a duplicate for every [substrate]. Average of the duplicate results was taken. The error bar represents standard error of the mean of the independent experiments.

| Parameters | α -FXIIa | β -FXIIa |
|---|-----------------|----------------|
| V_{max} (pmol/s) | 43.46±2.07 | 71.33±6.64 |
| k_{cat} (s^{-1}) | 15.52±0.74 | 25.47±2.37 |
| K_M (mM) | 0.17±0.02 | 0.25±0.05 |
| k_{cat} / K_M ($L \text{ mol}^{-1} s^{-1}$) | 91204 | 101880 |

With respect of hydrolysis of the chromogenic substrate (S-2302), the activity parameter (k_{cat}) of β -FXIIa is slightly higher than that of α -FXIIa (**Table 5.4**). This finding is consistent with the work reported by a study showing that the activity of β -FXIIa is higher than α -FXIIa [106] . This would be due to the presence of a single, shorter amino acid sequence in β -FXIIa when compared to α -FXIIa, which enables the enzyme to speedily convert the substrate molecules to the product molecule. β -FXIIa has slightly lower affinity to the chromogenic substrate, S-2302, than does α -FXIIa; this maybe indicates that although α -FXIIa binds to the substrate more strongly than does β -FXIIa, it produces less conversion of the substrate to the product. However, with respect of S-2302, the catalytic efficiency (or specificity) of these proteases is quite similar.

K_M for β -FXIIa (0.25 ± 0.05 mM) and α -FXIIa (0.17 ± 0.02 mM) of the current study is identical to what has been found in the other studies. According to a study[189], K_M is equal to 0.190 mM for both forms of FXII. Based on the current observation and the observation of the same study, k_{cat} values of α -FXIIa (15.52 ± 0.74 s⁻¹ and 15 ± 2 s⁻¹ respectively) and β -FXIIa (25.47 ± 2.37 s⁻¹ and 15.52 ± 0.74 s⁻¹ respectively) are approximately similar[189]. This indicates that the result of the current study is in agreement with what has been found previously. Hence, this validates appropriate enzymology and characterization of the recombinant coagulation FXII catalytic domain constructs.

In the subsequent sections, similar analysis was performed for FXII zymogen, FXIIac, FXIIc, HISTF- β FXII, and MBP- β -FXIIa.

5.4.2 Amidolytic activity of FXII zymogen, FXIIac, and FXIIc in comparison with β -FXIIa and α -FXIIa.

The same assays and steps, described above for α -FXIIa and β -FXIIa, were carried out in order to characterize catalytic activity of FXII zymogen and the different recombinant variants of the protease domain. It was observed that one pmol of the enzymes, FXII zymogen, FXIIac and FXIIc, did not show any amidolytic effect on 0.6 mM S-2302 in comparison to β -FXIIa and α -FXIIa, (**Figure 5.10 and 5.11**) whereas the same concentration of α -FXIIa and β -FXIIa produced substantial amidolytic cleavage on the substrate.

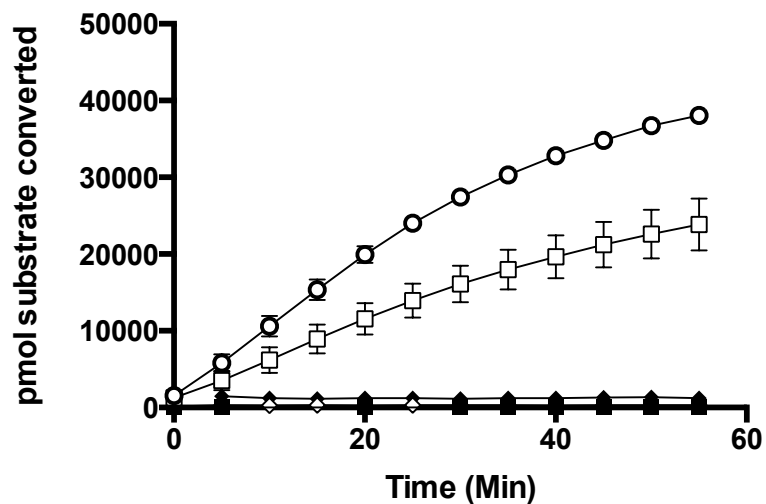


Figure 5.10 Comparative time dependent assay of the different commercial forms and recombinant variants of FXII. Number of picomoles of product (per pmol of enzyme) was generated by hydrolysis of 0.6 mM S-2302 by various forms of FXII. Average of twelve independent experiments for α -FXIIa and β -FXIIa and three experiments for other FXII forms were used. In each experiment a duplicate was used for the [substrate]; average of the duplicate values was taken. The error bar is standard error of the mean of all the independent experiments. The following symbols indicate the different enzymes: (FXII zymogen, ■), (FXIIc, ◆), (FXIIac, ◇), (α -FXIIa, ◻), (β -FXIIa, ○).

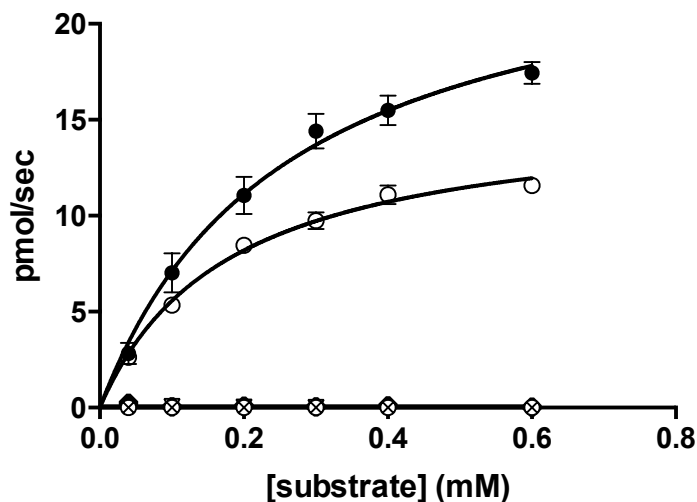


Figure 5.11 Activity of different forms of FXII. Amidolytic activity (pmol/sec/ pmol of the proteases) of various forms of FXII versus different [substrate] (mM) was plotted. FXIIc and FXIIac behave as FXII zymogen. Average of twelve experiments for α -FXIIa, and β -FXIIa and three experiments for the other FXII forms were used. In each independent experiment a duplicate was used for each [substrate]; average of the duplicate values was taken. The error bar is standard error of the mean of all the independent experiments. The following symbols indicate the different enzymes: (FXII zymogen, \bullet), (FXIIc \square), (FXIIac, \blacktriangle), (β -FXIIa, \blacklozenge), (α -FXIIa, \circ).

FXII zymogen, FXIIc, and FXIIac behave similarly and did not show amidolytic activity in comparison with the active; this indicates that they have a protease domain in inactive state. With respect to FXII zymogen, the reason of inactivity would be that the zymogen form (proenzyme) is usually in inactive state. The amidolytic activity of the recombinant forms of the catalytic domain was further examined using higher concentration of the chromogenic substrate, S-2302, and higher concentration of fresh batches of the enzymes.

FXIIc showed an extremely weak amidolytic effect, which is 15000 and 1000 times less than that of human β -FXIIa and α -FXIIa respectively, even though higher concentration of the recombinant protein (2500 times) and higher concentration of S-2302 (1.6 times) were used in the assay of the recombinant protein (**Figure 5.12**).

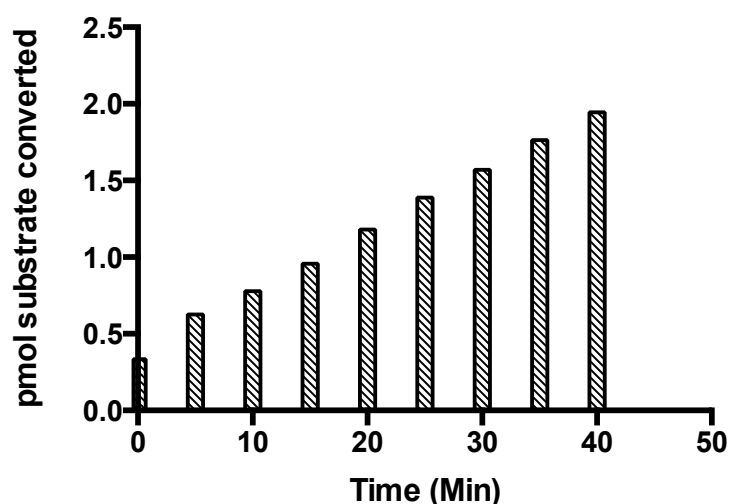


Figure 5.12 Amidolytic activity of FXIIc. When compared to β -FXIIa and α -FXIIa, at 40-min time point, FXIIc caused release of a very small amount of pNA (picomoles of product per pmol of FXIIc) as a result of its extremely weak hydrolytic effect on S-2302. In each experiment a duplicate was used; average of the duplicate values was taken. The concentration of the protein construct was 25 μ M (2500 times more than that of the commercially available activated forms) and S-2302 was 1mM (1.6 times more than the maximum concentration used in the assays of the commercially available activated forms).

The first cause of inactivity (or extremely weak amidolytic activity) of FXIIc in comparison with β -FXIIa and α -FXIIa may have been the presence of extra residues (an arginine followed by a serine residue) at N-terminus of the recombinant protease domain. To test this hypothesis, the amidolytic activity was also performed for FXIIac lacking Arg and Ser residues at N-terminus.

However, FXIIac also showed a weak hydrolytic effect, which is approximately 150 and 100 times less than that of human native type β -FXIIa and α -FXIIa respectively, although higher concentration of the recombinant enzyme, 100 times, and S-2302, 1.6 times, was used in the assay of FXIIac (Figure 5.13). However, compared to FXIIac, 100-time less amidolytic activity of FXIIc may have been the presence of the extra N-terminus residues in the latter recombinant form. This finding would indicate that FXIIc and FXIIac have zymogen-like behaviour. From activity side, the zymogen-like behaviour of both FXIIc and FXIIac was used as a preliminary attempt to further characterize these proteins in relation with their crystal structures[173].

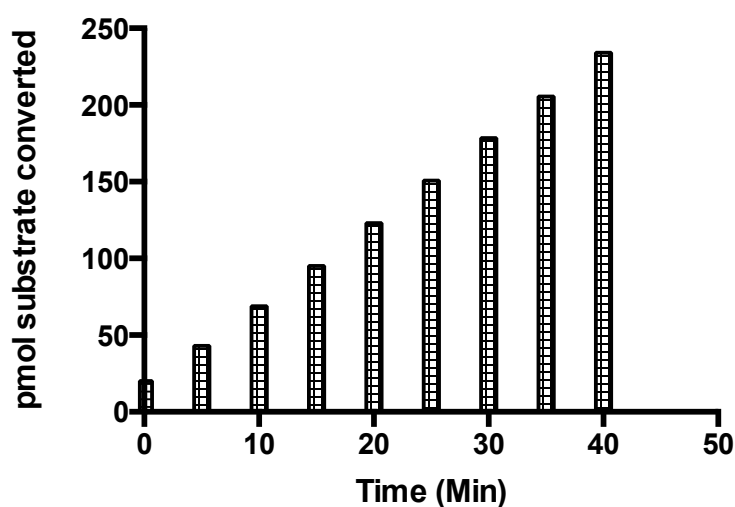


Figure 5.13 Amidolytic effect of FXIIac. Compared to β -FXIIa and α -FXIIa, at 40-min time point, FXIIac produced release of a slight amount of the coloured product (picomoles of product per pmol of FXIIac). In each experiment, a duplicate was used; average of the duplicate values was taken. The concentration of the enzyme construct was 1 μ M (100 times more than that of β -FXIIa and α -FXIIa) and S-2302 was 1mM (1.6 times more than the maximum concentration used in the β -FXIIa and α -FXIIa assays).

The catalytic domain could be in the zymogen form and needs to be activated by negative surface agents. To test this assumption, autoactivation assays were performed (**section 5.3.3**). The third possible cause could be absence of the peptide fragment of the proline-rich region. In the wild type FXIIa, Cys466 of the catalytic domain disulphide bonds with Cys340 of the remnant peptide from the proline-rich region. To test this postulation, the effect of this fragment on the catalytic activity of FXIIac was evaluated (**section 5.3.4**). The fourth possible cause would be the loss of both Cys466-Cys340 disulphide bond and the peptide fragment and or substitution of the cysteine residue, Cys466, by serine; this reason was analysed in the section of amidolytic activity of HISTF- β FXII (**section 5.3.6**). The last possible reason is absence of the remnant peptide having the glycosylated Asn335; this could play an important role in the catalytic activity. To test this hypothesis, MBP- β -FXIIa having the glycosylated peptide was tested for the amidolytic activity in comparison with the commercially available activated forms, clarified in the last section below.

5.4.3 Autoactivation of FXII zymogen and the recombinant catalytic domains

The aim of this experiment was to activate FXII zymogen through autoactivation i.e. conversion of the zymogen from an inactive conformation to the catalytically active conformation by the negative surface agents. This would be used as a useful guide to perform autoactivation assay for the recombinant variants of the catalytic domain and rationalize their zymogen-like behaviour, described below in detail. The second aim was to examine if

binding sites for the activators exist within the recombinant catalytic domain of FXIIc and FXIIac. The third objective behind this assay was to compare the effect of the negative surface agents alone and in combination with Zn^{2+} on the recombinant variants. Polyphosphate, kaolin and dextran (with and without zinc ion) were used as negative surface agents and incubated with FXII zymogen; then to verify activation of FXII, the mixture was supplemented with S-2302 and the process of amidolytic cleavage was monitored by the optimized colorimetric assay using spectrophotometer. These agents were able to convert FXII zymogen to FXIIa and the activation process was probably elicited by attachment of these agents to the binding domains in the heavy chain (Fibronectin, kringle and EGF-like domains) and or to the proline-rich region domain. The result showed successful activation, although the process was very slow and the activated FXII did not show full amidolytic cleavage compared to α -FXIIa and β -FXIIa (**Figure 5.14**). It was also observed that the amount of the product generated by combination of the activators and zinc is higher than that of the activators alone. The reason behind this difference could be that Zn^{2+} is necessary for modulation or conformational change of FXII independent on the negatively charged surfaces. Subsequently, the process of autoproteolysis of FXII on such surfaces can be accomplished. The conformational change could be the result of binding of Zn^{2+} to four binding sites located within the domains of the heavy chain of FXII zymogen, which are fibronectin and EGF-like domains.

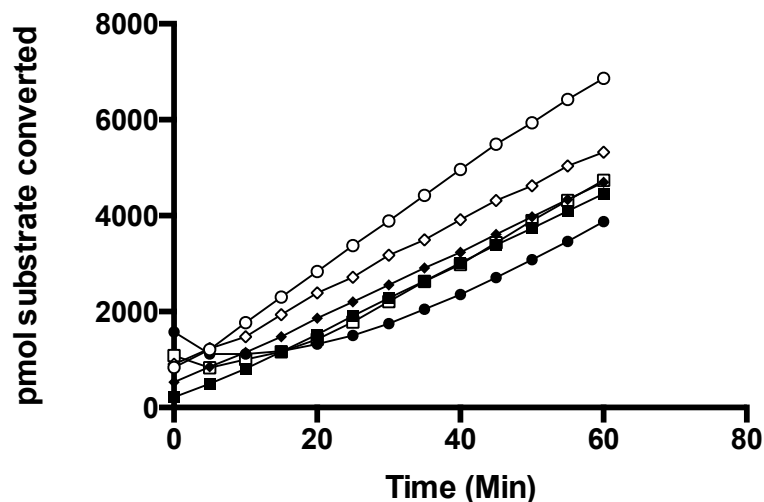


Figure 5.14 Autoactivation of human FXII zymogen. The activation was triggered by the negative surface agent $\pm \text{Zn}^{2+}$, and then the activated form of FXII hydrolysed 0.6mM substrate. Y-axis is the amount of product reflecting the amidolytic breakdown of S-2302 by activated FXII. Average of three independent experiments was analysed; in every independent experiment a duplicate was used and average of the duplicate values was taken. The following symbols indicates activator-zymogen combinations: (100 $\mu\text{g/ml}$ poly-p 20, ■), (1 $\mu\text{g/ml}$ DS, ●), (1 $\mu\text{g/ml}$ DS+ 10 μM ZnSO₄, ◇), (100 $\mu\text{g/ml}$ poly-p 20+ 10 μM ZnSO₄, □), (100 $\mu\text{g/ml}$ kaolin, ▲), (100 $\mu\text{g/ml}$ kaolin + 10 μM ZnSO₄, ○). DS is dextran sulphate and poly-p20 is polyphosphate p-20.

To examine whether FXIIac and FXIIC are in the inactive state and need to be activated by the negative surface agents, activation of the proteins with Poly-p, kaolin and dextran sulphate $\pm \text{Zn}^{2+}$ was carried out, even though they lack the heavy chain and the fragment of the proline-rich region. Amidolytic activity was performed using the colorimetric assay. The recombinant protease domains were still not able to hydrolyse the substrate (**Figure 5.15 and 5.16**).

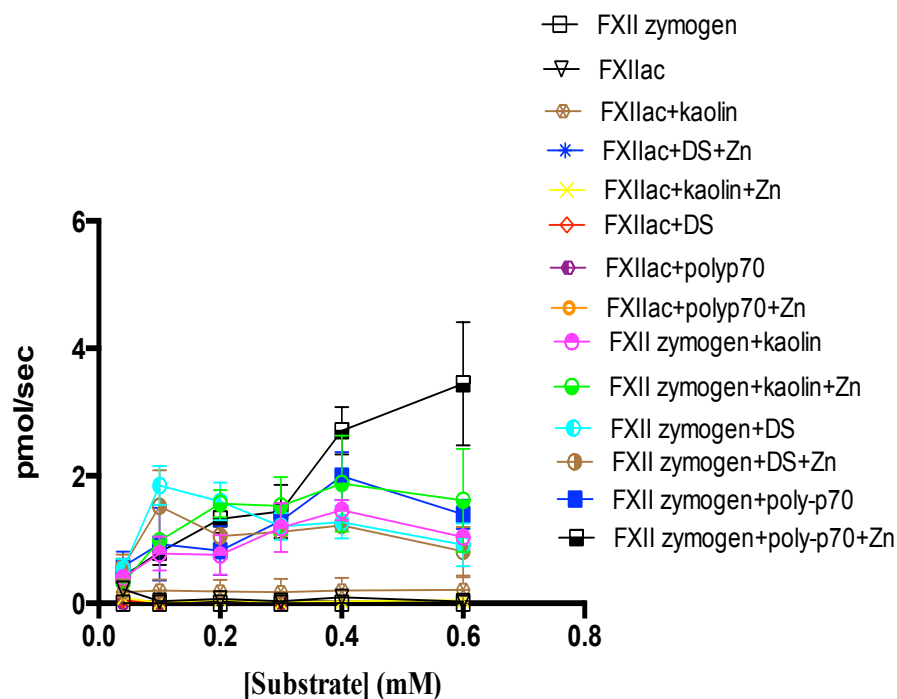


Figure 5.15 Autoactivation of the different forms of FXII. The surfactants, DS, kaolin, and poly-p70, alone or in combination with Zn^{2+} were used for the purpose of activation. Cleavage of S-2302 in the FXII zymogen-activator assay indicates that the zymogen was converted to the activated form of FXII, although the autoactivation process was very slow. The absence of release of the coloured product in FXIIac-activator assay denotes that the activation of FXIIac was not produced. Y-axis is product generation (pmol/s/pmol of FXII); X-axis is the different [S-2302]. The average of data of 3 independent experiments was taken. In every single experiment a duplicate was used for each [substrate]. Average of the duplicate results was calculated. DS is dextran sulphate. The error bar is standard error of the mean of the independent experiments.

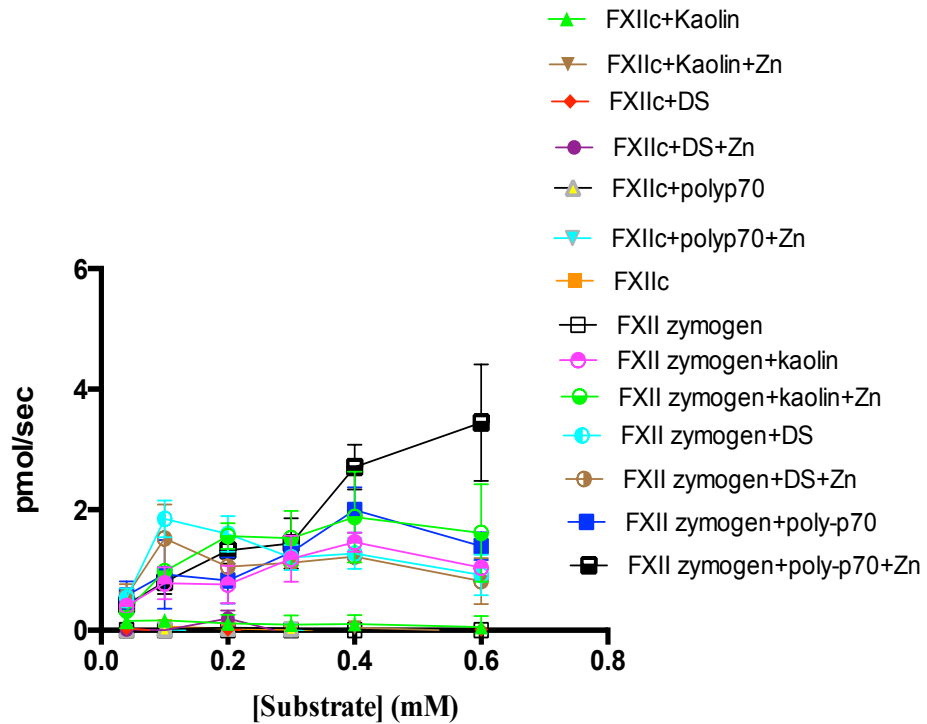


Figure 5.16 Autoactivation of the different forms of FXII. Generation of the coloured product from the amidolytic breakdown of S-2302 in FXII zymogen-activator assay implies that the zymogen was activated, although the autoactivation process was very slow. Lack of the coloured product in the FXIIc-activator assay means that the activation of the protein construct was not produced. The initial velocities of generation of the products, reflecting activity of these coagulation proteases, were defined as pmol/s/pmol of FXII versus different substrate concentrations. The average of data of 3 independent experiments was taken. In every single experiment a duplicate was used for each [substrate]. Average of the duplicate results was calculated. DS is dextran sulphate. The error bar is standard error of the mean of all the independent experiments.

This would suggest that the activation of the recombinant proteins failed to occur and they were kept in the inactive conformation. A possible reason elucidating this observation is that the recombinant enzymes lack the peptide

fragment of the proline-rich region. To examine this hypothesis, the peptide fragment was used for activation purpose.

5.4.4 Investigation of the activation of FXIIac by NGPLSCGQR / NGPLSCGQRLRKSLSMTR beta stump peptides

With respect to the hypothesis explained above, inactivity of the recombinant protease constructs could be due to lack of the peptide fragments of the proline-rich region. These peptide fragments are NGPLSCGQR (335-343 of the proline-rich region from N-terminus to C-terminus) and NGPLSCGQRLRKSLSMTR (335-353 of the proline-rich region from N-terminus to C-terminus). To test this assumption, each peptide was added to FXIIac and the mixture was incubated for activation purpose. Then, the construct was tested on the different concentrations of the chromogenic substrate for amidolytic activity. Cleavage of the chromogenic substrate was not observed for both NGPLSCGQR and NGPLSCGQRLRKSLSMTR experiments (**Figure 5.17**).

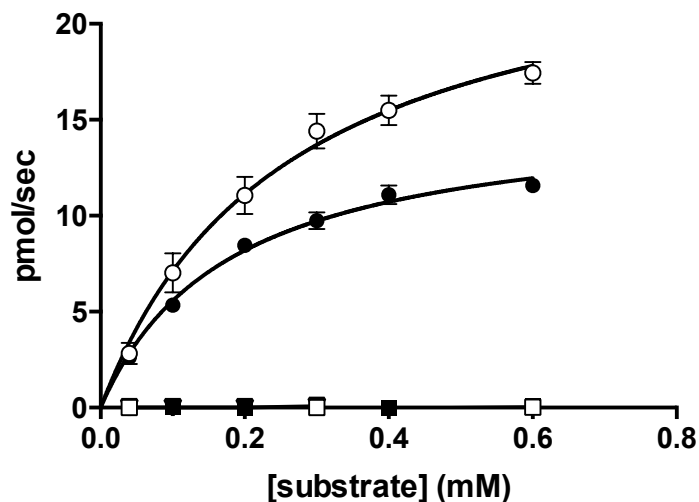


Figure 5.17 Failure of activation of FXIIac by NGPLSCGQR or NGPLSCGQRLRKSLSMTR beta stump peptides. Y-axis represents the activity (pmol/s/pmol of FXIIac) of the protein construct in comparison with FXIIa forms. In every single experiment, two wells were used as a duplicate for each [substrate]. Average of the duplicate results was taken. The error bar is standard error of the mean of the three independent experiments for FXIIac and twelve independent experiments for human FXIIa. The following symbols denote the different forms: (FXIIac + NGPLSCGQR, ■), (FXIIac + NGPLSCGQRLRKSLSMTR, □), (α -FXIIa, ●), (β -FXIIa, ○).

Hence, this suggests that the peptides would not be able to activate the catalytic domain of the protein constructs without disulphide bonding to it. This would be due to the presence of serine instead of cysteine in the catalytic domain (Cys466 was replaced by Ser); Ser466 was not able to bond with Cys340; this condition is different from what is usually present in the wild type β -FXIIa; in which Cys466 bonds to Cys340 of NGPLSCGQR peptide. To test the fourth hypothesis, the amidolytic activity was performed for HISTF- β FXII generated in bacteria. In HISTF- β FXII, Cys340-Cys466 disulphide

bond exists between the nonglycosylated peptide fragment and the catalytic domain.

5.5.5 Investigation of the role of the remnant peptide bound to the catalytic domain via Cys340-Cys466 in the catalytic activity of the protease domain

In order to test the fourth hypothesis: both Cys340-Cys466 disulphide bond and the peptide fragment would be important for the catalytic activity of FXIIa, the amidolytic activity of HISTF- β FXII was performed in comparison with β -FXIIa and α -FXIIa. The recombinant protein at 0.01 μ M (1 pmol) did not cleave 0.6 mM S-2302. However, at 1 μ M, 100-fold higher concentration, the recombinant protein caused weak hydrolytic effect, which is approximately 12 and 8.5 times less than that of 10 nM β -FXIIa and 10 nM α -FXIIa respectively (**Figure 5.18 and 5.19**).

It is noticed that the hydrolytic effect of 1 μ M HISTF- β FXII on 0.6 mM S-2302 is approximately 10 and 1250 times more than that of FXIIac and FXIIc respectively, even though higher concentration of S-2302, 1.6 times, was used in the amidolytic assay of the latter two recombinant forms. The reason of higher amidolytic activity of HISTF- β FXII when compared to that of FXIIac and FXIIc would be the presence of the remnant peptide bound to the catalytic domain by Cys340 - Cys466 in the former recombinant form.

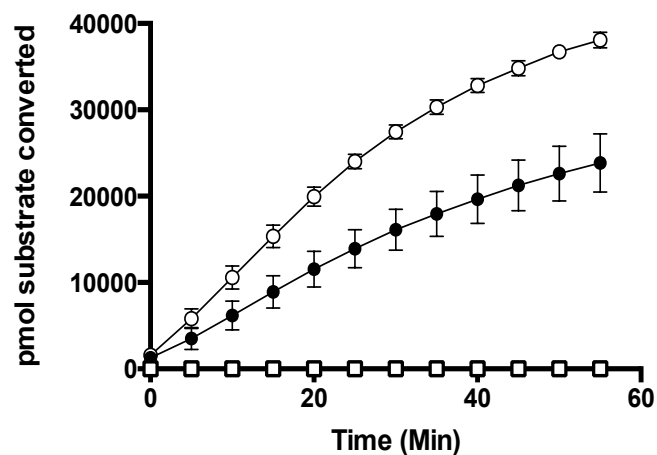


Figure 5.18 Comparative time dependent assays of human FXIIa (α -FXIIa and β -FXIIa) forms and HISTF- β FXII. Number of picomoles of product (per pmol of enzyme) was generated by hydrolysis of 0.6 mM S-2302 by various forms of FXII. Average of twelve independent experiments for α -FXIIa and β -FXIIa and three for HISTF- β FXII was taken. In each experiment a duplicate was used for each [substrate]; average of the duplicate values of all the independent experiments was taken. The error bar is standard error of the mean of all the independent experiments. The following symbols indicate the different enzymes: HISTF- β FXII \square , α -FXIIa, \bullet , and β -FXIIa, \circ .

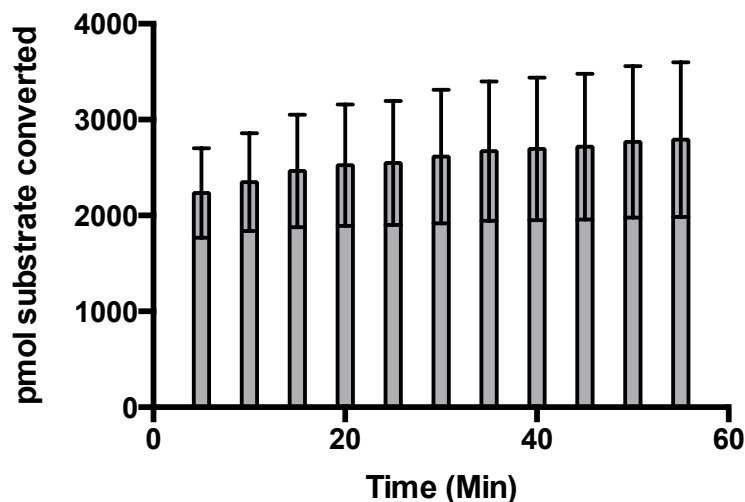


Figure 5.19 Weak amidolytic activity of HISTF- β FXII. HISTF- β FXII caused weak hydrolytic cleavage of 0.6 mM S-2302 in comparison with β -FXIIa and α -FXIIa. In each experiment, a duplicate was used; average of the duplicate values was taken. The concentration of the protein construct was 1 μ M (100 times more than that of β -FXIIa and α -FXIIa). The error bar is standard error of the mean of all the independent experiments.

The possible reason of lack or reduction in the amidolytic activity of HISTF- β FXII in comparison with that of human FXIIa would be nonglycosylation form of Asn335 of the remnant peptide due to lack of posttranslational modification and glycosylation process in the machinery system of bacteria. The commercially activated forms (β -FXIIa and α -FXIIa), purified from human plasma, have the glycosylated peptide fragment because the liver cells, generating FXII, have post-translational system producing protein modifications involving glycosylation. Hence, to test this last hypothesis, the glycosylated form of the peptide fragment, linked to the protease domain via Cys340-Cys466, was tested for hydrolytic activity as explained below

5.5.6 Investigation of the functional role of the glycosylated peptide fragment bound to the catalytic domain via Cys340-Cys466

The aim of this section was to evaluate the last hypothesis, to justify the functional role of the glycosylated remnant peptide in the catalytic activity of the protease domain. As shown (**Figure 5.20 and 5.21**), MBP- β -FXIIa (from the insect cells, *Drosophila Schneider 2 cells*) behaved as human FXIIa in the time dependent hydrolysis of S-2302. Its affinity and activity of is comparable with that of the human FXIIa (**Table 5.5**). This finding is consistent with the last assumption: MBP- β -FXIIa generated from insect (from the insect cells, *Drosophila Schneider 2 cells*) and FXIIa purified from human plasma are anticipated to be functionally similar as the conformation of their catalytic domain are supposed to be structurally similar due to the fact that the peptide fragment of both of them were likely to be glycosylated by post-translational modification system. The *Drosophila Schneider 2 cells* system would be important for generating functional FXIIa catalytic domain in which the catalytic domain bound to the fragment of the proline-rich domain having glycosylated Asn335 and a disulphide bond existing between Cys466 and Cys340. Hence, the glycosylated fragment would have an essential role in the full catalytic activity of FXII protease domain. However, the glycosylated form of FXIIa (MBP- β -FXIIa) would be problematic for the future structural study (crystallography study) because its addition and trimming tends to be heterogeneous.

It can also be concluded that the presence of the bioengineered fragments (HIS tag, MBP, and thrombin site) does not have effect on the cleavage of the substrate by the enzyme.

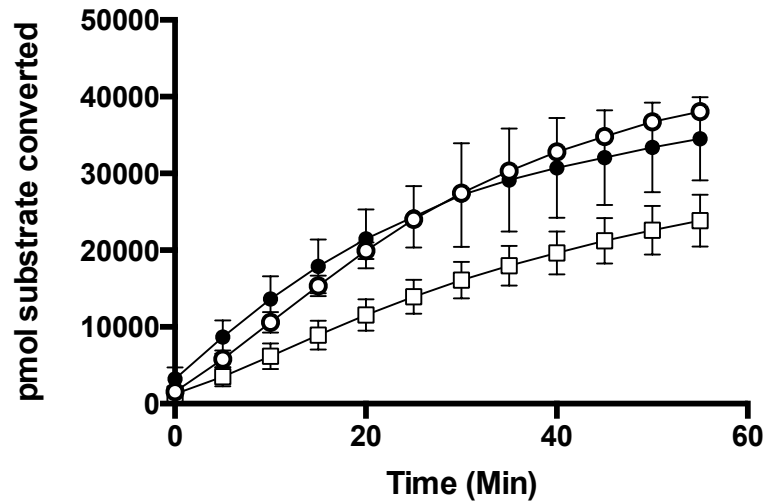


Figure 5.20 Comparative time dependent assays of human FXIIa (α -FXIIa and β -FXIIa) forms and MBP- β -FXIIa generated in *Drosophila Schneider 2 cells*. Number of picomoles of product (per pmol of enzyme) was generated by hydrolysis of 0.6 mM S-2302 by various forms of FXII. Average of twelve independent experiments for α -FXIIa and β -FXIIa and three experiments for MBP- β -FXIIa was used. In each experiment a duplicate was used for the [substrate]; average of the duplicate values was taken. The error bar is standard error of the mean of all the independent experiments. The following symbols are different enzymes : (α -FXIIa, \square), (MBP- β -FXIIa, \bullet), (β -FXIIa, \circ).

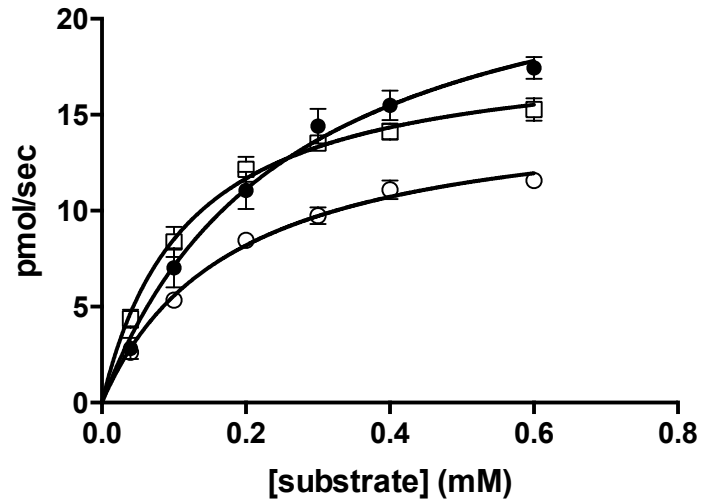


Figure 5.21 Activity MBP-β-FXIIa in comparison with α-FXIIa and β-FXIIa. Activity (pmol/sec/ pmol of the proteases) of the different forms of FXII versus different [substrate] (mM). MBP-β-FXIIa generated in *Drosophila Schneider 2 cells* behaves as human FXIIa. Average of twelve experiments for α-FXIIa, and β-FXIIa and three experiments for MBP-β-FXIIa was taken. In each independent experiment a duplicate was used for each [substrate]; average of the duplicate values was taken. The error bar is standard error of the mean of all the independent experiments. The following symbols are different enzymes: (MBP-β-FXIIa, □), (β-FXIIa, ●), (α-FXIIa, ○).

Table 5.5 Kinetic parameter values of Kinetic hydrolysis of S-2302 by MBP- β -FXIIa using average of three experiments. In every single experiment two wells was used as a duplicate for every [substrate]. Average of the duplicate results was taken. The error represents standard error of the mean of all the independent experiments.

| Parameters | MBP-β-FXIIa |
|---|-------------------------------------|
| V_{max} (pmol/s) | 56.04 \pm 7.15 |
| k_{cat} (s^{-1}) | 20.01 \pm 2.55 |
| K_M (mM) | 0.17 \pm 0.05 |
| k_{cat} / K_M ($L \cdot mol^{-1} \cdot s^{-1}$) | 117705 |

5.5 Conclusion

It was concluded that FXIIc, FXIIac, and HISTF- β FXII do not have any amidolytic activity in comparison with human β -FXIIa and α -FXIIa. However, at high concentration of both S-2302 and these recombinant proteins, extremely weak amidolytic activity was noticed, indicating that they displayed zymogen-like behaviour. From activity side, the zymogen-like behaviour of both FXIIc and FXIIac was used as an initial effort to further characterize these proteins in correlation with their crystal structures. Following treatment with the activators, FXIIac and FXIIc were not able to cleave S-2302. Nonexistence of the peptide fragment of the proline-rich region was supposed to be responsible for the unsuccessful autoactivation. FXIIac, following addition of the beta stump peptides (NGPLSCGQR or NGPLSCGQRLRKSLSMTR), did not hydrolyse S-2302, suggesting that Cys340-Cys466 disulphide bond between the peptide fragment and the catalytic domain would be essential for the catalytic activity of FXIIa. Compared to FXIIc and FXIIac, the higher activity of HISTF- β FXII could be due to the presence of the peptide fragment bound to the catalytic domain of HISTF- β FXII by Cys340-Cys466. Failure of autoactivation of FXIIc and FXIIac suggests that the catalytic domain would not have binding sites for the activators. The lower amidolytic activity of FXIIc in comparison with FXIIac would be due the presence of the extra residues at N-terminus of the former recombinant form. MBP- β -FXIIa behaved as β -FXIIa and α -FXIIa. The full amidolytic activity of MBP- β -FXIIa would be due to the existence of the

glycosylated form of the peptide fragment that would be present in MBP- β -FXIIa due to its expression in the *Drosophila Schneider 2 cells* whereas it would be absent in HISTF- β FXII due to its expression in bacteria. It would also propose that the presence of the bioengineered fragments (HIS tag, MBP, and thrombin site) doesn't have any effect on the cleavage of the substrate by MBP- β -FXIIa.

Chapter 6: General discussion, significance of the current project, and future plan

6.1 General discussion

Cardio-Cerebral-Vascular diseases are the first leading cause of death in the world during the past decade. Occlusion of blood vessels by stable thrombus formation is one of the main causes of the diseases [190].

Factor XII-deficient animal models have proposed that this protein contributes to steady thrombosis that can cause obstruction of blood vessels and loss of blood supply to the brain, which is termed as ischemic stroke. Contrary to other blood coagulation factors, deficiency in FXII is not related with abnormal bleeding in patients or in animals [172][124].

These findings propose that specific inhibition of FXII could be an attractive medicine and a new method of anticoagulation to treat or prevent pathological thrombosis that could have a lower risk for haemorrhage and a safer anticoagulation profile than the currently available non-selective, broad-spectrum anticoagulants, such as warfarin, or novel direct thrombin and FXa inhibitors [129][130][131, 132], [167-170].

Specific inhibition of FXIIa needs exploring the main residues helping to recognize its specific substrate and or investigating the potential target residues important for its specific inhibitor, known as CHFI, existing naturally in corn seeds. This information mainly needs the crystal structure of CHFI-FXIIa complex, which has not been solved yet. As an alternative strategy, the information on CHFI-FXII interaction would be attained from the individual

crystal structure of each of FXIIa and CHFI. The crystal structure of CHFI revealed that the protein has no particular, atypical central inhibition loop compared to that of the other serine protease inhibitors lacking inhibitory activity against FXIIa. The structure of FXIIa has not been revealed yet. Lack of information on FXIIa and or CHFI-FXIIa complex structure created an obstacle in the approach of studies trying to rationalize the reason of selectivity of CHFI.

Hence, the goal of the current PhD was to pharmacologically investigate into FXII-CHFI interaction and FXII function. This was used as an early attempt and strategy to understand the molecular mechanism of inhibition of FXIIa by CHFI and of FXIIa function, which is highly informative for designing low molecular weight inhibitors as safe anticoagulants. The project was carried through the following, logical route directions : first, developing an efficient expression and purification system for generating soluble and functional recombinant native type CHFI and establishing an inhibitory activity assay against FXIIa to verify the proper function of the recombinant protein that was, together, necessary for ascertaining a principal assay and a reference guide to generating and testing the different recombinant variants of CHFI with the desired point mutations guided by a proper prediction study of CHFI-FXII interaction, second, to investigate into the hypothesis of the tight-binding property of CHFI via different approaches of enzyme inhibition mechanisms and kinetic data analysis, third, to investigate into the function of FXII by examining the effect of Cys466 and glycosylated peptide remnant from the proline-rich region on the function of the catalytic domain via characterizing the different recombinant variants of the catalytic domain of FXIIa, FXIIc,

FXIIac, HISTF- β FXII, and MBP- β -FXIIa (generated by R Manna, a PhD student in the structural biology group/ Emsley group, and M Pathak, a research assistant in the structural biology group/ Emsley group).

In the current study an effective protocol for soluble expression and single step purification for the recombinant CHF1 was first recognized using pCOLD I-GST vector and the bacterial expression systems, BL21 DE3 and origami™2 (DE3). Inhibition activity, representing the inhibition effect of CHF1 different forms on the catalytic activity of FXIIa enzyme, was measured by the influence of rHIS-GST-CHF1, rHIS-GST and commercial CHF1 on the amount of pNA generated from hydrolytic breakdown of S-2302 by the enzyme. rHIS-GST tag as a negative control didn't display any inhibitory effect whereas the recombinant wild type CHF1 (rHIS-GST-CHF1) showed tremendous and full inhibitory activity against FXIIa; this verifies the following points. First, the recombinant protein is as active inhibitor as commercial CHF1 and is properly folded following expression, purification and storage. Second, rHIS-GST tag cannot affect the molecular interaction between CHF1 and FXIIa and the inhibition effect is entirely due to the recombinant CHF1 bound to rHIS-GST tag via HRV3C protease linker. This finding can be used as a principal assay and a reference guide for assessing the inhibitory activity of the mutants against FXIIa in the characterization study of CHF1-FXIIa interaction.

With respect to the prediction study, it was anticipated that the residues of interest exist on the surface of the central inhibition loop projecting away from the body of CHF1. It is expected that the fully exposed Arg34 could have a

principal role in the inhibition of FXIIa. Arg34 at P1 position is likely to extend into the S1 pocket of FXII catalytic domain and bind to a potential target residue, Asp592. It is expected that one nitrogen atom of the guanidinium group of Arg34 forms a hydrogen bond of 2.7 Å with Asp592 of FXII, whereas the other nitrogen atom forms a hydrogen bond of 2.4 Å with Gly621 on FXII. The carbonyl oxygen of Arg34 is anticipated to be situated in the oxyanion hole, interacting with hydroxyl group of Ser598 of the catalytic triad and producing Michaelis complex. The catalytic triad is composed of Ser598, His447, and Asp597. Gly596 could also contribute to the catalytic reaction triggered by the catalytic triad. Hence, Arg34 would fill the space of S1 pocket and make a primary contribution to the affinity for the CHF1 inhibition of FXII protease domain.

Trp22 and Arg43 located at either ends of the central inhibition loop i.e. N-terminus and C-terminus respectively are anticipated to be the key interaction residues for inhibition of FXIIa. They would be defined as important factors helping to elucidate specificity of CHF1 toward FXIIa. It was predicted that a pocket is created by loop 99 of FXII catalytic domain into which Trp22 inserts. Within the pocket, Gln450 at position S13 of FXII could interact with Trp22 at position P13 of CHF1 by forming a hydrogen bond. Arg43 at position P9' of CHF1 would be expected to form a salt bridge with Asp452 at S9' on the exposed surface of FXIIa. Asp452 can probably be used to both define the exosite for substrate cleavage as well as to define the binding site for CHF1.

On the basis of these observed interactions, the central residues, Arg34, and the two key residues, Trp22 and Arg43, were mainly chosen for point mutation. It is hypothesized that Arg34 would play a main, significant role in the function of CHF1. Trp22 and Arg43 would behave as two key interaction residues.

To validate the prediction study by the experimental investigation into CHF1-FXII interaction, site directed mutagenesis was used for the desired point mutations. Guided by the established, effective expression and single-step purification system for generating soluble and functional recombinant rHIS-GST-CHF1 (which is the aim of chapter 2), soluble expression and purification of the different rHIS-GST-CHF1 mutants were performed. Characterization of the inhibitory activity of the mutant proteins of interest was performed using the developed, principal inhibition assay of rHIS-GST-CHF1 as a template. The central Arg34 at the very top of the fully exposed region of the CHF1 inhibition loop would play a crucial role in the inhibition function of CHF1 against human coagulation FXIIa. Trp22 at the N-terminus and Arg43 at the C-terminus of the central inhibition loop would be the two key residues for interaction of CHF1 with FXIIa. They can be considered as two factors important for elucidating the question of specific inhibitory activity of CHF1 toward the cognate enzyme.

On the basis of this finding, the different peptides mimicking the central inhibition loop of CHF1 were designed for the certain purposes elucidated below. With reference to the result of the characterization study of the different mutants, the central inhibition loop would be responsible for the

function of CHFI. The two key interaction residues with FXIIa would be present at N-terminus and C-terminus of the of the central loop peptide. The purpose of the peptide assay was firstly to evaluate the relevance of the central inhibition loop peptide in the inhibitory activity of the CHFI, second, to investigate the necessity of the Cys20-Cys44 disulphide-coupled peptide folding of the central inhibition loop for the function of the key residues, lastly, to further validate the importance of Arg34, Trp22, and Arg43 of the central inhibition loop for an initial approach to elucidating specific inhibition activity of CHFI toward coagulation FXIIa.

Cyclic and non-cyclic forms of the synthetic isolated peptide of CHFI central inhibition loop showed the same inhibition effectiveness, proposing that the Cys20-Cys44 disulphide bridge would be irrelevant for the inhibitory activity of the isolated peptide. The reason would be that the two key residues, Trp22 at the N-terminus and Arg43 at the C-terminus, would help the peptide fold around and negate the dependence on the Cys20-Cys44 disulphide bond.

From examining the tight-binding postulation, it was concluded that that CHFI behaves as a non-competitive inhibitor of the different forms of FXIIa in the pre-inhibition test. In contrast, it acts as a competitive inhibitor in the acute condition, proposing that CHFI is a competitive inhibitor either with slow degree of reversibility or irreversible property due to tightness of binding. Reversibility assay supports that CHFI is an inhibitor with slow degree of dissociation. The competitive inhibition behaviour of CHFI is likely to be resulted from the following potential mechanisms. The first could be that Arg43 of CHFI inhibition loop and the Arg of the tripeptide Pro-Phe-Arg, S-

2302, compete for binding to the negatively charged target, Asp452, located on the surface of FXIIa; this would function as a non-active site interaction surfaces, or an exosite, on the surface of FXIIa. This site would probably be necessary for recognizing and cleaving both S-2302 and CHFI with high specificity. The second possible mechanism would be that Arg34 of CHFI and Arg of the tripeptide substrate compete for binding to the active site of FXIIa. The negatively charged S1 pocket of FXII would accommodate the positively charged side chain of Arg34 of CHFI, enabling this residue to compete with the Arg of the tripeptide substrate for binding to the catalytic triad of FXII. Therefore, both CHFI and S-2302 can undergo hydrolytic breakdown resulting in the generation of the chromophore, p-nitroaniline, from S-2302 and cleavage of Arg34-Leu35 on the surface of CHFI inhibition loop. Hence, there would be a similarity in the site of interaction of S-2302 and CHFI on FXIIa enzyme and this phenomenon is considered as a characteristic feature of competitive inhibition. Noncompetitive behaviour of CHFI may be due to slow degree of dissociation due to noncovalent, tight binding of CHFI inhibition loop to FXIIa, resulting in a more stable E-I (enzyme-inhibitor) complex. This effect would be due to the interaction of Arg43 of CHFI with the potential target residue, Asp452, expected to function as a non-active site interaction surface, or an exosite, on the surface of FXIIa (described fully in chapter 3). Several hydrogen bonds that could be made between the interaction key residues of CHFI and the other potential target residues on FXII enzyme would contribute to a more E-I complex. As described comprehensively in chapter 2, Arg34 would hydrogen bond to both Asp592 and Gly621 in the S1 pocket of FXII. Trp22 and Gly32 of CHFI could also form hydrogen bonds

with Gln450 and Trp618 of FXII respectively. Noncovalent, tight binding is a characteristic feature of the standard mechanism of the canonical inhibitors. The conclusion of the current study is in agreement with the studies hypothesizing that CHFI is expected to follow standard mechanism of inhibition. With respect to this mechanism, both the intact inhibitor (CHFI) and its ligated product (regenerated CHFI) can hinder the active site[141],[136, 156].

With respect to the investigation into FXII function, it was found that FXIIc, FXIIac, and HISTF- β FXII are not amidolytically active in comparison with human β -FXIIa and α -FXIIa. However, at high concentration of both S-2302 and these recombinant proteins, tremendously weak amidolytic activity was observed, meaning that they showed zymogen-like behaviour. From activity side, the zymogen-like behaviour of both FXIIc and FXIIac was used as a preliminary attempt to further characterize these proteins in relationship with their crystal structures [173] . Following treatment with the activators, FXIIac and FXIIc were not able to cleave S-2302. Lack of the peptide fragment of the proline-rich region was anticipated to be responsible for the failed autoactivation. FXIIac, following addition of the beta stump peptides (NGPLSCGQR or NGPLSCGQRLRKSLSMTR), did not cleave S-2302, proposing that Cys340-Cys466 disulphide bond between the peptide fragment and the catalytic domain would be crucial for the catalytic activity of FXIIa. In comparison to FXIIc and FXIIac, the higher activity of HISTF- β FXII could be due to the occurrence of the peptide fragment bound to the catalytic domain of HISTF- β FXII by Cys340-Cys466. Failure of autoactivation of FXIIc and FXIIac suggests that the catalytic domain would not have binding sites for the

activators. The lower amidolytic activity of FXIIc in comparison with FXIIac would be due the existence of the extra residues at N-terminus of the former recombinant form. MBP- β -FXIIa behaved as β -FXIIa and α -FXIIa. The full amidolytic activity of MBP- β -FXIIa would be due to the presence of the glycosylated form of the peptide fragment that would be present in MBP- β -FXIIa as a result of its expression in *Drosophila Schneider 2 cells* whereas it is likely to be nonexistent in HISTF- β FXII due to its expression in bacteria. It would also propose that the presence of the bioengineered fragments (HIS tag, MBP, and thrombin site) doesn't have any effect on the cleavage of the substrate by MBP- β -FXIIa.

Cumulatively, an efficient system for soluble expression, single step purification and proper storage of functional, wild type rHIS-GST-CHF1 was for the first time identified. The fully functional recombinant protein was verified via establishing an inhibition test against FXIIa. The developed expression, purification and inhibition assays were used as a fundamental guide to both generating and characterizing the mutant proteins of interest that were made on the basis of an appropriate docking of CHF1-FXIIa interaction. For the first time, the current investigation into the question of specificity of CHF1 against FXII revealed that the central Arg34 at the very top of the fully exposed region of CHF1 inhibition loop plays a central role in the inhibition function of CHF1 toward FXIIa. In addition, this study identified Trp22 at the N-terminus and Arg43 at the C-terminus of the central inhibition loop as a two key interaction residues with FXIIa. Tight-binding property of CHF1 was verified by using different strategies of kinetic mechanisms and kinetic data analysis. This behaviour could be due to non-active site interaction and or

numerous hydrogen bonds between the key interaction residues and their potential targets on FXIIa. With respect to the investigation into FXIIa function, It was observed that both Cys340-Cys466 and glycosylated peptide fragment of the proline-rich region would have a functional role for the full catalytic activity of FXII protease domain.

6.2 Significance of this study

This study identified the key important residues on the exposed surface of CHF1 and their potential target residues on the surface of FXIIa that would have a fundamental role in the mechanism of selective and tight binding interaction of CHF1 with FXIIa. This project is highly informative as an early approach to design novel, specific and safe anticoagulants for the treatment of thrombosis and its complications.

6.3 Future plan

There are different lines along which the current study can be developed in the future.

6.3.1 Prediction studies of CHF1 interaction with other proteases

In order to further investigate the specificity of CHF1 against FXII vs. other proteases, further docking studies could be done of CHF1 with other coagulation factors or serine proteases having sequence homology with FXII. . Results from a most recent study, carried out in 2015 [191], and showed that CHF1 has inhibitory activity against trypsin, plasmin and FXI. The potency of inhibition of CHF1 against trypsin and FXIIa is almost similar whereas its potency towards plasmin and FXI is 200 times lower than that towards both these proteases. This would give rise to a notion that in order to understand the high affinity of CHF1 for trypsin for example, a macromolecular docking between CHF1 and trypsin would be necessary. The key interaction residues of CHF1 with FXIIa found in this study may have the same importance or there may be other residues of interest to explain the reason of high potency of CHF1 for trypsin. As a different strategy, prediction studies of CHF1 against plasmin and FXI are also a relevant approach to explain the lower effectiveness of CHF1 when interacting with the proteases.

6.3.2 Generation and inhibitory activity of different CHF1 mutants

On the basis of the predicted interactions in the macromolecular docking studies proposed above, different CHF1 mutants with desired point mutations

can be produced. Then, as an experimental validation of the docking models, inhibitory activity of the CHFI different recombinant variants can be conducted against the proteases of interest. This would support and validate the key interactions predicted.

6.3.3 Point mutations of the potential target residues of CHFI in FXII

The model used in this study predicted that Asp592, Gln450, and Asp452 of the FXII protease are involved in binding to CHFI. It would be important to validate their significance for binding. This can be done by point mutation and then checking for inhibition by CHFI. In addition, point mutation of Asn335 would be necessary in order to further validate the importance of glycosylated Asn335 for full catalytic activity of FXII protease domain.

6.3.4 Inhibitory activity of the different forms of the isolated peptides of CHFI against other proteases that have sequence homology with FXII

To further investigate the notion of protease selectivity, synthetic peptides could be explored. They could be used to evaluate the relevance of the central inhibition loop in the inhibitory activity of CHFI against the other proteases, to investigate the necessity of Cys20-Cys44 disulphide-coupled peptide folding of the inhibition loop for the inhibition function, and to further validate the importance of the point mutations suggested to be made on the basis of the docking studies described above. This would be essential to understand if there is an additional factor that determines specificity of the key interaction residues for the potential targets on FXIIa. For example, steric effects outside the catalytic loop region may underlie the specificity of action of CHFI.

6.3.5 Reversibility assay of CHF1 mutants

For the purpose of understanding the potential role of hydrogen bonds and the non-active site surface salt bridge in the slow dissociation property of CHF1, reversibility assay for CHF1 recombinant variants having the important point mutations may be done. The mutants missing the key interaction residues, in particular R43, could loss tight-binding inhibition property.

6.3.6 Using the CHF1 isolated peptide as a template for pharmacophore-based drug design.

The inhibition loop peptide of CHF1 can be used as a model for ligand-based drug design. The minimum requirement for the inhibitory activity of the peptides generated from rounds of the combinatorial synthesis, for example, through peptidomimetics would be the presence of tryptophan and arginine at either ends of the peptides with an arginine centrally positioned. Screening of the peptides against FXII and other closely related proteases would be needed to improve selectivity and affinity against the target protein, FXIIa. Appropriately optimised peptides could undergo further *ex vivo* ADME (administration, distribution, metabolism and excretion) and *in vivo* pharmacokinetics profile prediction as well as toxicity assessment. Finally, suitable peptides could be evaluated *in vivo* for their potential efficacy (see next section).

6.3.7 Preclinical studies of candidate peptides

A lead peptide that has favourable pharmacokinetic profile and acceptable toxicity may be tested in vivo to study the effect on thrombosis and bleeding effects or other signs and symptoms related to the inhibition of FXIIa using mice with thromboembolism, stroke and pulmonary embolism, models. This would be significant to estimate the efficiency and efficacy and the therapeutic window of the peptide-drug like molecule.

6.3.7 Point mutations of the potential target residues of the CHF1-FXII model

On the target protein (FXIIa) side, point mutations of the potential target residues, Asp592, Gln450, and Asp452, would be necessary for validating their significance for binding. In addition, point mutation of Asn335 would be necessary in order to further validate the importance of glycosylated Asn335 for full catalytic activity of FXII protease domain.

6.3.8 Crystallization studies of FXIIa, CHF1-FXII, and the lead peptide generated from pharmacophore-based drug design

To further validate the key interaction residues of CHF1-FXIIa, crystallisation studies could be performed. These could be done with CHF1 itself, isolated as recombinant proteins, or with any suitable loop peptide as defined above. The potential target residues on FXII can be used for novel, direct or target- based drug design.

References

1. Hall, J.E., *Guyton and Hall Textbook of Medical Physiology*. 11th edition. Elsevier Saunders, Philadelphia, 2006. p. 457-490.
2. Marieb, E.N. and Hoehn K., *Human Anatomy & Physiology*. 9th edition. Boston Pearson, 2013. p. 649–50.
3. Clemetson, K.J., *Platelets and primary haemostasis*. *Thromb Res*, 2012. **129**(3): p. 220-4.
4. Davie, E.W., Fujikawa K., and Kisiel W., *The coagulation cascade: initiation, maintenance, and regulation*. *Biochemistry*, 1991. **30**(43): p. 10363-70.
5. De Meyer, S.F., et al., *Binding of von Willebrand factor to collagen and glycoprotein Ibalpha, but not to glycoprotein IIb/IIIa, contributes to ischemic stroke in mice--brief report*. *Arterioscler Thromb Vasc Biol*, 2010. **30**(10): p. 1949-51.
6. Bode, A.P., Read M.S., and Reddick R.L., *Activation and adherence of lyophilized human platelets on canine vessel strips in the Baumgartner perfusion chamber*. *J Lab Clin Med*, 1999. **133**(2): p. 200-11.
7. Sadler, J.E., *Biochemistry and genetics of von Willebrand factor*. *Annu Rev Biochem*, 1998. **67**: p. 395-424.
8. Brass, L., *Understanding and evaluating platelet function*. *Hematology Am Soc Hematol Educ Program*, 2010. **2010**: p. 387-96.

9. Chou, T.C., *New mechanisms of antiplatelet activity of nifedipine, an L-type calcium channel blocker*. Biomedicine (Taipei), 2014. **4**: p. 24.
10. Brass, L., et al., *Signal transduction during platelet plug formation*. In: *Michelson AD (ed.). Platelets, 2nd edition*. 2007(San Diego, CA, Elsevier.): p. p.359-346
11. Moroi, M. and Jung S.M., *A mechanism to safeguard platelet adhesion under high shear flow: von Willebrand factor-glycoprotein Ib and integrin alphabeta-collagen interactions make complementary, collagen-type-specific contributions to adhesion*. J Thromb Haemost, 2007. **5**(4): p. 797-803.
12. De Meyer, S.F., et al., *Antiplatelet drugs*. Br J Haematol, 2008. **142**(4): p. 515-28.
13. Hutchison, C.A., et al., *Mutagenesis at a specific position in a DNA sequence*. J Biol Chem, 1978. **253**(18): p. 6551-60.
14. Cattaneo, M., *Platelet P2 receptors: old and new targets for antithrombotic drugs*. Expert Rev Cardiovasc Ther, 2007. **5**(1): p. 45-55.
15. Savi, P., et al., *Clopidogrel: a review of its mechanism of action*. Platelets, 1998. **9**(3-4): p. 251-5.
16. Vogler, E.A. and Siedlecki C.A., *Contact Activation of Blood Plasma Coagulation: A Contribution from the Hematology at Biomaterial Interfaces Research Group The Pennsylvania State University*. Biomaterials, 2009. **30**(10): p. 1857-69.

17. Offermanns, S., et al., *Defective platelet activation in G alpha(q)-deficient mice*. Nature, 1997. **389**(6647): p. 183-6.
18. Offermanns, S., *Activation of platelet function through G protein-coupled receptors*. Circ Res, 2006. **99**(12): p. 1293-304.
19. Bach, R., Nemerson Y., and Konigsberg W., *Purification and characterization of bovine tissue factor*. J Biol Chem, 1981. **256**(16): p. 8324-31.
20. Broze, G.J., Jr., Girard T.J., and Novotny W.F., *Regulation of coagulation by a multivalent Kunitz-type inhibitor*. Biochemistry, 1990. **29**(33): p. 7539-46.
21. Kang, S. and Niemetz J., *Purification of human brain tissue factor*. Thromb Haemost, 1988. **59**(3): p. 400-3.
22. Broze, G.J., Jr., et al., *Purification of human brain tissue factor*. J Biol Chem, 1985. **260**(20): p. 10917-20.
23. Panasiuk, A., et al., *Increase in expression of monocytic tissue factor (CD142) with monocytes and blood platelet activation in liver cirrhosis*. Blood Coagul Fibrinolysis, 2007. **18**(8): p. 739-44.
24. Sakai, T., et al., *Binding of human factors VII and VIIa to a human bladder carcinoma cell line (J82). Implications for the initiation of the extrinsic pathway of blood coagulation*. J Biol Chem, 1989. **264**(17): p. 9980-8.
25. Steffel, J., Luscher T.F., and Tanner F.C., *Tissue factor in cardiovascular diseases: molecular mechanisms and clinical implications*. Circulation, 2006. **113**(5): p. 722-31.

26. Morrissey, J.H., *Tissue Factor and Factor VII Initiation of Coagulation, in Hemostasis and Thrombosis: Basic Principles and Clinical Practice*. . 2001(Lippincott Williams and Wilkins: Philadelphia.): p. 89-101.
27. Nemerson, Y. and Repke D., *Tissue factor accelerates the activation of coagulation factor VII: the role of a bifunctional coagulation cofactor*. Thromb Res, 1985. **40**(3): p. 351-8.
28. Radcliffe, R. and Nemerson Y., *Mechanism of activation of bovine factor VII. Products of cleavage by factor Xa*. J Biol Chem, 1976. **251**(16): p. 4749-802.
29. Masys, D.R., Bajaj S.P., and Rapaport S.I., *Activation of human factor VII by activated factors IX and X*. Blood, 1982. **60**(5): p. 1143-50.
30. Bauer, K.A., et al., *Factor IX is activated in vivo by the tissue factor mechanism*. Blood, 1990. **76**(4): p. 731-6.
31. Tracy, P.B., Nesheim M.E., and Mann K.G., *Coordinate binding of factor Va and factor Xa to the unstimulated platelet*. J Biol Chem, 1981. **256**(2): p. 743-51.
32. Mann, K.G., et al., *Surface-dependent reactions of the vitamin K-dependent enzyme complexes*. Blood, 1990. **76**(1): p. 1-16.
33. Monkovic, D.D. and Tracy P.B., *Activation of human factor V by factor Xa and thrombin*. Biochemistry, 1990. **29**(5): p. 1118-28.
34. Nesheim, M.E., Taswell J.B., and Mann K.G., *The contribution of bovine Factor V and Factor Va to the activity of prothrombinase*. J Biol Chem, 1979. **254**(21): p. 10952-62.

35. Suzuki, K., Dahlback B., and Stenflo J., *Thrombin-catalyzed activation of human coagulation factor V*. J Biol Chem, 1982. **257**(11): p. 6556-64.
36. Lorand, L. and Konishi K., *ACTIVATION OF THE FIBRIN STABILIZING FACTOR OF PLASMA BY THROMBIN*. Arch Biochem Biophys, 1964. **105**: p. 58-67.
37. Seligsohn, U., et al., *Activation of human factor VII in plasma and in purified systems: roles of activated factor IX, kallikrein, and activated factor XII*. J Clin Invest, 1979. **64**(4): p. 1056-65.
38. van Dieijen, G., et al., *The role of phospholipid and factor VIIIa in the activation of bovine factor X*. J Biol Chem, 1981. **256**(7): p. 3433-42.
39. Rapaport, S.I., *Inhibition of factor VIIa/tissue factor-induced blood coagulation: with particular emphasis upon a factor Xa-dependent inhibitory mechanism*. Blood, 1989. **73**(2): p. 359-65.
40. Davie, E.W. and Ratnoff O.D., *WATERFALL SEQUENCE FOR INTRINSIC BLOOD CLOTTING*. Science, 1964. **145**(3638): p. 1310-2.
41. King, M.W., *Blood Coagulation. The Medical Biochemistry Page*. Available in: <http://themedicalbiochemistrypage.org/bloodcoagulation.html>. 2009.
42. Colman, R.W., *Contact Activation Pathway: Inflammatory, Fibrinolytic, Anticoagulant, Antiadhesive and Antiangiogenic Activities, in Hemostasis and Thrombosis: Basic Principles and Clinical Practice*. 2001 (Lippincott Williams and Wilkins: Philadelphia): p. 103-121.
43. Furie, B. and Furie B.C., *Molecular and cellular biology of blood coagulation*. N Engl J Med, 1992. **326**(12): p. 800-6.

44. Mann, K.G., *Biochemistry and physiology of blood coagulation*. Thromb Haemost, 1999. **82**(2): p. 165-74.
45. Gailani, D. and Renne T., *The intrinsic pathway of coagulation: a target for treating thromboembolic disease?* J Thromb Haemost, 2007. **5**(6): p. 1106-12.
46. Davie, E.W. and Kulman J.D., *An overview of the structure and function of thrombin*. Semin Thromb Hemost, 2006. **32 Suppl 1**: p. 3-15.
47. Jenny, N.S. and Mann, K.G., *Thrombin, in Hemostasis and Thrombosis: Basic Principles and Clinical Practice*. 2001(Lippincott Williams and Wilkins): p. 171-189.
48. Rand, M.D., Kalafatis M., and Mann K.G., *Platelet coagulation factor Va: the major secretory platelet phosphoprotein*. Blood, 1994. **83**(8): p. 2180-90.
49. Gailani, D. and Broze G.J., Jr., *Factor XI activation in a revised model of blood coagulation*. Science, 1991. **253**(5022): p. 909-12.
50. Naito, K. and Fujikawa K., *Activation of human blood coagulation factor XI independent of factor XII. Factor XI is activated by thrombin and factor XIa in the presence of negatively charged surfaces*. J Biol Chem, 1991. **266**(12): p. 7353-8.
51. Lord, S.T., *Fibrinogen and fibrin: scaffold proteins in hemostasis*. Curr Opin Hematol, 2007. **14**(3): p. 236-41.
52. Hantgan, R.R., et al., *Fibrinogen structure and physiology*. In: *Hemostasis and Thrombosis: Basic Principles and Clinical Practice* (ed. by Colman R.W., Hirsh

- J., Marder V.J., Clowes A.W. and George J.N.). 2001 (Lippincott Williams and Wilkins, Philadelphia, PA.): p. 203–232.*
53. Wagner, D.D., Urban-Pickering M., and Marder V.J., *Von Willebrand protein binds to extracellular matrices independently of collagen*. Proc Natl Acad Sci U S A, 1984. **81**(2): p. 471-5.
54. Huang, P.Y. and Hellums J.D., *Aggregation and disaggregation kinetics of human blood platelets: Part III. The disaggregation under shear stress of platelet aggregates*. Biophysical Journal, 1993: p. 354-361.
55. Bock, S.C., *Antithrombin III and Heparin Cofactor II, in Hemostasis and Thrombosis: Basic Principles and Clinical Practice*. 2001(Lippincott Williams and Wilkins: Philadelphia): p. 321-333.
56. Madsen, D.E., et al., *C1-inhibitor polymers activate the FXII-dependent kallikrein-kinin system: Implication for a role in hereditary angioedema*. Biochim Biophys Acta, 2015. **1850**(6): p. 1336-42.
57. Rosenberg, R.D. and Damus P.S., *The purification and mechanism of action of human antithrombin-heparin cofactor*. J Biol Chem, 1973. **248**(18): p. 6490-505.
58. Jin, L., et al., *The anticoagulant activation of antithrombin by heparin*. Proc Natl Acad Sci U S A, 1997. **94**(26): p. 14683-8.
59. Rao, L.V. and Rapaport S.I., *Studies of a mechanism inhibiting the initiation of the extrinsic pathway of coagulation*. Blood, 1987. **69**(2): p. 645-51.

60. Adams, R.L. and Bird R.J., *Review article: Coagulation cascade and therapeutics update: relevance to nephrology. Part 1: Overview of coagulation, thrombophilias and history of anticoagulants*. *Nephrology (Carlton)*, 2009. **14**(5): p. 462-70.
61. Renne, T., et al., *Defective thrombus formation in mice lacking coagulation factor XII*. *J Exp Med* 202(2), 2005: p. 271-281.
62. Forsgren, M., et al., *Molecular cloning and characterization of a full-length cDNA clone for human plasminogen*. *FEBS Lett*, 1987. **213**(2): p. 254-60.
63. Bezerra, J.A., et al., *Plasminogen deficiency leads to impaired remodeling after a toxic injury to the liver*. 1999(*Proc Natl Acad Sci U S A* 96(26): 15143-15148.).
64. Walker, F.J., *Regulation of activated protein C by a new protein. A possible function for bovine protein S*. *J Biol Chem*, 1980. **255**(12): p. 5521-4.
65. Esmon, C.T. and Owen W.G., *Identification of an endothelial cell cofactor for thrombin-catalyzed activation of protein C*. *Proc Natl Acad Sci U S A*, 1981. **78**(4): p. 2249-52.
66. Sturn, D.H., et al., *Expression and function of the endothelial protein C receptor in human neutrophils*. *Blood*, 2003. **102**(4): p. 1499-505.
67. de Boer, J.P., et al., *Alpha-2-macroglobulin functions as an inhibitor of fibrinolytic, clotting, and neutrophilic proteinases in sepsis: studies using a baboon model*. *Infect Immun*, 1993. **61**(12): p. 5035-43.

68. Moroi, M. and Aoki N., *Isolation and characterization of alpha2-plasmin inhibitor from human plasma. A novel proteinase inhibitor which inhibits activator-induced clot lysis.* J Biol Chem, 1976. **251**(19): p. 5956-65.
69. Elisen, M.G., et al., *Protein C inhibitor acts as a procoagulant by inhibiting the thrombomodulin-induced activation of protein C in human plasma.* Blood, 1998. **91**(5): p. 1542-7.
70. Polgar, L., *The catalytic triad of serine peptidases.* Cell Mol Life Sci, 2005. **62**(19-20): p. 2161-72.
71. Di Cera, E., *Serine proteases.* IUBMB Life, 2009. **61**(5): p. 510-5.
72. Yang, Y., et al., *Serine proteases of parasitic helminths.* Korean J Parasitol, 2015. **53**(1): p. 1-11.
73. Hedstrom, L., *Serine protease mechanism and specificity.* Chem Rev, 2002. **102**(12): p. 4501-24.
74. Citarella, F., et al., *Structure/function analysis of human factor XII using recombinant deletion mutants. Evidence for an additional region involved in the binding to negatively charged surfaces.* Eur J Biochem, 1996. **238**(1): p. 240-9.
75. Elsa S. Henriquesa, W.B.F., Nathalie Reuterc, André Meloa, David Brownd, José and B.M. A.N.F. Gomesa, Marco A.C. Nascimento & Maria João Ramosa, *The search for a new model structure of b-Factor XIIIa.* Journal of Computer-Aided Molecular Design KLUWER/ESCOM Kluwer Academic Publishers., 2001. **15**: p. 309–322.

76. Stavrou, E. and Schmaier A.H., *Factor XII: what does it contribute to our understanding of the physiology and pathophysiology of hemostasis & thrombosis*. Thromb Res, 2010. **125**(3): p. 210-5.
77. Konings, J., et al., *Factor XIIIa regulates the structure of the fibrin clot independently of thrombin generation through direct interaction with fibrin*. Blood, 2011. **118**(14): p. 3942-51.
78. Konings, J., et al., *Factor XIIIa regulates the structure of the fibrin clot independently of thrombin generation through direct interaction with fibrin*. Blood, 2011. **118**(14): p. 3942-51.
79. Yamada, K.M., *Cell surface interactions with extracellular materials*. Annu Rev Biochem, 1983. **52**: p. 761-99.
80. Clarke, B.J., et al., *Mapping of a putative surface-binding site of human coagulation factor XII*. J Biol Chem, 1989. **264**(19): p. 11497-502.
81. Samuel, M., Samuel E., and Villanueva G.B., *Histidine residues are essential for the surface binding and autoactivation of human coagulation factor XII*. Biochem Biophys Res Commun, 1993. **191**(1): p. 110-7.
82. Baglia, F.A., Jameson B.A., and Walsh P.N., *Identification and characterization of a binding site for factor XIIIa in the Apple 4 domain of coagulation factor XI*. J Biol Chem, 1993. **268**(6): p. 3838-44.
83. Rojkaer, R. and Schousboe I., *Partial identification of the Zn²⁺-binding sites in factor XII and its activation derivatives*. Eur J Biochem, 1997. **247**(2): p. 491-6.

84. Mahdi, F., et al., *Factor XII interacts with the multiprotein assembly of urokinase plasminogen activator receptor, gC1qR, and cytokeratin 1 on endothelial cell membranes*. Blood, 2002. **99**(10): p. 3585-96.
85. Bradford, H.N., Pixley R.A., and Colman R.W., *Human factor XII binding to the glycoprotein Ib-IX-V complex inhibits thrombin-induced platelet aggregation*. J Biol Chem, 2000. **275**(30): p. 22756-63.
86. Henderson, L.M., et al., *Assembly of contact-phase factors on the surface of the human neutrophil membrane*. Blood, 1994. **84**(2): p. 474-82.
87. Hasan, A.A., Zisman T., and Schmaier A.H., *Identification of cytokeratin 1 as a binding protein and presentation receptor for kininogens on endothelial cells*. Proc Natl Acad Sci U S A, 1998. **95**(7): p. 3615-20.
88. Mahdi, F., et al., *Expression and colocalization of cytokeratin 1 and urokinase plasminogen activator receptor on endothelial cells*. Blood, 2001. **97**(8): p. 2342-50.
89. Schmaier, A.H. and Larusch G., *Factor XII: new life for an old protein*. Thromb Haemost, 2010. **104**(5): p. 915-8.
90. Schousboe, I., *Pharmacological regulation of factor XII activation may be a new target to control pathological coagulation*. Biochem Pharmacol, 2008. **75**(5): p. 1007-13.
91. McMullen, B.A. and Fujikawa K., *Amino acid sequence of the heavy chain of human alpha-factor XIIIa (activated Hageman factor)*. J Biol Chem, 1985. **260**(9): p. 5328-41.

92. Pixley, R.A., et al., *A monoclonal antibody recognizing an icosapeptide sequence in the heavy chain of human factor XII inhibits surface-catalyzed activation.* J Biol Chem, 1987. **262**(21): p. 10140-5.
93. Citarella, F., et al., *Identification of a putative binding site for negatively charged surfaces in the fibronectin type II domain of human factor XII--an immunochemical and homology modeling approach.* Thromb Haemost, 2000. **84**(6): p. 1057-65.
94. Wiley, H.S., Shvartsman S.Y., and Lauffenburger D.A., *Computational modeling of the EGF-receptor system: a paradigm for systems biology.* Trends Cell Biol, 2003. **13**(1): p. 43-50.
95. Chien, P., et al., *Modulation of the human monocyte binding site for monomeric immunoglobulin G by activated Hageman factor.* J Clin Invest, 1988. **82**(5): p. 1554-9.
96. Cool, D.E., et al., *Characterization of human blood coagulation factor XII cDNA. Prediction of the primary structure of factor XII and the tertiary structure of beta-factor XIIa.* J Biol Chem, 1985. **260**(25): p. 13666-76.
97. Ravon, D.M., et al., *Monoclonal antibody F1 binds to the kringle domain of factor XII and induces enhanced susceptibility for cleavage by kallikrein.* Blood, 1995. **86**(11): p. 4134-43.
98. Lynch J, S.-M.Z., *Physiological Effects of the Plasma Kallikrein-Kinin System: Roles of the Blood Coagulation Factor XII(Hageman Factor).* J Clinic Toxicol, 2012. **2**:e105. doi:10.4172/2161-0495.1000e105.

99. Chen, X., et al., *Ordered adsorption of coagulation factor XII on negatively charged polymer surfaces probed by sum frequency generation vibrational spectroscopy*. *Anal Bioanal Chem*, 2007. **388**(1): p. 65-72.
100. Schmaier, A.H., *The elusive physiologic role of Factor XII*. *J Clin Invest*, 2008. **118**(9): p. 3006-9.
101. Kishimoto, T.K., et al., *Contaminated heparin associated with adverse clinical events and activation of the contact system*. *N Engl J Med*, 2008. **358**(23): p. 2457-67.
102. Kaminishi, H., et al., *Activation of blood clotting factors by microbial proteinases*. *FEMS Microbiol Lett*, 1994. **121**(3): p. 327-32.
103. Kannemeier, C., et al., *Extracellular RNA constitutes a natural procoagulant cofactor in blood coagulation*. *Proc Natl Acad Sci U S A*, 2007. **104**(15): p. 6388-93.
104. Smith, S.A., et al., *Polyphosphate modulates blood coagulation and fibrinolysis*. *Proc Natl Acad Sci U S A*, 2006. **103**(4): p. 903-8.
105. Maas, C., et al., *Misfolded proteins activate Factor XII in humans, leading to kallikrein formation without initiating coagulation*. *J Clin Invest*, 2008. **118**(9): p. 3208-18.
106. Fujihara, N., et al., *Characterization of factor XII Tenri, a rare CRM-negative factor XII deficiency*. *Ann Clin Lab Sci*, 2004. **34**(2): p. 218-25.

107. Bernardo, M.M., et al., *Surface-independent acceleration of factor XII activation by zinc ions. I. Kinetic characterization of the metal ion rate enhancement*. J Biol Chem, 1993. **268**(17): p. 12468-76.
108. Schousboe, I., *Contact activation in human plasma is triggered by zinc ion modulation of factor XII (Hageman factor)*. Blood Coagul Fibrinolysis, 1993. **4**(5): p. 671-8.
109. LaRusch, G.A., et al., *Factor XII stimulates ERK1/2 and Akt through uPAR, integrins, and the EGFR to initiate angiogenesis*. Blood, 2010. **115**(24): p. 5111-20.
110. Colman, R.W. and Schmaier A.H., *Contact system: a vascular biology modulator with anticoagulant, profibrinolytic, antiadhesive, and proinflammatory attributes*. Blood, 1997. **90**(10): p. 3819-43.
111. Kolte D, Z.S., *What we have learned from Structure of High Molecular Weight Kininogen*. J Clin Toxicol 2011. **1**(102e). doi:10.4172/2161-0494.1000102e).
112. Schmeidler-Sapiro, K.T., Ratnoff O.D., and Gordon E.M., *Mitogenic effects of coagulation factor XII and factor XIIIa on HepG2 cells*. Proc Natl Acad Sci U S A, 1991. **88**(10): p. 4382-5.
113. Gordon, E.M., et al., *Factor XII-induced mitogenesis is mediated via a distinct signal transduction pathway that activates a mitogen-activated protein kinase*. Proc Natl Acad Sci U S A, 1996. **93**(5): p. 2174-9.

114. Fernando, A.N., et al., *Assembly, activation, and signaling by kinin-forming proteins on human vascular smooth muscle cells*. Am J Physiol Heart Circ Physiol, 2005. **289**(1): p. H251-7.
115. Mavrogiannis, L., Kariyawasam K.P., and Osmond D.H., *Potent blood pressure raising effects of activated coagulation factor XII*. Can J Physiol Pharmacol, 1997. **75**(12): p. 1398-403.
116. Tankersley, D.L., Alving B.M., and Finlayson J.S., *Preparation of beta-XIIa (Hageman factor fragment) from human plasma*. Thromb Res, 1982. **25**(4): p. 307-17.
117. DeLa Cadena R, W.Y., Colman RW, *Contact activation pathway: inflammation and coagulation*. In: Colman RW, Hirsh J, Marder VJ, Salzman EW, eds. *Hemostasis and Thrombosis: Basic Principles and Clinical Practice*. 3rd ed. Philadelphia, Pa: JB Lippincott Co; 219-240. 1994.
118. Ratnoff, O.D. and Colopy J.E., *A familial hemorrhagic trait associated with a deficiency of a clot-promoting fraction of plasma*. J Clin Invest, 1955. **34**(4): p. 602-13.
119. Renne, T., et al., *In vivo roles of factor XII*. Blood, 2012. **120**(22): p. 4296-303.
120. Ponczek, M.B., Gailani D., and Doolittle R.F., *Evolution of the contact phase of vertebrate blood coagulation*. J Thromb Haemost, 2008. **6**(11): p. 1876-83.
121. Kleinschnitz, C., et al., *Targeting coagulation factor XII provides protection from pathological thrombosis in cerebral ischemia without interfering with hemostasis*. J Exp Med, 2006. **203**(3): p. 513-8.

122. Pauer, H.U., et al., *Targeted deletion of murine coagulation factor XII gene-a model for contact phase activation in vivo*. *Thromb Haemost*, 2004. **92**(3): p. 503-8.
123. Renne, T., et al., *Defective thrombus formation in mice lacking coagulation factor XII*. *J Exp Med*, 2005. **202**(2): p. 271-81.
124. Stoll, G., Kleinschnitz C., and Nieswandt B., *Molecular mechanisms of thrombus formation in ischemic stroke: novel insights and targets for treatment*. *Blood*, 2008. **112**(9): p. 3555-62.
125. Halbmayer, W.M., et al., *The prevalence of factor XII deficiency in 103 orally anticoagulated outpatients suffering from recurrent venous and/or arterial thromboembolism*. *Thromb Haemost*, 1992. **68**(3): p. 285-90.
126. Lammle, B., et al., *Thromboembolism and bleeding tendency in congenital factor XII deficiency--a study on 74 subjects from 14 Swiss families*. *Thromb Haemost*, 1991. **65**(2): p. 117-21.
127. Burton, R.A., et al., *Identification of an ordered compact structure within the recombinant bovine fibrinogen alphaC-domain fragment by NMR*. *Biochemistry*, 2006. **45**(7): p. 2257-66.
128. Olson, N.C., et al., *Coagulation factor XII genetic variation, ex vivo thrombin generation, and stroke risk in the elderly: results from the Cardiovascular Health Study*. *J Thromb Haemost*, 2015. **13**(10): p. 1867-77.

129. van Montfoort, M.L. and Meijers J.C., *Anticoagulation beyond direct thrombin and factor Xa inhibitors: indications for targeting the intrinsic pathway?* *Thromb Haemost*, 2013. **110**(2): p. 223-32.
130. Kenne, E. and Renne T., *Factor XII: a drug target for safe interference with thrombosis and inflammation.* *Drug Discov Today*, 2014. **19**(9): p. 1459-64.
131. Baeriswyl, V., et al., *Development of a selective peptide macrocycle inhibitor of coagulation factor XII toward the generation of a safe antithrombotic therapy.* *J Med Chem*, 2013. **56**(9): p. 3742-6.
132. Baeriswyl, V., et al., *A Synthetic Factor XIIa Inhibitor Blocks Selectively Intrinsic Coagulation Initiation.* *ACS Chem Biol*, 2015. **10**(8): p. 1861-70.
133. Jones, S. and Thornton J.M. Thornton, *Principles of protein-protein interactions.* *Proc Natl Acad Sci U S A*, 1996. **93**(1): p. 13-20.
134. Apostoluk, W. and Otlewski J., *Variability of the canonical loop conformations in serine proteinases inhibitors and other proteins.* *Proteins*, 1998. **32**(4): p. 459-74.
135. Krowarsch, D., et al., *Canonical protein inhibitors of serine proteases.* *Cell Mol Life Sci*, 2003. **60**(11): p. 2427-44.
136. Behnke, C.A., et al., *Structural determinants of the bifunctional corn Hageman factor inhibitor: x-ray crystal structure at 1.95 Å resolution.* *Biochemistry*, 1998. **37**(44): p. 15277-88.
137. Laskowski, M.J., Qasim M.A., and S.M. Lu, *Interaction of standard mechanism, canonical protein inhibitors with serine proteinases. In: protein-*

Protein Recognition, pp. 228–279, Kleanthous C. (ed.), Oxford University Press, Oxford. 2000.

138. Korsinczky, M.L., et al., *Solution structures by 1H NMR of the novel cyclic trypsin inhibitor SFTI-1 from sunflower seeds and an acyclic permutant*. J Mol Biol, 2001. **311**(3): p. 579-91.
139. Bode, W. and Huber R., *Structural basis of the endoproteinase-protein inhibitor interaction*. Biochim Biophys Acta, 2000. **1477**(1-2): p. 241-52.
140. Otlewski, J., Krowarsch D., and Apostoluk W., *Protein inhibitors of serine proteinases*. Acta Biochim Pol, 1999. **46**(3): p. 531-65.
141. Laskowski, M., Jr. and Kato I., *Protein inhibitors of proteinases*. Annu Rev Biochem, 1980. **49**: p. 593-626.
142. Bode, W. and Huber R., *Natural protein proteinase inhibitors and their interaction with proteinases*. Eur J Biochem, 1992. **204**(2): p. 433-51.
143. Jackson, R.M. and Russell R.B., *The serine protease inhibitor canonical loop conformation: examples found in extracellular hydrolases, toxins, cytokines and viral proteins*. J Mol Biol, 2000. **296**(2): p. 325-34.
144. Ng, T.B., *In Advances in Phytomedicine Volume 3, Naturally Occurring Bioactive Compounds*, ed.by Rai, M., Carpinella, M.C. 2006(Elsevier, Radarweg 29, PO box 211, 1000 AE Amsterdam, The Netherlands): p. 409-410.
145. Lei, M.G. and Reeck G.R., *Combined use of trypsin-agarose affinity chromatography and reversed-phase high-performance liquid*

- chromatography for the purification of single-chain protease inhibitor from corn seeds. J Chromatogr, 1986. 363(2): p. 315-21.*
146. Wen, L., et al., *Nucleotide sequence of a cDNA clone that encodes the maize inhibitor of trypsin and activated Hageman factor. Plant Mol Biol, 1992. 18(4): p. 813-4.*
147. Ling, L., *Distribution of trypsin inhibitors in plant food stuffs. Master thesis, Kansas state university. . 1972.*
148. Hazegh-Azam, M., et al., *The corn inhibitor of activated Hageman factor: purification and properties of two recombinant forms of the protein. Protein Expr Purif, 1998. 13(2): p. 143-9.*
149. Hansson, K.M., et al., *The effect of corn trypsin inhibitor and inhibiting antibodies for FXIa and FXIIa on coagulation of plasma and whole blood. J Thromb Haemost, 2014. 12(10): p. 1678-86.*
150. CHEN, I. and MITCHELL H.L., *Phytochemistry, 1973. Volume 12(2 Department of Biochemistry, Kansas State University, Manhattan, KS 66502, U.S.A.): p. 327–330.*
151. Swartz, M.J., et al., *Isolation and characterization of trypsin inhibitor from opaque-2 corn seeds. J Biol Chem, 1977. 252(22): p. 8105-7.*
152. Hojima, Y., Pierce J.V., and Pisano J.J., *Hageman factor fragment inhibitor in corn seeds: purification and characterization. Thromb Res 1980. 20: 149–62*

153. Hojima, Y., P. J.V., and P. J.J., *Plant inhibitors of serine proteinases: hageman factor fragment, kallikreins, plasmin, thrombin, factor Xa, trypsin, and chymotrypsin. Thromb Res* 1980; 20: 163–71.
154. Chong, G.L. and Reeck G.R., *Interaction of trypsin, beta-factor XIIa, and plasma kallikrein with a trypsin inhibitor isolated from barley seeds: a comparison with the corn inhibitor of activated Hageman factor. Thromb Res*, 1987. **48**(2): p. 211-21.
155. Ratnoff, O.D., *Studies on the inhibition of ellagic acid-activated Hageman factor (factor XII) and Hageman factor fragments. Blood*, 1981. **57**(1): p. 55-8.
156. Mahoney, W.C., et al., *Amino acid sequence and secondary structural analysis of the corn inhibitor of trypsin and activated Hageman Factor. J Biol Chem*, 1984. **259**(13): p. 8412-6.
157. Chen, M.S., et al., *α -Amylases from three species of stored grain Coleoptera and their inhibition by wheat and corn proteinaceous inhibitors. Insect Biochem. Mol. Biol.* 22:, 1992: p. 261-268.
158. Chen, Z.Y., et al., *A Corn Trypsin Inhibitor with Antifungal Activity Inhibits *Aspergillus flavus* alpha-Amylase. Phytopathology*, 1999. **89**(10): p. 902-7.
159. Chen, Z.Y., et al., *Resistance to *Aspergillus flavus* in Corn Kernels Is Associated with a 14-kDa Protein. Phytopathology*, 1998. **88**(4): p. 276-81.

160. Chen, Z.Y., et al., *Inhibition of plant-pathogenic fungi by a corn trypsin inhibitor overexpressed in Escherichia coli*. Appl Environ Microbiol, 1999. **65**(3): p. 1320-4.
161. Ansell, J., et al., *The pharmacology and management of the vitamin K antagonists: the Seventh ACCP Conference on Antithrombotic and Thrombolytic Therapy*. Chest, 2004. **126**(3 Suppl): p. 204S-233S.
162. Becker, R.C., et al., *The primary and secondary prevention of coronary artery disease: American College of Chest Physicians Evidence-Based Clinical Practice Guidelines (8th Edition)*. Chest, 2008. **133**(6 Suppl): p. 776S-814S.
163. Kleinschmidt, S. and Seyfert U.T., *Heparin-associated thrombocytopenia (HAT)--still a diagnostic and therapeutical problem in clinical practice*. Angiology, 1995. **46**(1): p. 37-44.
164. King, D.J. and Kelton J.G., *Heparin-associated thrombocytopenia*. Ann Intern Med, 1984. **100**(4): p. 535-40.
165. Hirsh, J., et al., *Heparin: mechanism of action, pharmacokinetics, dosing considerations, monitoring, efficacy, and safety*. Chest, 1995. **108**(4 Suppl): p. 258S-275S.
166. Symons, G., *Anticoagulation: where have we come from and where are we going? The evidence for and against novel anticoagulants*. S Afr Med J, 2014. **104**(2): p. 143-6.

167. Quinlan, D.J. and Eriksson B.I., *Novel oral anticoagulants for thromboprophylaxis after orthopaedic surgery*. *Best Pract Res Clin Haematol*, 2013. **26**(2): p. 171-82.
168. Broussalis, E., et al., *Latest developments in anticoagulant drug discovery*. *Drug Discov Today*, 2014. **19**(7): p. 921-35.
169. Levine, M.N., et al., *Hemorrhagic complications of anticoagulant treatment: the Seventh ACCP Conference on Antithrombotic and Thrombolytic Therapy*. *Chest*, 2004. **126**(3 Suppl): p. 287S-310S.
170. Levine, M.N., et al., *Hemorrhagic complications of anticoagulant treatment*. *Chest*, 2001. **119**(1 Suppl): p. 108S-121S.
171. Siegal, D.M., Garcia D.A., and Crowther M.A., *How I treat target-specific oral anticoagulant-associated bleeding*. *Blood*, 2014. **123**(8): p. 1152-8.
172. Woodruff, R.S., et al., *Inhibiting the intrinsic pathway of coagulation with a factor XII-targeting RNA aptamer*. *J Thromb Haemost*, 2013. **11**(7): p. 1364-73.
173. Pathak, M., et al., *Coagulation factor XII protease domain crystal structure*. *J Thromb Haemost*, 2015. **13**(4): p. 580-91.
174. Hayashi K, K.C., *pCold-GST vector: a novel cold-shock vector containing GST tag for soluble protein production*. *Protein Expr Purif.* , 2008 **62**(1):120-7. doi: **10.1016/j.pep.**(1): p. 120-7.

175. Stojan, J., *Enzyme Inhibition*, in: H.J. Smith, C. Simons (Eds.), . *Enzymes and Their Inhibition*, Drug Development, 2005 (CRC Press, London, chapter 4): p. 149-169.
176. Cleland, W.W., , *Steady State Kinitics*, in: P.D. Boyer (Ed.), *The Enzymes*, 3rd ed., Vol. 2, . (Academic Press, New York): 1970. p.1-65.
177. Saboury, A.A., *Enzyme Inhibition and Activation: A General Theory*. J. Iran. Chem. Soc., Vol. 6, No. 2, June 2009, pp. 219-229.
178. Copeland, R., *Evaluation of enzyme inhibitors in drug discovery: A guide for medicinal chemists and pharmacologists*. Hoboken, New Jersey. John Wiley & Sons., Inc., 2013. 5.2:133-135.
179. Taylor, K., *Enzyme Kinetics and Mechanisms*. **Kluwer Academic publishers** 2004. (9.2.2): p. 124-125.
180. Baker, G., Dunn S., and Holt A., *Handbook of Neurochemistry and Molecular Neurobiology* Practical Neurochemistry Methods, Practical Enzymology, Reversible, Irreversible, Tight-Binding Inhibitors 2007. **(5.1.1)** p. 114-115.
181. Vauquelin, G., et al., *New insights in insurmountable antagonism*. *Fundam Clin Pharmacol*, 2002. **16**(4): p. 263-72.
182. Cairo, C.W., Simon J.B., and Golan D.E., '*Drug-Receptor interaction, Fundamentals in Pharmacology*' in *Principles of Pharmacology : The Pathophysiologic Basis of Drug Therapy* ed.by Golan, D. E., Tashjian, A. H., Jr., Armstrong,E.J. and Armstrong A. W.Philadelphia. Lippincott Williams and Wilkins. 2005: p. 23-25.

183. Wu, G., *Assay development : Fundamentals and Practices*. John Wiley and Sons. 2010. chapter 3. p. 95-96.
184. Chen, W.W., Niepel M., and Sorger P.K., *Classic and contemporary approaches to modeling biochemical reactions*. Genes Dev, 2010. **24**(17): p. 1861-75.
185. Michaelis, L., et al., *The original Michaelis constant: translation of the 1913 Michaelis-Menten paper*. Biochemistry, 2011. **50**(39): p. 8264-9.
186. Matyska, L. and Kovar J., *Comparison of several non-linear-regression methods for fitting the Michaelis-Menten equation*. Biochem J, 1985. **231**(1): p. 171-7.
187. Bjorkqvist, J., et al., *Defective glycosylation of coagulation factor XII underlies hereditary angioedema type III*. J Clin Invest, 2015. **125**(8): p. 3132-46.
188. Shan, J., et al., *Expression, refolding, and activation of the catalytic domain of human blood coagulation factor XII*. Protein Expr Purif, 2003. **27**(1): p. 143-9.
189. Silverberg, M., et al., *Autoactivation of human Hageman factor. Demonstration utilizing a synthetic substrate*. J Biol Chem, 1980. **255**(15): p. 7281-6.
190. WHO, <http://www.who.int/mediacentre>. 2012.
191. Baeriswyl, V., et al., *A Synthetic Factor XIIa Inhibitor Blocks Selectively Intrinsic Coagulation Initiation*. ACS Chem Biol, 2015. **10** (8) p.1861-70

Appendix

Publication

Article:

Pathak M, Wilmann P, Awford J, Li C, Hamad BK, Fischer PM, Dreveny I, Dekker LV, Emsley J. Coagulation factor XII protease domain crystal. *J Thromb Haemost structure*. 13(4):580-9. doi: 10.1111/jth.12849 (2015).

Conference paper:

Rosa Manna, Badraldin Hamad, Jonas Emsley. EXPRESSION PURIFICATION AND ACTIVITY ASSAYS OF HUMAN FXII. FINAL PROGRAMME Joint British Society for Haemostasis & Thrombosis, UK Platelet Group & United Kingdom Haemophilia Centre Doctors Organisation- Annual Scientific and general meeting, The Royal College of Surgeons of Edinburgh (2014).